

**DESCRIPTION OF A TRANSIENT CAUSED BY THE SWITCHING-OFF
OF ONE OF THE FOUR OPERATING MCP
AT NOMINAL REACTOR POWER AT NPP KALININ UNIT 3**

V. A. Tereshonok, V. S. Stepanov, V. V. Ivchenkov, V. A. Pitilimov
(VNIAES)

S. P. Nikonov (RRC “Kurchatov Institute“)

July 2008

CONTENT

Abbreviations.....	3
1 Initial data	8
2 Measuring and recording devices	10
3 Analysis of the transient caused by switching-off of one MCP of the four operated.....	11
Conclusions.....	84
Annex A. Reactor core load.....	85
Annex B. Arrangement of the ionization chamber channels, control rods of CPS and their groups' assignment, thermal control sensors at FA outlets and the arrangement of the SPND.....	86
Annex C. Division of the reactor core in 60 °-symmetry sectors, layout of FA, CPS control rods and CPS CR group allocation, layout of thermal control sensors at FA outlets and assemblies with SPND	87
Annex D. Location of the temperature monitoring casings in the primary circulation loops	88
Annex E. Parameters recorded by UBLS	89
Annex F. Parameters recorded by ICMS	103
Annex G. Parameters recorded by MMS.....	121

ABBREVIATIONS¹

АЗ/РР	- reactor protection
АКНП /NFC	- neutron flux control system
АРМ/АРС	- automatic reactor power controller
АЭС/NPP	- nuclear power plant
БРУ-СН/FASB-HL	- fast acting steam bypass valves for house loads
БПУ/MCR	- main control room
ВВЭР/WWER-	reactor WWER
ВД/HP	- high pressure
ВКВ/UES	- upper end switch
ВПЭН /AFWP-	auxiliary feedwater pump
ГПК /MSH	- main steam header
ГЦН /MCP	- main circulation pump
ДПЗ/SPND	- self powered neutron detector
D7/D7	- secondary side deaerator D7
ИК/ICh	- ionization chamber
КГТН/СНТР	- condenser hydro-turbine pump
КД/PRZ	- pressurizer
КНДР/ТНС	- secondary side condenser
КСН/ISC	- internal house loads collector
КЭН-1(2)/СР-1(2)	- condenser pump of the first (second) stage
«Н»	- mode of APC to maintain reactor power
НД/LP	- low pressure
НКВ/LES	- low end switch
НС РЦ/SL-RH-	shift leader of the reactor hall
ОР/CR	- control rods
ПВД /HP-PH	- high pressure pre-heater
ПГ /SG	- steam generator
ПЗ-1/PP-1	- pre-protection – 1-st stage
ПК/PC	- primary circuit
ПНД/LP-PH	- low pressure pre-heater

¹ For better traceability, the abbreviations are given both in their original (Russian) spelling and as translated into English (RU/EN)

ПД-1/OR-1 - first sub-range scale of NFC
 ПД-2/OR-2 - second sub-range scale of NFC
 «Per. N»/«Contr. N» - mode of TEC to maintain the TG load
 «Per. P»/«Contr. P» - mode of TEC to maintain pressure in the MSH
 POM/LRPC - load-off and reactor power controller
 PY/RF - reactor facility
 СБВУ/UBLS - upper level unit control system
 СБПК /ICMS - in-core monitoring system
 СПП/SSSH - steam separator and steam superheater
 СУЗ/CPS - reactor control and protection system
 СЭК/MMS - measurement-monitoring system
 «Т» - APC mode to maintain pressure in MSH
 ТБС/FA - fuel assembly
 ТБСА/АФА - „alternative“ fuel assembly
 ТГ/TG - turbine generator
 ТП/TC - thermocouple
 ТП1(2)/TC1(2)- the 1st (2nd) set of thermocouples
 ТПН /TFWP - turbo-feedwater pump
 ТС/RT - resistance thermometer
 ТЭН/ТЕН - tube electroheater (in PRZ)
 ЦВД /HPTP - high pressure turbine part
 ЦНД /LPTP - low pressure turbine part
 ЭЧСР/TEC - turbine electronic controller
 $C_{6к}/C_B$ - concentration of boric acid in the coolant, g/kg
 $G_{БПЭHj} /G_{j-AFWP}$ - feedwater flow rate at pressure side of AFWP_j, (j = 1, 2), m³/h, t/h
 G_{D7-j} /G_{D7-j} - condensate flow rate of the j-th deaerator (j = 1, 2), m³/h, t/h
 $G_{ПBi} / G_{i-SG}$ - feedwater flow rate of SG_i, (i=1,2,3,4), m³/h, t/h
 $G_{HP-PHj} /G_{j-HP-PH}$ - feedwater flow rate of HP-PH_j, (j = 1, 2), m³/h, t/h
 $G_{подп} /G_{PC-supply}$ - make-up flow rate in PC, m³/h, t/h
 $G_{прод} /G_{blowdown}$ - blow-down flow rate in PC, m³/h, t/h
 $G_{ПTi} /G_{loop-i}$ - coolant flow rate in the i-th loop of PC (i= 1,2,3,4), m³/h, t/h
 G_p /G_r - coolant flow rate through the reactor, m³/h, t/h
 $G_{спп} /G_{SSSH}$ - flow rate of heating steam to SSSH, t/h
 $G_{ТПHj} /G_{TFWPj}$ - feed water flow rate at pressure side of TFWP_j, (j=1, 2), m³/h, t/h
 H_i - insertion depth of the CR_i group of CPS, i = 1, 2, ... , 10, cm, %

K_q	- FA relative power (core power radial peaking factor), rel. unit
$K_{q \max}$	- max. value of the FA relative power, rel. unit
K_v	- core power peaking factor, rel. unit
$K_{v \max}$	- max. core power peaking factor, rel. unit
$L_{д7-j} / L_{D7-j}$	-condensate level in the j-th deaerator ($j = 1, 2$), mm, cm
$L_{кд} / L_{PRZ}$	- coolant level in pressurizer, cm
L_{SGi}	- SG _i water level ($i = 1,2,3,4$), mm, cm
$L_{пвд-j} / L_{j-HP-PH}$	- HP-PH _j water level, ($j = 1, 2$), mm, cm
$L_{пнд-j} / L_{j-LP-PH}$	- LP-PH _j water level, ($j = 1, \dots, 5$), mm, cm
L_{sd}	- water level of the turbine condenser, mm
$N_{1к} / N_{PC}$	- reactor thermal power calculated on the basis of the coolant parameters in the primary circuit, MW, % N_{nom}
$N_{2к} / N_{SC}$	- reactor thermal power calculated on the basis of feed water parameters of the SGs, MW, % N_{nom}
$N_{акз} / N_{core}$	- average reactor thermal power, MW, % N_{nom}
$N_{акнп} / N_{NFC}$	- reactor thermal power calculated on the basis of NFC records, MW, % N_{nom}
$N_{гиди} / N_{MCPi}$	- electrical power consumed by the motor of MCP _i , ($i = 1, 2, 3, 4$), MW
$N_{дпз} / N_{DCS}$	- reactor thermal power calculated on the basis of SPND, MW, % N_{nom}
$N_{ниki} / N_{nfi}$	- reactor power calculated on the basis of data from the i-th measurement channel of the operational range of NFC ($i=1, \dots, 6$), MW, % N_{nom}
$N_{ном} / N_{nom}$	- nominal reactor power
$N_{итi} / N_{PC-loop-i}$	- loop _i power of primary circuit, ($i=1, 2, 3, 4$), MW
$N_{тек} / N_{actual}$	- actual reactor power, MW, % N_{nom}
$N_{эл} / N_{el}$	- TG electrical power (active), MW
N_i	- reactor power according to the i-th measurement channel of OR-1 NFC
$n_{тпнj} / n_{TFWPj}$	- rotation speed of TFWP _j , ($j = 1,2$), min^{-1}
$P_{1к} / P_{PC}$	- PC pressure, MPa
$P_{аз} / P_{core}$	- core outlet pressure, MPa
$P_{впэhj} / P_{AFWP}$	- feedwater pressure at the pressure side of AFWP _j , ($j = 1, 2$), MPa
$P_{гнк} / P_{MSH}$	- MSH pressure, MPa
$P_{д7-j} / P_{D7-j}$	- D7 _j pressure, ($j = 1, 2$), MPa
$P_{кнсб} / P_{CC}$	- pressure in the condenser collector, MPa
$P_{кч} / P_{ISC}$	- ISC pressure, MPa
$P_{кэH1-j} / P_{CP-1-j}$	- CP-1 _j pressure at pressure side, ($j = 1, 2, 3$), MPa
$P_{кэH2-j} / P_{CP-2-j}$	- CP-2 _j pressure at pressure side, ($j = 1, \dots, 5$), MPa

- $P_{от6i} / P_{extr-i}$ - steam pressure at the j-th turbine stage outlet, ($i = 1, \dots, 8$), MPa
- $P_{пвi} / P_{SG-i}$ - feed water pressure at SG_i inlet, ($i = 1, \dots, 4$), MPa
- $P_{пвдj} / P_{HPH-j}$ - feed water pressure at HP-PH_j outlet, ($j = 1, 2$), MPa
- $P_{пгi} / P_{SGi}$ - SG_i steam pressure, ($i = 1, \dots, 4$), MPa
- $P_{спп} / P_{SSSH}$ - SSSH outlet pressure, MPa
- $P_{тпнj} / P_{TFWPj}$ - overpressure at pressure side of j-TFWP ($j = 1, 2$), MPa
- P_{HPTPi} / P_{HPTP} - HPTP_i outlet pressure, ($i = 1, \dots, 8$), MPa
- $S_{опу-чhj} / S_{FASB-HLj}$ - position of pressure control valve of FASB-HL_j, ($j = 1, 2$), %
- $S_{очi} / S_{main-i}$ - position of the main water level control valve of SG_i , ($i = 1, \dots, 4$), %
- $S_{пуски} / S_{start-i}$ - position of the start-up water level control valve of SG_i , ($i = 1, \dots, 4$), %
- $S_{пк} / S_{cv}$ - control valve position, %
- $S_{пк\ пнд-j} / S_{cv\ LP-PH-j}$ - position of the level control valve of LP-PH_j, ($j = 3, 4, 5$), %
- $S_{пki} / S_{CV-i}$ - position of high pressure control valve of TG_i , ($i = 1, \dots, 4$), %
- $T_{1к} / T_{PC}$ - mean coolant temperature in the primary circuit, °C
- T_{BX} / T_{inlet} - mean (by four operating MCP) coolant temperature at core inlet, °C
- $T_{гi} / T_{hot-i}$ - hot leg coolant temperature of the loop_i, ($i = 1, \dots, 4$), °C
- $T_{кнсб} / T_{cc}$ - temperature in the condenser collector, °C
- $T_{пвi} / T_{SG-i}$ - SG_i , inlet feed water temperature, ($i = 1, \dots, 4$), °C
- $T_{пвдj} / T_{HP-PH-j}$ - HP-PH_j downstream feed water temperature, ($j = 1, 2$), °C
- $T_{пвдj\ вх} / T_{HP-PH-j\ in}$ - HP-PH_j inlet feed water temperature, ($j = 1, 2$), °C
- $T_{пвдj\ вых} / T_{HP-PH-j\ out}$ - HP-PH_j outlet feed water temperature, ($j = 1, 2$), °C
- $T_{спп} / T_{SSSH}$ - heating steam temperature upstream SSSH, °C
- T_{xi} / T_{ci} - cold leg coolant temperature of the loop_i, ($i = 1, \dots, 4$), °C
- $T_{цв} / T_{HPTP}$ - water temperature at turbine condenser inlet, °C
- $T_{цвj} / T_{HPTP-j}$ - outlet water temperature at the j-th turbine condenser, ($j = 1, 2$), °C
- $T_{цвд} / T_{HPTP}$ - steam temperature at the outlet of HPTP, °C
- $T_{эф} / T_{ef}$ - full power effective days of reactor operation, (eff. days)
- $T_{итг1} / T_{ич1}$ - hot leg coolant temperature of the i-th loop, ($i = 1, \dots, 4$)
on the basis of the resistance thermometer measurements, °C
- $T_{итгx} / T_{ичt}$ - cold leg coolant temperature of the i-th loop, ($i = 1, \dots, 4$)
on the basis of the resistance thermometer measurements, °C
- $T_{итг1-j} / T_{ич1-j}$ - hot leg coolant temperature of the i-th loop, ($i = 1, \dots, 4$)
on the basis of the j-th thermocouple measurements of the first set, °C
- $T_{итг2-j} / T_{ич2-j}$ - hot leg coolant temperature of the i-th loop, ($i = 1, \dots, 4$)

- on the basis of the j-th thermocouple measurements of the second set, $^{\circ}\text{C}$
- $T_{\text{итпх1-j}}/T_{\text{итс1-j}}$ - cold leg coolant temperature of the i-th loop, ($i = 1, \dots, 4$)
on the basis of the j-th thermocouple measurements of the first set, $^{\circ}\text{C}$
- $T_{\text{итпх2-j}}/T_{\text{итс2-j}}$ - cold leg coolant temperature of the i-th loop, ($i = 1, \dots, 4$)
on the basis of the j-th thermocouple measurements of the second set, $^{\circ}\text{C}$
- T_k - outlet coolant temperature of FA_k , $^{\circ}\text{C}$
- $\Delta P_{\text{гппи}}/\Delta P_{\text{MCPi}}$ - pressure difference of MCP_i , ($i = 1, \dots, 4$), MPa
- $\Delta P_{\text{итг}}/\Delta P_{\text{SGi}}$ - pressure difference of SG_i , ($i = 1, \dots, 4$), MPa
- $\Delta P_p/\Delta P_r$ - pressure difference of reactor, MPa
- ΔT_k - coolant heat-up of FA_k , ($k = 1, \dots, 95$), $^{\circ}\text{C}$
- $\Delta T_{k \text{ max}}$ - maximum coolant heat-up of FA, $^{\circ}\text{C}$
- $\Delta T_{\text{ити}}/\Delta T_{\text{ит}}$ - coolant average heat-up in the i-th loop ($i = 1, \dots, 4$), $^{\circ}\text{C}$
- $\Delta T_{\text{итн1}}/\Delta T_{\text{итс1}}$ - coolant heat-up in the i-th loop ($i = 1, \dots, 4$), averaged on the basis of thermocouples' measurements of the first set, $^{\circ}\text{C}$
- $\Delta T_{\text{итн2}}/\Delta T_{\text{итс2}}$ - coolant heat-up in the i-th loop ($i = 1, \dots, 4$), averaged on the basis of thermocouples' measurements of the second set, $^{\circ}\text{C}$
- $\Delta T_{\text{итн1-j}}/\Delta T_{\text{итс1-j}}$ - coolant heat-up in the i-th loop ($i = 1, \dots, 4$), on the basis of j-the thermocouple measurement of the first set, $^{\circ}\text{C}$
- $\Delta T_{\text{итн2-j}}/\Delta T_{\text{итс2-j}}$ - coolant heat-up in the i-th loop ($i = 1, \dots, 4$), on the basis of j-the thermocouple measurement of the second set, $^{\circ}\text{C}$
- $\Delta T_{\text{итс}}/\Delta T_{\text{ит}}$ - coolant heat-up in the i-th loop ($i = 1, \dots, 4$), on the basis of measurement data of the resistance thermometers, $^{\circ}\text{C}$
- $\delta W_{\text{аз}}/\delta W_{\text{core}}$ - axial offset calculated on the basis of reconstructed power distribution in the core, %
- $\delta W_{\text{дпз}}/\delta W_{\text{дс}}$ - axial offset calculated on the bases of SPND readings, %
- τ - actual time, h, min, s
- Δ - change of a value

1 INITIAL DATA

The first fuel loading of the reactor core in Unit 3, NPP Kalinin consists of AFA developed by OKBM (experimental engineering bureau) in Nizhni Novgorod, with uranium-gadolinium fuel and without burnable absorbers. Till the burnup of 96 eff. days the core load had five types of AFA:

- 48 FA with U_{235} -enrichment of 1.3 %;
- 42 FA with U_{235} -enrichment of 2.2 %;
- 37 FA with average U_{235} -enrichment of 2.98 % (303 fuel rods with 3 %-enrichment, 9 gadolinium fuel rods with 2.4 %-enrichment);
- 24 radial profiled FA with average U_{235} -enrichment of 3.9 % (243 fuel rods with 4 %-enrichment, 60 fuel rods with 3.6 %-enrichment, 9 gadolinium fuel rods with 3.3 %-enrichment);
- 12 radial profiled FA with average U_{235} -enrichment of 3.9 % (240 fuel rods with 4 %-enrichment, 66 fuel rods with 3.6 %-enrichment, 6 gadolinium fuel rods with 3.3 %-enrichment).

It should be mentioned that AFA have stiffening fins which like the leading tubes and spacers were made of zirconium alloy (E-635).

After the operation of this fuel load during 96 effective days a defected FA with coordinates 07-32 (FA with initial U_{235} -enrichment of 2.2 % weight metal) was replaced by a “fresh” standard FA with U_{235} -enrichment of 1.6 % weight metal. The spacers and the leading tubes of this FA were made of stainless steel.

The fuel loading map in the reactor core of Unit 3 NPP Kalinin after the replacement of the defected AFA by a standard FA is demonstrated in Annex A. The scheme in this annex also demonstrates the layout of CR CPS rods and their distribution in the groups.

The scheme in Annex B shows the layout of ionizing chambers channels (in the biological shield of the reactor); CR of CPS and their assignment in groups; ICMS thermal control sensors locations at FA outlets; assemblies with SPND in the leading (central) FA tubes; primary circuit loop nozzles' locations.

Ionisation chambers KNK-15 and KNK-53M are used at Unit 3 NPP Kalinin for the neutron flux measurements during power operation from 10^{-2} to 120 % N_{nom} . Ionization chamber couples (KNK-15 + KNK-53M), which are located on one suspender are installed in the channels of the biological shield No. 2, 12, 22 (1st set) and channels No. 7, 17, 27 (2nd set). There, ionization chambers KNK-15 are installed (729 ± 10) mm higher, whereas the ionization chamber KNK-53M – (875 ± 10) lower than the level of the reactor core centre. Ionization chambers KNK-53M operate either separately in the 1st operation sub-range of NFC (OR-1) or in combination with the ioniza-

tion chamber KNK-15 in the 2nd operation sub-range (OR-2). During power operation higher than 1 % N_{nom} , the power control and power excursion take place in the range OR-2 (combination of KNK-15 and KNK-53M).

The core schema in Annex C shows conditionally accepted division of FA locations in the reactor core into 6 sectors with a 60⁰-symmetry together with layout of CR of CPS and their assignment in groups; ICMS thermocouples' locations (at FA-outlets) and SPND sensors' locations.

The schema in Annex D shows the locations of the casings of the temperature measurement devices in the main circuit as well as the table of KKS of ICMS thermal control sensors and the corresponding numbering of the temperature devices' casings located in the primary loops.

According to the measurement system established at the NPP the positions of CR of CPS are given with respect to the position of the lower end switches (LES). They are located 17.25 cm higher than the bottom of the reactor core. With the length of the reactor core of 355 cm and the distance between the lower and the upper end switches of 352 cm, it turns out that the CR of CPS when withdrawn from the reactor core (while $H = 352$ cm, then $H = 100$ %) are 14.25 cm higher than the upper end of the core. Thus, the upper end of the core corresponds to the positions of CR of CPS $H = 337.75$ cm = 96 %.

The data of the power load timetable (necessary to calculate the fuel burnup) for Unit 3 NPP Kalinin from the beginning of the first fuel cycle up to the day when the experiment with the switching off of one MCP took place, are provided separately on a digital medium. Additionally, tables are supplied with the daily averaged effective operation time of the reactor; boron concentration history; history of the position of the tenth group of CR of CPS; average thermal reactor power history and the electrical power history of the turbine generator.

2 MEASURING AND RECORDING DEVICES

Measuring and recording in this dynamic mode were conducted by standard devices i. e. by the upper block level system – (CBBY/UBLS) and by the ICMS as well as by means of additional measurement equipment (a system of experimental control COK/SEC).

The list of parameters recorded by the UBLS, (with periodicity of 1 s) is given in Annex F. The aperture of recording for directly measured signals is 0.1 % of the sensor's scale maximal value.

The list of parameters recorded by ICMS with time step 1 s is given in Annex G. The signal recordings aperture is not available for them. It should be mentioned that the currents of the SPND were recorded taking into account of the background sensors currents, i. e. with the deduction of background sensors currents.

The list of parameters recorded by the SEC computer with frequency of 10 Hz is given in Annex H, the aperture of parameter recordings is missing. The signals have been taken from plant standard sensors and systems. The NFC system have recorded the reactor power only in the sub-range OR-1 which was determined by the signals of the ionization chambers (Type KNK-53M9), located in the lower part of the core.

Data recorded by UBLS, ICMS and SEC is provided on the CD.

On CD can be found information for the CR of CPS positions recorded by the systems UBLS, ICMS and SEC in cm related to the position of the rigid end-stops which are located 10 cm lower than the lower end switches and 7.25 cm higher than the bottom of the reactor core.

3 ANALYSIS OF THE TRANSIENT CAUSED BY SWITCHING-OFF OF ONE MCP WHILE THE OTHER THREE REMAIN IN OPERATION

Initial steady state reactor parameters are shown in Table 1, in column „Initial state“ (data from ICMS, with exception of C_B which is determined by laboratory analysis). Values of FA relative power and heat-up of the coolant in FA are shown in the core schema of Fig. 1 and 2 (line „initial state“). The operational state of the loop equipment and control systems are without changes, as designed. The reactor was Xe_{135} poisoned. The boron concentration in the coolant of the primary circuit, pressurizer and deaerator of the feed water was balanced. The APC was operating in mode „T“ and, respectively, TEC was in mode «Control N».

At 20:30:02 on 02.10.2005 (time recorded by UBLS) the shift leader of the reactor manually switched off MCP-1 (YD10D01 - one of the four operated) from the control room.

The time histories (“0” on the time scale corresponds to the time 20:30:02) of the main parameters of the PC and SC are presented in the following Figures:

- Fig. 3 – 81 parameters recorded on ICMS and UBLS;
- Fig. 82 – 100 data recorded on of the additional SEC.

Parameters recorded at the end of the transient caused by the switching off of MCP-1 are shown in Table 1 (the column “end state”) and on the core map of Fig. 1, 2 (the line “end state”).

After 1.41 s (here and below from the moment of the switching off of MPC-1) and upon the signal “load off #2 switch off ¼ MCP PP-1 1KO” the LRPC load-off algorithm started with the insertion at first, the CR group #10 (from the initial position $H_{10} = 82.95\%$) and after that by reaching $H_{10} = 50\%$ - both CR groups #10 and #9 (from the upper end switches-UES).

Upon actuation of PP-1, the APC switched from mode „T“ into mode „H“ and so eliminated the control role of CPS. At the same time TEC switched on from mode “Control N” into “Control R”.

At the 73th s of the transient, by $N_{ifco} = 67.2\% N_{nom}$ (recorded by ICMS), LRPC stopped the reactor load-off process. After completing of LRPC procedure, the automatic power control (APC) switched on to CPS in mode “N” and then maintained the “neutron” power of the reactor in the range from 66.2 % to 67.0 % N_{nom} (Fig. 5, 6).

During the reactor load-off the CR group #10 was inserted from 82.95 % to 43.18 %, whereas the group #9^l up to 92.61 % (from the BES). The reactor power recorded by NFC was reduced from 98.83 to 67.2 % N_{nom} , with the average reduction gradient of $dN_{nfc}/d\tau = -0.452\% N_{nom}/s = -27.1\% N_{nom}/min$. The lower gradient of load reduction in the time interval from the 42nd s to the 73^d s is apparently due to termination of the temperature increase at core inlet (see Fig. 18

– 23), and so terminating the impact of the negative feedback of the coolant temperature, that increased (up to the 42nd s of the transient) the gradient of power reduction due to the increase of T_{inlet} . The decrease of T_{inlet} after 42 s of the process caused an insertion of additional positive reactivity into the core $\Delta\rho = (\partial\rho/\partial T)\cdot\Delta T_{inlet}$, which interfered reactor power reduction from LRPC.

According Fig. 4, the reactor power recorded by the measurement channel #2 of OR-2 of NFC in the time period from 14th to 35th s of the process exceeded the power identified by other measurements channels. It is due to the fact, that the channel #2 (see Annex C) is situated at the side of core sector #2 where streams mainly cooled-down coolant from the cold leg of loop #2 (see Fig. 45, 16, 17), which causes higher power generation in this sector due to negative temperature feedbacks.

During the TG load-off the HP control valves changed their position as shown in Fig. 50 (recorded by the UBLS, with aperture of recording) and in Fig. 95 (data of SEC, without aperture of recording). El-power of TG reduced from the initial value of 983 MW in the time from the 10th to the 18th s of the transient to 967 MW. The control valves (Fig. 95) partly closed from the initial positions 47.6, 29.4, 36.5 and 34.3 % to respectively 47.6, 28.6, 35.5 and 33.6 % at the 15th s. By the 30th s of the process, N_{el} reduced rapidly to 828 MW due to the partly closure of the control valves till the 29th s respectively to 33.7, 21.6, 27.3 and 27.3 %. As a result of pressure decrease in the main steam collector (Fig. 85) the control valves opened at the 39th s respectively to 36.4, 23.2, 29.0 and 29.0 %, which caused the increase of N_{el} by the 40th s up to 845 MW. Then the control valves have been closing partly till approximately the 222th s of the transient, and their positions reached respectively 26.6, 16.6, 21.2 and 22.6 %. For that time N_{el} decreased till the 222th s to 622 MW. Then, approximately by the 235th s, control valves partly re-opened up to 26.7, 16.7, 21.5 and 22.8 %, which caused an increase of the electrical power up to 627 MW and stabilized at this level.

Fig. 3 denotes electrical power consumption history of MCP 1-4. It can be see that the reduction of N_{MCP1} to 0 took place within 1 s. After switching off of MCP-1 a slight drop of N_{MCP2} , N_{MCP3} and N_{MCP4} is observed due to the reduction of the hydraulic resistance of the PC as a result of the coolant flow reduction.

The time-dependent changes of pressure differences of MCP1-4 and in the reactor are presented in Fig. 7, 83. Figure 83 shows that particularly at the 70th s the values ΔP_{MCPi} ($i = 1, 2, 3, 4$) and ΔP_p have reached their minimal (for this mode) values and after that have stabilized. The pressure differences of MCP1-4 and of the reactor before and after switching off of MCP-1 are listed in Table 1.

The change of the flow direction in the loop 1 began approximately at the 25th s after the switching off of MCP-1 at ΔP_{MCP-1} approximately equal to 0.29 MPa (see e. g., Fig. 16, 17, 45).

Time histories of the coolant flow rate in the 4 PC loops and in the reactor are shown in Fig. 9 (ICMS data). It should be mentioned that the values G_{PC} and G_R are not very reliable till the 70th s of the transient and especially for time moment of the run out mode of the MCP after its switching off because the ICMS has not a calculation model for this conditions. An increase in the flow rate of loops #2, 3, 4 with running MCP is caused by the reduction of the hydraulic resistance in PC (most of all in the core) due to the reduction of the flow rate.

Fig. 8 shows the time histories of loops' thermal power and reactor power, calculated on the bases of PC coolant measured data. It should be mentioned, that in the interval approximately up to the 150th s the values $N_{PC-loop-i}$ ($i = 1, 2, 3, 4$) and N_{IK} are not reliable.

Time histories of the reactor power calculated in various ways (N_{PC} , N_{SC} , N_{DCS} , N_{core}), also the reactor power recorded by NFC (N_{NFC}) and the TG electrical power ($N_{el.}$) are shown in Fig. 4. The exact definition of N_{PC} , N_{SC} and indirect also N_{core} under the conditions of fast changing parameters (for all, that of flow rates and temperatures) without consideration of the coolant transportation time (delay time) like it is done in the ICMS, is generally impossible. In that sense, the values N_{PC} , N_{SC} and N_{core} in the interval approximately till the 150th s of the transient are not reliable. The strong lapse in the $N_{SC}(\tau)$ evolution at the time interval approximately from the 44th to the 49th s of the process is due to the disturbance in the recording of the SG-1 feedwater flow rate cause by its abrupt decrease (Fig. 61).

In that way, the reactor power can only be evaluated on the basis of the data recorded by NFC and DCS till the 150th s of the transient.

PC pressure histories are presented in Fig. 10, 11, 84 and $P_{PC}(\tau)$ history in Fig. 84 (data without recording aperture). Analysing the results in Fig. 84, it can be seen that the initial PC pressure of 15.52 MPa, grew insignificantly by the 10th s (up to 15.55 MPa) due the coolant heat-up in the core caused by the reduced flow rate. From the time period after the 30th to the 90th s it dropped from 15.54 to 15.12 MPa due to the PC coolant temperature decrease caused by reactor power load reduction controlled through LRPC. For this period the coolant flow rates in all loops and through the core are practically stabilized, and the steam pressure reduction in SGs with operating MCP remained also practically constant up to the 137th s (with minor reduction of T_{PC} and with all heaters of the pressurizer in operation). Later on the pressure in the PC began to increase and reached 15.47 MPa by the 300th s. with practically constant temperature of the coolant (due to the operation of the electroheaters in the pressurizer).

The coolant level in PRZ recorded by the UBLS (Fig. 10) increased from the initial value 841.6 cm approximately by the 10th s up to 844.7 cm, and then from the 30th s to the 136th s of the transient it has decreased to 751.5 cm.; later on, starting from the 215th s of the process it began to

grow smoothly reaching 763 cm by the 288th s. L_{PRZ} (recorded by MMS) insignificantly increased (Fig. 84) from the initial value of 859 cm to 866 cm till the 22th s, and then, by the 136th s it reduced to 790 cm, later on increased smoothly and stabilized at the 260th s at a level of 800 cm. The difference in the values of L_{PRZ} (recorded by the upper level control measurements and the MMS) are due to the fact, that the UBLS data considers the corrections for the coolant temperature in the pressurizer whereas the MMS data do not take that into account.

According to the UBLS records (Fig. 12) after the load-off of process was completed and reactor parameters stabilized, the make-up flow rate insignificantly increased whereas the blow-down flow rate insignificantly decreased. On the other hand, it can be seen in Fig. 13 that the position of valve TK32S02 changed from appr. 34 % in the initial state to appr. 40 % in the final state, whereas the changes occurred mostly in the interval from the 86th to the 150th s.

Figure 51 (UBLS records), Fig. 85 and Fig. 86 (MMS records) show the time history of SG vapour pressure. It should be mentioned that P_{SGi} ($i = 1, 2, 3, 4$) recorded by UBLS (Fig. 51) are by (0.02 – 0.04) MPa higher than the analogous records of MMS (Fig. 85). It is due to the fact that the pressure measuring sensors are located not in the SG but in the fresh steam pipes. MMS records the values of just these sensors whereas UBLS records considered (though, hard to say how precisely) the corrections for pressure losses in the region length from SGs to the places of the sensors' locations. Further are analysed the SC pressure histories recorded by MMS (Fig. 85 and 86), and then are added some corrections on the basis of data recorded by UBLS.

According to Fig. 85 the steam pressure in SG-1 decreased sharply from initially 6.21 MPa to 5.8 MPa by the 25th s (due to the loop-1 power reduction), and then, from the 29th s to the 31th s it dropped to 5.77 MPa. After the coolant flow reverse in the loop-1 took place, the pressure increased to 5.92 MPa in the interval from the 36th to 47th s and later on it was changing like $P_{MSH}(\tau)$. It should be mentioned that in the time interval from the 20th to the 129th s the SG-1 pressure was lower than the steam pressure in MSH. The SG2-4 pressure, which initially were 6.22, 6.24 and 6.26 MPa, unevenly and insignificantly decreased in relation to the initial values in the intervals (17 – 24 s), (16 – 27 s) and (19 – 26 s) due to the reduction of P_{MSH} caused by the reactor power reduction parallel to a minor reduction of N_{ei} . Then it increased respectively to 6.37, 6.32 and 6.30 MPa by the 39th, 37th and the 40th s (due to the power increase in loops #2-4 caused by the increase of the coolant flow rate and temperature and to the increase of P_{MSH} as a result of the decrease of N_{ei}). Later on the pressure decreased respectively up to the 129th, 135th and 131th s (whereas mostly intensively by the 89th – 90th s due to the reactor power reduction by LRPC, thus reaching the minimum values of 6.13, 6.09 and 6.02 MPa, whereupon practically stable reactor power was reached and $P_{MSH}(\tau)$ could be determined. The fact that the pressure in SG-4 reduced most sharply

from the 38th s, becoming at the end lower than P_{SG2} and P_{SG3} , is due to the power reduction in loop #4 as a result of flow mixing of the already cooled down coolant from the “hot” leg of loop #1 into loop #4.

Steam pressure in MSH (Fig. 85) reduced from the initial value 6.01 MPa to 5.87 MPa by the 21th s (due to the reactor power reduction, and, but by a minor load -off of TG), and then increased up to 6.014 MPa by the 37th s (due to the sharp reduction of N_{el} by the 30th s as it is can be seen in Fig. 50 and 51), and then reduced to 5.89 MPa by the 65th s (due to the reactor power reduction and slow load-off of TG). After completion of reactor load-off, due to insufficient load-off of TG, the pressure P_{MSH} reached 5.86 MPa by the 130th s, after that it started to increase smoothly (due to the smooth closure of control valves) becoming practically stable by 300th s at a value of 6.0 MPa.

According to ICMS records (Fig. 51) steam pressure in SG-2, 3 and 4 with initial values 6.29, 6.24 and 6.24 MPa, reached maximal values 6.41, 6.35 and 6.35 MPa, by the 35th – 37th s and dropped to minimal values 6.15, 6.12 and 6.04 MPa by the 131th s.

Figure 56 (UBLS records) shows the time history of steam pressure in the house loads collector and the valve position of FASB-HL. Figure 100 denotes the time history of P_{ISC} recorded by MMS. According to Fig. 100 the steam pressure in ISC decreased from the initial value 1.186 MPa to 0.737 MPa by the 120th s and then (due to the opening of valves in the 1st and 2nd device of FASB-HL – Fig. 56) it increased and reached 1.072 MPa by the 248th s. In the initial phase the valves of the 1st and 2nd device of FASB-HL were closed (Fig. 56). Starting from the 36th s, the valve of the 1st device of FASB-HL began to open and reached 57 % by the 133th s. At the 65th s the valve of the 2nd device of FASB-HL began to open and reached the position of 44 % by the 132th s. Afterwards the position of FASB-HL’s valves did not change.

The water level evolutions in SGs are shown in:

– Figures 57, 89, 90 – recorded on the basis of the measurements of the 2-chamber level measurement devices;

– Figures 58, 91, 92 – recorded on the basis of the measurements of the 1-chamber level measurement devices.

According to Fig. 89, 90 (data without recording aperture) L_{SG1} from the initial value of 165 mm, changed by +14 mm by the 13th s and then decreased by the 30th s with -73 mm (apparently due to the steam increase in SG-1 after the sharp reduction of P_{SG1}), and later it increased to +191 mm by the 76th s (due to the sharp power reduction of loop #1 after the flow reverse), and after that began to decrease (most fast till the 180th s) becoming practically stable at the 390th s thus a different of +10mm resulted compared with the initial value. There, the main feed water control valve of SG-1 began to close from the 35th s and closed practically completely at the 52th s (Fig.

62). The starter valve of the feed water controller partly closed to 49 % in the interval from the 44th to 51th s, then opened up to 55 % by the 55th s, and later on partly dropped to 24 % by the 72th s changing after that its position (mostly to open) maintaining the water level in SG-1.

Water levels in SG2-4 (Fig. 89 and 90) related to the initial values respectively 185, 165 and 161 mm increased by +7, +25 and +36 mm at the 22th, 25th and 23th s respectively (possibly due to reduction of heat transfer in SG-2-4 at the beginning of the flow rate reduction and the coolant speed in loops #2-4), then they began relatively sharply to increase (due to power increase in loops #2, 3 and 4 and thus leading to increase of flow rates and coolant heat-up in the loops). Maximum deviations from the initial values of minus 174, minus 126 and minus 134 mm were reached at 63, 67 and 60 s and then, due to additional opening of the main and the starting feed water valve of SG-2-4 as well as due to the power reduction of loops #2, #3 and #4 and also the integral reactor power, they increased to values different from the initial ones by minus 44, minus 1 and minus 3 mm at 132, 171 and 132 s respectively. Then, due to the closure of the starting control valves to the initial positions as well as due to the closure and the following smoothly partial opening of the main feedwater valves of SG-2 -3 -4, (Fig. 62) they began to stabilize. Relatively quickly has stabilized the level L_{SG4} (Fig. 90), beginning approximately from the 340th s it returned to initial value very fast. The water level in SG-2 at 270 s reached a level change of -85 mm, and after that it began to increase and at 420 s it stabilized at a slightly different value from the initial one. The water level in SG-3 decreased during the stabilisation to -65 mm (at the 364th s) and then it began to grow, reaching practically the initial value at 465s. After the SG water levels drop by more than 100 mm at the 48th s, the both AFWP were actuated (Fig. 94).

The main feed control valves of SG-2-4 with initial positions of 59, 71 and 58 %, opened during the transient respectively to 84 % (at the 64th s), to 100 % (at the 79th s) and to 66 % (at the 49th s), and closed to respectively 50 % (at the 138th s), to 68 % (at 168th s) and to 30 % (at the 130th s).

The records of one-chamber level measurement devices denoted the following (Fig. 91 and 92):

– L_{SG1} with initial value of 2218 mm reduced by the 21th s to minus 142 mm, and increased by +205 mm by the 53th s, then it smoothly reduced and stabilized practically by the 450th s with a difference of +25 mm in comparison with the initial state;

– L_{SG2} , L_{SG3} and L_{SG4} with initial values of 2203, 2196 and 2214 mm increased by the 13th, 18th and 15th s respectively by +13, +23 and +22 mm, and then the water levels reduced respectively by the 69th, 72th and 48th s to minus 114, minus 90 and minus 126 mm. After that they increased by the 122th, 170th and 129th s respectively to minus 44, +4 and +3 mm and finally their

stabilisation began and completed respectively by the 480th, 465th and 360th s at values different from the initial ones by respectively minus 39, minus 12 and +2 mm.

SGs feedwater flow rates evolutions are shown in Fig. 61 (records of the ICMS) and in Fig. 87 (records of MMS). According to the MMS records, the SG-1 feed water flow rate volume increased from the initial value of 1463 m³/h by the 29th s to 1577 m³/h (apparently due to the reduction of P_{SG1}), and then, by the 50th s it reduced to 152 m³/h (closure of the feed water main control valve of SG-1), and approximately by the 75th s it reduced practically to zero (partial closure of the feedwater starting control valve of SG-1 – Fig. 62). Later, G_{SG1} began to increase approximately from the 175th s (reduction of L_{SG1} and step-by-step partial opening of the feed water starting valve of SG-1). Concerning the data from ICMS (Fig. 61), during the measurement time interval of about (33 – 38) s there has been a device malfunction of recording $G_{fw1}(\tau)$. The minimal value of G_{fw1} , recorded approximately at the 120th s denotes 109 t/h. After the 145th s G_{SG1} has began slowly to increase and at the 300th s reached the value of 154 t/h. At first the SG-2, 3, 4 feedwater flow rates reduced slightly (at the (30 – 37)th s) and then increased by the (52 – 54)th s; later decreased according to the heat sinking through SG-2-4.

SG feed water pressure histories are shown in Fig. 63, 88. The changes of P_{fw_i} ($i = 1, 2, 3, 4$) during the transient have been determined by feed water flow rates (Fig. 61, 87) and pressure in SG (Fig. 51, 85).

The TFWP #1, #2 rotational speed histories and the feed water flow rates at the pressure side as recorded by UBLS are shown in Fig. 59. Apart from the feed water flow rates at the pressure side of TFWP #1, #2, Fig.60 denotes also the FW-pressure at the pressure sides (recorded by UBLS). Figure 93 shows the rotational speed change during the transient of TFWP #1, #2 recorded by MMS. According to Fig. 93, n_{TFWP1} and n_{TFWP2} with initial values of respectively 3068 and 3053 r/min decreased from the 20th s till the 37th and 34th s respectively to 3041 and 3027 r/min (insignificant partial closure of the feed water main control valves of SG and a pressure reduction in SG), and then increased respectively by the 52th and 53th s up to 3097 and 3083 r/min (partial opening of the feed water main control valves to SG-2-4 and an increase of P_{SG2} , P_{SG3} and P_{SG4}). Then they began to decrease according to the thermal power of the reactor relieved mostly into SG-2, 3, 4 (partial closure of the feed water control valves of SG and a pressure reduction in SG). During the time interval from the 112th to 153th s there was an increase of the rotational speed of TFWP-2 (maximum of 2990 r/min during $\tau = 142$ s), whereas the rotation speed of TFWP-1 reduced. The flow rates at the pressure site of TFWP-1, 2 in principle were following their rotational speed (Fig. 59).

Figure 67 shows the time-dependences of the feed water flow rates in the lines of HP-PH as recorded by the in-core monitoring system and Fig. 68 shows the analogous dependences of flow rates, as well as the pressure values in the lines of HP-PH recorded by UBLS. The form of the curves of $G_{\text{HP-PH } 1}(\tau)$ and $G_{\text{HP-PH } 2}(\tau)$ are close to the average flow rates dependences at the pressure sides of TFWP (Fig. 59). A minor increase of pressure in the lines of HP-PH in the time interval from the 40th to approximately the 58th s (Fig. 67) is apparently a result of the cut-off of the steam line connection of HP-PH (s., e. g. Fig. 69 and 65).

According to Fig. 69 (recorded by UBLS) it follows:

- the levels in HP-PH #6- 1, 2 increased from the 55th to the 50th s respectively to 3156 and 2954 mm; as a result of the water level growth, the HP-PH were approximately at the 45th and 60th s switched off at first group “B” and after that - the group “A”;
- the level control valves of HP-PH #6-1, 2 with a water discharge line into THC opened from appr. 47 % in the intervals (125 – 145) and (145 – 157) s to appr. 99 %;
- the level control valves in HP-PH #6-1, 2 with water discharge line into D7 in the intervals (133 – 145) and (146 – 157) s from the position 45 % closed respectively to zero and to 10 %;
- the level control valves in HP-PH #7-1 in the interval (133 – 156) s partially opened from 21 to 29 %, and the respective the valve HP-PH #7-2 in the interval (146 – 158) s partially opened from the position 41 % to the position 30 %.

The feed water temperature evolution at HP-PH inlets and outlets is shown in Fig.65. It should be mentioned that the water temperature sensors downstream HP-PH are installed upstream the water inlets of CHTP.

The inlet SG feed water histories are shown in Fig.64. It can be seen that the main decrease of $T_{\text{fw}2}$ and $T_{\text{fw}4}$ occurred by the 380th s, whereas that of $T_{\text{fw}3}$ took place by the 407th s.

Figure 66 denotes the water temperature evolution at the pressure side of CHTP. According to the figure this temperature increased starting from the initial value 262.9 °C at the 123th s to the 133th to 264.8 °C, and then, from the 292th to the 300th s it decreased reaching practically the initial value (to 263 °C).

Figure 52 shows the time history of the heating steam flow rate to SSSH and the position of the control valve in the line of steam flow to the SSSH. According to this figure Scv did not changed. The flow rate of the heating steam to the SSSH reduced from the initial value 496 t/h to 459 t/h by the 21th s (steam generation reduction in SG), and then, by the 33th s, it increased up to 505 t/h (due to the partial closure of the control valves $T\Gamma$ – Fig. 95), after that, by the 57th s it increased relatively soon to 447 t/h (steam reduction in SG), and later the flow rate has followed the change of the thermal power transferred to the secondary circuit and it was changing in counter-phase to the sequential change of TG control valves positions.

Figure 53 shows the temperature and the pressure time-dependences of the heating steam upstream SSSH and in the condensate collector. According to the figure, the heating steam temperature upstream SSSH and in the condensate collector did not change (within the recording aperture) and had respectively 274.2 and 272.3 °C. The heating steam pressure upstream SSSH and in the condensate collector dropped (within the recording aperture) from the initial values of respectively 5.727 and 5.652 MPa in the time intervals from the 6th to the 17th s of the process and from the 9th to the 20th s of the process respectively to 5.689 and 5.570 MPa, then it increased in the intervals from respectively the 43th to the 55th s and from the 32th to the 42th s to respectively 5.730 and 5.628 MPa; later it began to increase again from the 162th and 150th s respectively and reached 5.872 and 5.800 MPa at the 295th and 278th s.

Figure 54 shows the time histories of the steam temperature downstream SSSH #1-4 (low pressure) and at the outlet of the high pressure part. According to the figure, the steam temperature at the outlet of the high pressure part began to decrease from the initial value of 153.5 °C at 47th s and reached 144.2 °C at the 277th s. The steam temperature at the downstream of SSSH #1-4 (low pressure part) increased, starting from the initial values 255.3, 255.3, 254.8 and 255.1 °C at the 103th, 123th, 127th and 109th s and reached at the 291th, 232th, 294th and 204th s respectively 261.0, 259.0, 259.8 and 258.5 °C, remaining afterwards practically the same.

Figure 55 depicts the time histories of the steam pressure at the in-takes #1-3 of the turbine and at the HPTP #1-4 (recorded by UBLS). The changes of the steam pressure at turbine in-takes #1-8 recorded by MMS are shown in Fig. 97 – 99. It should be mentioned that the pressure measurement channels in the 6th (Fig. 98) and the 7th (Fig. 99) intakes were out of order.

The D #7-1, 2 changes of the water flow rate and the changes in the positions of the main and starting water level control valves of the of D7-1, 2 are shown in Fig.70. The figure proves that for the time period of the transient the flow rates in D7 recorded by UBLS in the interval from the 13th to the 214th s reduced from the initial values of 3000 m³/h (D7-1) and respectively 3052 m³/h (D7-2) to 1788 and 1765 m³/h, and then, by the 300th s they slightly increased to 1956 and 1986 m³/h. In the interval from the 161th to the 174th s an increase of the condenser flow rates in D7-1, 2 took place (approximately by 300 m³/h in each one). The position of the starting control valve in D7-1, 2 practically did not change and stayed opened at about 49 %. The position of the main control valve of the water level in D7-1,2 sharply changed to 63 % from an initial position of 45 % in the time interval 15 – 40 s, and then, in the interval from the 53th to the 57th s it changed sharply from 62 to 49 %; later, in the interval (171 – 181) s it changed from 17 % to zero. Beginning from the 203th s the main control valve of the water level began to open and reached the position of 24 % at the 300th s.

During the transient the water level in the deaerators (Fig. 71) changed from the initial value of 2509 mm within the limits of 2488 to 2598 mm.

Figure 72 shows D7-1, 2 pressure histories and the change of the control valves' positions of in heating steam supply into the deaerator columns. According to the figure, the pressure in the deaerator D7-1 и D7-2 reduced to 0.582 and 0.581 MPa from the initial values of 0.596 and 0.598 MPa respectively starting from the 23th to the (128 – 131)th s, and then, from the 178th to respectively the 224th and the 234th s it increased to 0.611 and 0.615 MPa, later, from the 256th to the 295th s it reduced to 0.594 and 0.593 MPa. The positions of control valves at heating steam supply into the deaerator columns practically did not change till the 30th s and has the values respectively 21.6 and 22.6 %, and then, by the 178th s they increased to 37.4 and 39.4 % (due to the steam pressure reduction in the secondary circuit and the water level increase in D7-1, 2), after that, by the 242th s they dropped to respectively 31.1 and 32.4 % (the increase of the water level in D7-1,2 was stopped).

Figure 73 shows graphs of time histories of the condensate water levels in LP-PH #3-5 and the positions of the level control valves in the same LP-PH. The figure denotes that $L_{LP-PH-3}$ increased to 550 mm from the initial value of 330 mm starting at approximately the 21th s and continuing to the 99th s and then it dropped to 25 mm approximately by the 200th s, changing then insignificantly till the 289th s and it increased again to 100 mm by the 293th s. The condensate level in LP-PH-4 changed insignificantly: in the initial state it denoted 327 mm, and by the 39th s it raised to 334 mm, and then it dropped to 276 mm by the 165th s, and till the 300th s it raised again till 345 mm. The water level of $L_{LP-PH-5}$ practically did not change till the 30th s staying at 34 mm, and then it sharply increased to 575 mm by the 65th s changing till the 100th s within the range of (575 – 592) mm, then, sharply dropped to 25 mm by the 119th s, and later it raised again from 32 to 421 mm in the interval from the 131th to 285th s. The position of the level control valve of LP-PH #3 did not change till the 149th s and was open to 75 %, then, by the 169th s it changed to 40 %. The position of the level control valve of LP-PH #4 was 68 % till the 140th s and then it reduced to 60 % by the 154th s.

Figure 75 denotes the condensate level history of LP-PH #2 recorded by level measurement devices based on 1000 и 1600 mm, and also the time history of the positions of the main and starting water level control valves of LP-PH #2. It can be seen that L_{LPH-2} measured by the level measurement device with a basis of 1000 mm increased from the initial value of 742 mm to 889 mm starting at the 180th to 235th s, and then by the 300th s it dropped to 647 mm. The condensate level recorded by the measurement device with a basis of 1600 mm, which has initially a value of 221 mm, was changing approximately till the 258th s in the range of (200 – 313) mm, and then it dropped to 140 mm by the 292th s. The position of the water level main control valve of LP-PH #2

did not change till the 211th s staying at 63 %, then it reduced to appr. 20 % by the 224th s, and then it increased to 36 % in the time period from the 287th to 300th s. The position of the starting control valve for the level control of LP-PH #2 practically did not change.

Figure 76 shows the condensate levels history of LP-PH #1 (shown by two separate level measurement devices), and the average water level history of LP-PH #1. According to this figure the condensate level $L_{LP-PH1-1}$ increased from the initial value 62 mm in the time interval from the 63th to the 198th s from 74 to 288 mm and changed later insignificantly. The condensate level in $L_{LP-PH1-2}$, which was 31 mm in the initial state practically did not change till the 126th s and then raised to 127 mm by the 228th s and began to decrease smoothly starting from the 285th s thus becoming 108 mm by the 300th s.

Figure 74 denotes the coolant temperature histories in various measurement points from the suction area of CP #1 to the outlet of LP-PH #5. According to this figure the LP-PH#5 temperature at the outlet began to decrease approximately from the 46th s. As a result of this, the coolant temperature decreased by the 273th s from 150 to 141 °C, which is due to the steam pressure decrease in the turbine in-takes of LP-PH (see Fig. 98, 99).

Figure 78 shows the pressure histories at the pressure side of CP-1 #1 and #3 (CP-1 #2 is in hot stand-by mode). Figure 77 shows the pressure histories at the pressure side of CP-2(#1 - #5). The pressure drop at the pressure sides of CP-2 in the interval from the 15th to 44th s is due to the additional partial opening of the main level control valve of D7 (Fig. 70). In principle, the pressure change at the pressure sides of CP-2 was in counter-phase to the change of the position of the level control valve of D7.

Condensate level histories of the first (SD11,12) and the second (SD13,14) groups of the turbine condensers are given in Fig. 79. The figure shows that in the interval from the 46th to the (276 – 278)th s the condensate level raised from 1017 mm to 1210 mm. The local minimum of $L_{sd11,12}(\tau)$ at $\tau = 57$ s and the maximum value of $L_{sd13,14}(\tau)$ with $\tau = 59$ s (pitches) are, in our opinion, due to the disturbances in the recording.

The pressure time history of the first (SD11,12) and the second (SD13,14) groups of the turbine condensers are depicted in Fig. 80 (recorded by UBLS) and in Fig. 96 (recorded by MMS). As MMS records show, the pressure in the turbine condenser at the 240th s (after the completion of the dynamic mode connected with the reduction of the reactor power from appr. 98.8 to 64.7 % N_{nom} (recorded by NFC)) reduced in relation to the initial values by appr. 0.7 kPa.

Figure 81 shows the circuit water temperature history at the inlet and outlet of the first and the second group of the turbine condensers. The figure denotes that the circuit water temperature at the outlet of the first group of condensers related to the interval from the 84th to the 271th s de-

creased by 1.6 °C, and at the outlet of the second group in the interval from the 80th to the 297th s it decreased by 2.1 °C.

The transient results of the loop temperature control by ICMS are shown in Fig. 14-43. These figures use the following notations:

– T_{ictc} , T_{icth} , T_{ict} – cold and hot leg coolant temperatures and the coolant temperature difference between the hot and the cold legs of the loop_{*i*} (*i* = 1, 2, 3, 4) of the primary circuit recorded by the resistance thermometers (RT);

– $T_{itcc1-j}$, $T_{itcc2-j}$ and ΔT_{itc1-j} – cold and hot leg coolant temperatures and the coolant temperature difference between the hot and the cold legs of the loop_{*i*} (*i* = 1, 2, 3, 4) of the primary circuit recorded by the *j*-th thermocouples (*j* = A,B,C) of the first set (TC-1);

– $T_{itcc2-j}$, $T_{itcc2-j}$ и ΔT_{itc2-j} – cold and hot leg coolant temperatures and the coolant temperature difference between the hot and the cold legs of the loop_{*i*} (*i* = 1, 2, 3, 4) of the primary circuit recorded by the *j*-th thermocouples (*j* = A, B, C) of the second set (TC-2);

– ΔT_{itcc1} and ΔT_{itc2} – coolant temperature difference between the cold and hot legs of the coolant temperature in the loop_{*i*} (*i* = 1, 2, 3, 4) of the primary circuit, averaged on all thermocouple measurements of the first (TC-1) and the second (TC-2) sets;

– T_{ci} , T_{hi} and ΔT_{ilt} – the average value of coolant temperature of all thermocouples (TC-1 and TC-2) and resistance thermometers (RT) for the cold and hot legs; the difference of the coolant temperature between the cold and hot legs of the loop_{*i*} (*i* = 1, 2, 3, 4) in the primary circuit.

The locations of the temperature monitoring casings in the primary loops (for all cold and hot legs) at Unit 3, NPP Kalinin are given in Annex D.

The measured data of some of the cold leg thermocouples in the PC-loops as: $T_{1tcc1-1}$ (Fig. 16), $T_{1tcc2-1}$ (Fig. 17), $T_{2tcc2-1}$ (Fig. 19), $T_{3tcc1-2}$ (Fig. 20), T_{3tcc} and T_{3tcc} (Fig. 21), T_{4tcc} and $T_{4tcc1-3}$ (Fig. 22) and $T_{4tcc2-3}$ (Fig. 23), are not taken into account by the analysis because these thermocouples did not have the required direct contact area with the coolant. Due to the same reasons the hot leg temperature measurement of $T_{2tSG1-3}$ (Fig. 28) was also not considered by the analysis.

It should be mentioned that by determining the average (measured by TC-1, TC-2 and RT) coolant temperature of the cold legs (Fig. 14), the average coolant temperature of the hot legs (Fig. 24) and the coolant average temperature differences between the hot and cold legs (Fig. 43) of PC-loops, the above listed thermocouple measurements are excluded for the calculations.

According to Fig. 16 the hot leg #1 coolant temperature recorded by TC-1, $T_{1tcc1-2}$ and $T_{1tcc1-3}$ began sharply to decrease from the initial values respectively 288.2 and 288.0 °C starting from the 7th s (due to increased cooling of SG-1 because of the flow rate and coolant flow speed reduction in loop #1) thus reaching at the 27th and 30th s the minimum values respectively 282.1 and 282.0 °C, and then sharply increasing (caused by the flow reverse in loop #1, which consists of

flow parts from cold legs #4 and #2, but mostly that of cold leg #4) and after that reaching at the 45th s maximum values 289.8 and 289.6 °C. Later it began to decrease practically parallel to the coolant changes in the cold leg #4 and completed the decrease by the 150th s at values 284.1 and 283.9 °C, afterwards (due to the increase in T_{c4}) raised and stabilized practically at appr. by the 276th s at values 285.0 and 284.9 °C.

As recorded by TC-2 (Fig. 17), the coolant temperature T_{1tc2-2} and T_{1tc2-3} decreased to 282.0 and 282.1 °C (initial value 288.2 °C) in the time period from 7 s to 28 s and to 30 s respectively, and then increased to 289.9 and 289.7 °C by the 46th s, later dropped to (284.0 – 284.1) °C by the 150th s, and after that increased to 285.1 °C by the 276th s becoming then practically stable.

The coolant temperature of cold leg 2 recorded by TC-1 (Fig. 18) increased from the initial value (287.8 – 287.9) °C in the interval from the 8th to the 44th s up to (290.3 – 290.4) °C (caused by the loop power increase due to: the increase coolant heat-up in the reactor, the decrease of flow rate in the reactor and the increase of the coolant flow rate in the loop as well as due to the steam pressure rise in SG-2 as a results of the partial closure of the control valves). Then, by the 139th s it decreased to 284.4 °C (most intensive decrease occurring till the 94th s) due to the decrease of the loop power caused by the reactor load-off mode of LRPC (also due to a partial mixing of a cooled-up coolant into the hot leg of this loop coming from the hot leg of loop #1) and due to the pressure decrease in SG2, later it slowly raised following the changes of $P_{SG2}(\tau)$ and getting practically stable by the 276th s at a value of 287.4 °C.

Recorded by TC2 (Fig. 19) the coolant temperature T_{2tc2-2} and T_{2tc2-3} from the initial value 287.9 °C grew from the 9th to 44th s up to 290.4 °C, and then, by the 145th s it decreased to 286.4 °C (having most significant decrease till the 94th s), and began to grow slowly thus getting stable by the 276th s at value 287.4 °C.

The cold leg #3 coolant temperature recorded by TC-1 T_{3tc1-1} and T_{3tc1-3} (Fig. 20) increased from the initial values 287.9 and 287.6 °C in the time interval from the 10th to (42 – 44)th s up to 290.3 and 289.9 °C (caused by the loop power increase due to the coolant heat-up in the reactor and the decreased flow rate through the reactor and the increased flow rate of the coolant in the loop as well as the steam pressure increase in SG-3 as a result of a relatively sharp partial closure of TG control valves by the 29th s). Later on, the coolant temperature decreased to 286.7 °C approximately by the 141th s (with most sharp decrease till the 94th s) due to the reactor power decrease, which continued till the 73th s with still LRPC being in operation and due to the steam pressure decrease in SG-3 caused by some delay of TG load-off, after which it increased according to the change in $P_{SG3}(\tau)$ and stabilizing at the 276th s at a level (287.7 – 287.8) °C.

According to Fig. 21 recorded by TC-2 the coolant temperature $T_{3tcc2-3}$ raised from the initial value $287.8\text{ }^{\circ}\text{C}$ at the 10^{th} to the 43^{th} s to $290.1\text{ }^{\circ}\text{C}$, and then, by the 148^{th} s it dropped to $286.9\text{ }^{\circ}\text{C}$ (reducing mostly fast till the 94^{th} s of the process), and then began to increase reaching stabilization at the 276^{th} s at a value of $287.9\text{ }^{\circ}\text{C}$.

The cold leg #4 coolant temperature $T_{4tcc1-1}$ recorded by TC-1 (Fig. 22) increased from the initial value $287.4\text{ }^{\circ}\text{C}$ in the interval from the 7^{th} to the 41^{th} s to $289.9\text{ }^{\circ}\text{C}$ (due to the loop power rise caused by the coolant flow rate and steam pressure increase in SG-4), and then, by the 142^{th} s it reduced to $283.7\text{ }^{\circ}\text{C}$ (the strong reduction was taking place till the 90^{th} s) due to the reactor power reduction by LRPC till the 74^{th} s and due to the mixing of a cooled-up coolant into the hot leg of this loop coming from the hot leg of loop #1, as well as due to the pressure reduction in SG-4. Then the temperature $T_{4tcc1-1}$ began to increase (following the rise of P_{SG4}) and it stabilized at the 276^{th} s at $284.8\text{ }^{\circ}\text{C}$.

The cold leg #4 coolant temperature recorded by TC-2 (see time-dependences $T_{4tcc2-1}$ and $T_{4tcc2-2}$ in Fig.23) with initial value $287.5\text{ }^{\circ}\text{C}$ began to increase and in the interval from the 9^{th} to the 41^{th} it became $(289.9 - 290.0)\text{ }^{\circ}\text{C}$, then by the 150^{th} s it reduced to $283.8\text{ }^{\circ}\text{C}$, and later on it started to increase and stabilized by the 276^{th} s at $(284.8 - 284.9)\text{ }^{\circ}\text{C}$.

The cold leg coolant temperature recorded by the resistance thermometers shows that (Fig. 15):

- The leg #1 temperature (initial value $288.0\text{ }^{\circ}\text{C}$) reduced to $283.0\text{ }^{\circ}\text{C}$ from the 10^{th} to the 33^{th} s, and then it increased to $288.5\text{ }^{\circ}\text{C}$ by the 50^{th} s, later on, it decreased by the 149^{th} s to $284.0\text{ }^{\circ}\text{C}$, followed by an increase to $284.9\text{ }^{\circ}\text{C}$ by the 294^{th} s after that reached practically a stable level;
- The leg #2, #3 and #4 temperatures (initial values 287.8 , 287.6 and $287.5\text{ }^{\circ}\text{C}$) increased from the 11^{th} to the 51^{th} , 54^{th} and the 46^{th} s up to 289.9 , 289.3 and $289.4\text{ }^{\circ}\text{C}$, then decreased by the 150^{th} s to 286.5 , 287.0 and $283.7\text{ }^{\circ}\text{C}$, and later on, by the 294^{th} s they increased to 287.3 , 287.7 and $284.8\text{ }^{\circ}\text{C}$ and practically reached a stable level.

The fact that the cold leg #4 coolant temperature at the end of the transient caused by the switching off of MCP-1, stabilized at a lower level than the analogue coolant temperature of loops #2 and #3, is due to the lower power of this loop caused by the mixing of coolant flow coming from the cooled-up hot leg of loop #1 into hot leg#4.

The hot leg #1 coolant temperature:

- according to Fig. 26 (as recorded by TC-1) the coolant temperature $T_{1TSG1-2}$ and $T_{1TSG1-3}$ had initial values of $317.3\text{ }^{\circ}\text{C}$ which have been changing insignificantly till the 32^{th} s (due to - till the moment of reverse flow in the loop took place which was caused by the cooled-up coolant entering into the core from this loop, and later on, right after the flow reverse disappeared due to the penetration of that coolant through the thermosensors which practically have not passed through

the SG until the moment of reverse flow have taken place). After that the coolant temperatures began sharply to decrease (due to coolant reverse flow development and its cooling down in the SG-1) and reached maximum values 269.7 and 271.6 °C at the 58th and 61th s, after which it increased relatively fast (by the 90th s) to 275.5 °C (practically, the coolant temperature began to reduce in the cold leg of this loop and formed a stable reverse flow in this loop), then it slightly changed (following the steam pressure change in SG-1) and became stable at the 270th s at values 276.9 and 276.6 °C;

– the coolant temperature $T_{1\tau SG2-1}$, $T_{1\tau SG2-2}$ and $T_{1\tau SG2-3}$ recorded by TC-2 (Fig. 27) (initial values 317.5, 317.0 and 317.1 °C) changed insignificantly by the first 32 s and denoted 317.1, 316.4 and 316.4 °C; by the 59th s they reduced to 271.3, 269.5 and 269.5 °C, and then, mostly by the 90th s, they increased and stabilized approximately at the 290th s at 276.7, 276.8 and 276.5 °C.

The hot leg #2 coolant temperature $T_{2\tau SG1-1}$ and $T_{2\tau SG1-2}$ (Fig. 28) recorded by TC-1 (initial values 316.4 and 317.1 °C) increased in the interval 5 -35 s to (319.7 – 319.8) °C (due to heat-up of the coolant in the reactor caused by the reduction of flow rate), and then, mostly by the 90th s, they decreased (due to the reactor power reduction by LRPC with stable coolant flow through the reactor, partially mixing of cooled-down flow from the hot leg #1, and also due to the reduction of P_{SG2} caused by the slow down TG load-off in this interval). Approximately at the 167th s, the temperatures reached the minimum value (310.8 – 310.9) °C, and then they began slowly to increase (due to the coolant temperature growth at the core inlet) and approximately at the 70th s they stabilized at values (311.5 – 311.6) °C.

The hot leg #2 coolant temperature $T_{2tch2-1}$, $T_{2tch2-2}$ and $T_{2tch2-3}$ (Fig. 29) recorded by TC-2 (initial 316.9, 317.3 and 317.3 °C) increased approximately from the 5th to the 33th, 37th and 36th s up to 319.9, 319.7 and 319.4 °C, and then, by the 150th s they decreased to 310.9, 310.7 and 310.5 °C (having the most significant coolant temperature reduction till the 90th s), after that they began to rise slowly and approximately by the 270th s stabilized at values 311.8, 311.6 and 311.4 °C.

It should be mentioned that bending points on the coolant temperature time-dependent curves (Fig. 28, 29) at $\tau = (15 - 16)$ s are caused by the specifics of the coolant temperature histories measured with the thermocouples at FA outlets in sector 2 (Fig. 45). These thermocouples were affected by the cooled-down flow of the cold leg #1 (till the change of the flow direction in this loop). It should be mentioned that the coolant flow swirling after FA outlet till the hot leg nozzles take place in counterclockwise.

The hot leg #3 coolant temperature:

– according to Fig. 30, the recorded by TC-1 coolant temperature $T_{3\tau SG1-1}$, $T_{3\tau SG1-2}$ and $T_{3\tau SG1-3}$ increased from the initial values 316.6, 316.6 and 316.3 °C up to 319.2, 319.6 and 319.4 °C in the interval from the 6th to the 42th s, and then they decreased to 312.3, 312.9 and 312.5 °C by the

150th s (with most significant reduction till the 90th s), later on they increase slowly stabilized at values 313.3, 313.7 and 313.4 °C by the 270th s;

– according to Fig. 31 recorded by TC-2 the coolant temperature $T_{3\text{rSG}2-1}$, $T_{3\text{rSG}2-2}$ and $T_{3\text{rSG}2-3}$ (initial values 316.5 °C, up to 319.2, 319.6 and 319.4 °C) increased in the interval from the 6th to 43th s, and then they decreased to 312.6, 312.9 и 312.6 °C by the 150th s (with most significant reduction till the 90th s), later on, they slightly increased and stabilized at values 313.3, 313.7 and 314.4 °C by the 270th s.

The reasons for the rise and the reduction of the hot leg #3 coolant temperature during the transient are the same as for the hot leg #2. The only one difference is that in this case there was no mixing of a cooled-down flow from the hot leg #1 into the hot leg #3.

The coolant temperature change of the hot leg #4 (Fig. 32 and 33) was less significant from the beginning of the process up to the 35th s than that in other hot legs where the MCP were in operation. That is due to the impact of the cooled-down coolant of the neighbouring hot leg #1 (s. Fig. 16 and 17) entering the core for the time period before the reverse flow appeared in this leg.

According to the records by TC-1 (Fig. 32), the coolant temperature $T_{4\text{tch}1-1}$, $T_{4\text{tch}1-2}$ and $T_{4\text{tch}1-3}$ (with initial values 317.3, 317.1 and 317.2 °C) reached at the 35th s values 318.1, 317.5 and 317.6 °C. The temperature $T_{4\text{rSG}1-1}$ increased by the 19th s up to 318.3 °C, and then, by the 27th s it decreased to 317.8 °C. By the 35th s it raised again to the abovementioned. During the transient $T_{4\text{rSG}1-2}$ and $T_{4\text{rSG}1-3}$ changed insignificantly until the 27th s but nevertheless they had the local minimum at the 27th s. The existence of the local minimum on the coolant temperature evolution in the hot leg #4 is due to the flow reverse in loop #1. Starting from the 35th to the 150th s the coolant temperature $T_{4\text{rSG}1-1}$, $T_{4\text{rSG}1-2}$ and $T_{4\text{rSG}1-3}$ decreased to 302.0, 302.8 and 304.0 °C (with most significant reduction till the 75th s), and then they slowly increased and approximately by the 270th s they stabilized at values 303.0, 304.1 and 305.1 °C. It should be mentioned that approximately from the 35th s the coolant temperature of the hot leg #4 was influenced by the flow mixing of the cooled-down coolant coming from the hot leg #1.

The coolant temperature change of hot leg #4 as recorded by TC-2 (Fig. 33) was analogous to the change as recorded by TC-1 (Fig. 32). According to Fig. 33, $T_{4\text{rSG}2-1}$, $T_{4\text{rSG}2-2}$ and $T_{4\text{rSG}2-3}$ changed starting from the initial values 317.1, 317.4 and 317.2 °C till the 35th s to values 317.5, 317.8 and 317.6 °C; and then, by the 150th s they reduced to 303.5, 302.7 and 303.7 °C, after which they insignificantly increased and became practically stable at the 270th s at values 304.9, 303.9 and 304.9 °C.

The coolant temperature in the hot legs as recorded by the resistance thermometers (Fig. 25), have the following evolutions:

– Loop #1: Starting from the initial value 317.4 °C the temperature increased up to 318.2 °C in the interval from the 9th to the 20th s, and by the 33th s it decreased to the initial value and dropped sharply to 278.4 °C by the 74th s after which it practically did not change and reduced to 277.4 °C by the 150th s. Later on it increased insignificantly and stabilized at 277.7 °C by the 270th s. The fact that T_{1TCr} at τ approximately equal to 60 s did not have the local minimum (see also Fig. 26, 27), is apparently due to the different azimuthal location of the resistance thermometers on the pipe with a diameter of 850 which is higher from the low pipe edge area where TC-1 and TC-2 are located (Annex D), and also due to a higher delay measuring time (measurement inertia) by the resistance thermometer;

– Loops #2 and #3: Starting from the initial values 314.5 and 316.1 °C the temperature increased respectively to 316.5 and 318.5 °C in the time interval from the 6th and 9th s to respectively the 41th and the 35th s, and then they reduced from 309.3 and 311.9 °C by the 150th s (with most fast reduction till the 104th s at temperatures respectively 310.1 and 312.5 °C). Later on they increased insignificantly and stabilized at values 309.9 and 312.5 °C at the 270th s. The $T_{2TCr}(\tau)$ evolution has at $\tau = 24$ s a bending point caused by the same reasons as the similar points on the time histories of the thermocouples (Fig. 28 and 29);

– Loop #4: Starting from the initial value 314.0 °C it increased from the 15th to the 37th s up to 317.0 °C, and then, by the 104th s it decreased to 299.0 °C and reached 298.8 °C by 150th s, after which it slightly increased and reached 299.1 °C at the 270th s.

Let's summarize shortly the analysis of the time histories of the coolant temperature differences between the hot and cold legs of the PC-loops during the transient, without taking into account the measured values (thermocouples records were not exact) for the following parameters: $\Delta T_{1TC1-1}(\tau)$ (Fig. 34), $\Delta T_{1TC2-1}(\tau)$ (Fig. 35), $\Delta T_{2TC1-3}(\tau)$ (Fig. 36), $\Delta T_{2TC2-1}(\tau)$ (Fig. 37), $\Delta T_{3TC1-2}(\tau)$ (Fig. 38), $\Delta T_{3TC2-1}(\tau)$ and $\Delta T_{3TC2-2}(\tau)$ (Fig. 39), $\Delta T_{4TC1-2}(\tau)$ and $\Delta T_{4TC1-3}(\tau)$ (Fig. 40) and $\Delta T_{4TC2-3}(\tau)$ (Fig. 41).

The below-considered coolant temperature differences between the hot and cold legs do not have much physical sense because by their calculation (carried out by the in-core monitoring system) the coolant temperature in the hot and cold legs are taken at the same time under the conditions of constantly changing parameters (flow rates and temperature in the PC). When performing the calculations of the studied differences it is necessary to take into account “transportation” characteristics (delay time) of the coolant in the PC-legs but there was not a consistent model applied for such consideration. However the analysis of the temperature changes between the hot and cold legs of PC-loops, without consideration the delay time during the transient is though approximate but still useful.

The coolant temperature differences between the hot and cold legs of loop #1 of the primary circuit as recorded by TC-1 - $\Delta T_{1TC1-2}(\tau)$ and $\Delta T_{1TC1-3}(\tau)$ (Fig. 34) (initial values 28.9 and 29.3 °C) increased in the interval from 7 to 29 s up to 34.5 and 34.7 °C (due to the heat-up of the coolant in the reactor caused by the decrease of the flow rate), and then, by the 58th s they dropped to minus 14.7 and minus 15.0 °C (caused by the cool-down of the coolant in SG-1 after the flow reversed in the loop). By the 90th s they increased to minus 9.1 °C (due to the completion of the reactor load-off by LRPC, thus slowing down the decreased of the coolant temperature in the cold leg of loop #4, mostly influencing T_{x1} , and leading to the stabilization of the flow rate in loop #1 and the heat exchange in SG-1). At the 180th s the temperature change stabilized at 8.3 °C.

As recorded by TC-2 (Fig. 35), the coolant temperature differences ΔT_{1TC2-2} and ΔT_{1TC2-3} (with initial value 29.0 °C) at first, beginning from the 7th to the 29th s, increased to 34.6 °C, and then, by the 58th s they decreased to minus 17.7 °C. By the 90th s they increased to minus 9.1 and minus 9.5 °C, and at the 180th s they stabilized at minus 8.5 °C.

The coolant temperature differences between the hot and cold legs of loop #2 in the primary circuit ΔT_{2TC1-1} and ΔT_{2TC1-2} , as recorded by TC-1 (Fig. 36), increased from the initial values 28.5 and 29.3 °C up to 30.0 and 30.2 °C in the interval from the 5th to the 14th s, and then, by the 19th s they slightly decreased to 29.8 and 30.1 °C. In the time interval 29 – 30 s they increased to 30.4 and 30.5 °C, after which they decreased to 24.7 °C by the 90th s, later on, followed a smooth decrease till the 210th s when and the temperature change reached 24.1 °C.

According to Fig. 37, the coolant temperature differences ΔT_{2TC2-2} and ΔT_{2TC2-3} as recorded by TC-2 increased from the initial value 29.4 °C in the time interval 5 - 13 s respectively up to 30.3 and 30.0 °C, and then, by the 19th s they decreased to 30.1 and 29.7 °C. By the 29th s a new rise took place, respectively to 30.5 and 30.3 °C, and then, by the 82th s they decreased sharply to 24.7 and 24.5 °C, followed by a smooth decrease and stabilization at 24.0 and 23.9 °C by the 210th s.

The specifics of the coolant temperature differences changes between the hot and the cold legs of loop #2 are related mostly to the specifics of the coolant temperature changes in the hot leg of this loop which were described before. The existence of local minimum points on the time histories of the above mentioned differences at $\tau = (12 - 15)$ s is caused by the cooled-down coolant flow coming from the neighbouring to the loop #1 cold leg, which has reached the core inlet before the flow has reversed and the cessation of these impacts when the flow stagnated and turned to the primary direction.

The coolant temperature differences between the hot and the cold legs of loop #3 ΔT_{3TC1-1} and ΔT_{3TC1-3} as recorded by TC-1 (Fig. 38), increased from the initial value 28.7 °C approximately from the 3th to the 29th s to approximately 30.0 and 30.4 °C (due to the increase of the coolant heat-

up in the reactor caused by the decrease of the flow rate), and then, by the 90th s they decreased to 26.2 and 26.4 °C (due to the continued reactor load-off mode of LRPC with small change of the coolant flow rate through the core), then they changed slightly and stabilized at the 240th s at values 25.3 and 25.7 °C.

As recorded by TC-2, the coolant temperature difference in loop #3 ΔT_{3TC2-3} (Fig. 39) (with from initial value 28.7 °C) increased to 30.3 °C in the time interval 5 - 29 s, then, by the 90th s it decreased to 26.1 °C, and stabilized at 25.5 °C approximately in the time period 220 – 240 s.

As recorded by TC-1, the coolant temperature difference between the hot and the cold legs of loop #4 ΔT_{4TC1-1} (Fig. 40) increased from the initial value 29.9 °C to 30.2 °C in the time interval 6 – 15 s, and then, by the 34th s it decreased to 29.0 °C, and approximately by 75th s it sharply reduced to 18.9 °C, after which it smoothly changed and reached at the 240th s 18.4 °C.

As recorded by TC-2, the coolant temperature differences between ΔT_{4TC2-1} and ΔT_{4TC2-2} (Fig. 41) increased from the initial values 29.6 and 29.9 °C to 29.8 and 30.3 °C in the time interval 4 - 8 s, and then, by the 34th s, they reduced to 28.3 and 28.7 °C. By the 75th s, differences sharply reduced to 20.3 and 19.8 °C, and later remained practically unchanged reaching 20.0 and 19.1 °C at the 240th s.

The specific behaviour of time histories of the coolant temperature difference between the hot and cold legs of loop #4 were mostly caused by the specifics of the coolant temperature change in the hot leg of this loop (see the above mentioned remarks). The reduction of the temperature difference by the (34 – 35)th s was caused by the coolant temperature increase in the cold leg of that loop (mostly due to the increase of P_{SG4}) and small change of the coolant temperature in the hot leg of the corresponding loop (due to entering into the core a cooled-down coolant flow from the cold leg #1 till the moment of flow reverse in the loop).

As recorded by the resistance thermometers, the difference of the coolant temperature between the hot and the cold legs (Fig. 42) is as follows:

– Loop #1: Starting from the initial value 29.4 °C the difference increased to 34.4 °C from the 10th to 33th s, and then, by the 67th s, it sharply decreased to minus 7.9 °C, later by the 90th s it increased to minus 6.4 °C, after which it smoothly decreased and stabilized at minus 7.0 °C at the 240th s;

– Loop 2: Starting from the initial value 26.5 °C it raised to 27.5 °C from the 7th to the 19th s practically without changing till the 40th s, and then, by the 90th s it decreased to 23.2 °C, after which it continued slightly to decrease and stabilized at 22.7 °C at the 160th s;

– Loop 3: Starting from the initial value 28.5 °C it raised to 30.1 °C from the 9th to the 34th s, and then, by the 90th s it decreased to 25.4 °C, after which it practically stabilized at the 210th to s 25.0 °C;

– Loop 4: Starting from the initial value $26.4\text{ }^{\circ}\text{C}$, it raised to $28.3\text{ }^{\circ}\text{C}$ from the 15^{th} to the 37^{th} s, and then, by the 56^{th} s it decreased to $23.1\text{ }^{\circ}\text{C}$. Later on, after some slowing down of the reduction it started again to decrease faster and at the 90^{th} s it reached $\Delta T_{4\text{TC}} = 15.2\text{ }^{\circ}\text{C}$. After that, the temperature difference practically did not increase, but oscillated about the average value $15.2\text{ }^{\circ}\text{C}$.

The “stepwise” decrease of $\Delta T_{4\text{TC}}$ was caused by the similar change of $T_{4\text{TCr}} = (\tau)$ (Fig. 25), which is due to the relatively strong influence of the flow mixing of the cooled-down coolant from the hot leg #1 into the hot leg #4 during the development and stabilisation of the reverse flow in the loop #1, and after that (when the loops’ and reactor’s flows reached stabilization), it is due to the load-off operation mode by LRPC.

Figure 44 – 49 show time histories of the coolant temperature at the FA outlet respectively in sectors 1-6 recorded by the ICMS (see also Annex C). These figures denote that the coolant temperature increased at the FA outlets with respect to the initial values by the following values:

- in sector #1 (Fig. 44) by $(2.2 - 3.9)\text{ }^{\circ}\text{C}$ at the $(42 - 46)^{\text{th}}$ s;
- in sector #2 (Fig. 45) by $(2.3 - 3.9)\text{ }^{\circ}\text{C}$ at the $(41 - 45)^{\text{th}}$ s;
- in sector #3 (Fig. 46) by $(2.3 - 4.1)\text{ }^{\circ}\text{C}$ at the $(41 - 48)^{\text{th}}$ s;
- in sector #4 (Fig. 47) by $(2.3 - 4.0)\text{ }^{\circ}\text{C}$ at the $(43 - 47)^{\text{th}}$ s;
- in sector #5 (Fig. 48) by $(2.3 - 3.9)\text{ }^{\circ}\text{C}$ at the $(42 - 47)^{\text{th}}$ s;
- in sector #6 (Fig. 49) by $(2.9 - 3.9)\text{ }^{\circ}\text{C}$ at the $(42 - 46)^{\text{th}}$ s.

Some local minimums (small pitches) on the $T_{\kappa}(\tau)$ curves of some FAs of sector 2 (Fig. 45) in the interval $18 - 22$ s have been caused by the impacts of the cooled-down coolant coming from the cold leg #1 and entering into the inlet region of these FA before the flow reverse in this loop have taken place. After reaching the maximal values during the transient, the FA outlet coolant temperature decreased mainly by the 150^{th} s. The most rapid reduction of T_c occurred till the 90^{th} s. The temperature reduction was caused by two reasons: 1) operation in power reduction mode of LRPC; 2) core inlet coolant temperature reduction (as a result of the cold legs #2, #3, #4 flow redistribution) due to the steam pressure decrease in the secondary circuit. Later the coolant temperature at the outlet for most of the FA increased (due to the cold legs’ coolant temperature rise in the loops with operating MCP) and began to stabilize from the 270^{th} s.

Table 1 – Main parameters of the primary and secondary circuit in the initial and the final state of the transient, caused by the switching off of MCP #1 while the other 3 MCPs remain in operation

Parameters	Values	
	Initial state	Final state
Date	02.10.2005	02.10.2005
Time, h:min:s	20:30:00	20:34:42
T _{eff. eff. days}	128.50	128.50
N _{core} , MW	2907	1946
N _{PC} , MW	2918	1926
N _{SC} , MW	2877	1938
N _{DCS} , MW	2887	1948
N _{NFC} , MW	2965	1996
N _{el} , MW	986	625
H ₁₋₈ , cm (%)	352 (100)	352 (100)
H ₁₀ , cm (%)	292 (82.95)	160 (45.45)
C _B , g/Kg	3.60	3.60
Tk _i , °C	288.14; 287.81; 287.69; 287.50	284.96; 287.40; 287.83; 284.80
ΔT _{loop<i>i</i>} , °C	29.23; 28.87; 28.74; 29.26	-7.98; 23.86; 25.40; 17.88
T _{inlet} , °C	287.79	286.68
ΔT _{loop} , °C	29.03	22.38
P _{PC} , MPa	15.52	15.46
ΔP _r , MPa	0.38	0.21
ΔP _{MCP<i>i</i>} , MPa	0.569; 0.564; 0.565; 0.562	0.153; 0.460; 0.448; 0.431
G _{loop<i>i</i>} , m3/h	22292; 22223; 21784; 21772	-7198; 24668; 24280; 24725
G _r , m3/h	88073	66475
L _{PRZ} , cm	860	780
L _{SG<i>i</i>} , cm	222; 220; 220; 222	229; 215; 216; 221
G _{i-SG} , t/h	1445; 1367; 1364; 1360	143; 1241; 1283; 937
T _{SG-i} , °C	215.70; 215.50; 216.40; 214.50	208.90; 201.70; 205.50; 201.10
P _{SG<i>i</i>} , MPa	6.27; 6.30; 6.25; 6.24	6.02; 6.27; 6.23; 6.16
P _{MSH} , MPa	6.02	5.99
δW _{DCS} , %	-6.06	-23.40
δW _{core} , %	-2.15	-20.70
K _{q max} /FA	1.27/08-25	1.29/12-21
ΔT _{c max} , °C/FA	28.71/08-25	27.69/08-25
K _{v max} /FA/layer	1.50/10-31/2	1.81/10-31/2

16 18 20 22 24 26 28 30 32 34 36 38 40 42

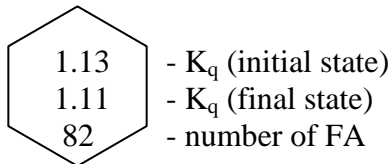
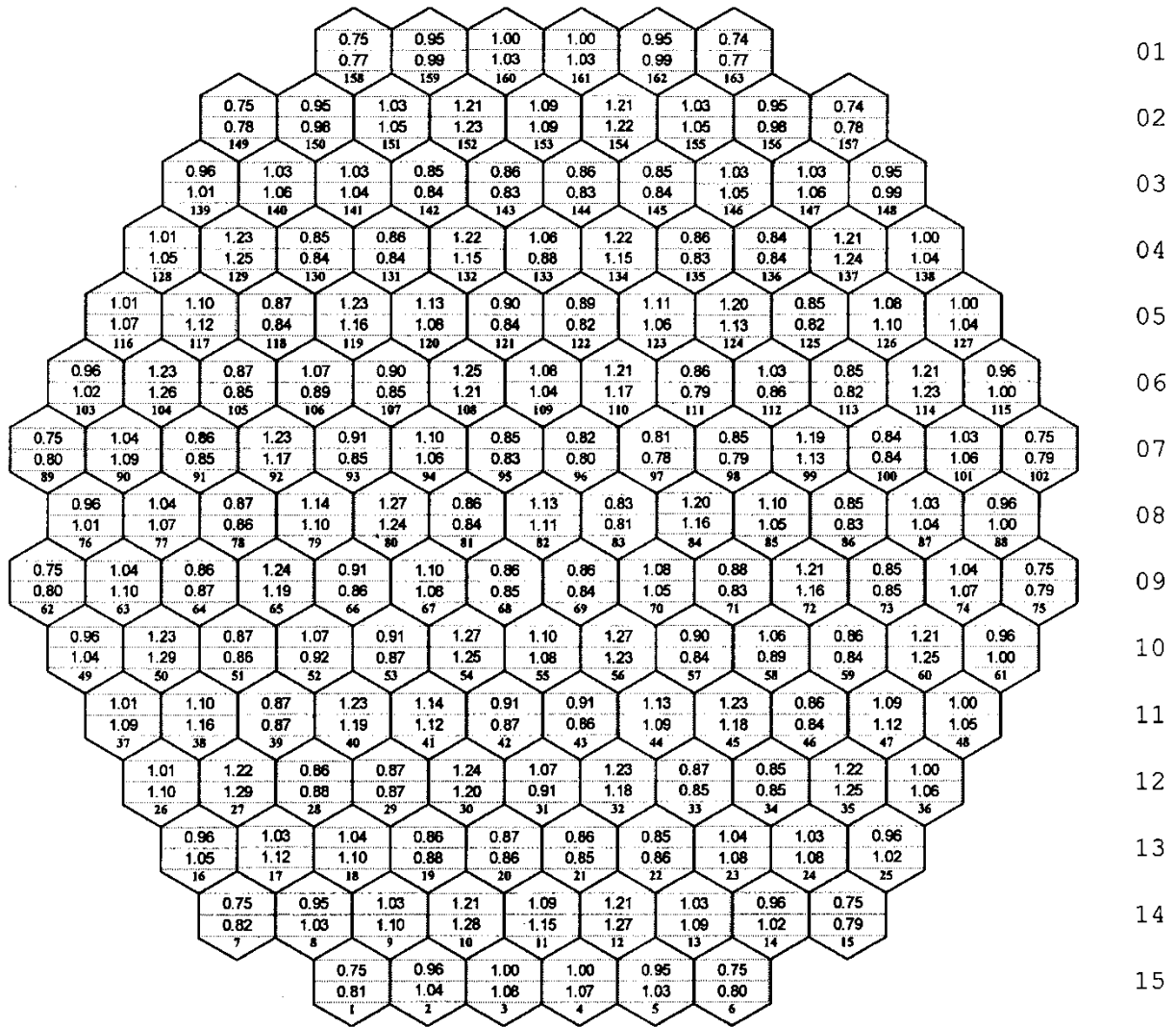


Fig. 1 – Relative power generation in FA

16 18 20 22 24 26 28 30 32 34 36 38 40 42

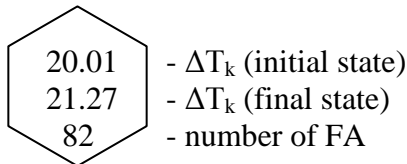
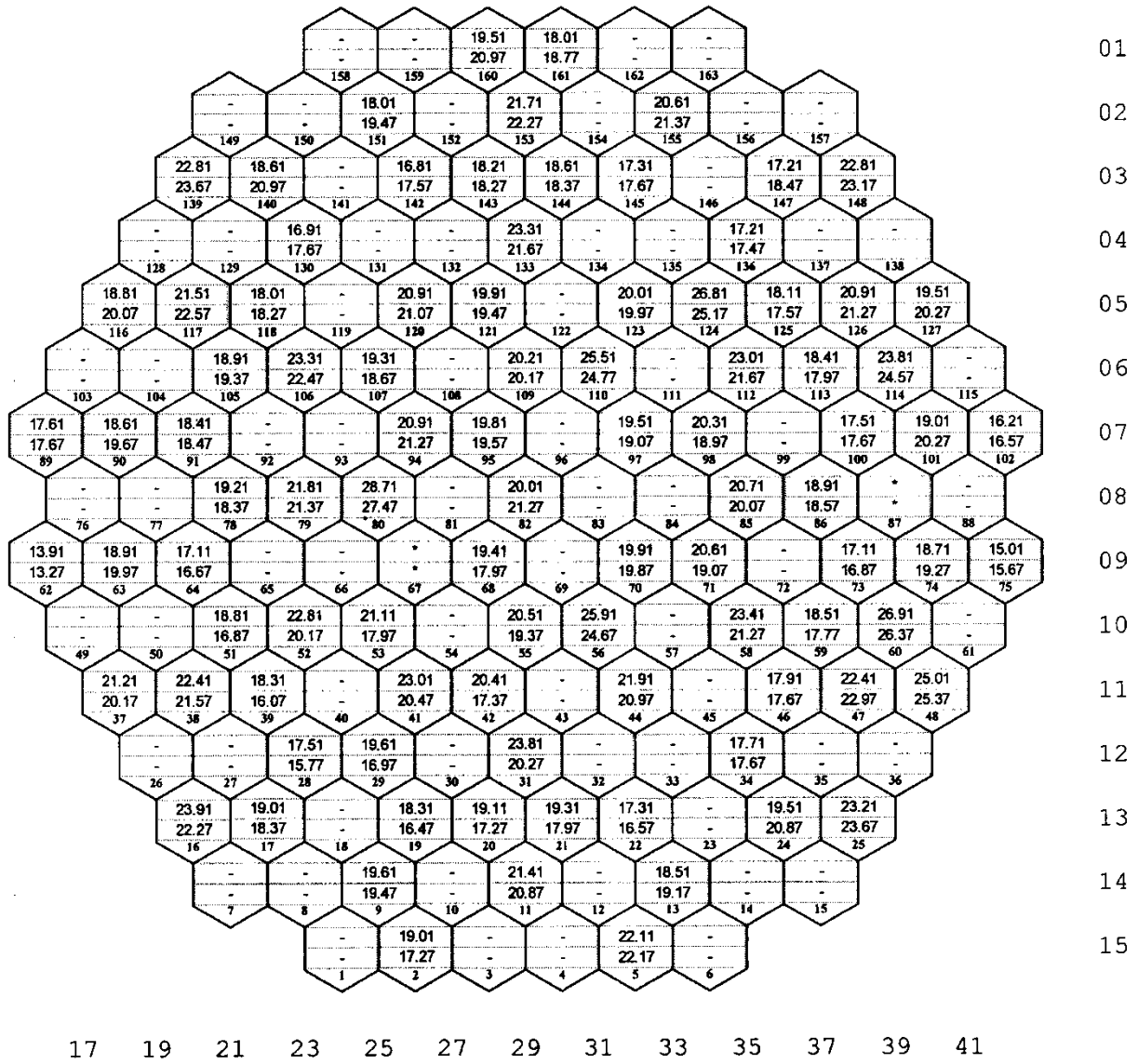


Fig. 2 – Coolant heat-up in FA recorded by the ICMS

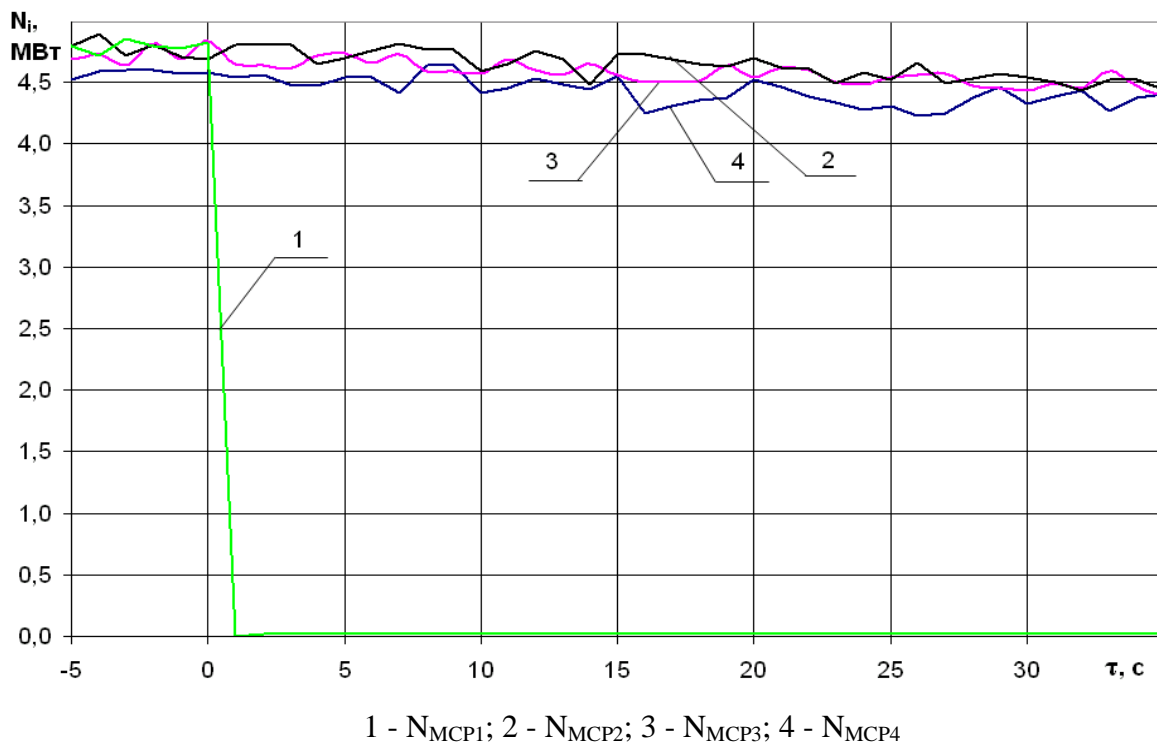


Fig. 3 – Power change of MCPs recorded by the ICMS during the transient caused by the switching off of MCP #1

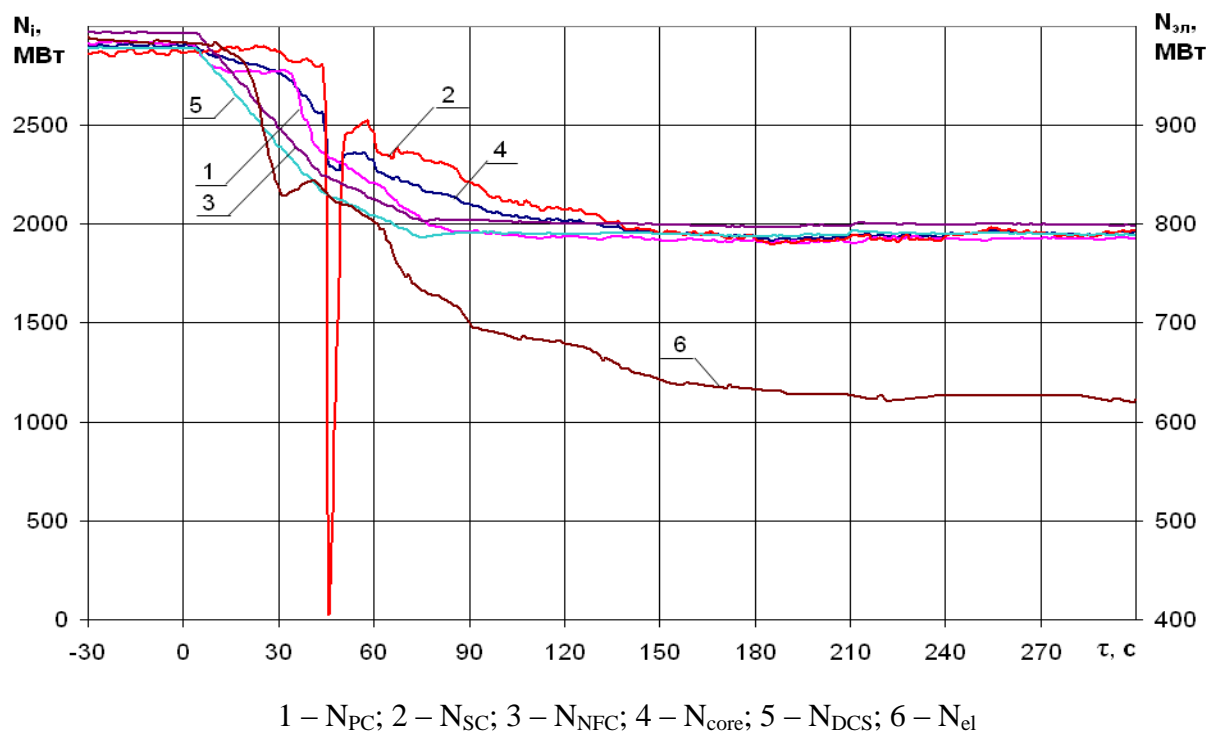


Fig. 4 – Time histories of integral reactor power, integral reactor power recorded by the NFC and electrical power of TG recorded by the UBL

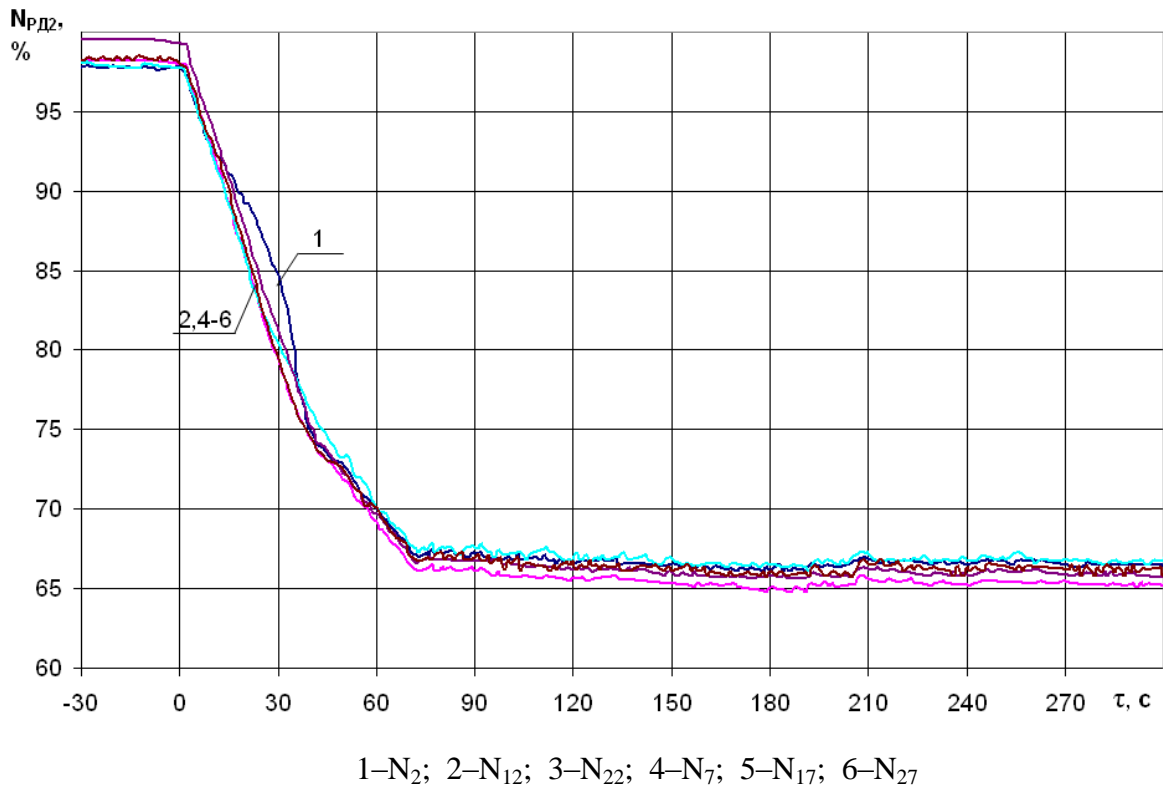


Fig. 5 – Reactor power change recorded by the different measurement channels OR-2 of NFC recorded by the UBLs

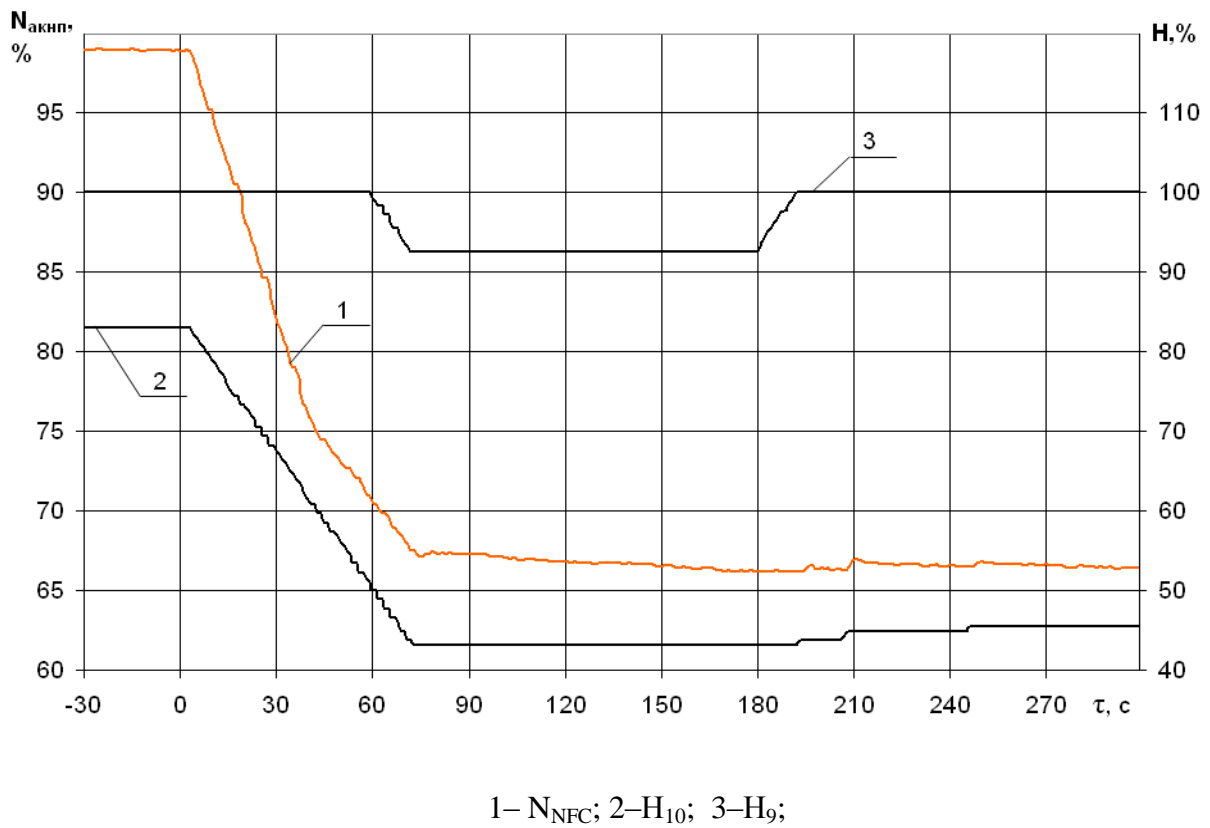


Fig. 6 – Change of CPS-group #10 and #9 positions and reactor power on the basis of NFC recorded by ICMS

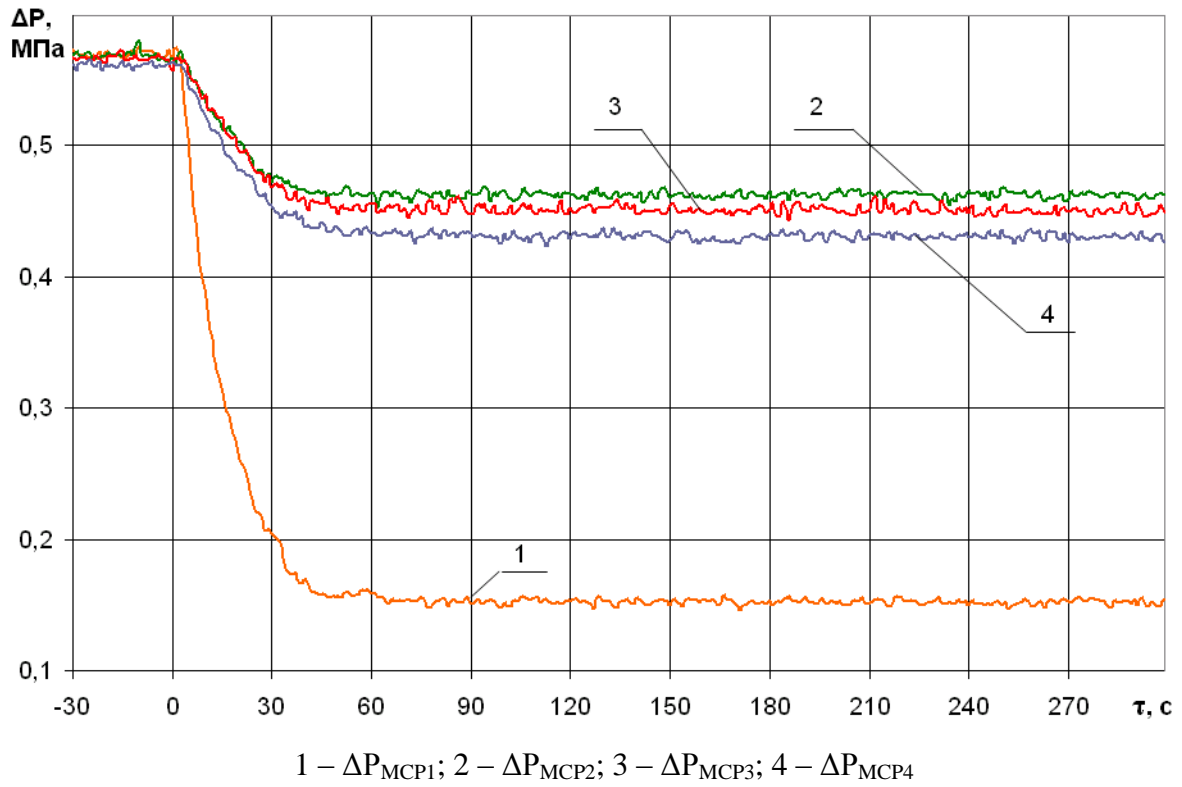


Fig. 7 – Change of the pressure differences of MCP-1–4 recorded by the ICMS

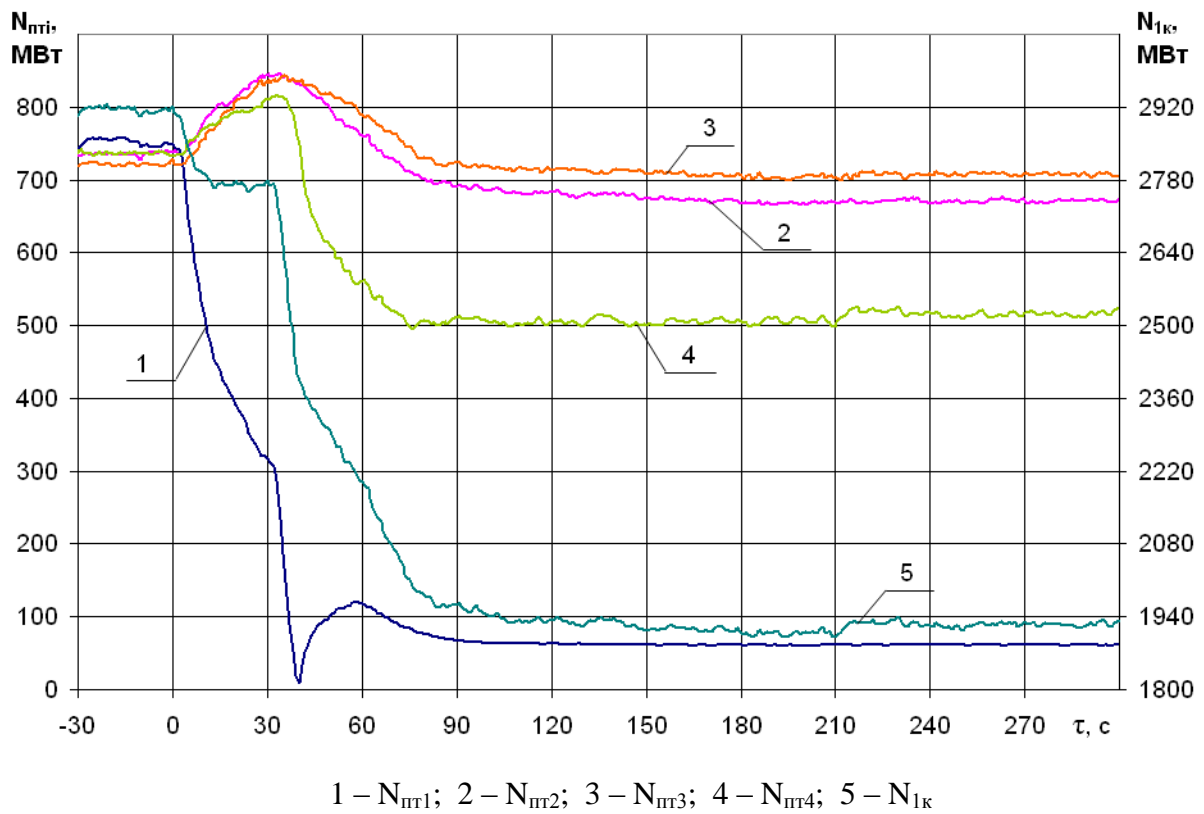


Fig. 8 – Thermal power histories of the primary loops and the integral reactor thermal power recorded by the ICMS

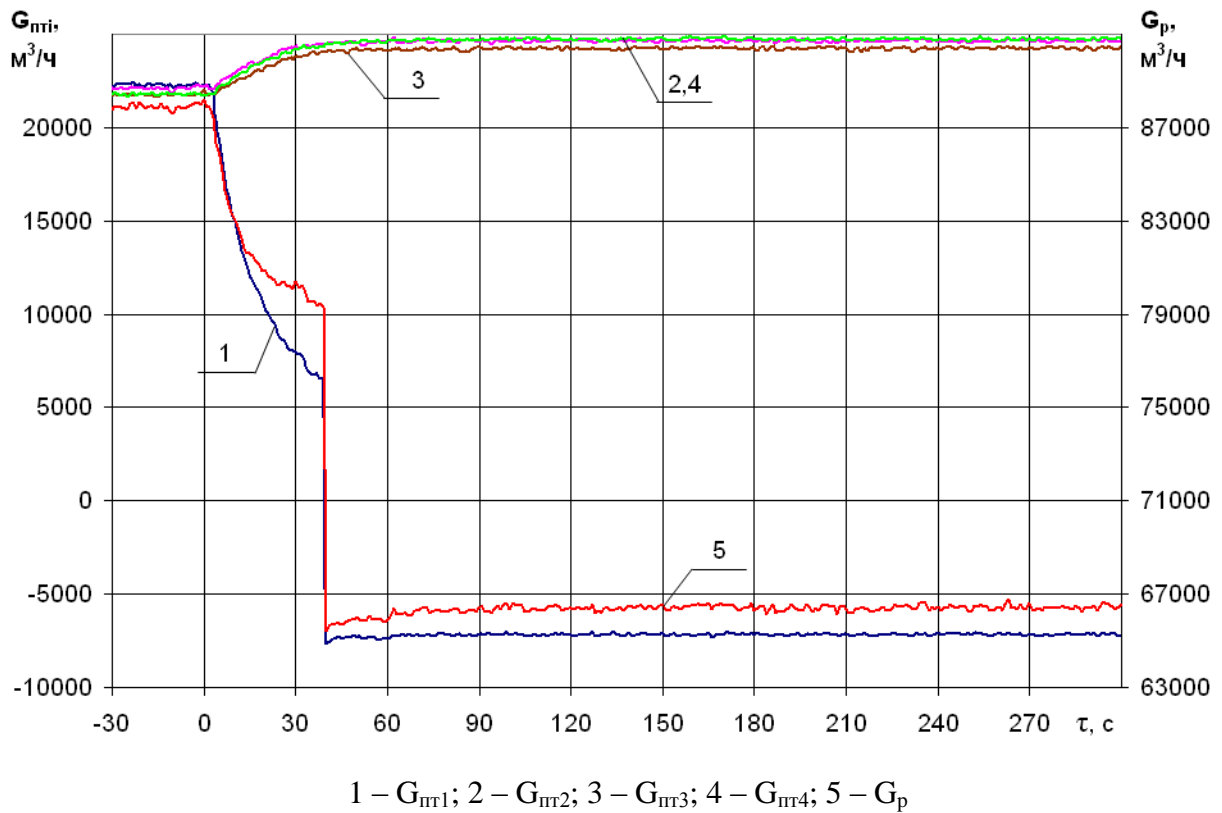


Fig. 9 – Coolant flow rates time histories of the primary loops and the reactor mass flow rate recorded by the ICMS

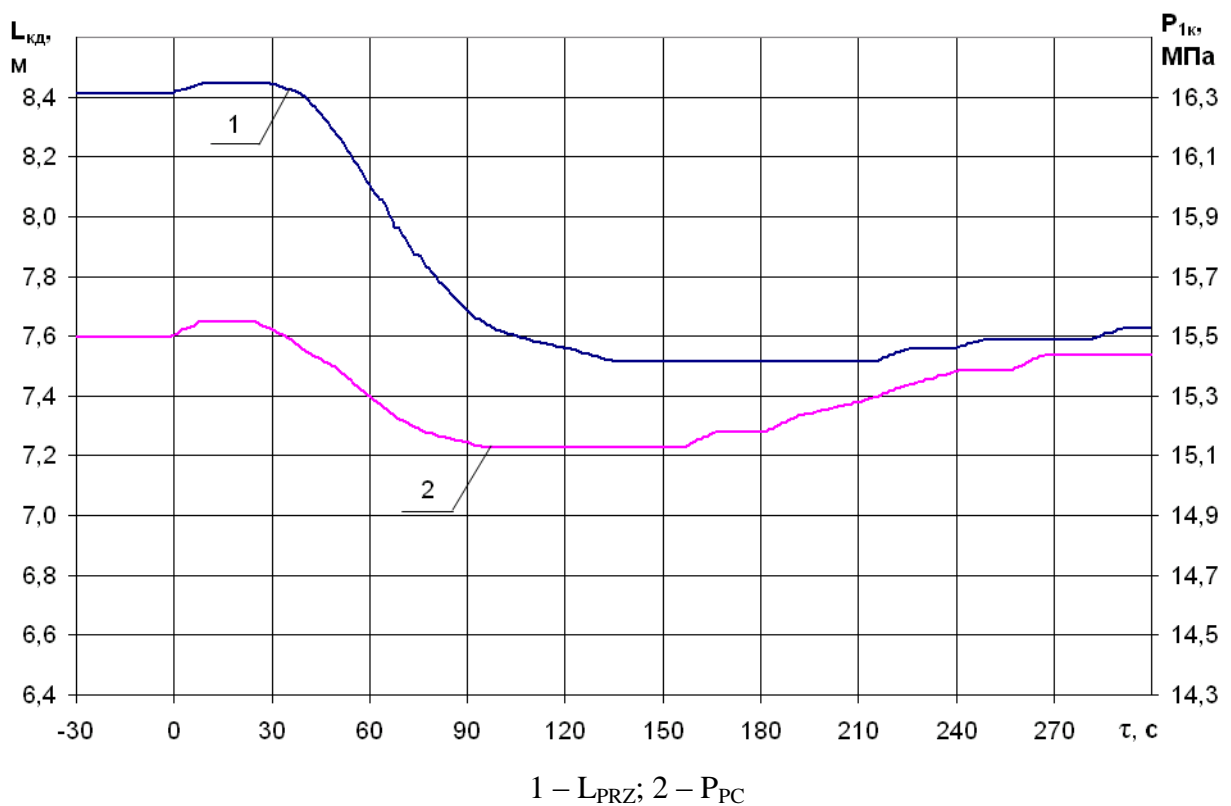


Fig. 10 – PRZ water level and PC-pressure change recorded by the UBLS

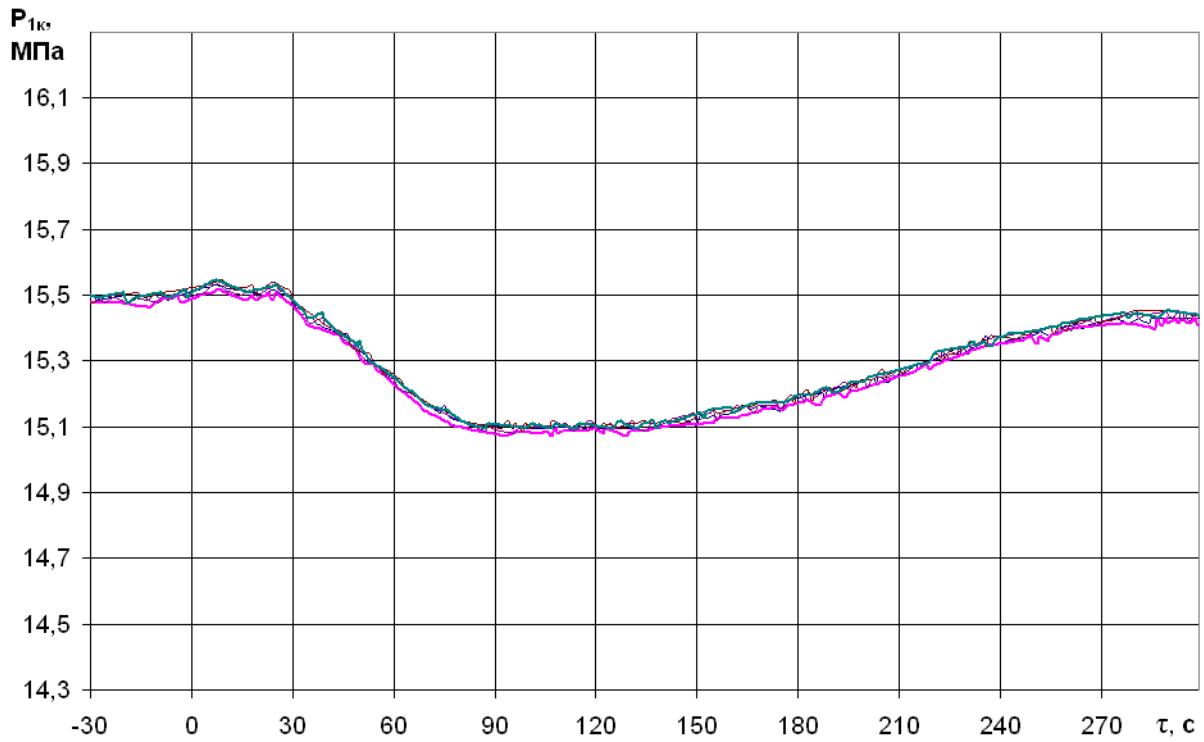
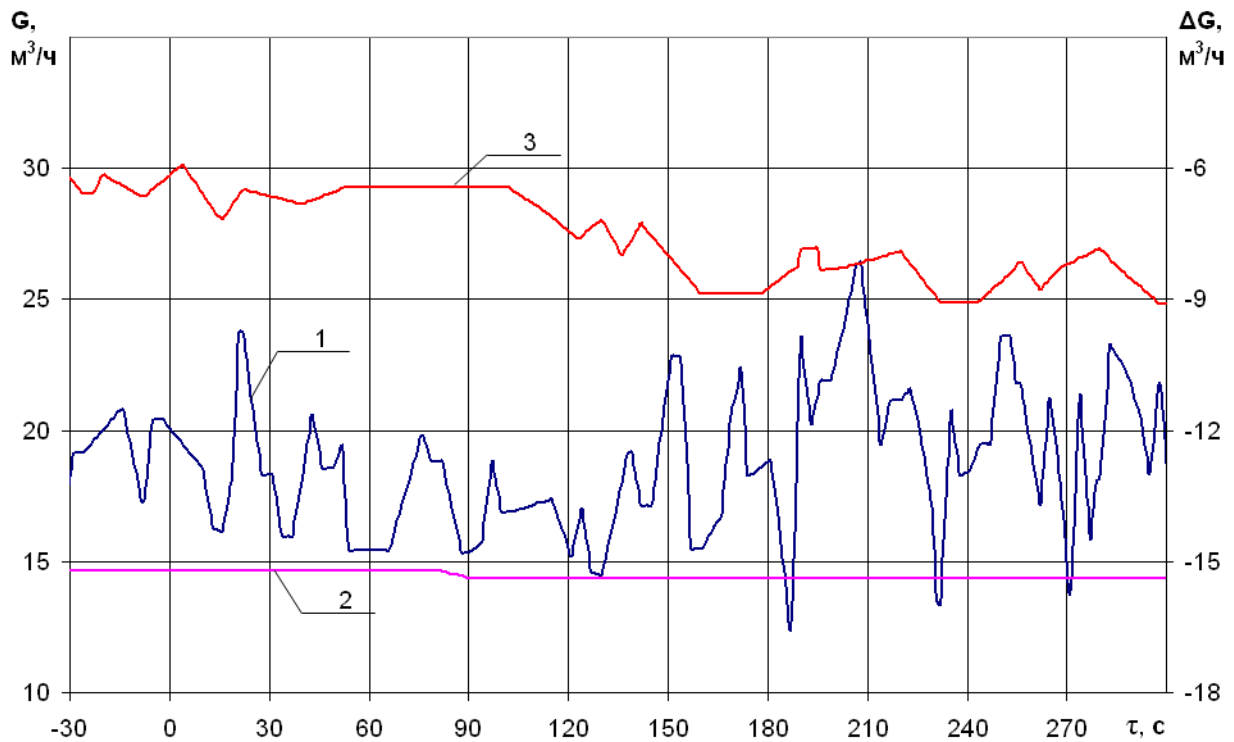
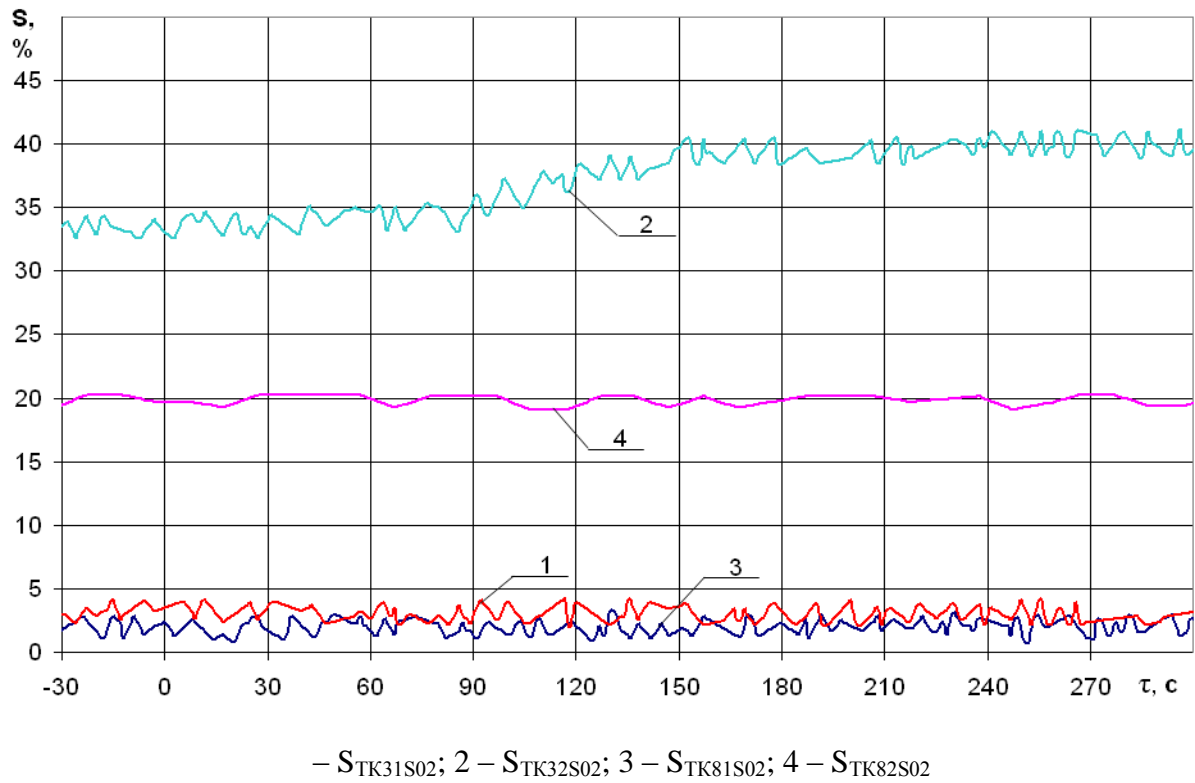


Fig. 11 – PC-pressure change by the reactor protection system (6 sensors) recorded by the UBL S



1 – $G_{\text{подп}}$; 2 – $G_{\text{прод}}$; 3 – $\Delta G_{\text{прод-под}}$

Fig. 12 - (controlling for power level 100% $N_{\text{ном}}$) Mass flow rate of make-up and blow-down systems and the difference between the blowdown and the make-up flow rate recorded by the UBL S



1

Fig. 13 – Change of the position of the make-up system valves (TK31,32S02) and of the blow-down system valves (TK81,82S02) recorded by the UBLS

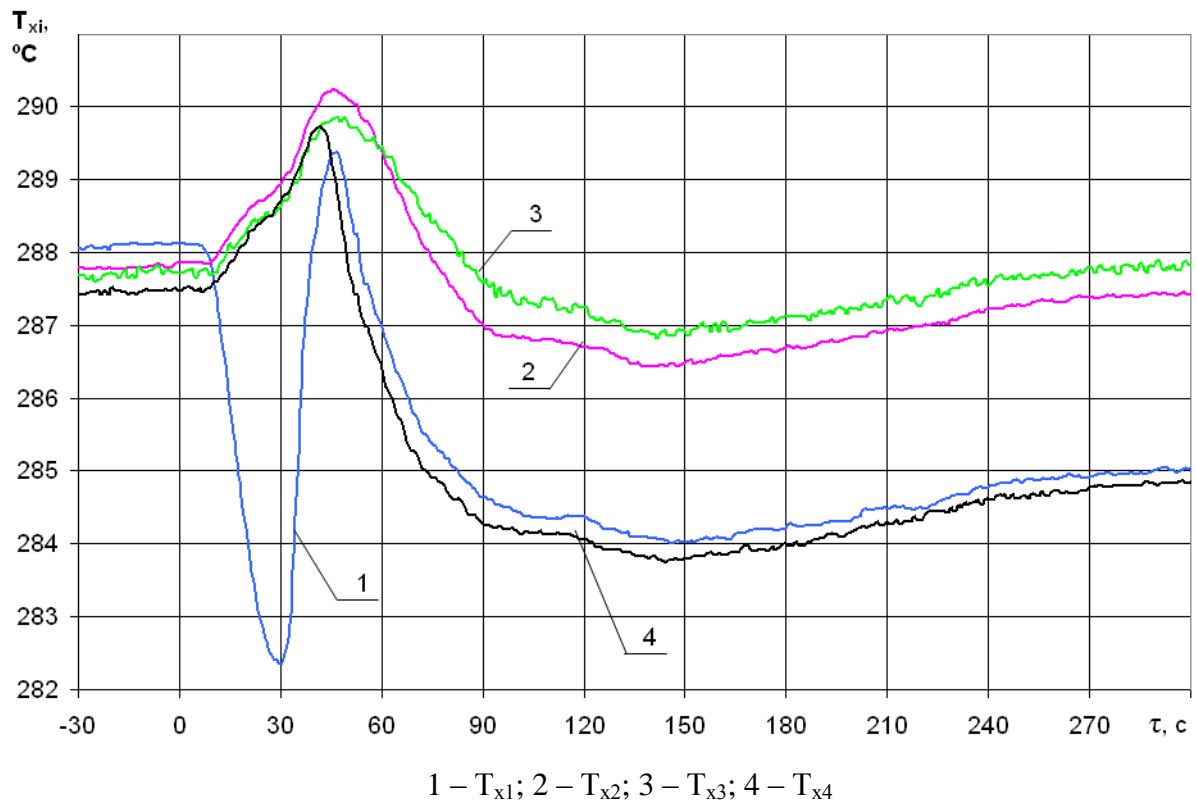


Fig. 14 – Mean coolant temperature histories of the cold legs of PC-loops recorded by the ICMS

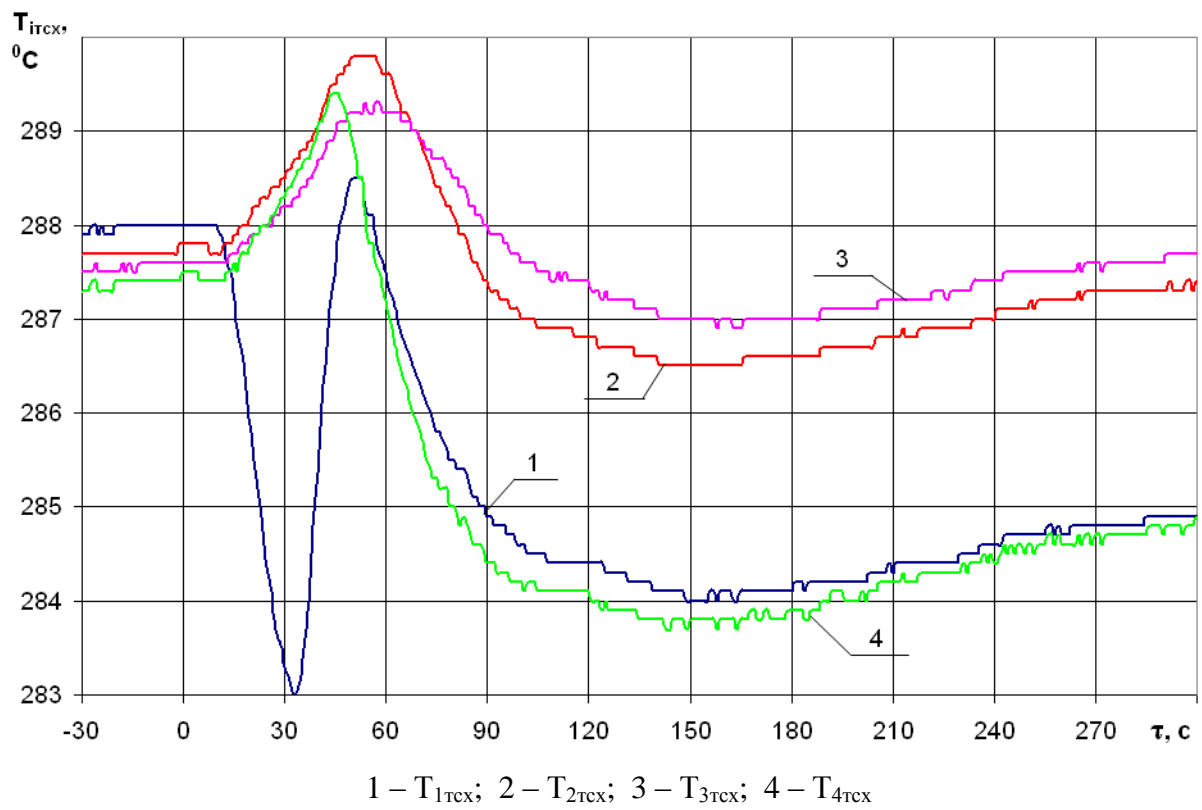


Fig. 15 – Mean coolant temperature histories of the cold legs of PC-loops recorded by the thermoresistors

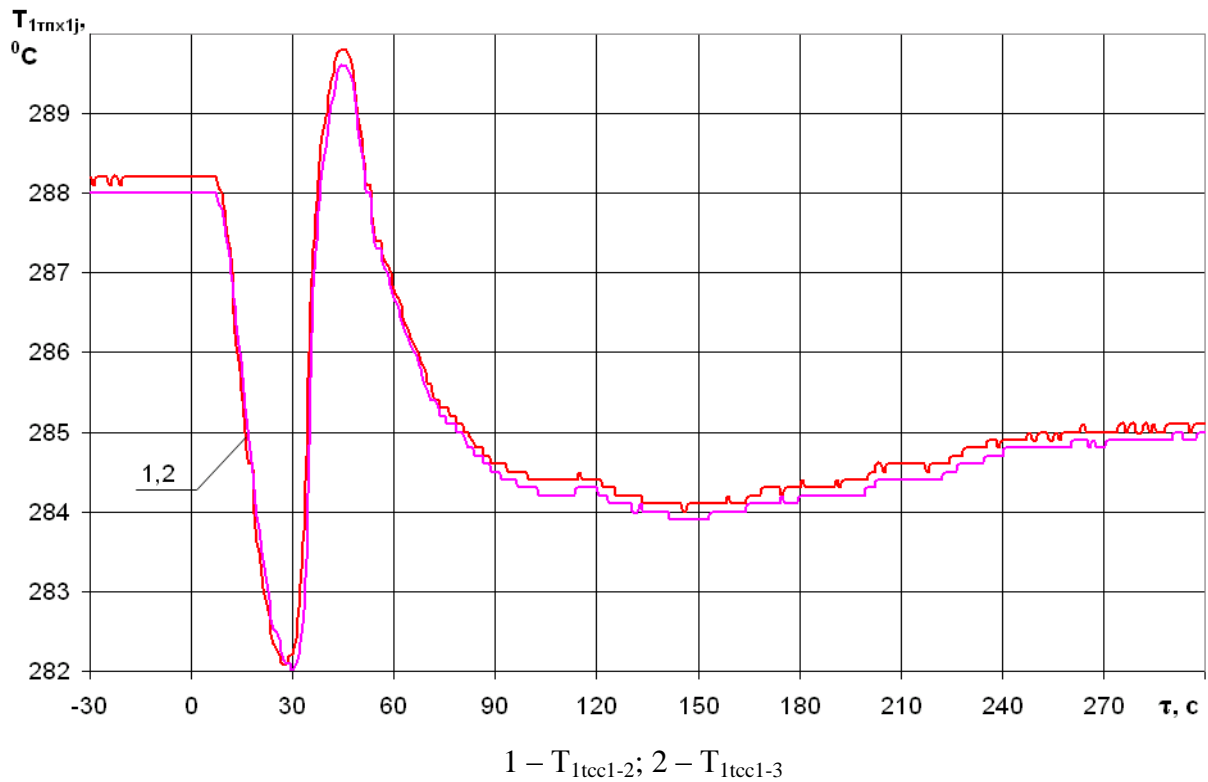


Fig. 16 – Cold leg #1 mean coolant temperature history recorded by the first set of thermocouples

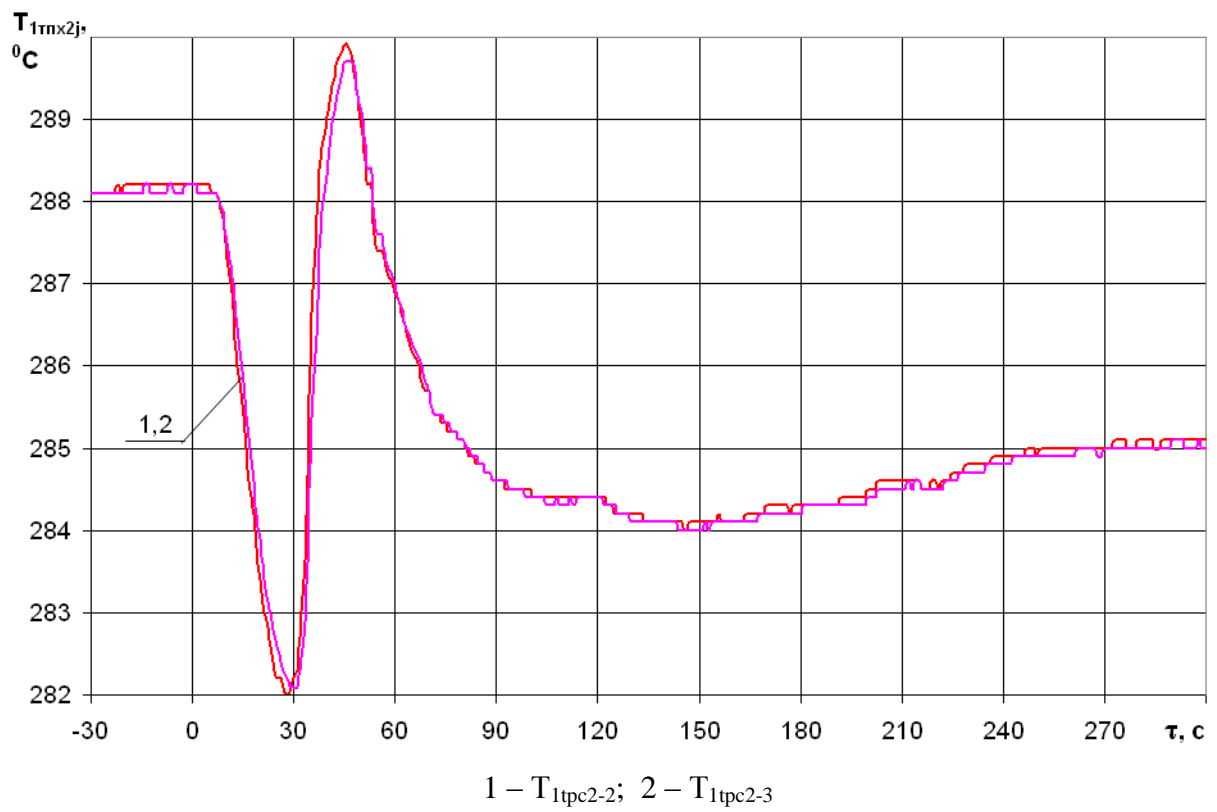


Fig. 17 – Cold leg #1 mean coolant temperature history recorded by the second set of thermocouples

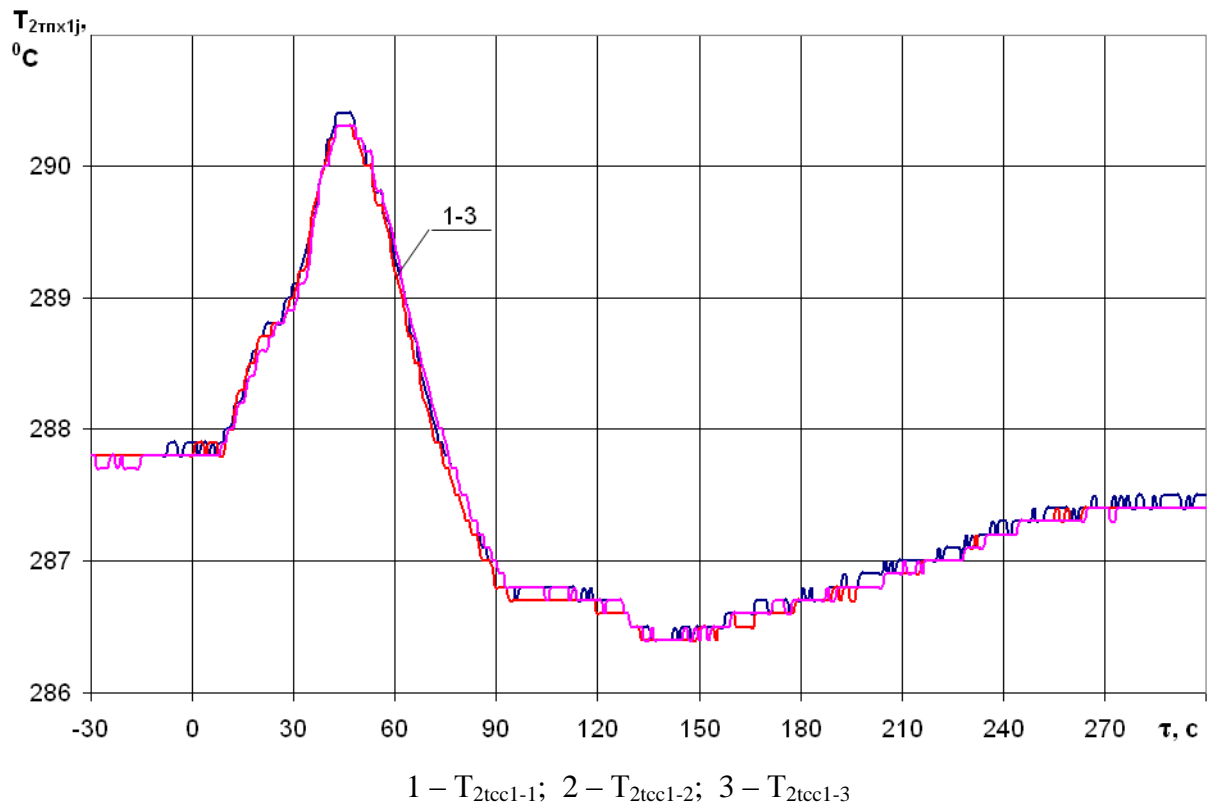


Fig. 18 – Cold leg #2 mean coolant temperature history recorded by the first set of thermocouples

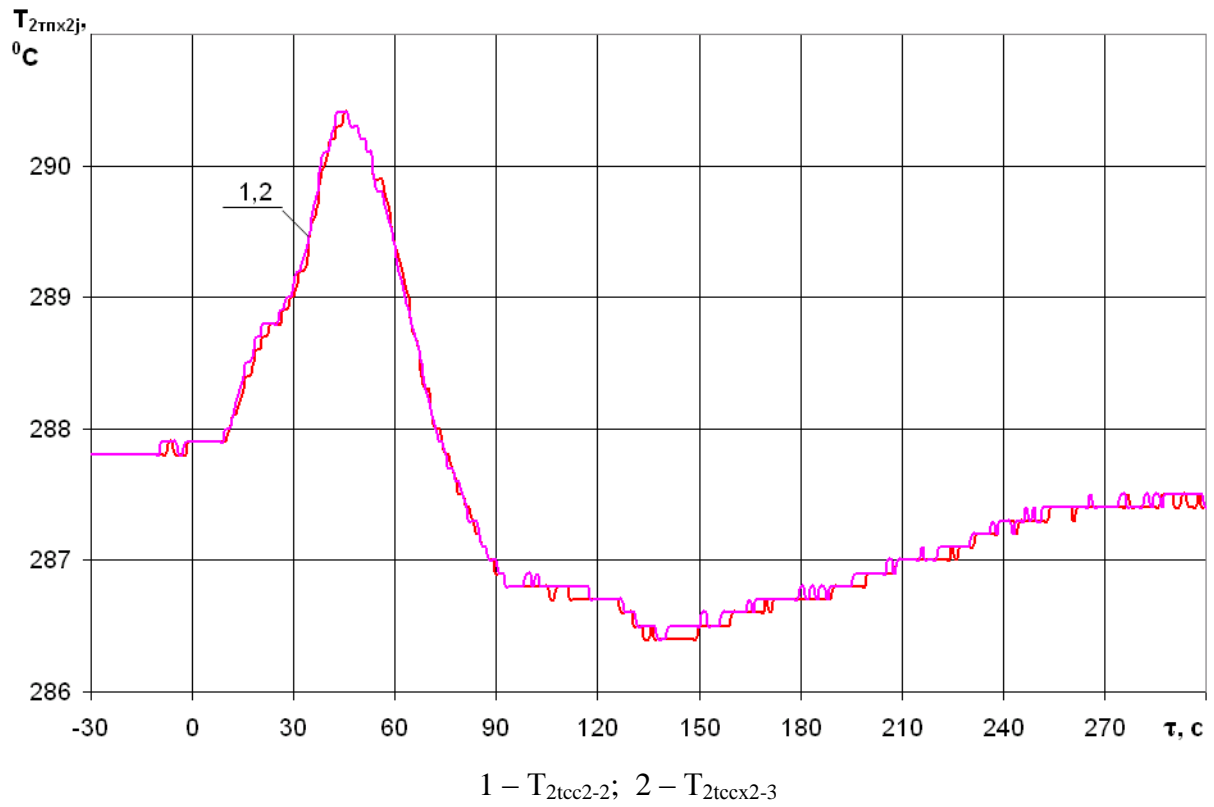


Fig. 19 – Cold leg #2 mean coolant temperature history recorded by the second set of thermocouples

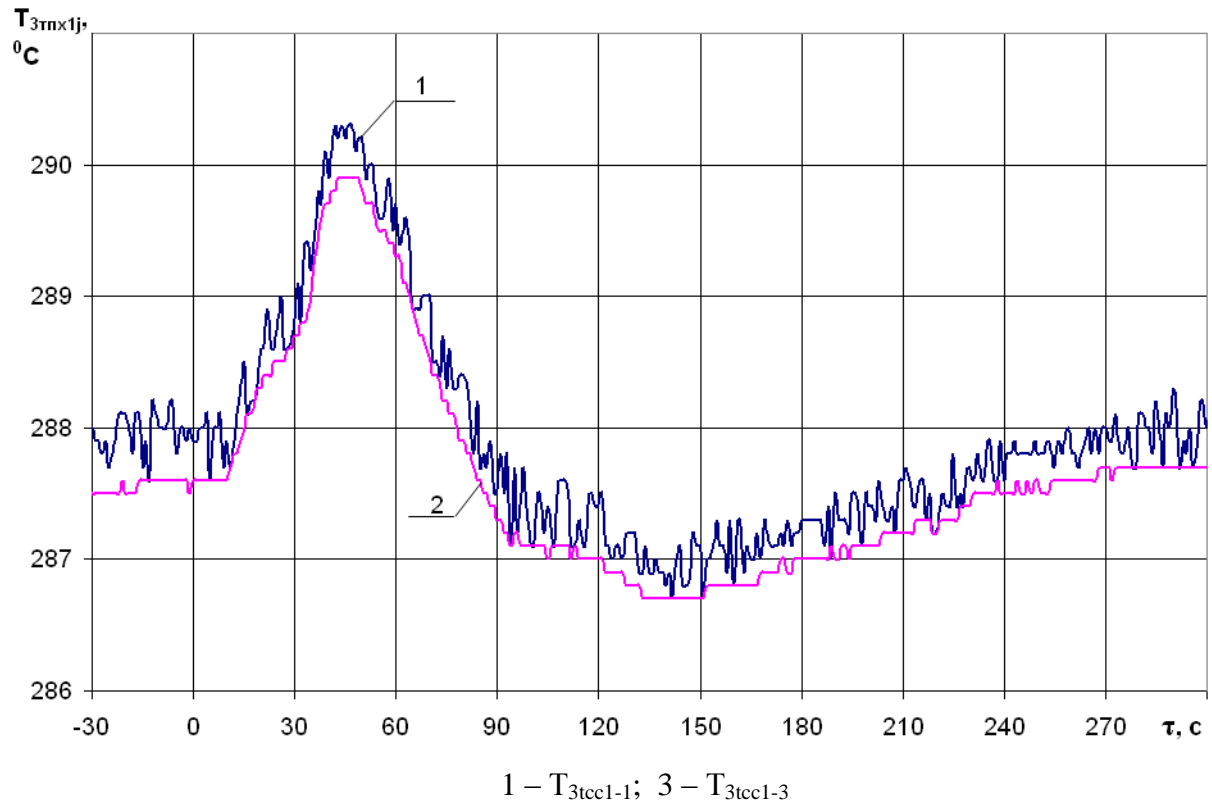


Fig. 20 – Cold leg #3 mean coolant temperature history recorded by the first set of thermocouples

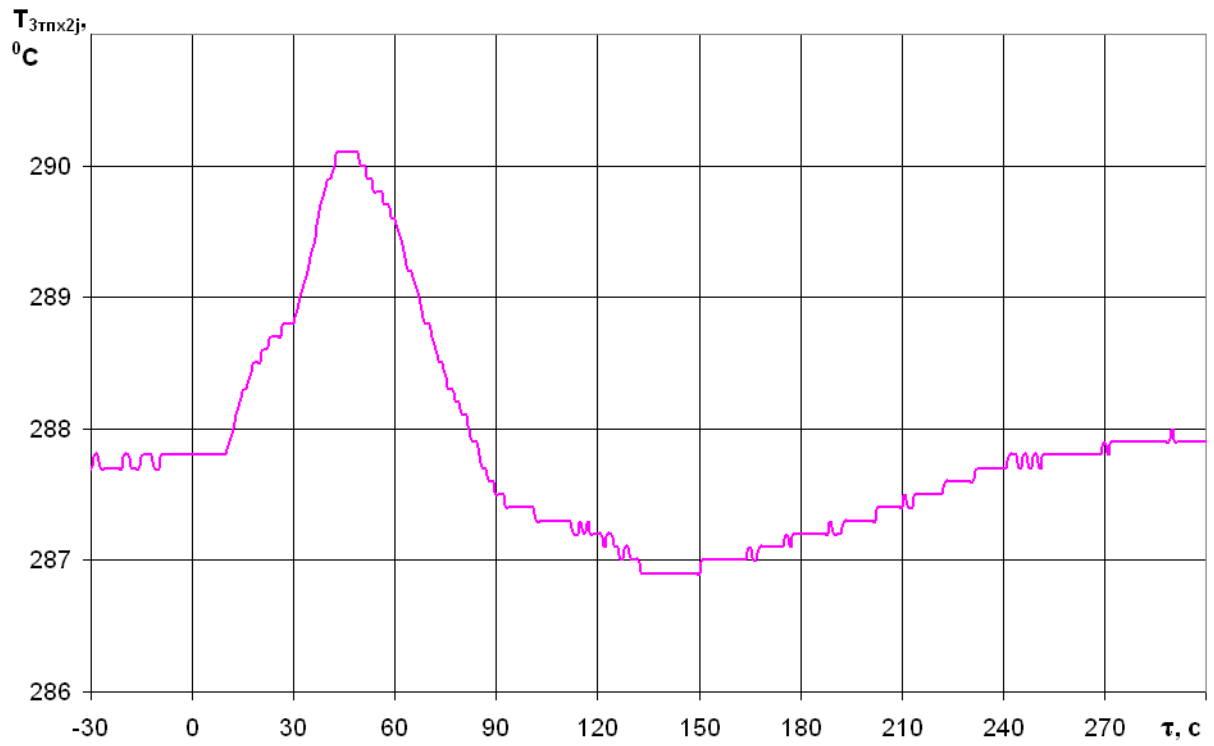


Fig. 21 – Cold leg #3 mean coolant temperature history recorded by the second set of thermocouples

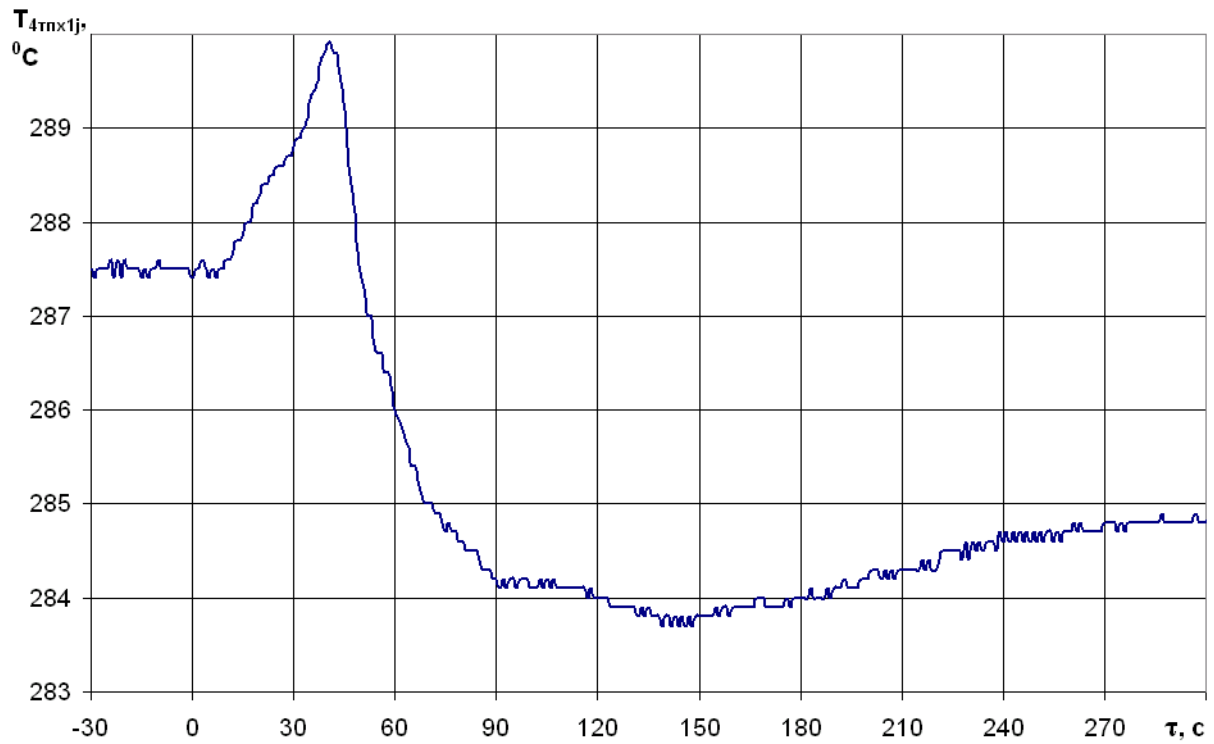


Fig. 22 – Cold leg #4 mean coolant temperature history recorded by the first set of thermocouples

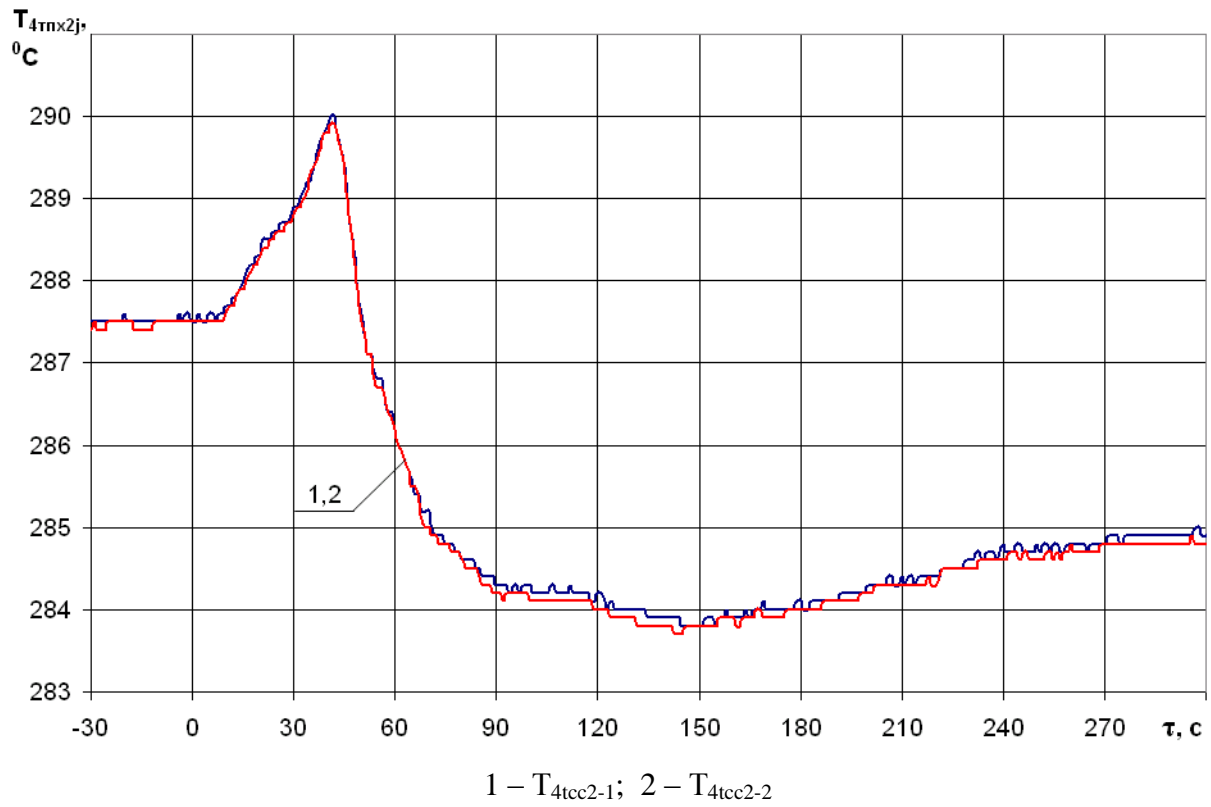


Fig. 23 – Cold leg #4 mean coolant temperature history recorded by the second set of thermocouples

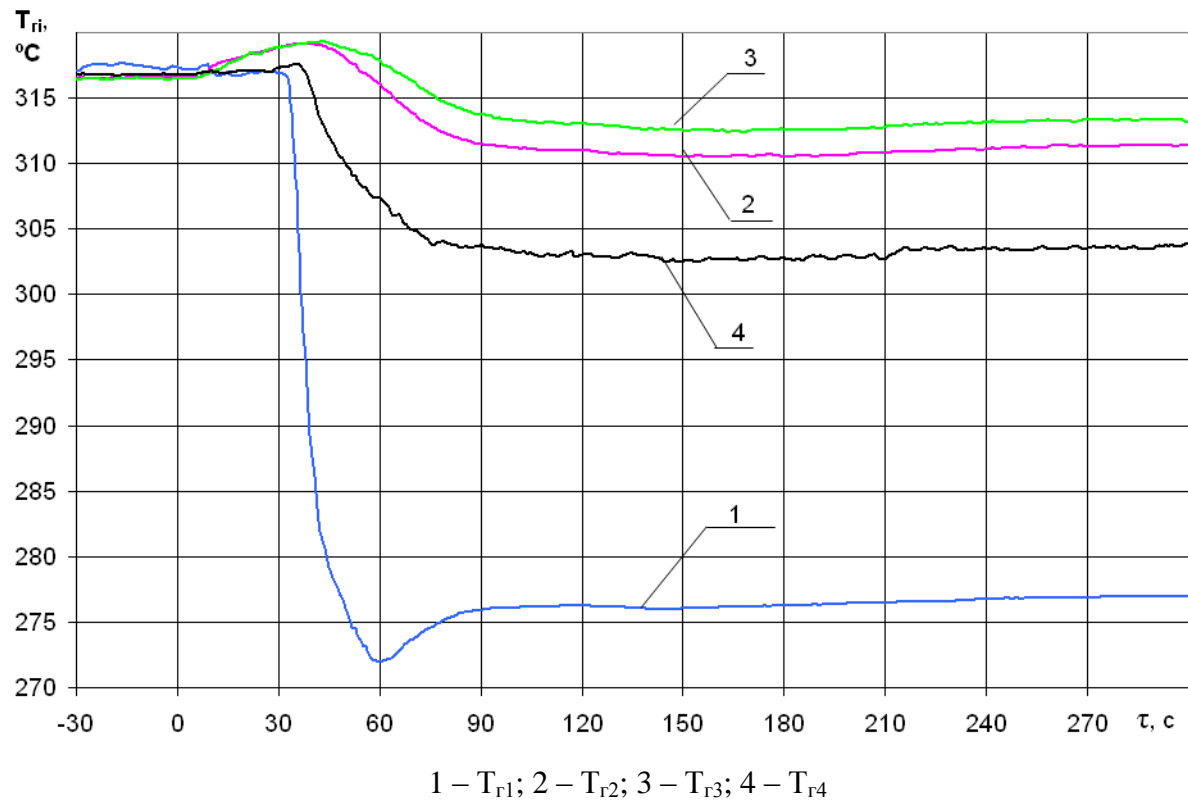


Fig. 24 – Mean coolant temperature histories of the hot legs of PC-loops recorded by the ICMS

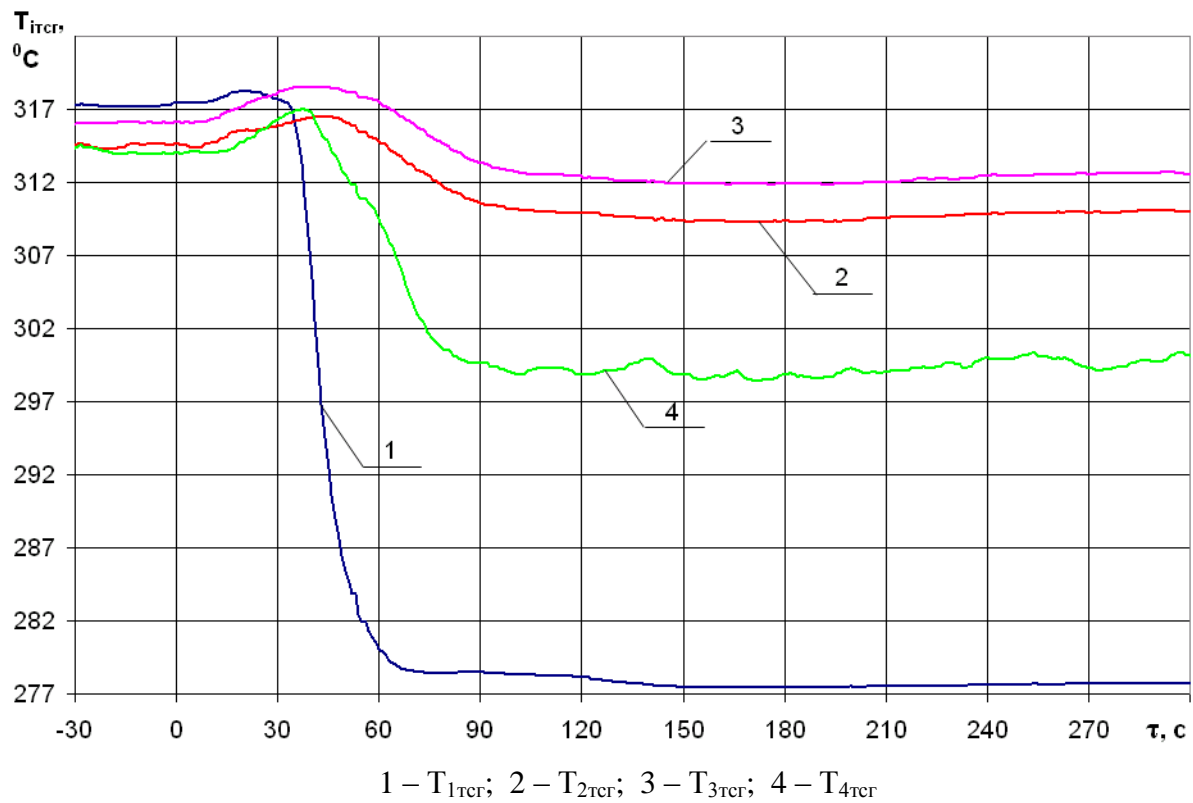


Fig. 25 – Mean coolant temperature histories of the hot legs of PC-loops recorded by the thermal resistors

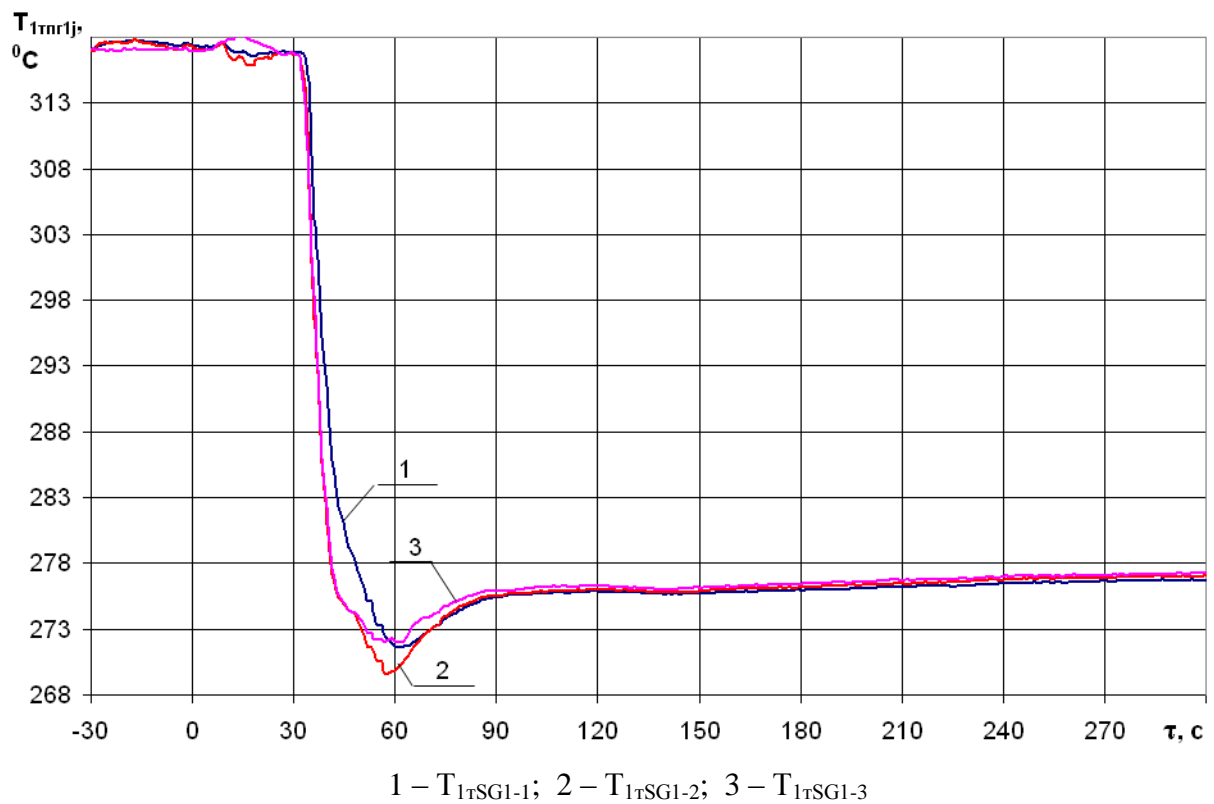


Fig. 26 – Hot leg #1 mean coolant temperature history recorded by the first set of thermocouples

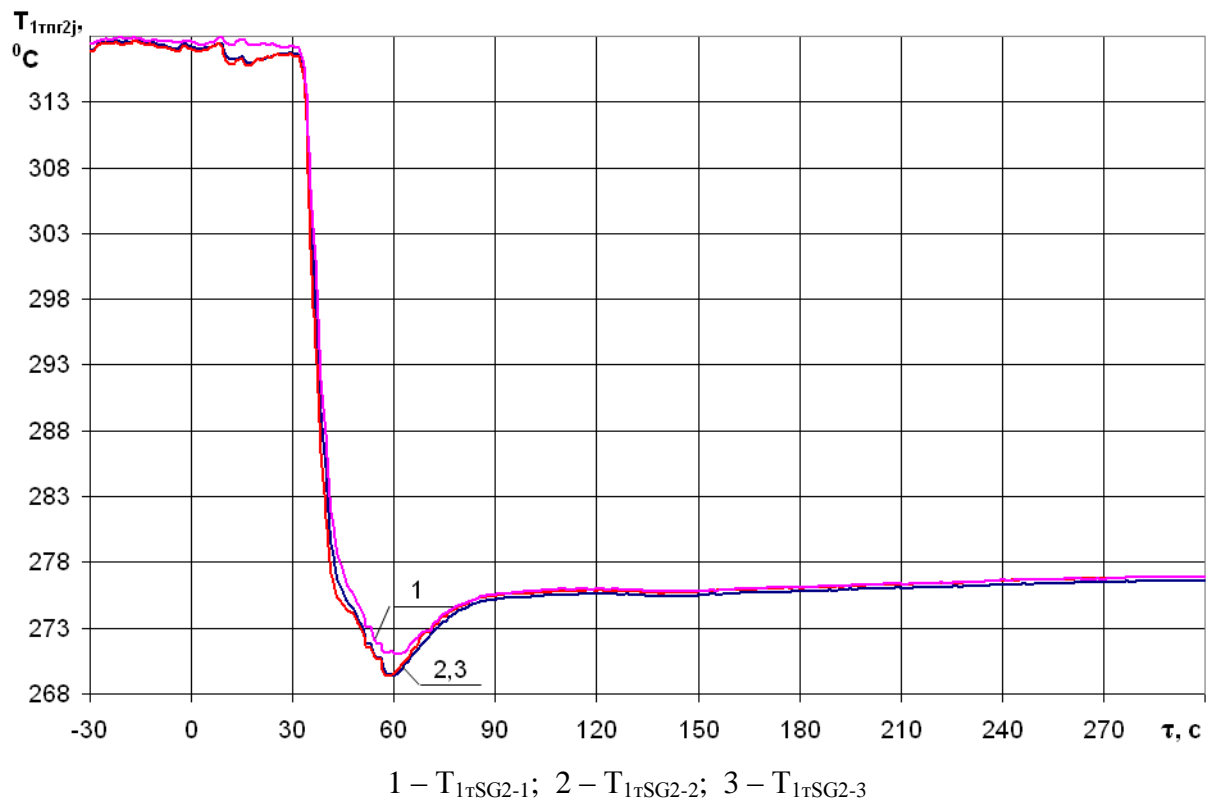


Fig. 27 – Hot leg #1 mean coolant temperature history recorded by the second set of thermocouples

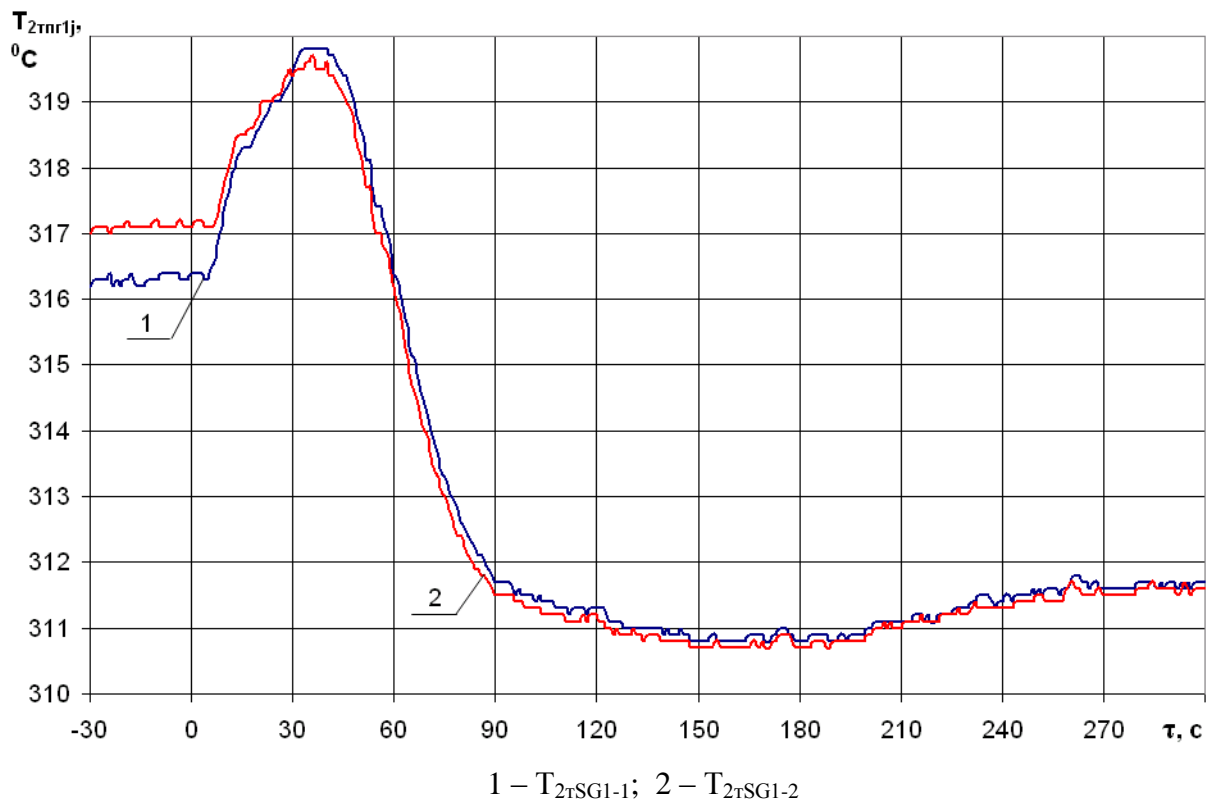


Fig. 28 – Hot leg #2 mean coolant temperature history recorded by the first set of thermocouples

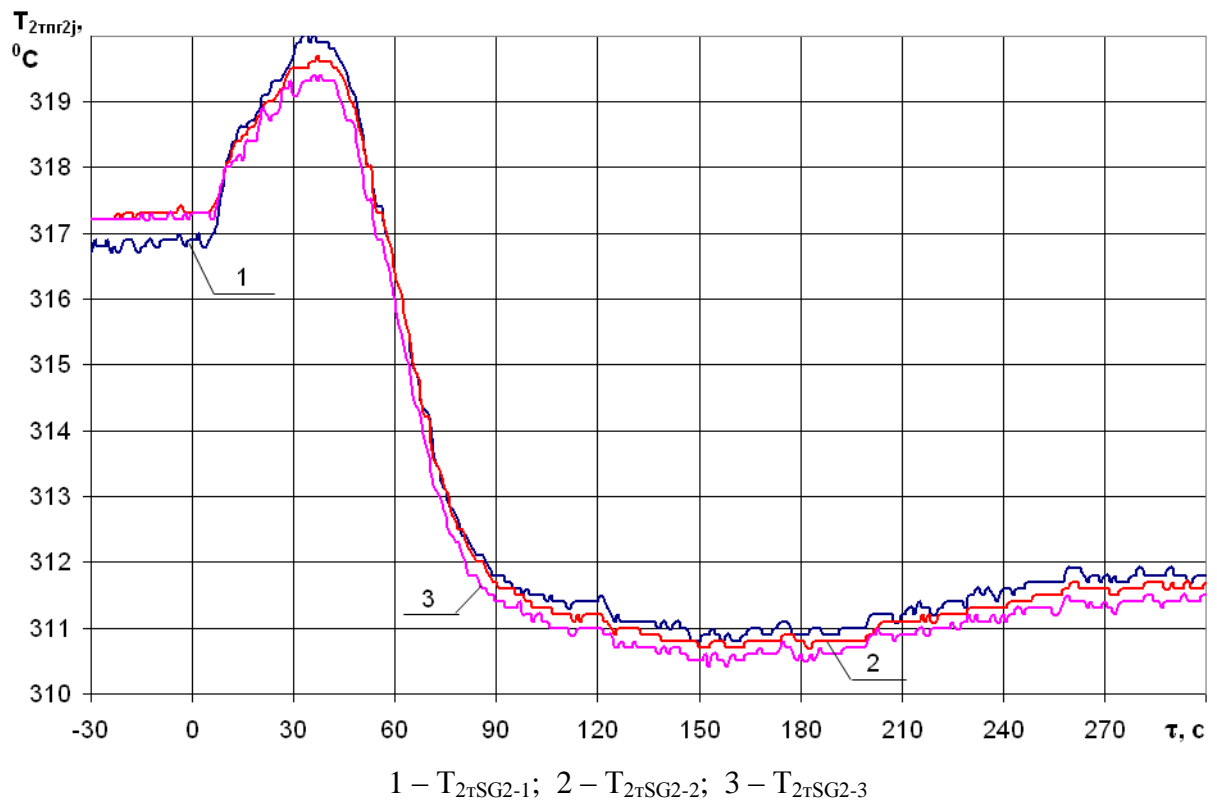


Fig. 29 – Hot leg #2 mean coolant temperature history recorded by the second set of thermocouples

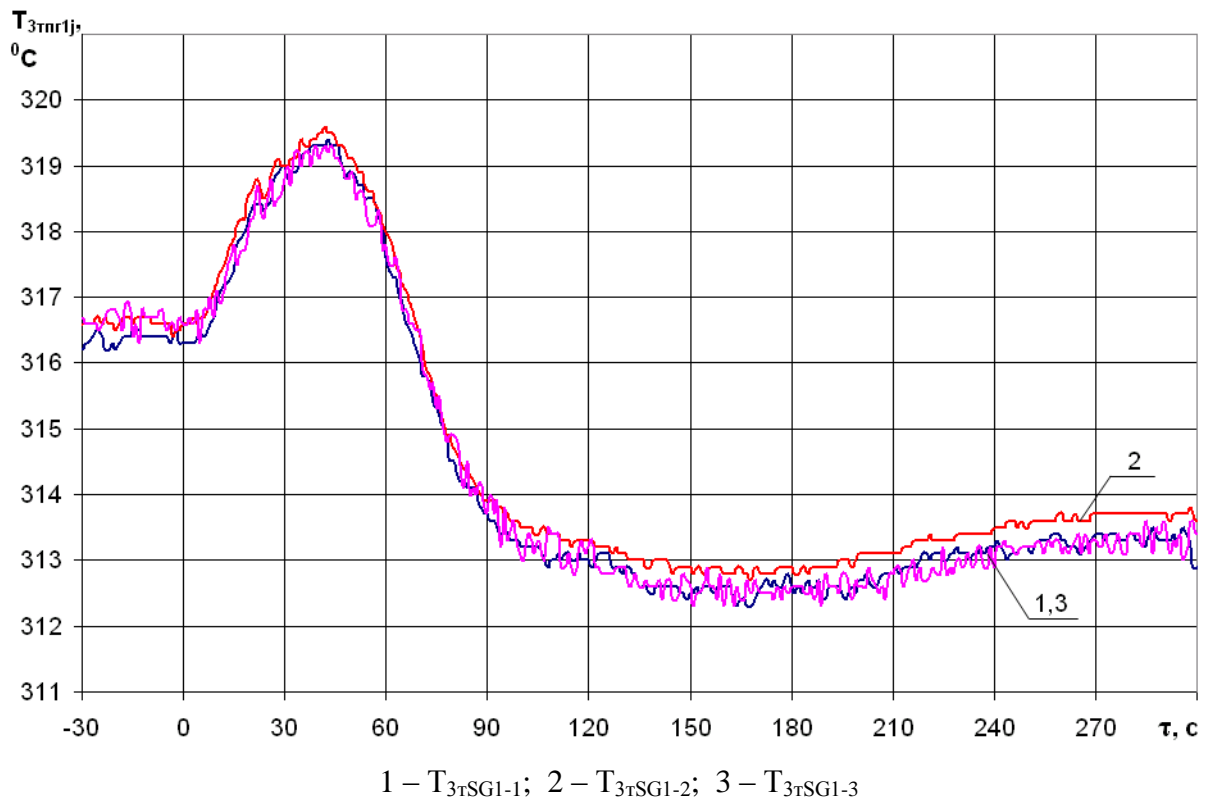


Fig. 30 – Hot leg #3 mean coolant temperature history recorded by the first set of thermocouples

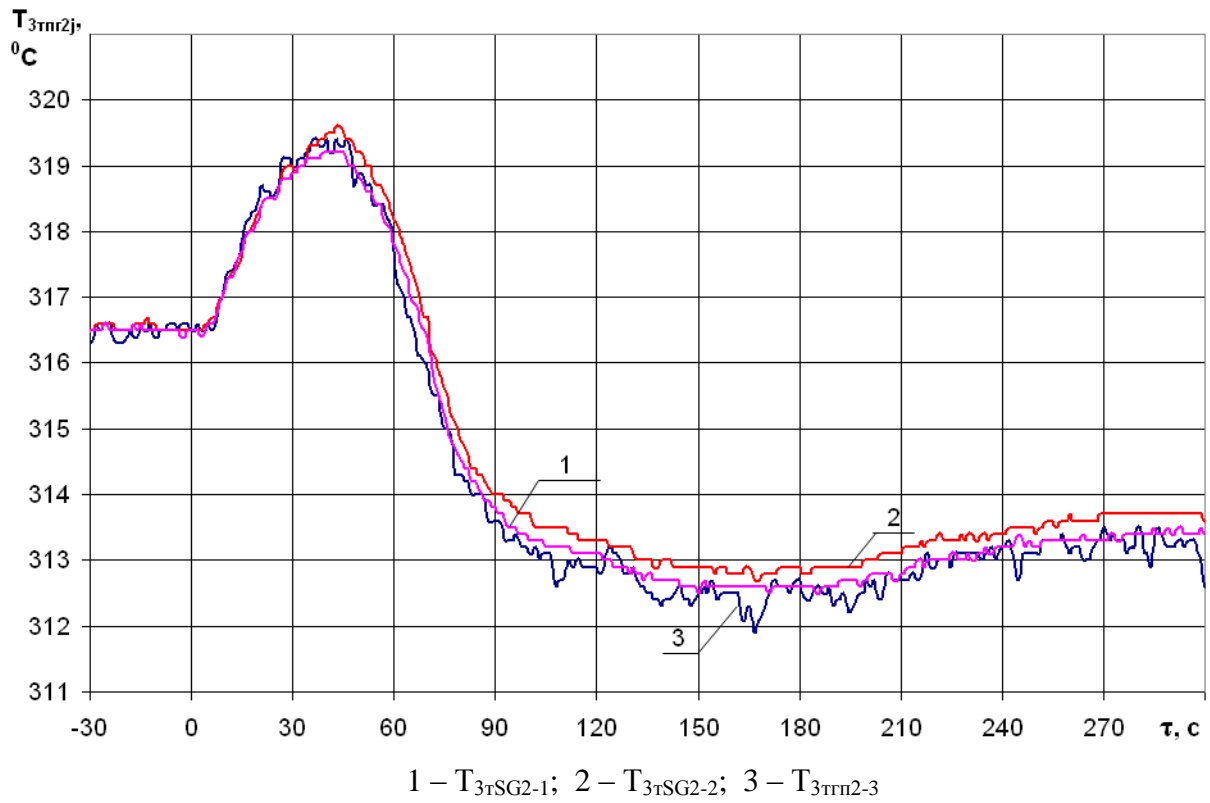


Fig. 31 – Hot leg #3 mean coolant temperature history recorded by the second set of thermocouples

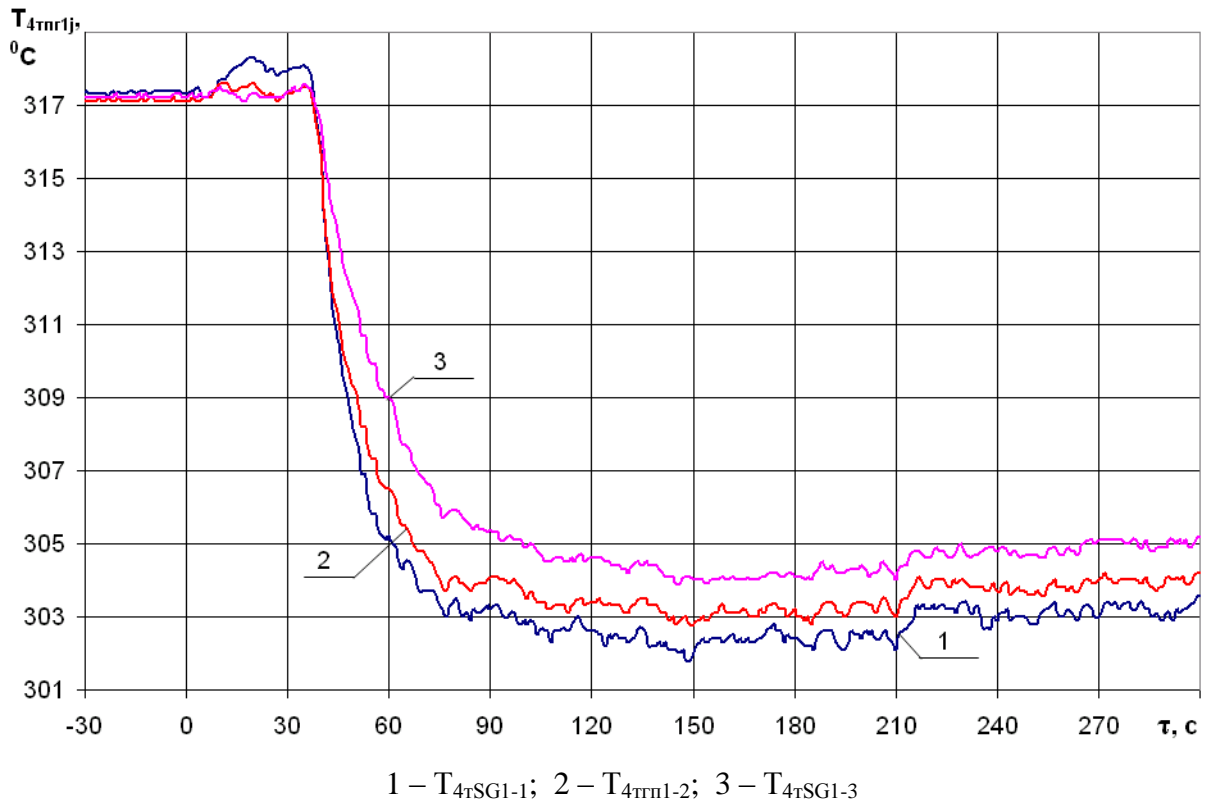


Fig. 32 – Hot leg #4 mean coolant temperature history recorded by the first set of thermocouples

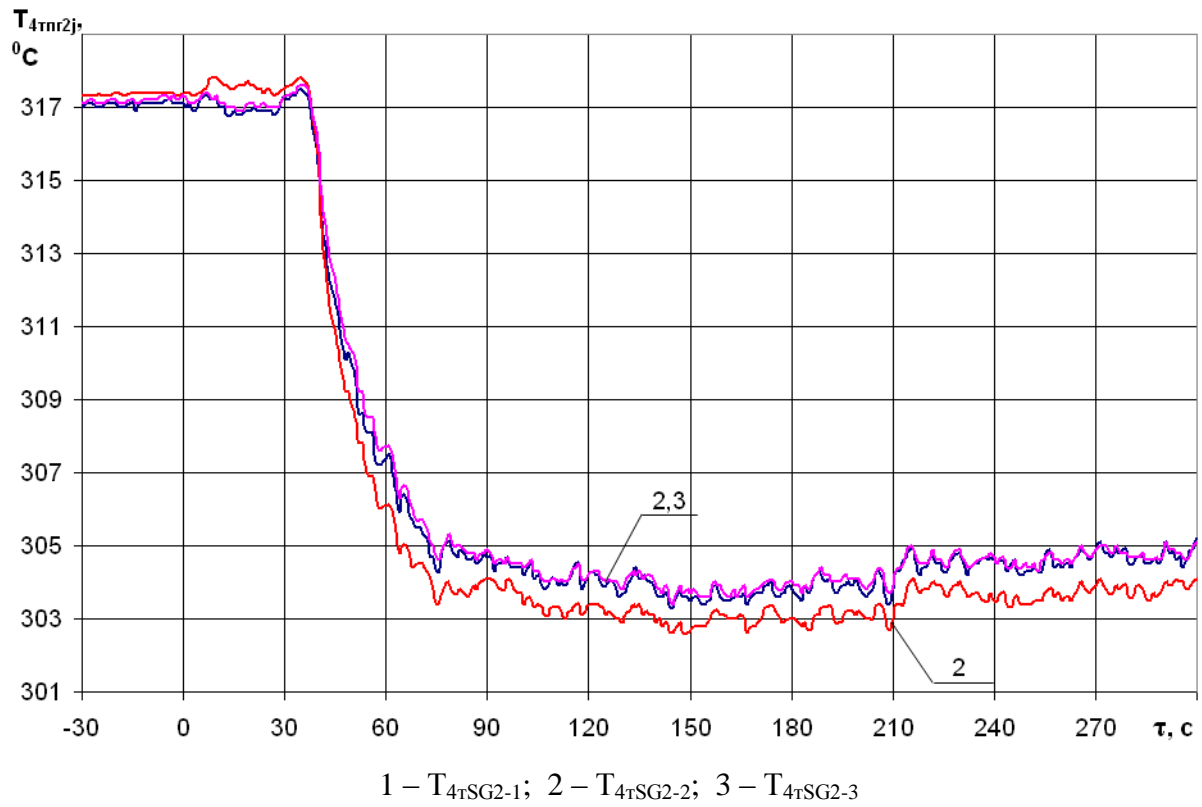


Fig. 33 – Hot leg #4 mean coolant temperature history recorded by the second set of thermocouples

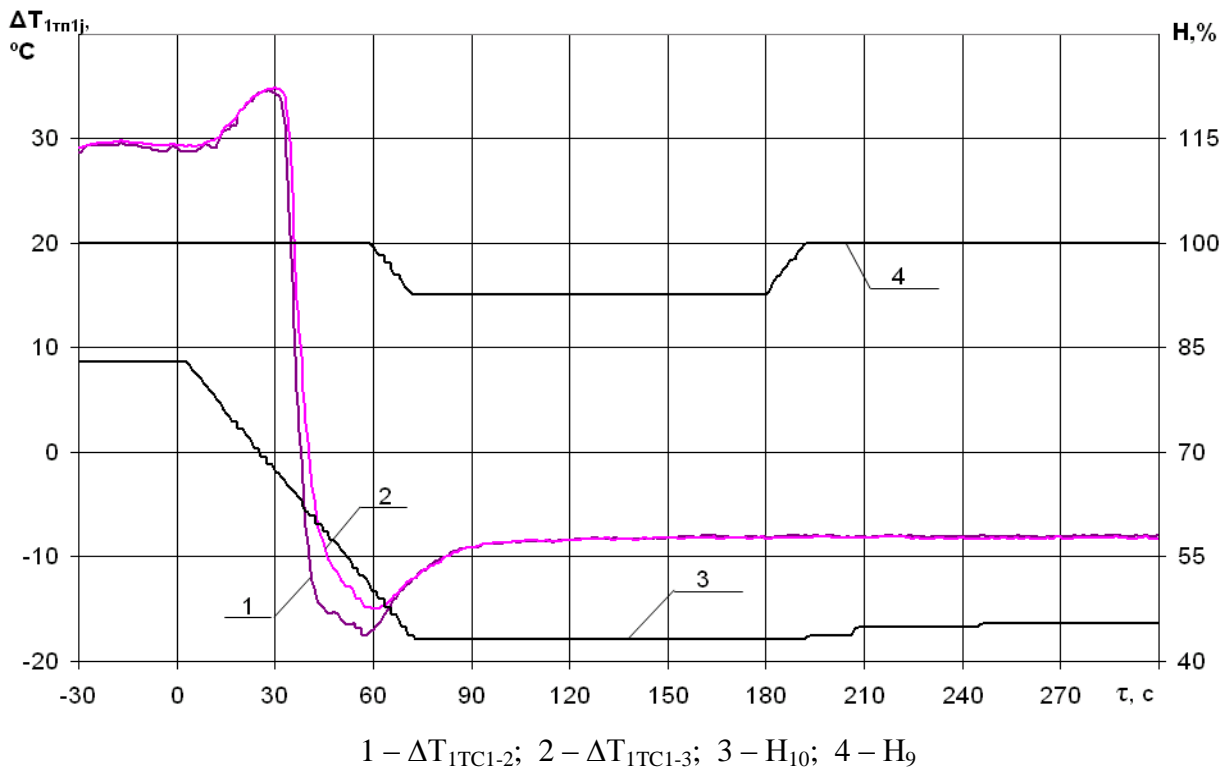


Fig. 34 – Change of CPS-group #10 and #9 positions and the coolant heat-up of loop #1 recorded by the first set of thermocouples

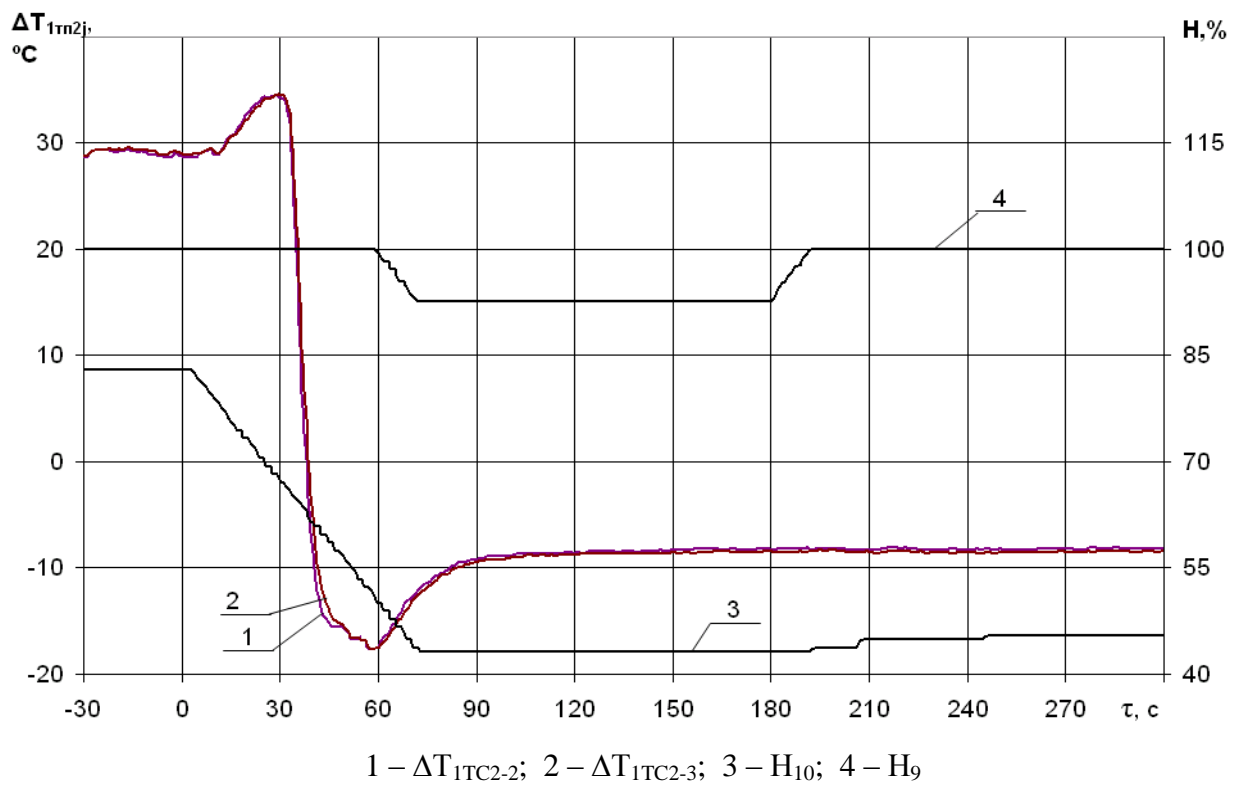


Fig. 35 – Change of CPS-group #10 and #9 positions and the coolant heat-up of loop #1 recorded by the second set of thermocouples

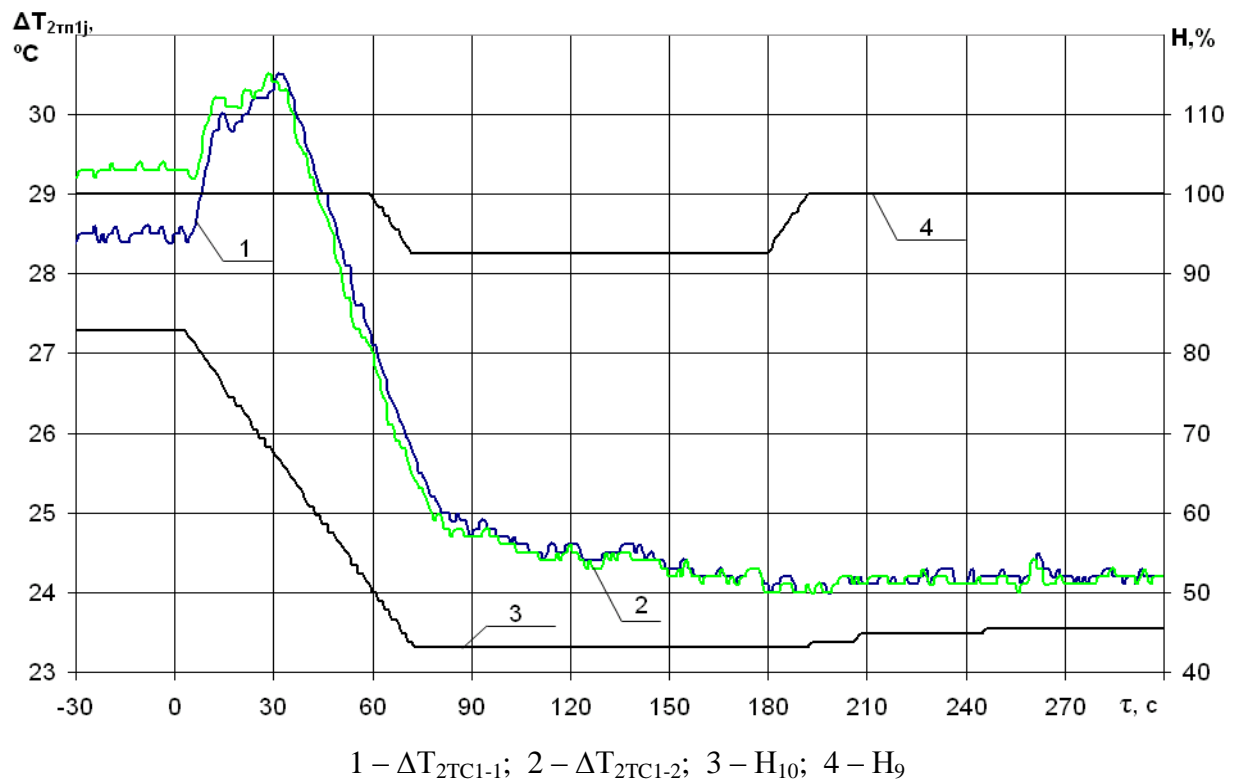


Fig. 36 – Change of CPS-group #10 and #9 positions and the coolant heat-up of loop #2 recorded by the first set of thermocouples

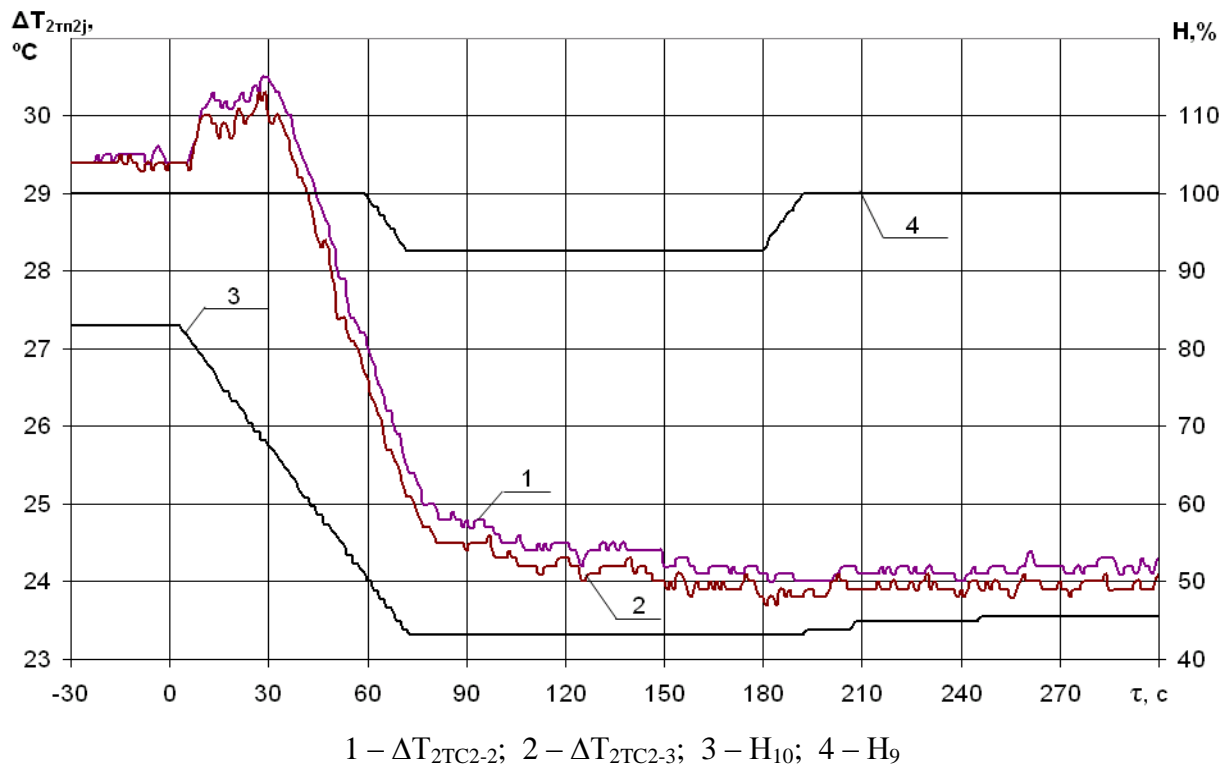


Fig. 37 – Change of CPS-group #10 and #9 positions and the coolant heat-up of loop #2 recorded by the second set of thermocouples

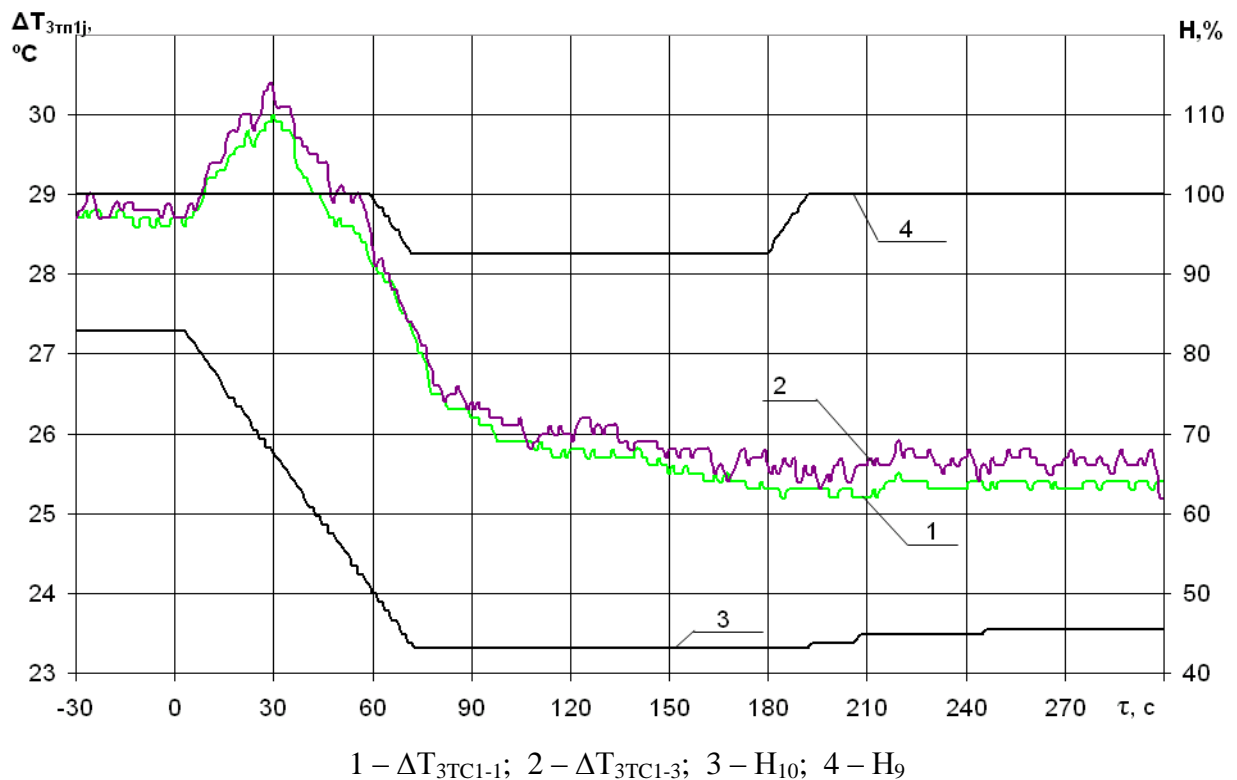


Fig. 38 – Change of CPS-group #10 and #9 positions and the coolant heat-up of loop #3 recorded by the first set of thermocouples

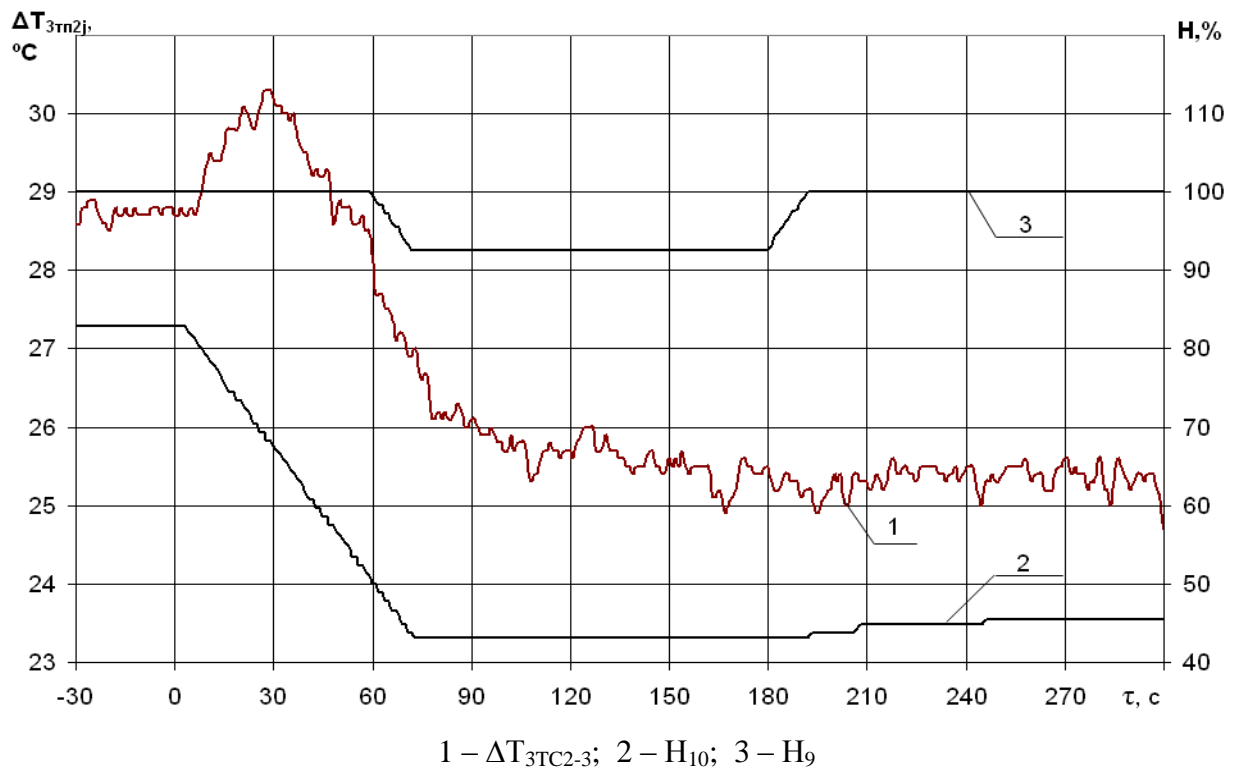


Fig. 39 – Change of CPS-group #10 and #9 positions and the coolant heat-up of loop #3 recorded by the second set of thermocouples

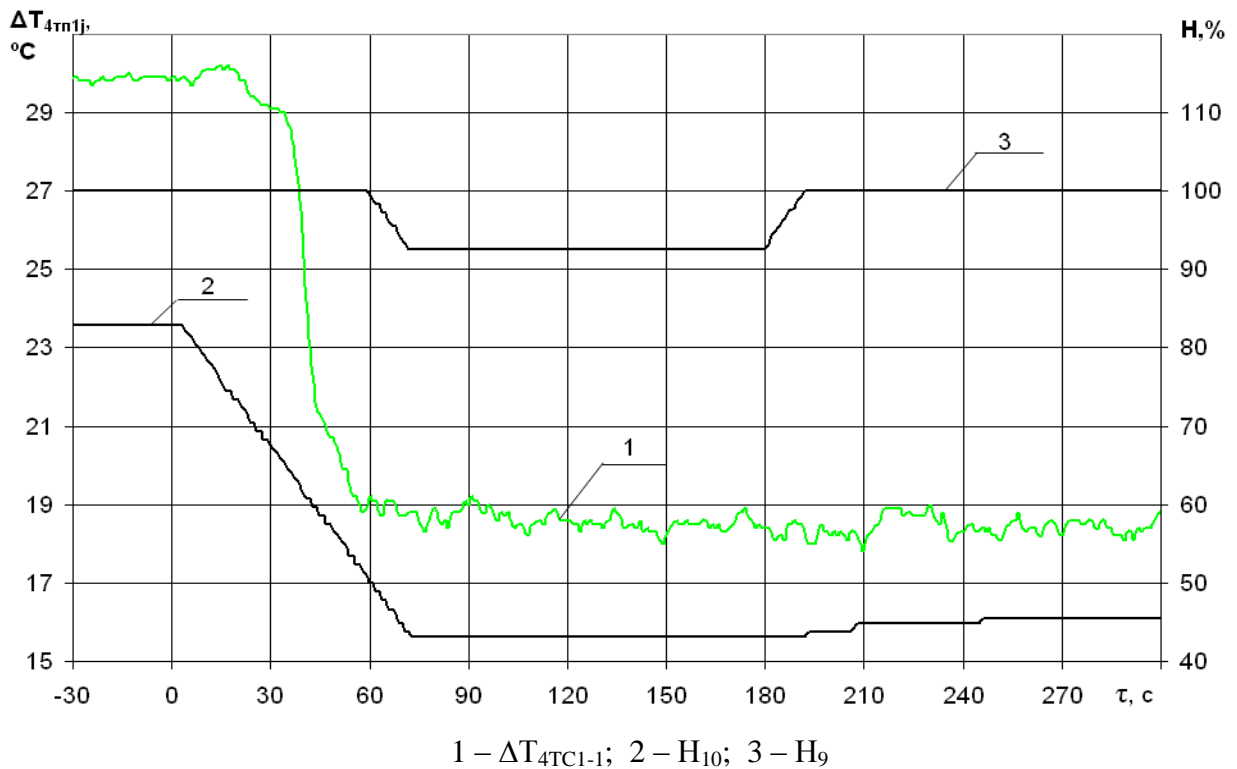


Fig. 40 – Change of CPS-group #10 and #9 positions and the coolant heat-up of loop #4 recorded by the first set of thermocouples

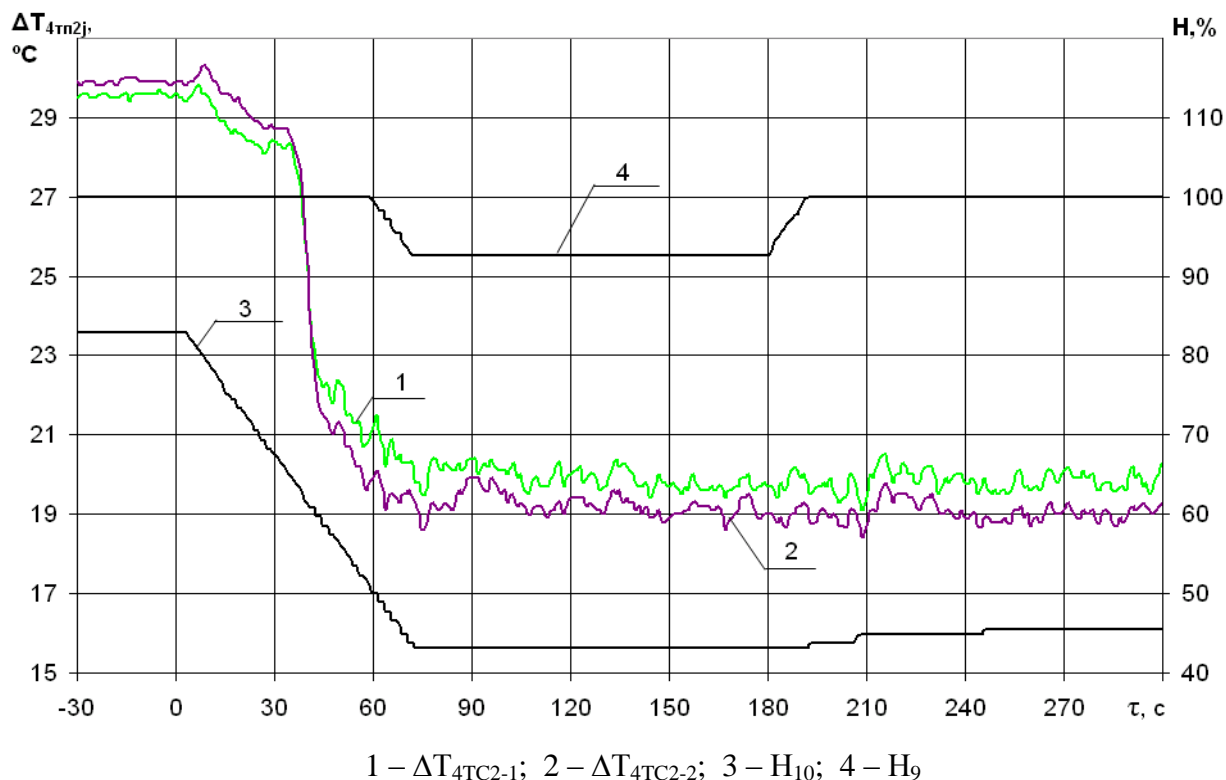


Fig. 41 – Change of CPS-group #10 and #9 positions and the coolant heat-up of loop #4 recorded by the second set of thermocouples

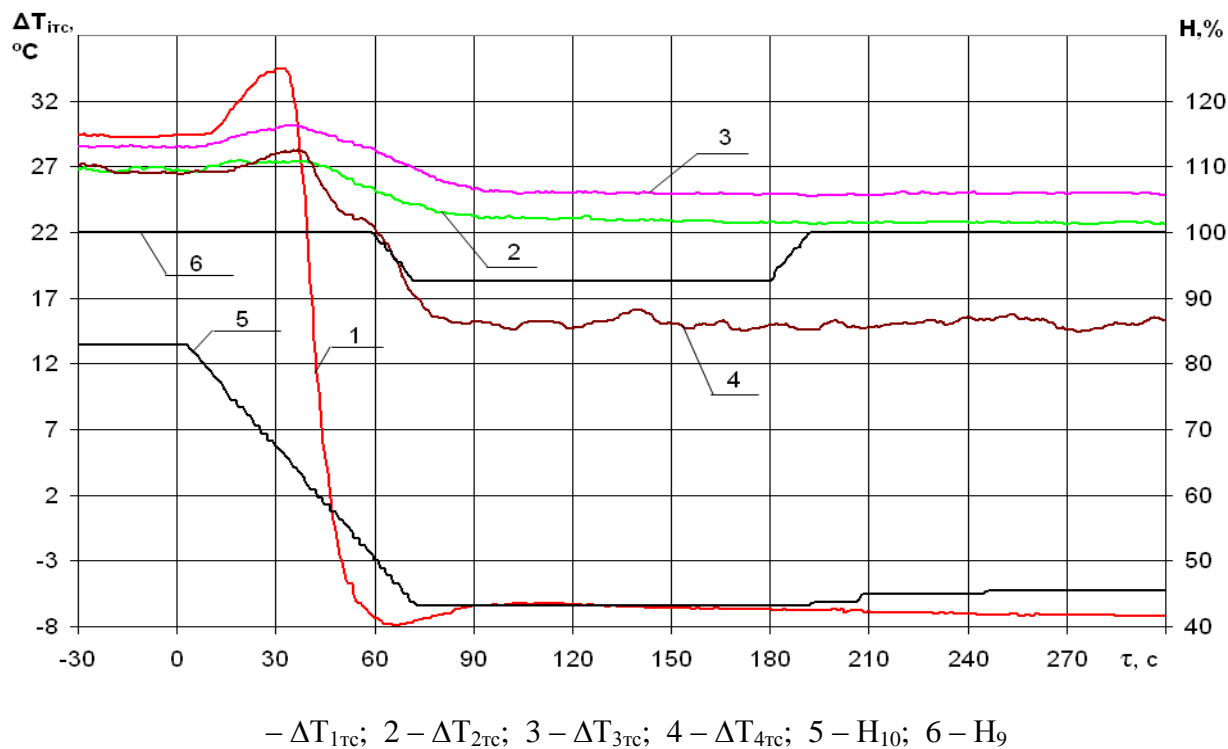


Fig. 42 – Change of CPS-group #10 and #9 positions and the coolant heat-up of all loops of PC recorded by the thermoresistors

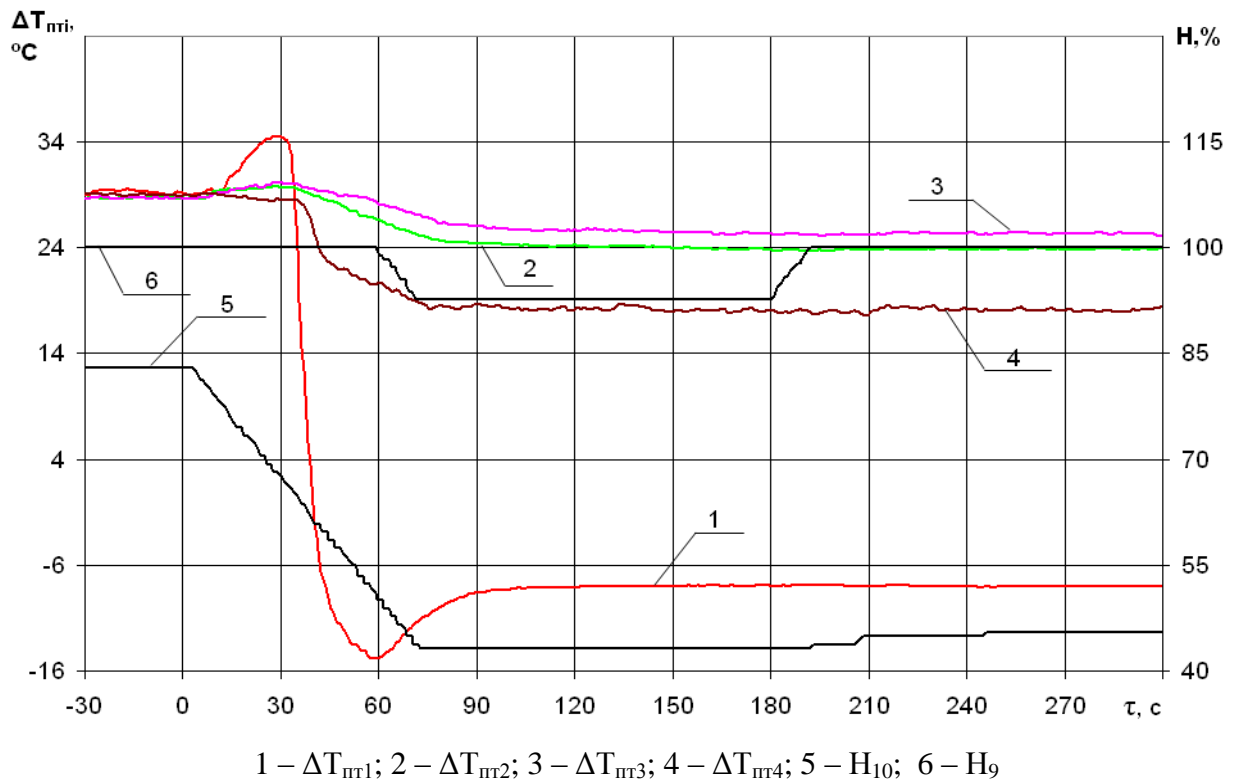


Fig. 43 – Change of CPS-group #10 and #9 positions and the coolant heat-up of all loops of PC recorded by the ICMS

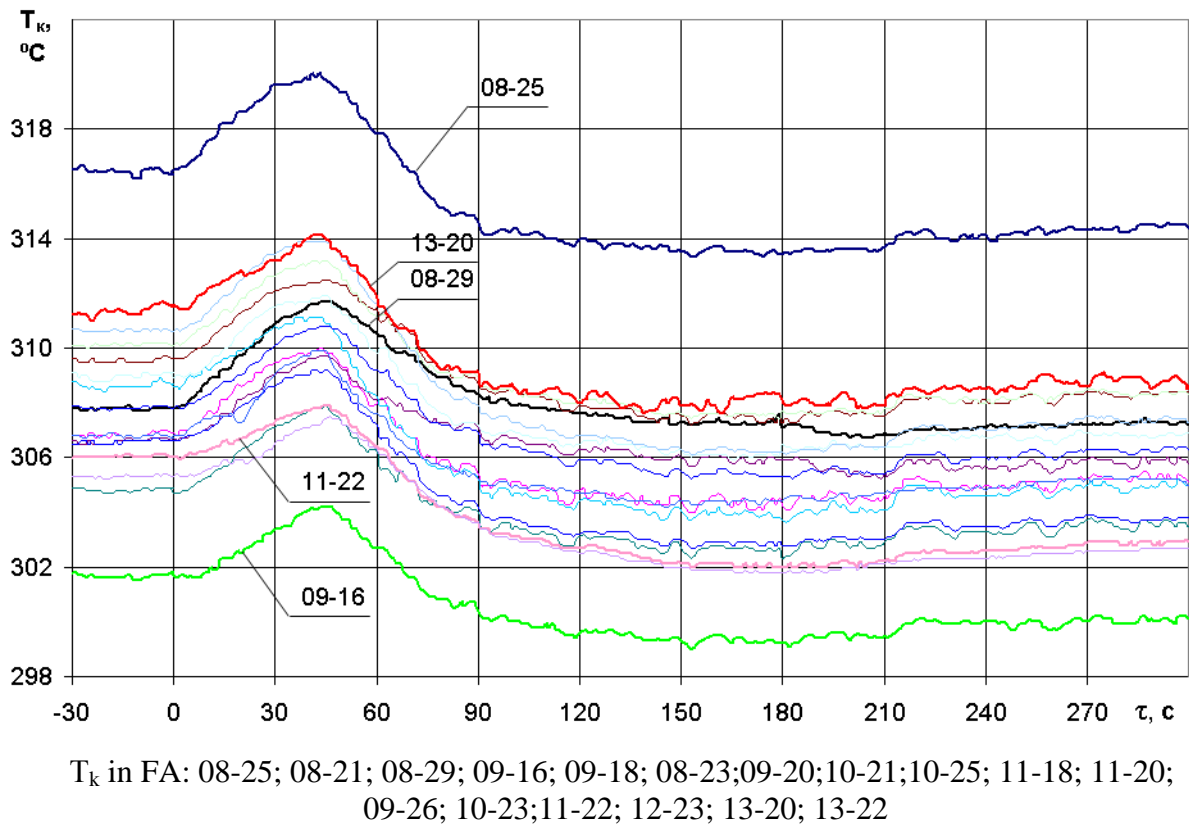
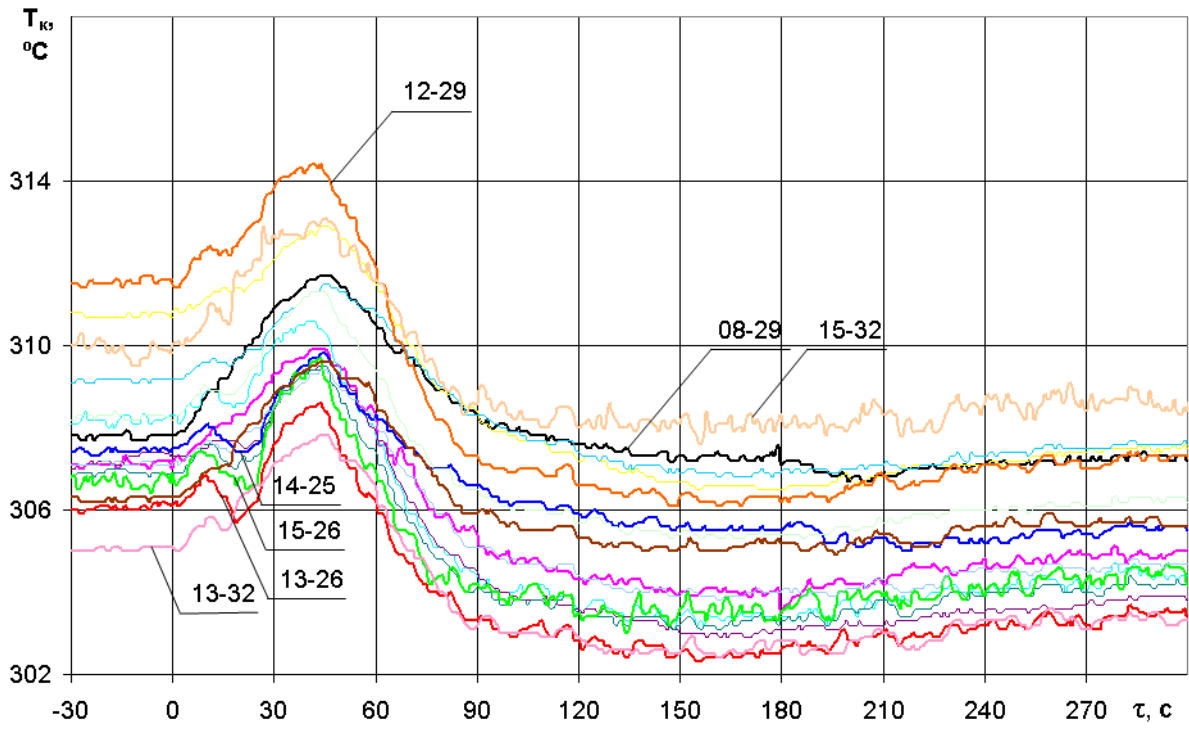
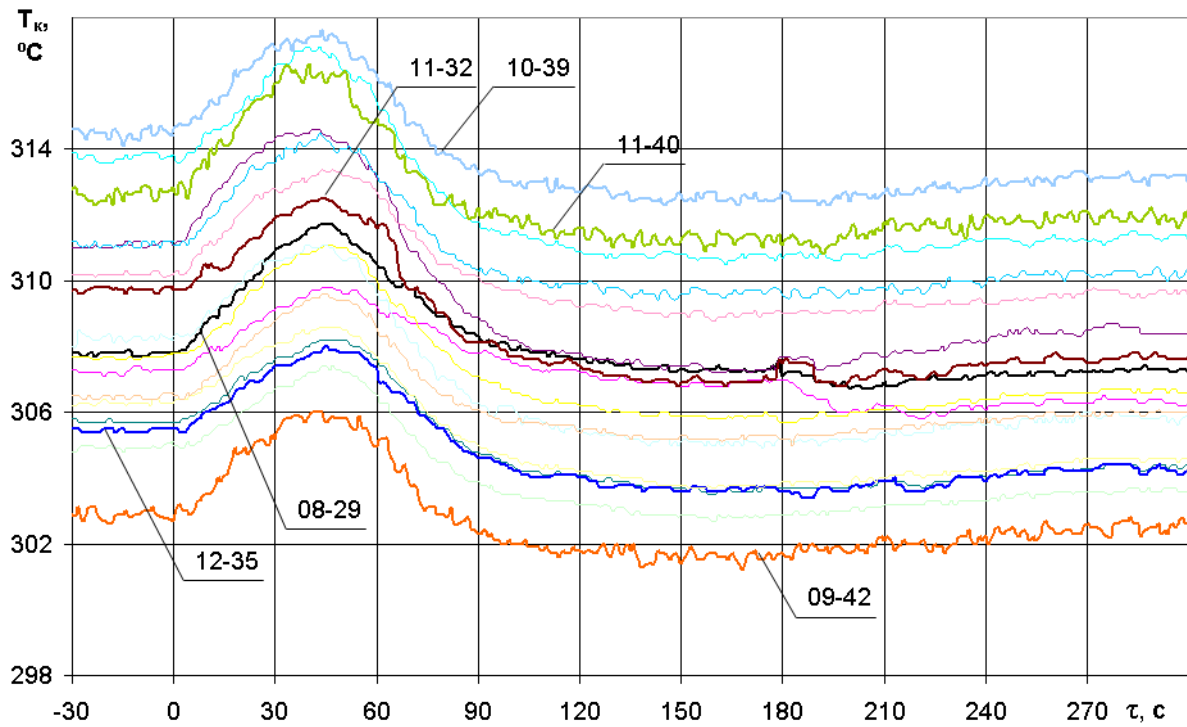


Fig. 44 – FA outlet coolant temperature histories of sector #1 recorded by the ICMS



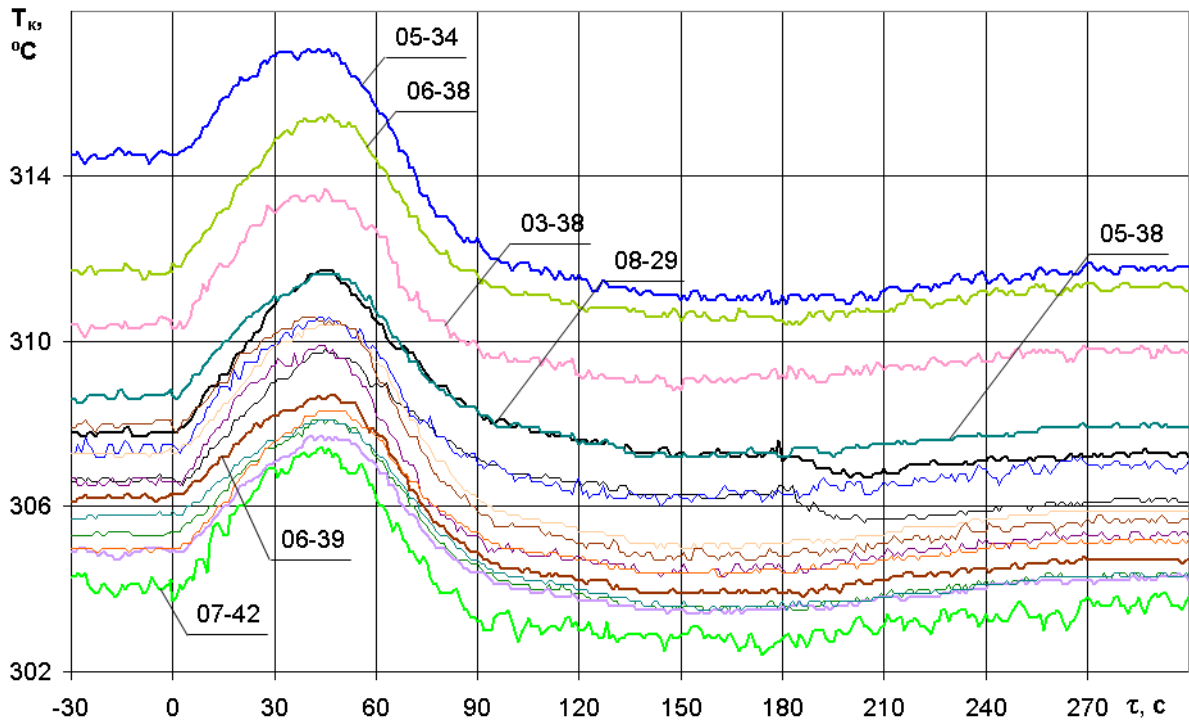
T_k in FA: 08-29; 09-28; 11-26; 11-28; 12-25; 13-26; 13-28; 4-25; 14-29; 15-26; 10-29; 12-29; 13-30; 13-32; 14-33; 15-32

Fig. 45 – FA outlet coolant temperature histories of sector #2 recorded by the ICMS



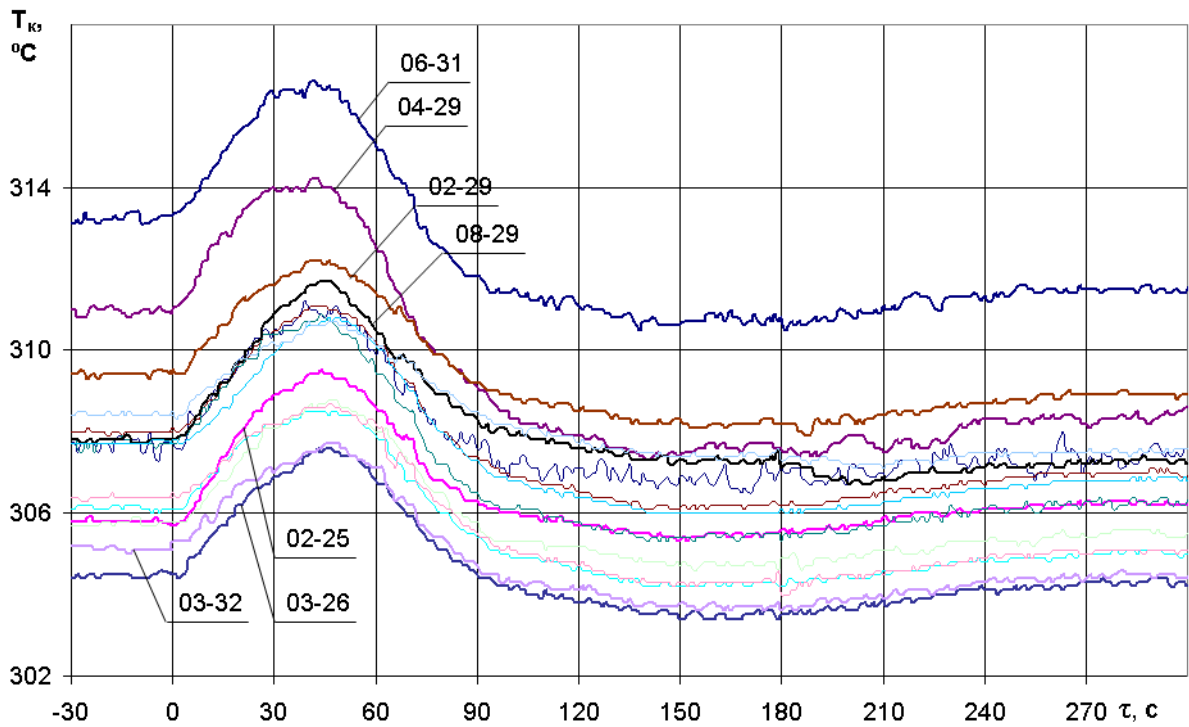
T_k in FA: 08-29; 13-36; 09-32; 10-31; 10-35; 11-32; 11-36; 12-35; 13-38; 09-34; 09-38; 10-37; 10-39; 11-38; 11-40; 09-40; 09-42

Fig. 46 – FA outlet coolant temperature histories of sector #3 recorded by the ICMS



T_k in FA: 08-29; 08-35; 07-40; 07-42; 08-37; 08-39; 05-38; 05-40; 06-39; 06-38; 07-32;
07-34; 07-38; 03-38; 04-35; 05-34; 05-36; 03-36

Fig. 47 – FA outlet coolant temperature histories of sector #4 recorded by the ICMS



T_k in FA: 01-28; 02-25; 03-36; 03-28; 04-29; 06-29; 05-28; 08-29; 05-32; 06-31; 01-30;
02-29; 02-33; 03-30; 03-32

Fig. 48 – FA outlet coolant temperature histories of sector #5 recorded by the ICMS

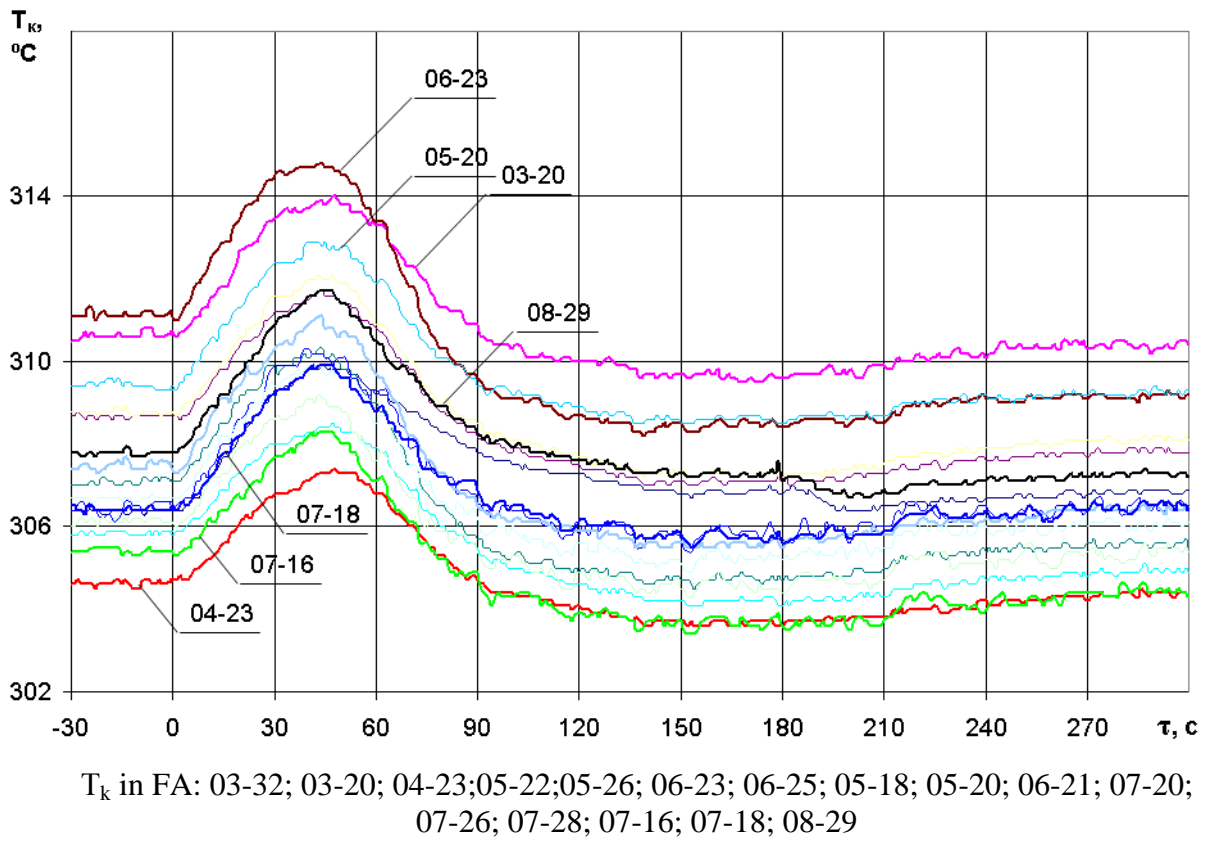


Fig. 49 – FA outlet coolant temperature histories of sector #6 recorded by the ICMS

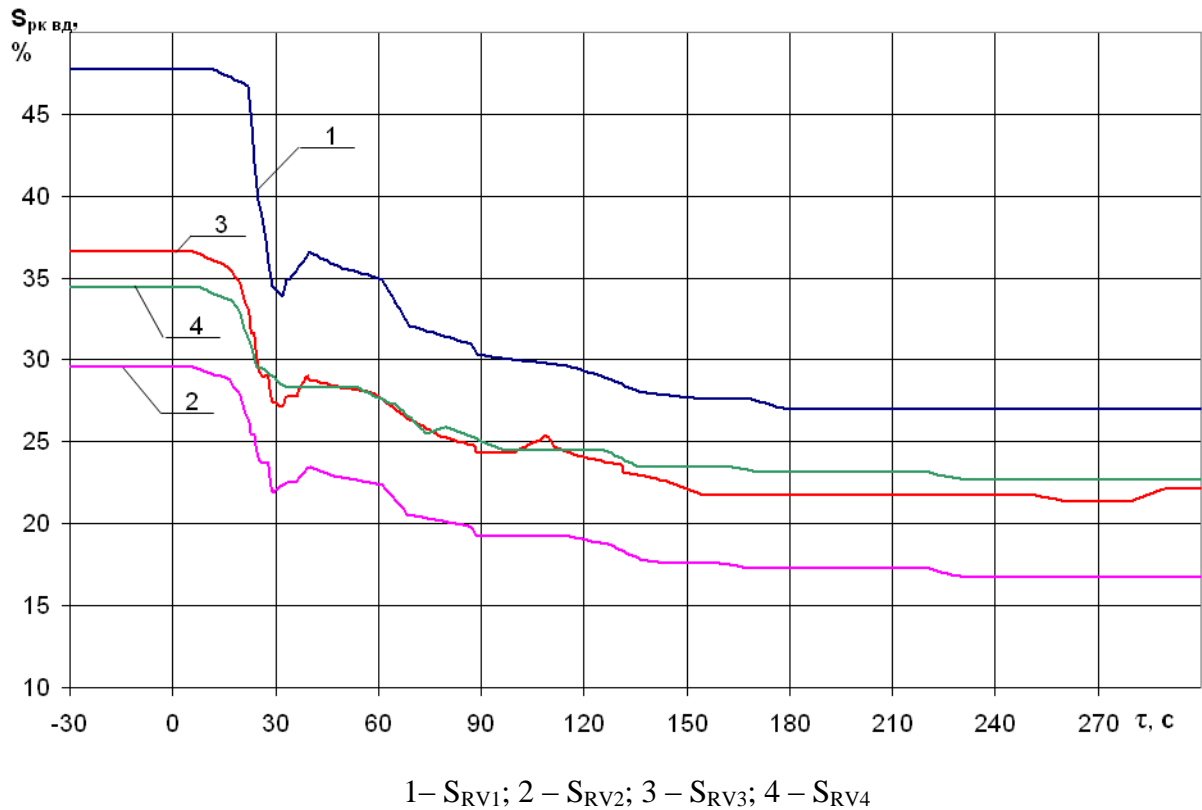


Fig. 50 – Change of the HP regulating valves' positions recorded by UBLS

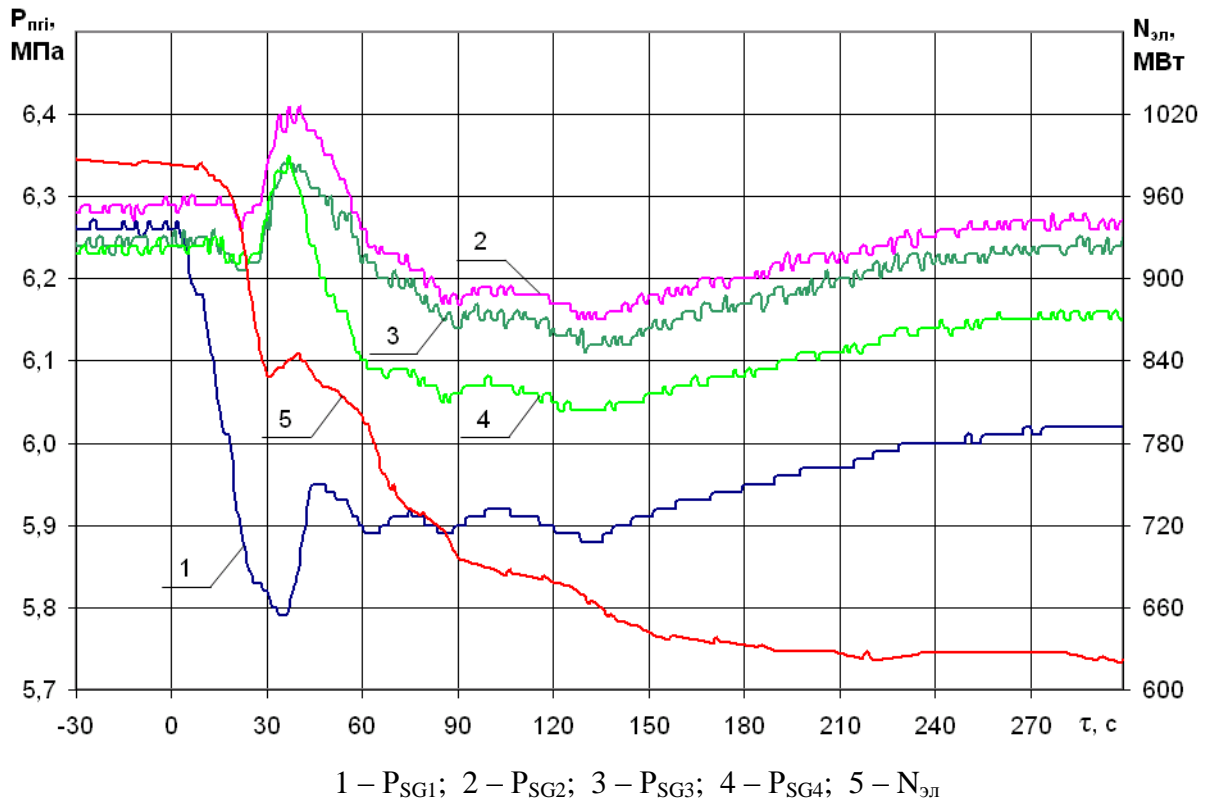


Fig. 51 – SG-#1–4 pressure histories and the electrical power history of TG recorded by the ICMS

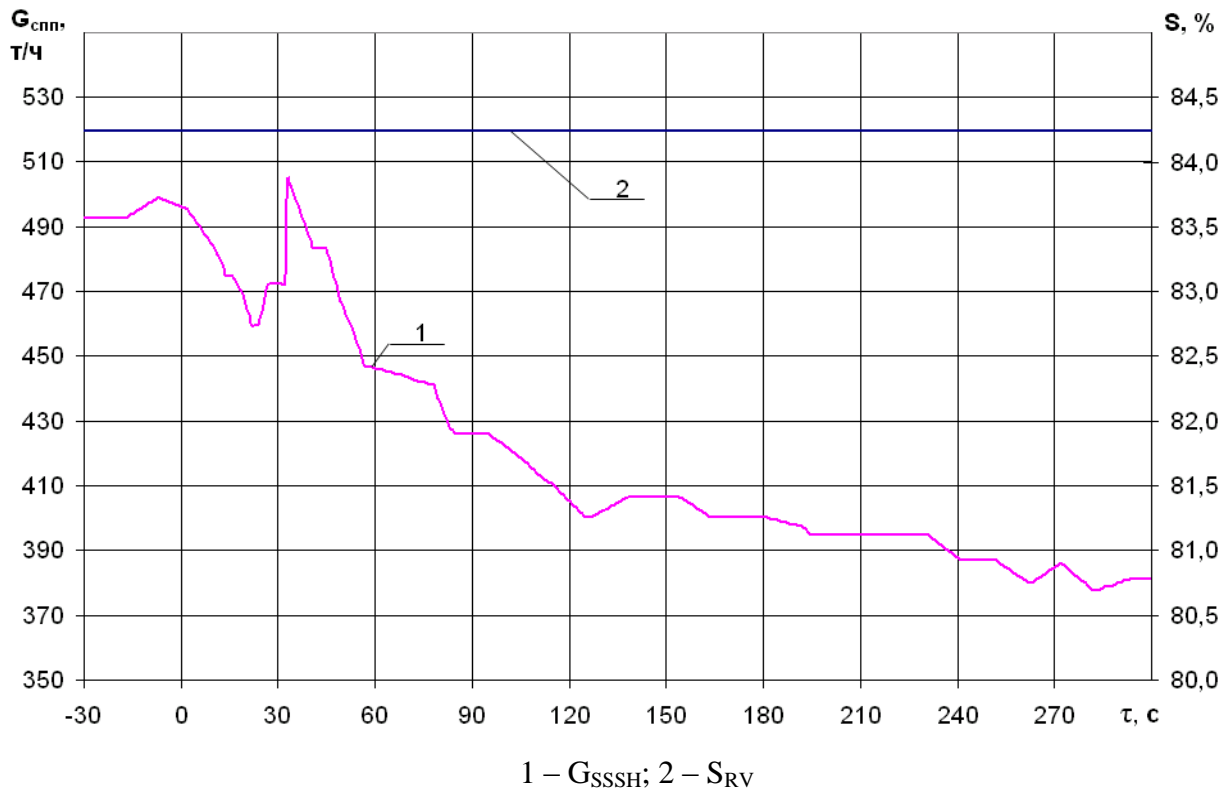


Fig. 52 – SSSH heating steam flow rate histories and the time history of the RV position on the steam supply line of the SSSH

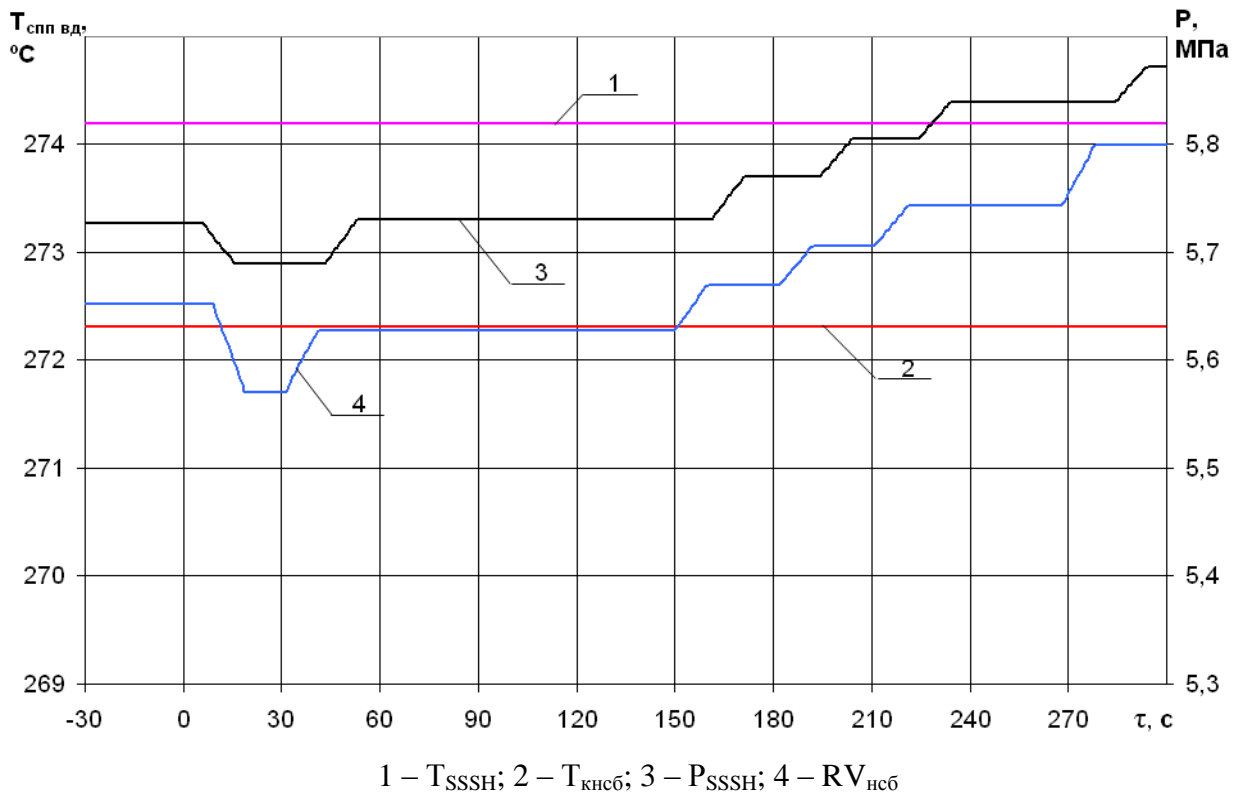


Fig. 53 – Temperature and pressure histories of the heating steam upstream the SSSH and in the condensate collector recorded by the UBLS

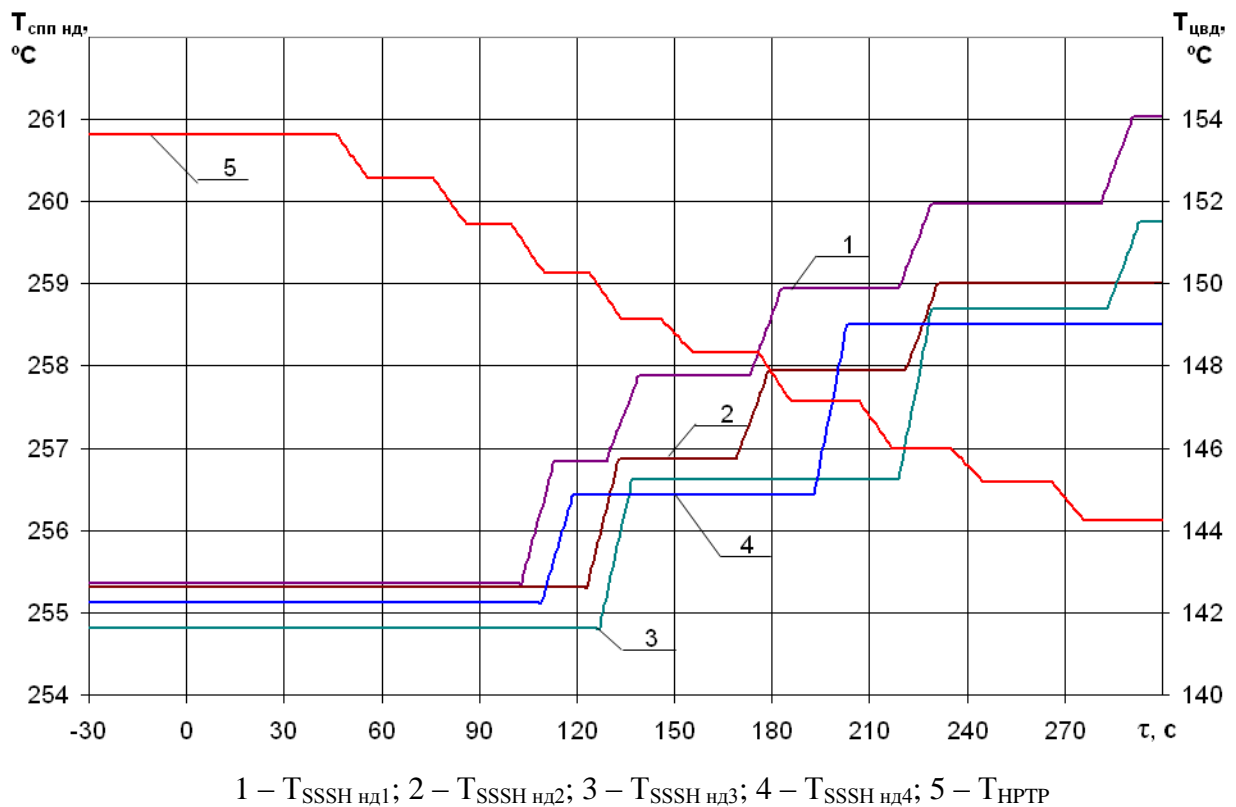


Fig. 54 – Steam temperature histories at the outlet of the HPTP and downstream of the low pressure SSSH1-4 recorded by UBLS

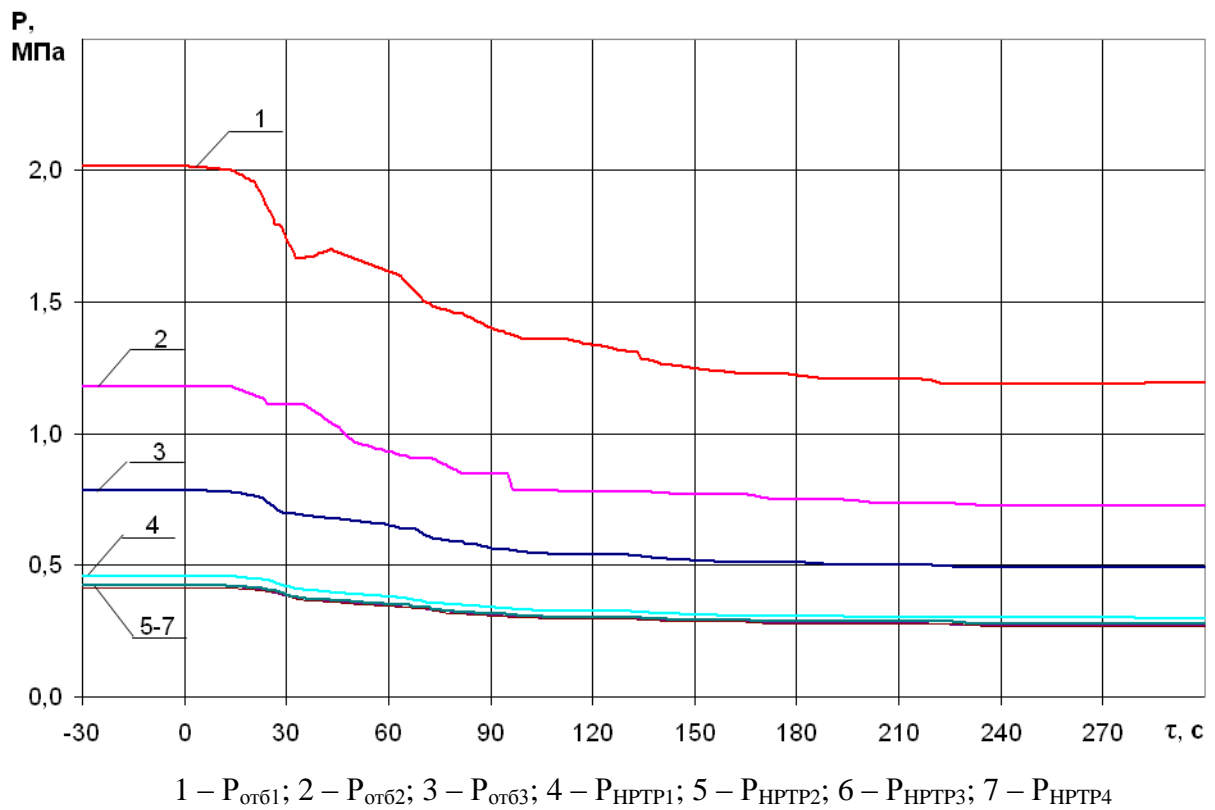


Fig. 55 – Steam pressure histories of the intakes #1-3 and at the outlet from HPTP #1-4 recorded by UBLS during

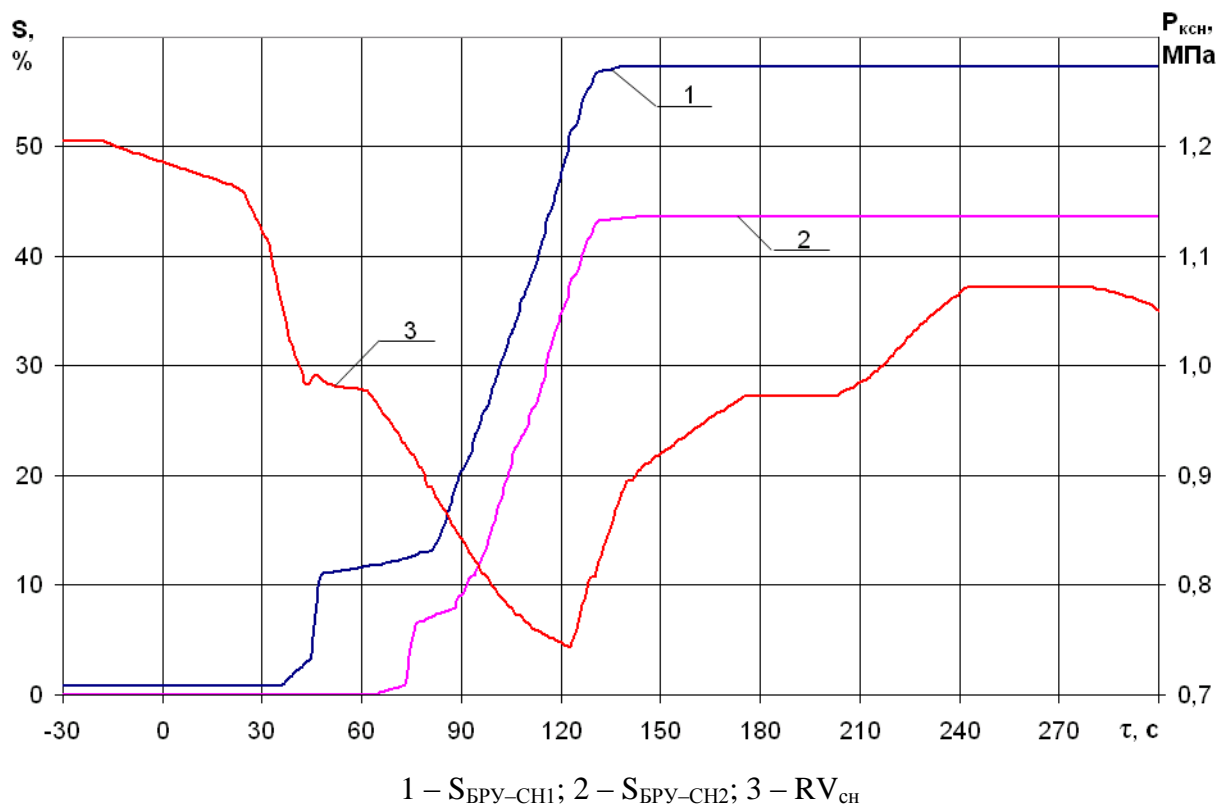
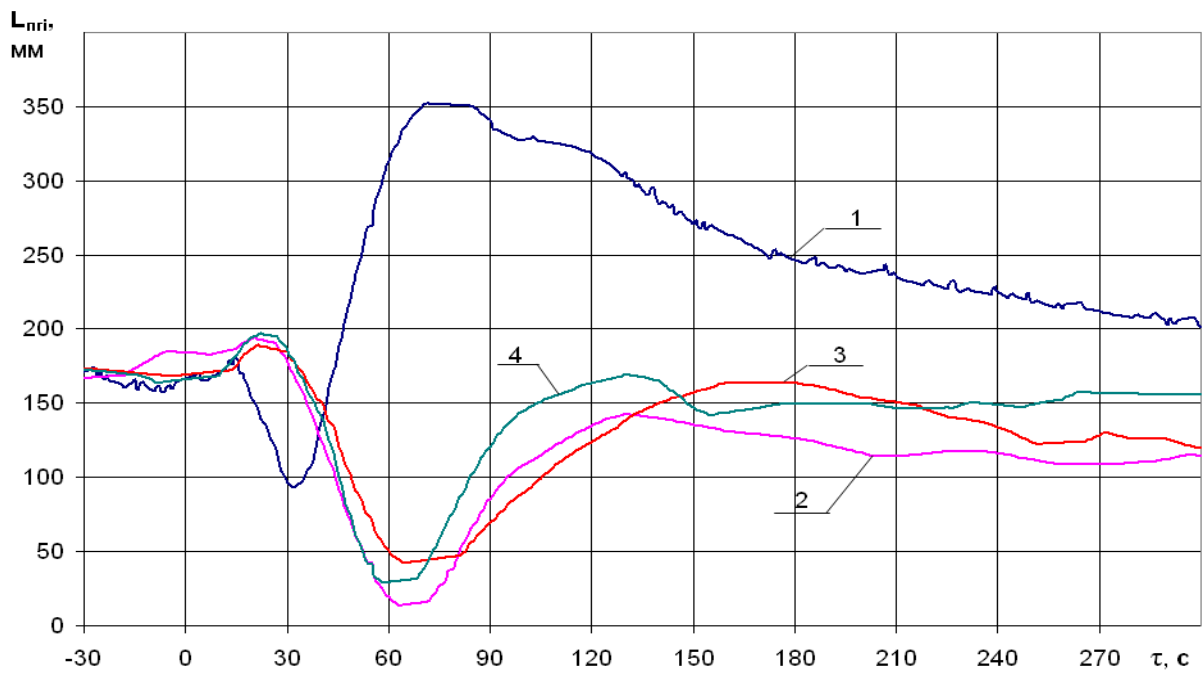
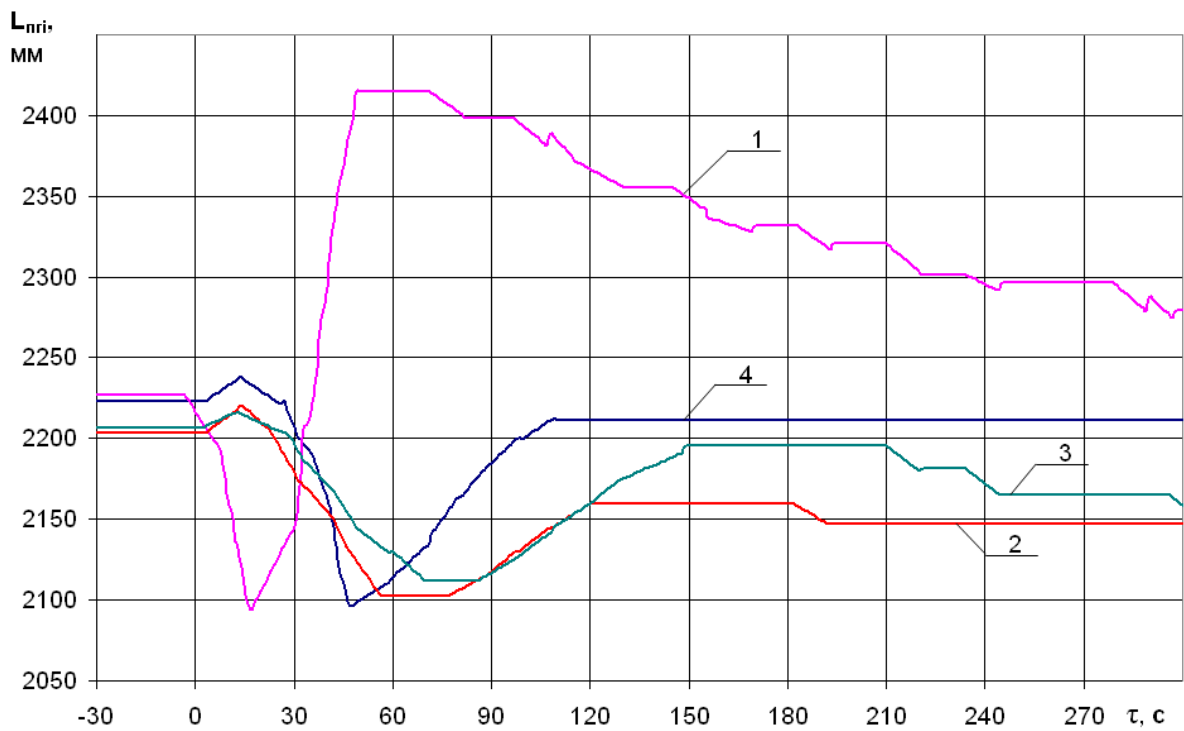


Fig. 56 – Change of the FASB-HL valve position and the pressure histories of ISC recorded by UBLS



1 – L_{SG1}; 2 – L_{SG2}; 3 – L_{SG3}; 4 – L_{SG4}

Fig. 57 – SG water level histories (measurements on “small” basis) by UBL5



1 – L_{SG1}; 2 – L_{SG2}; 3 – L_{SG3}; 4 – L_{SG4}

Fig. 58 – SG water level histories (measurements on “large” basis) by UBL5

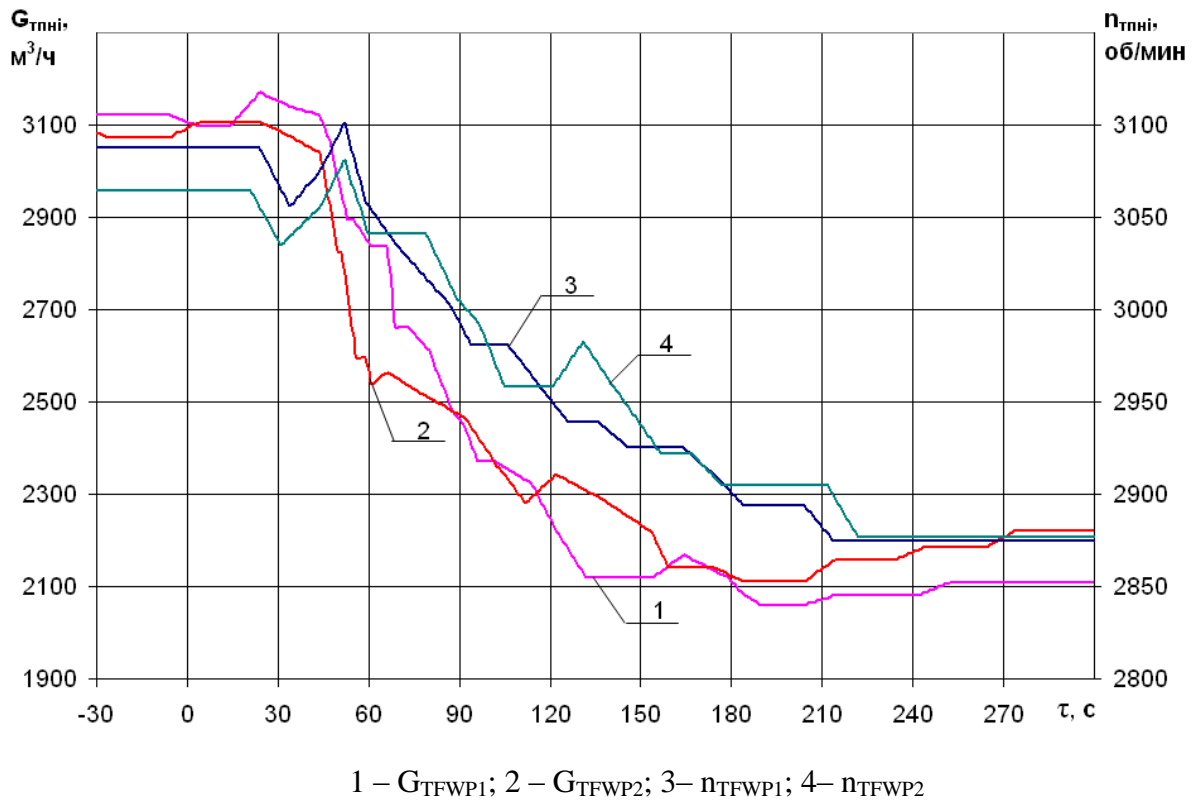


Fig. 59 – Change in flow rates of the feedwater at pressure side and the rotation speed of the turbine feedwater pumps recorded by the UBLS

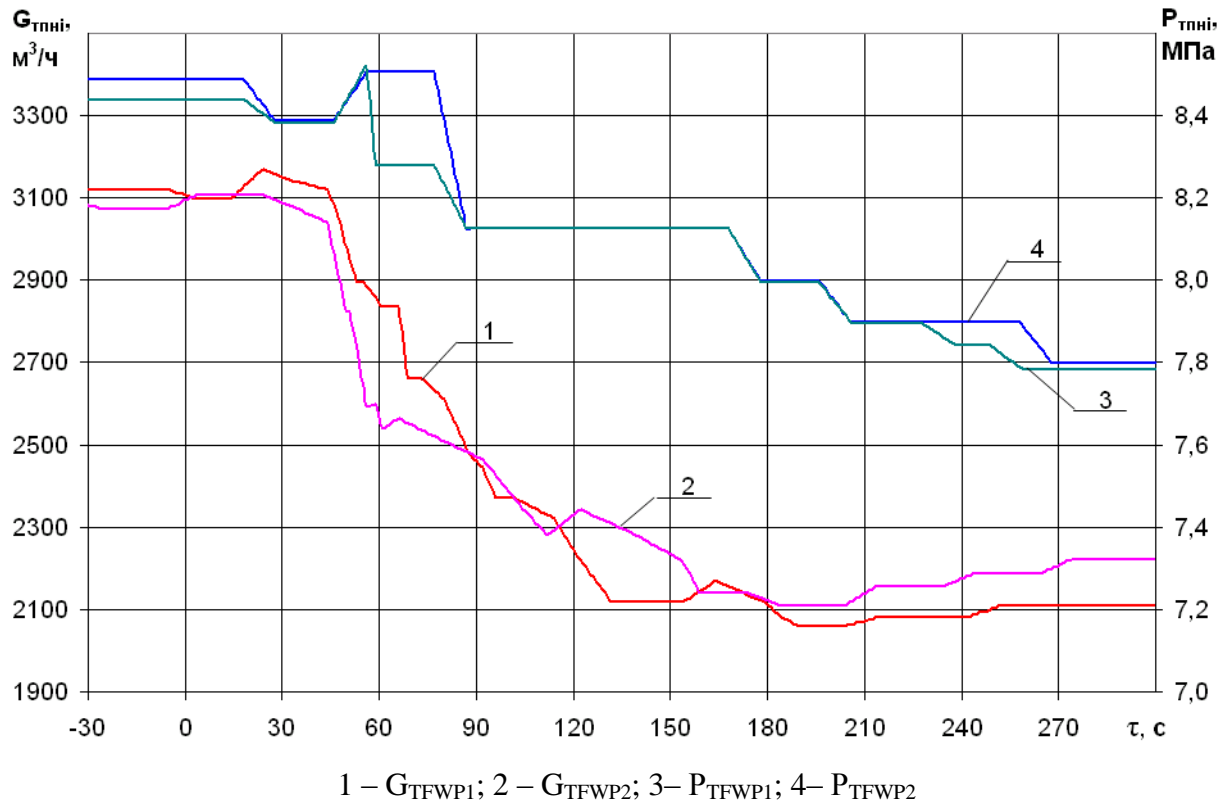


Fig. 60 – Feedwater flow rate histories and pressure at the pressure side of the TFWP-#1-2 recorded by UBLS

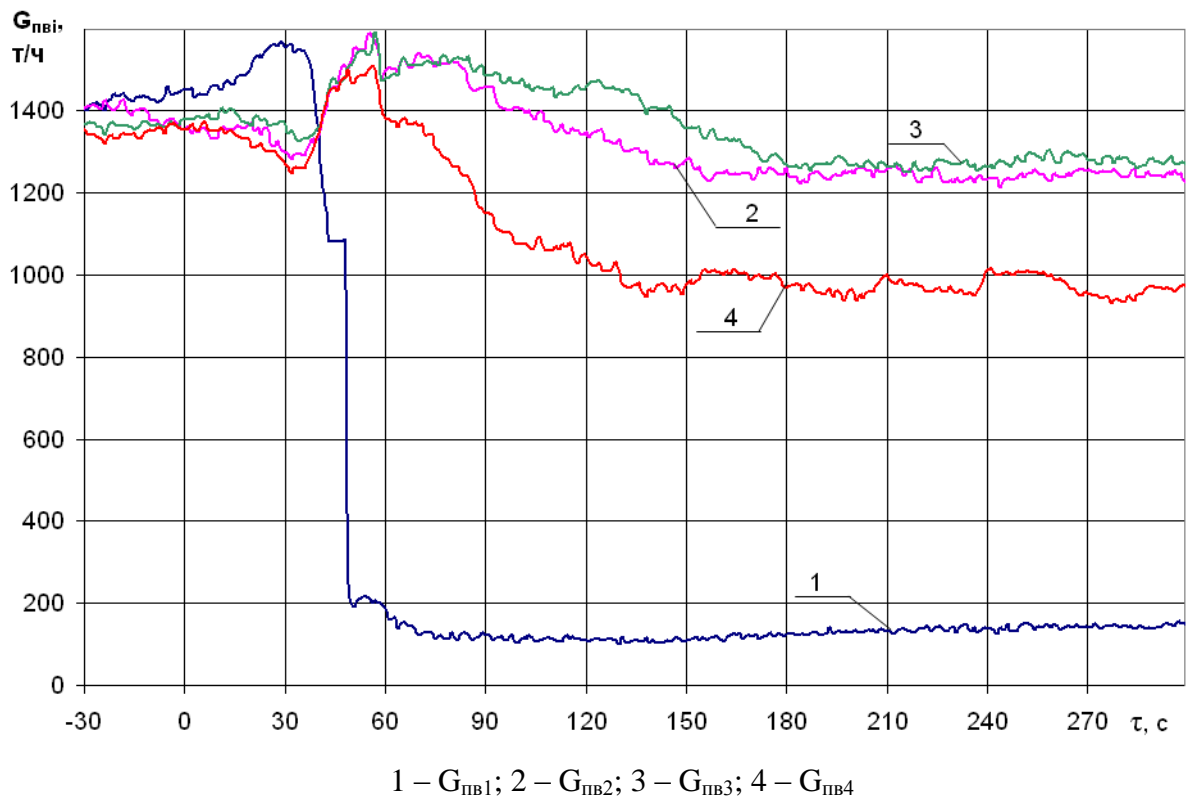


Fig. 61 – SG-1-4 feedwater flow rate histories recorded by ICMS

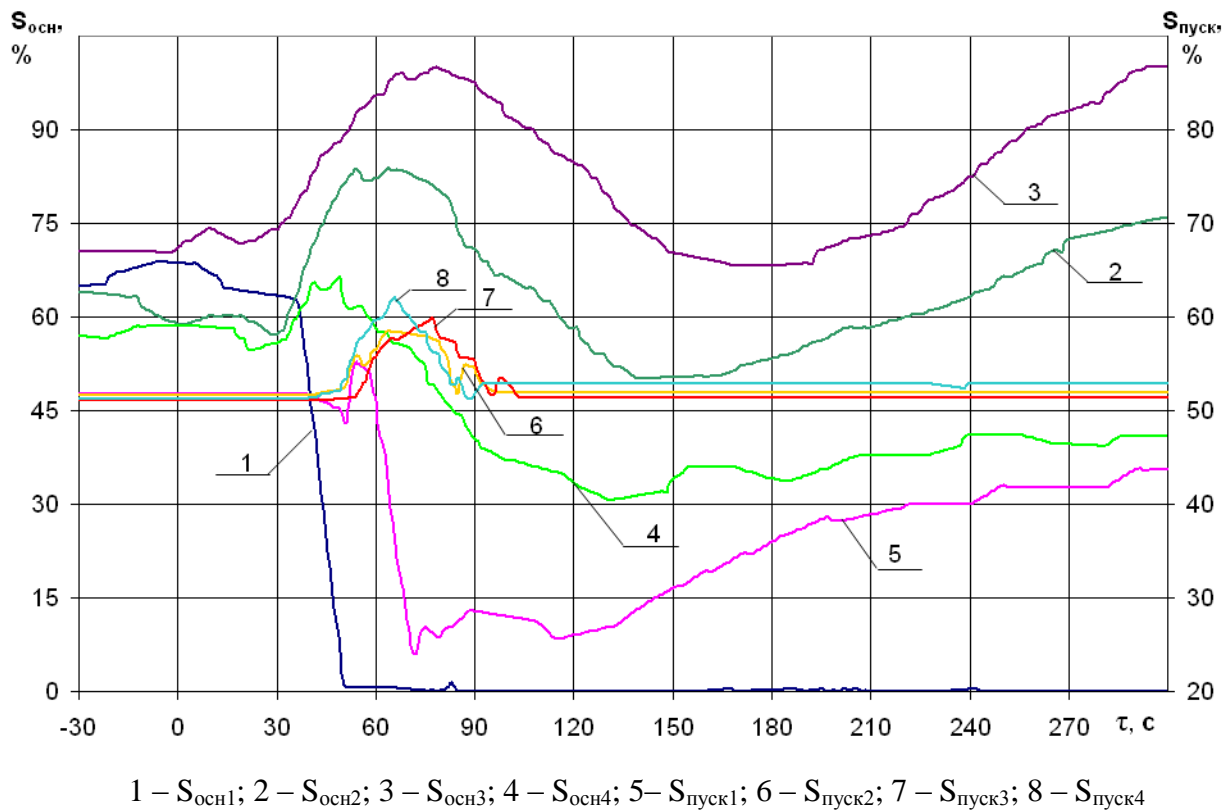


Fig. 62 – Degree of opening of the SG-1-4 feedwater main and starting valves recorded by the UBLS

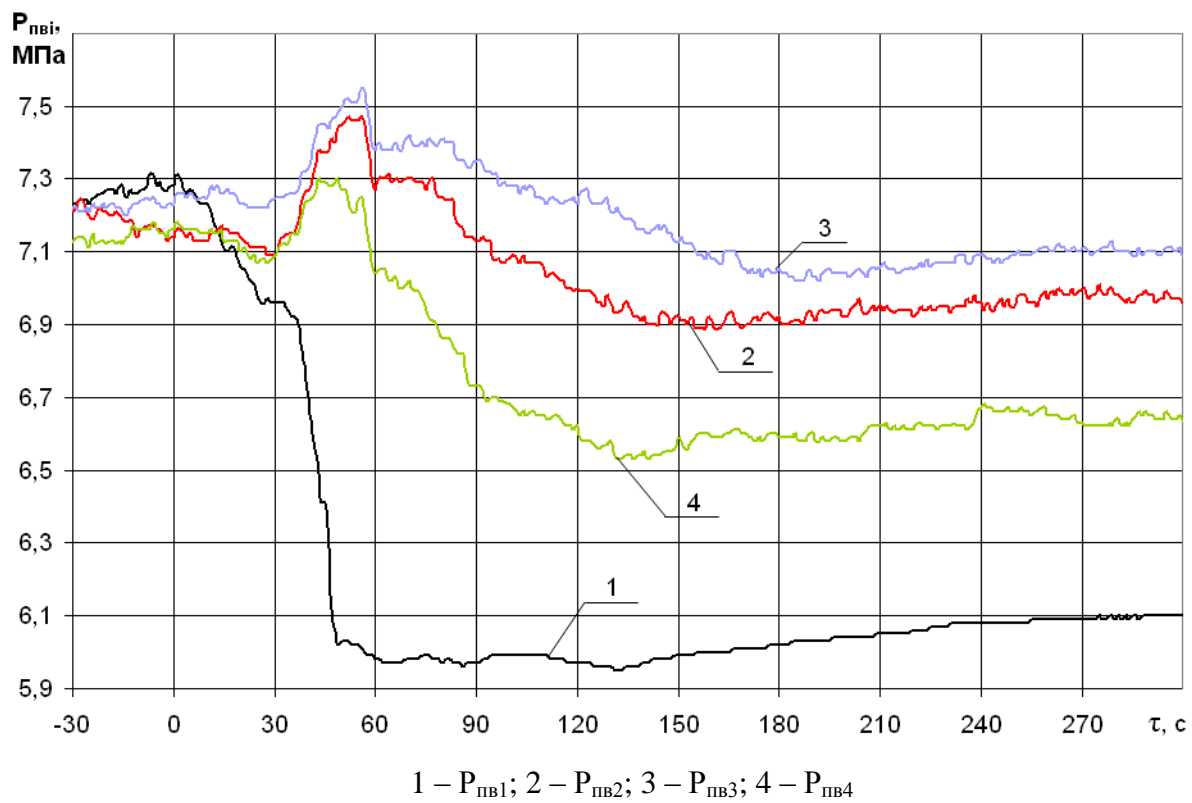


Fig. 63 – SG-1-4 feedwater pressure histories recorded by the ICMS

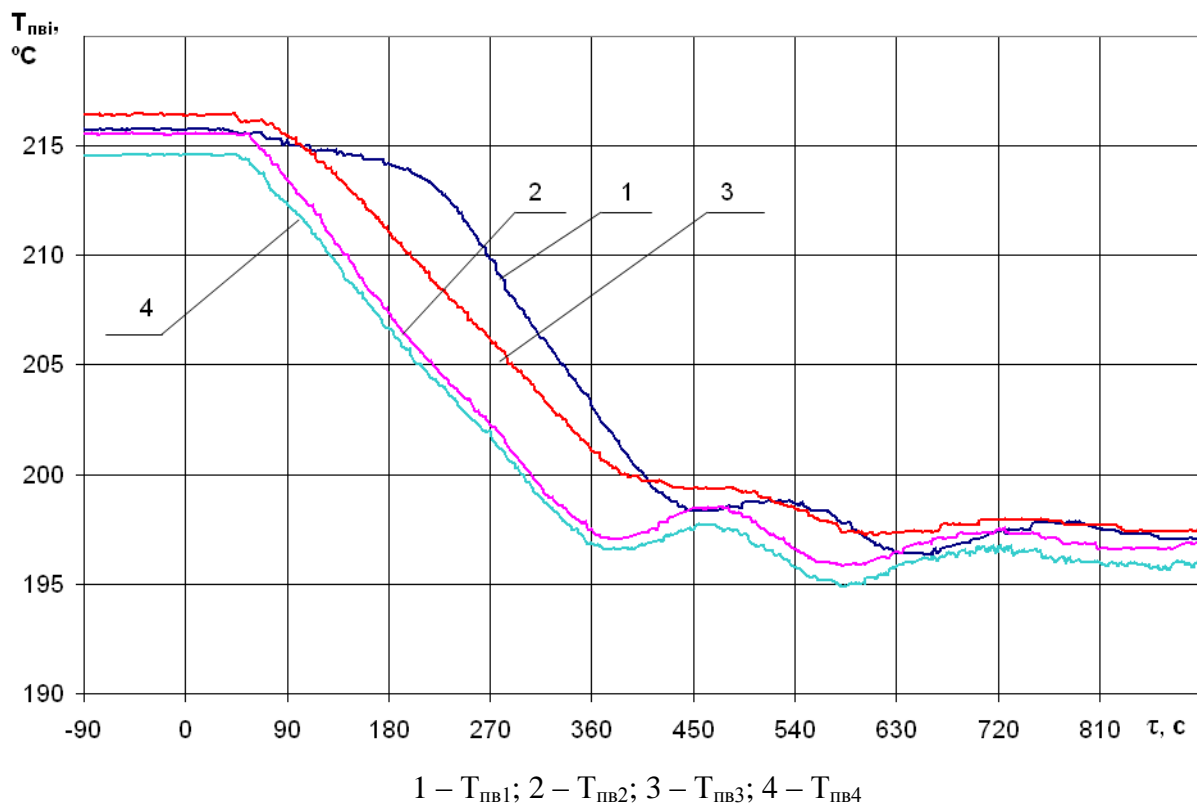


Fig. 64 – SG-1-4 feedwater temperature histories recorded by the ICMS

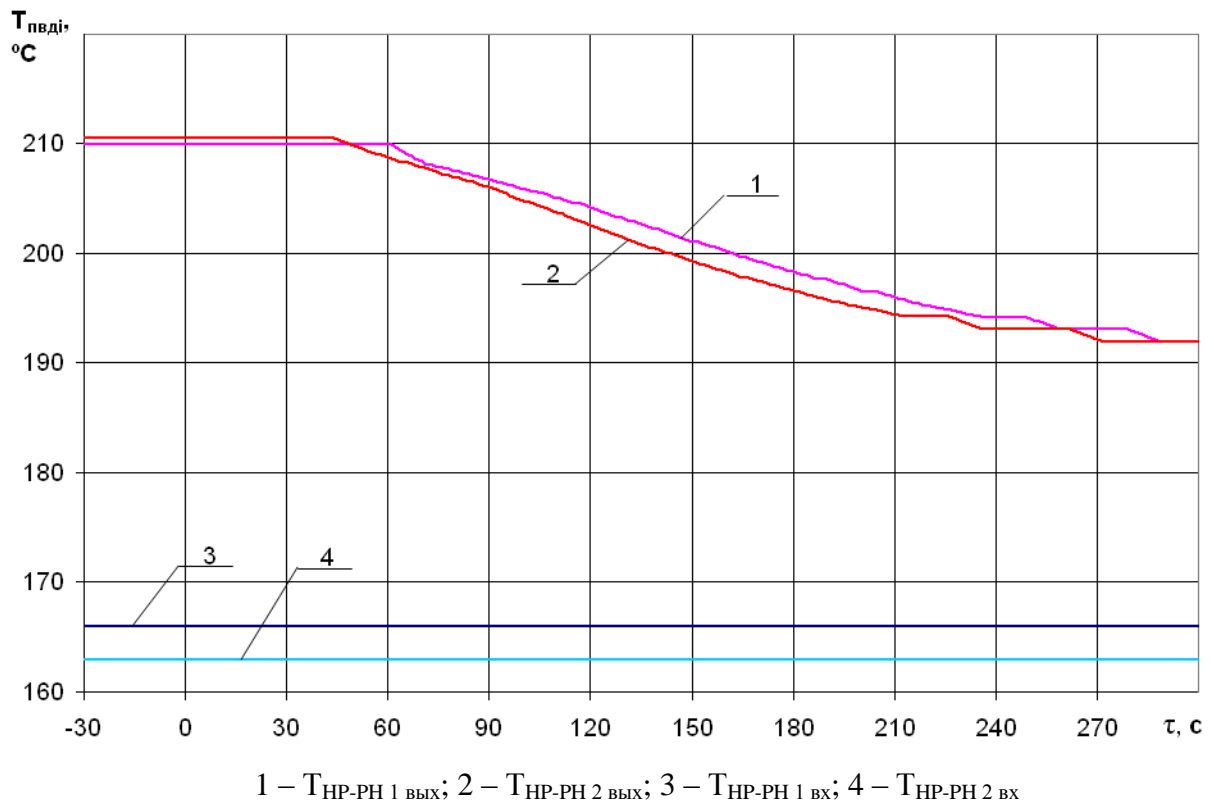


Fig. 65 – Inlet and outlet feedwater temperature histories of the HP-PH recorded by UBLS

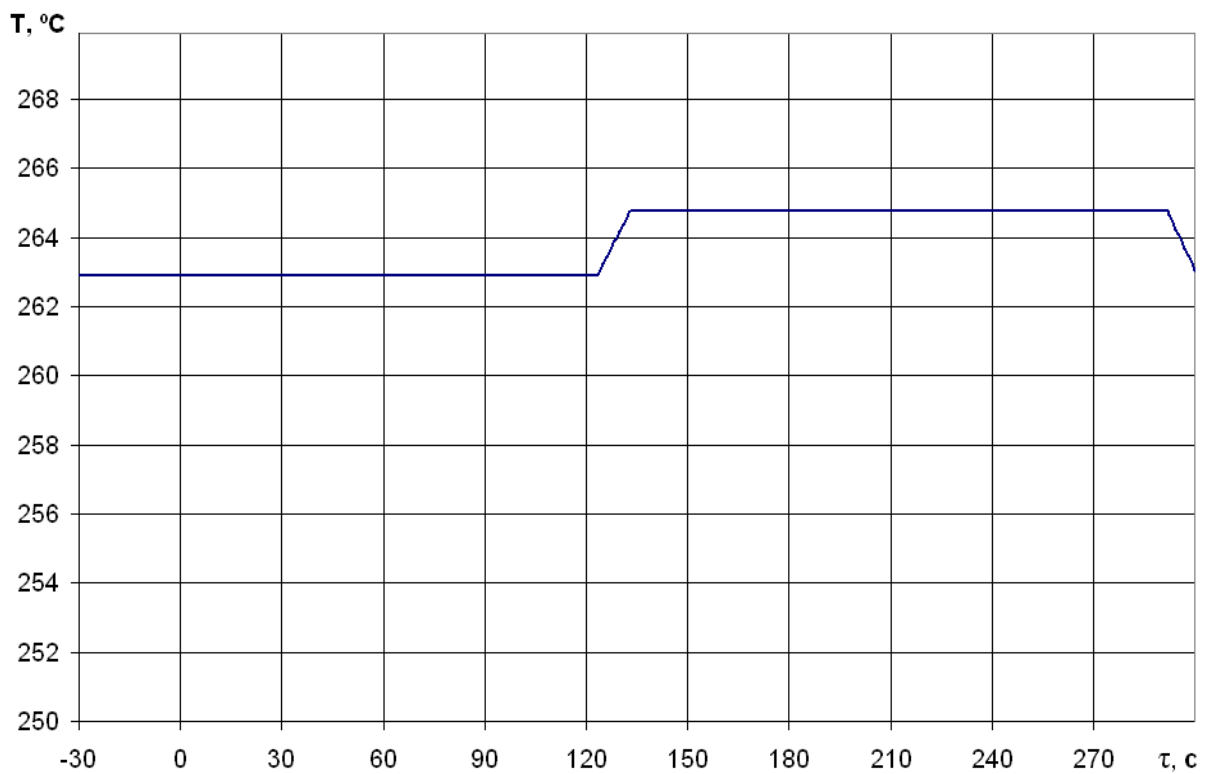


Fig. 66 – Feedwater temperature history at the pressure side of the condenser hydro-turbine pump recorded by UBLS

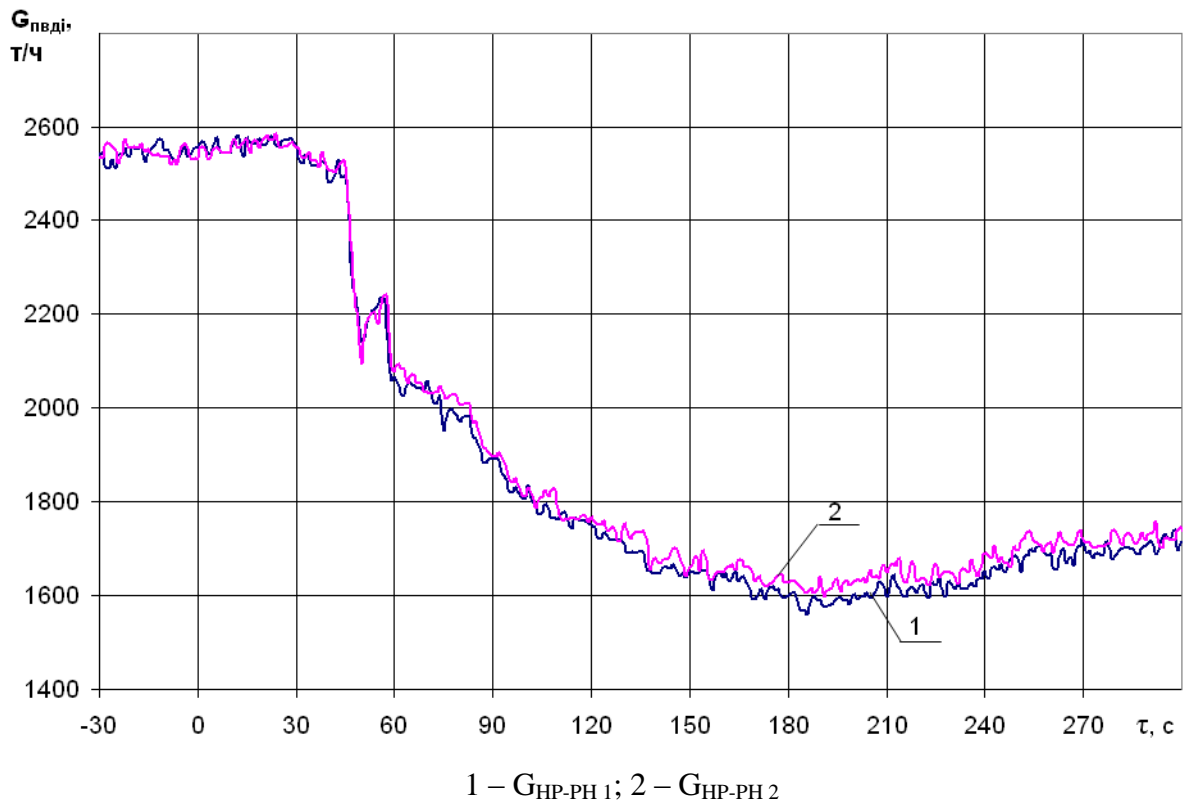


Fig. 67 – Feedwater flow rates of HP-PH lines recorded by the ICMS

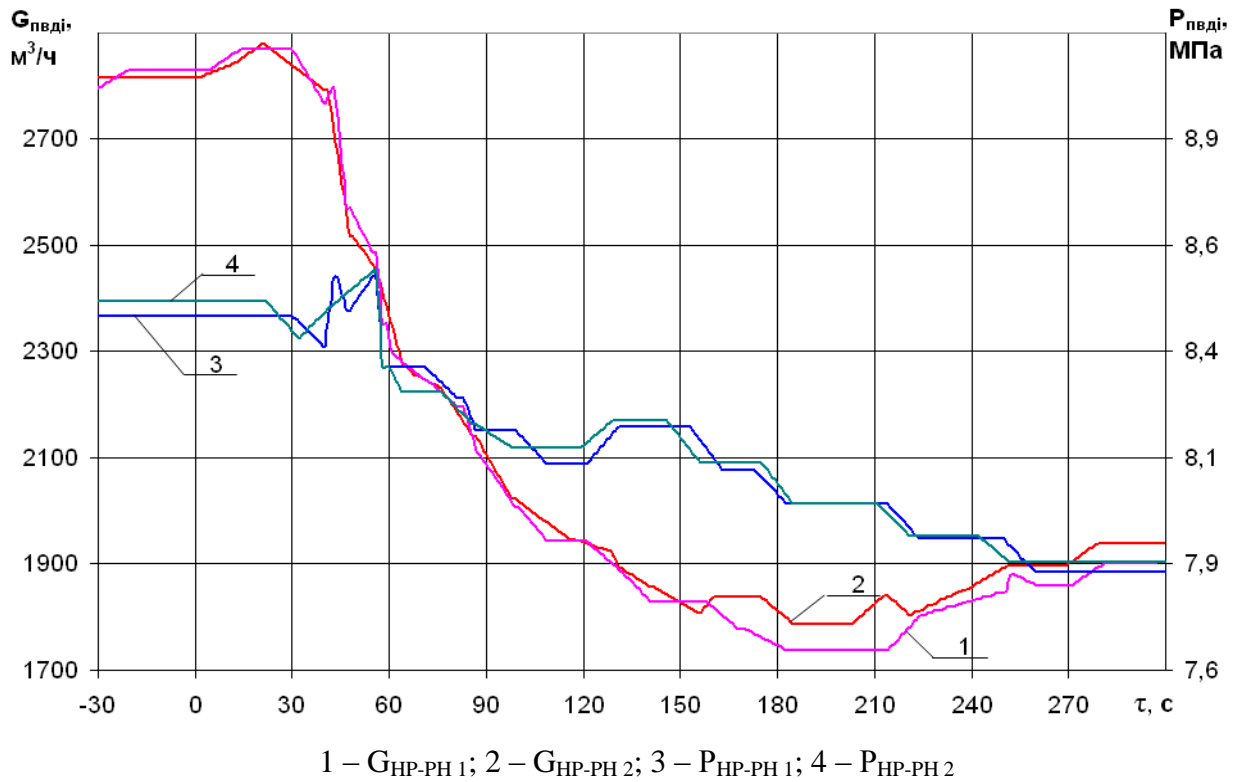
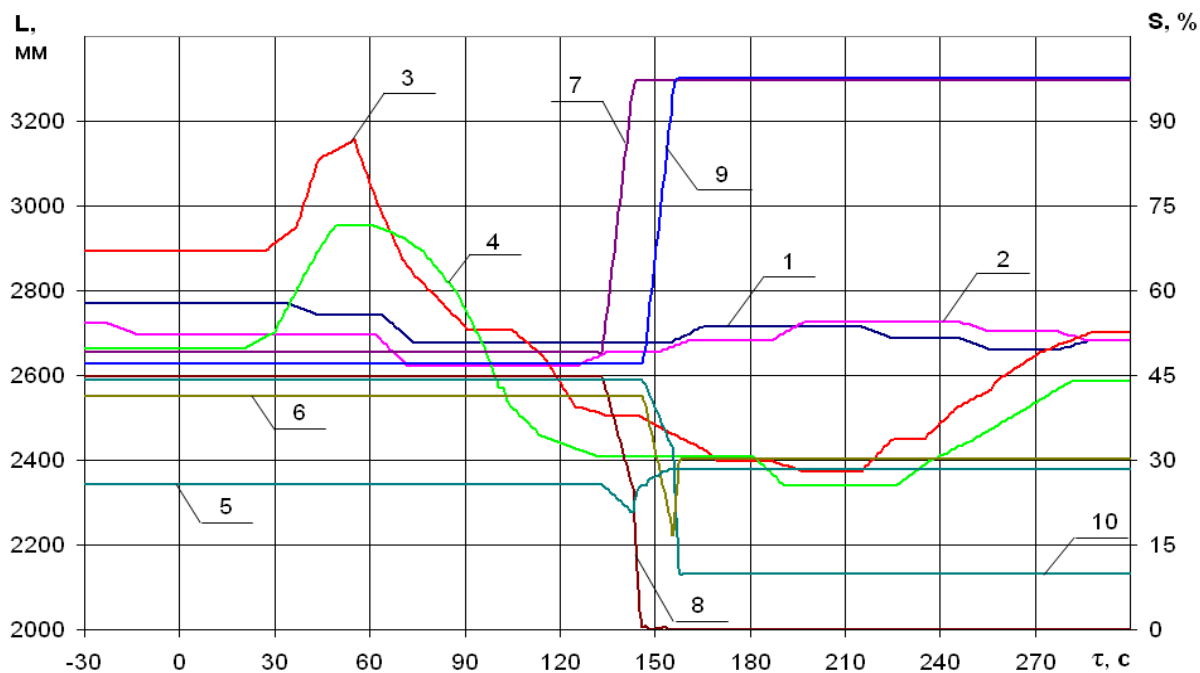
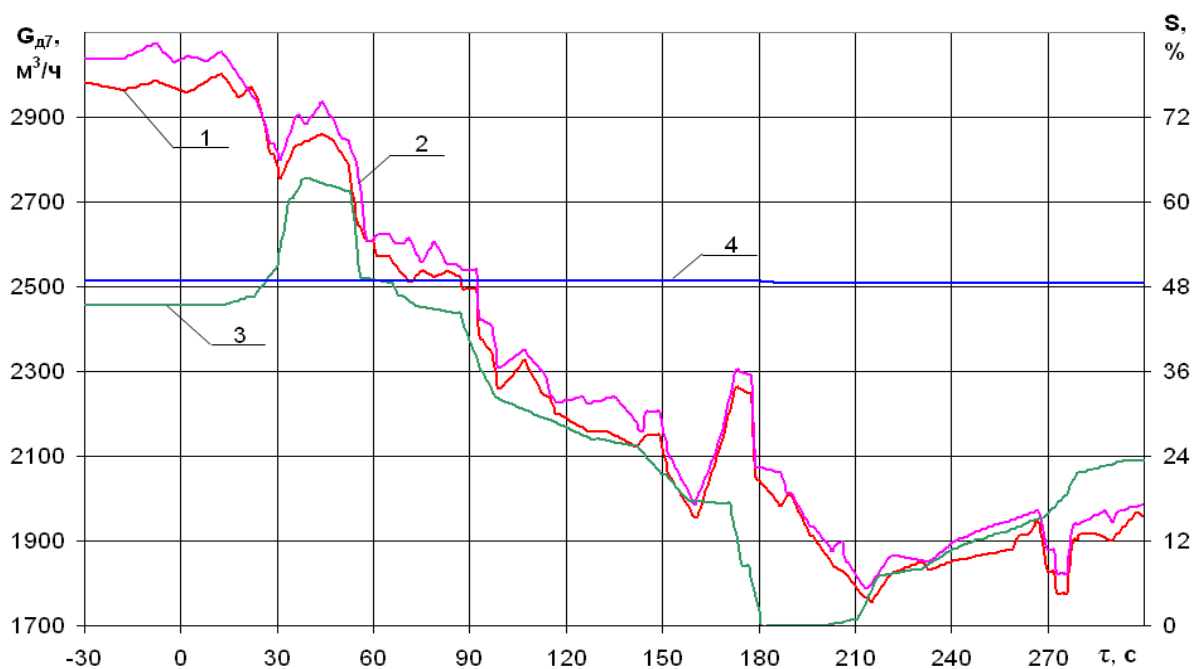


Fig. 68 – Feedwater flow rates of the HP-PH lines recorded by the UBLS



1 – $L_{HP-PH7-1}$; 2 – $L_{HP-PH7-2}$; 3 – $L_{HP-PH 6-1}$; 4 – $L_{HP-PH 6-2}$; 5 – $S_{RV ыр7-1}$; 6 – $S_{RV ыр7-2}$; 7 – $S_{RV ыр6-1}$ КНДР;
8 – $S_{RV ыр6-1 D7}$; 9 – $S_{RV ыр6-2 КНДР}$; 10 – $S_{RV ыр6-2 D7}$;

Fig. 69 – HP-PH #6,7 water level histories, position of the level regulator of the HP-PH #7-1,2, position of the level regulator of the of HP-PH #6-1,2 with the discharge of the condensate into THC and deaerator D-7 recorded by UBLS



1 – G_{D7-1} ; 2 – G_{D7-2} ; 3 – $S_{очн}$; 4 – $S_{пуск}$

Fig. 70 – Deaerator (D7) flow rate history and the positions of the main and starting level regulators recorded by UBLS

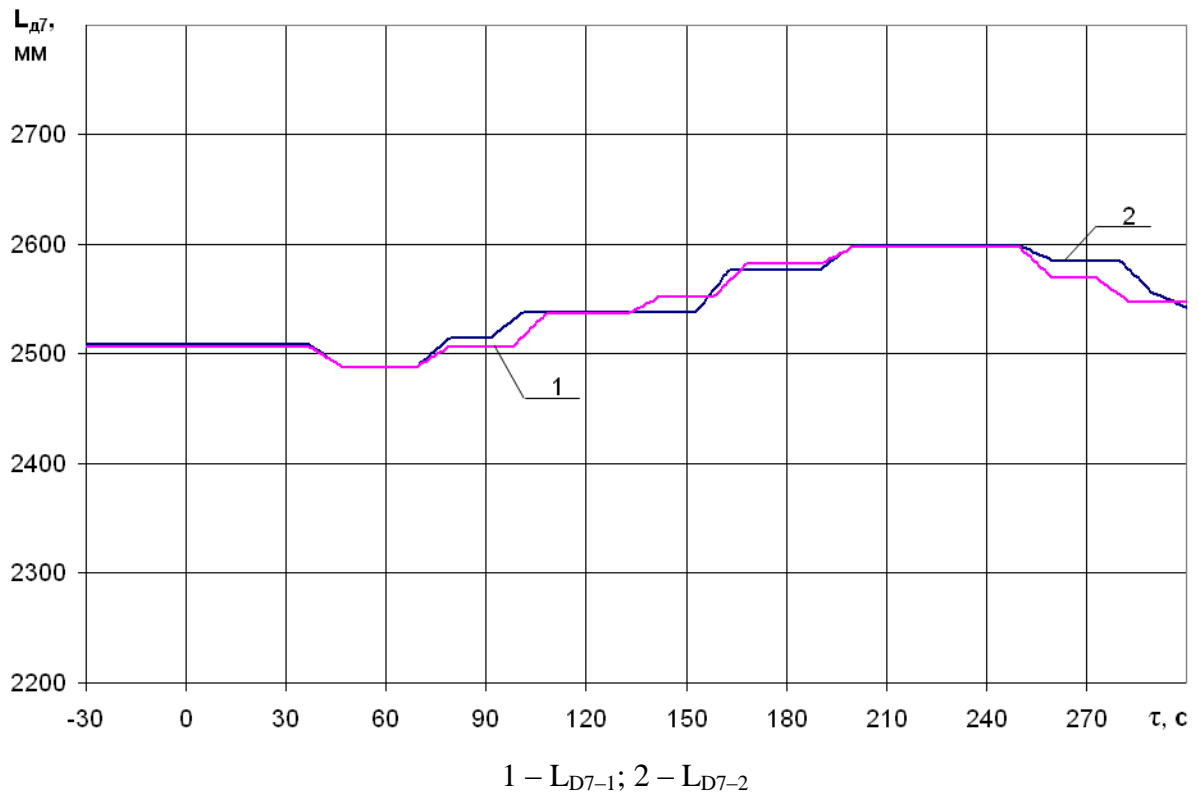


Fig. 71 – Deaerator (D7) water level histories recorded by the UBLS

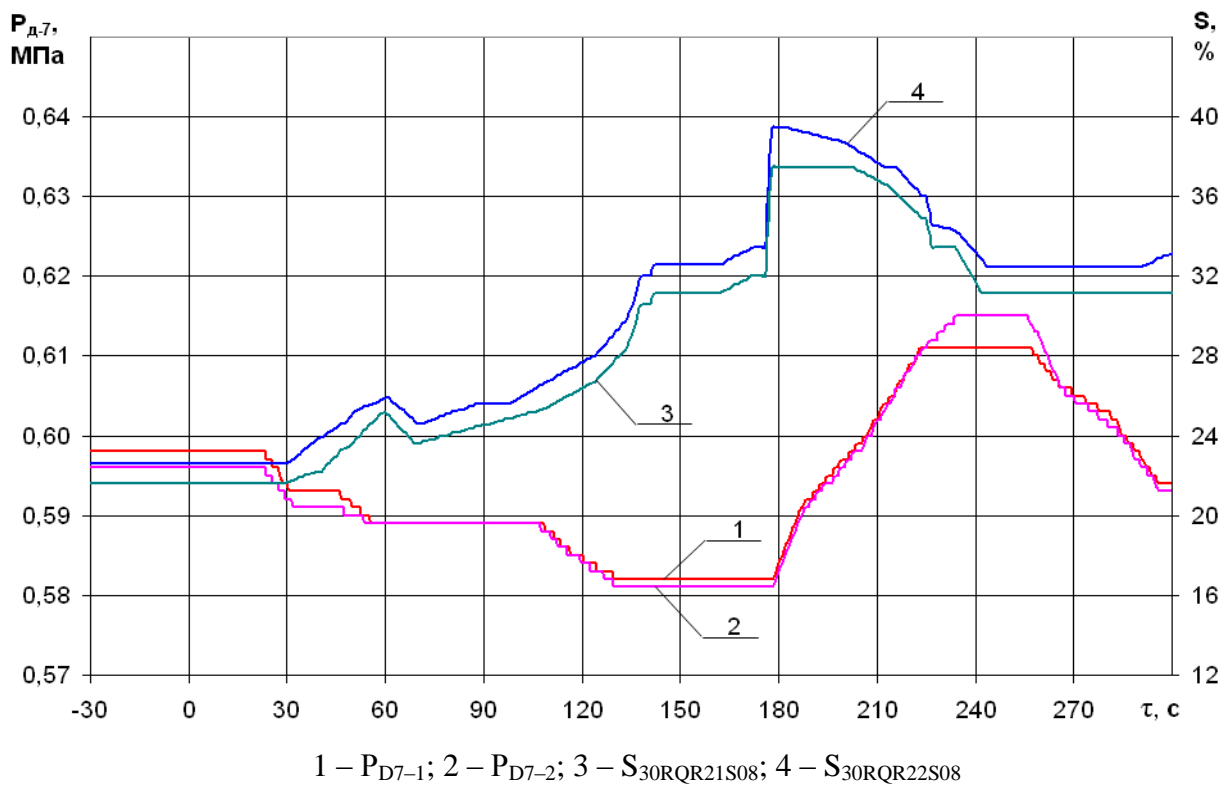


Fig. 72 – Deaerator (D7) pressure histories and the positions of the control valves of the heating steam supply into deaerator columns recorded by the UBLS

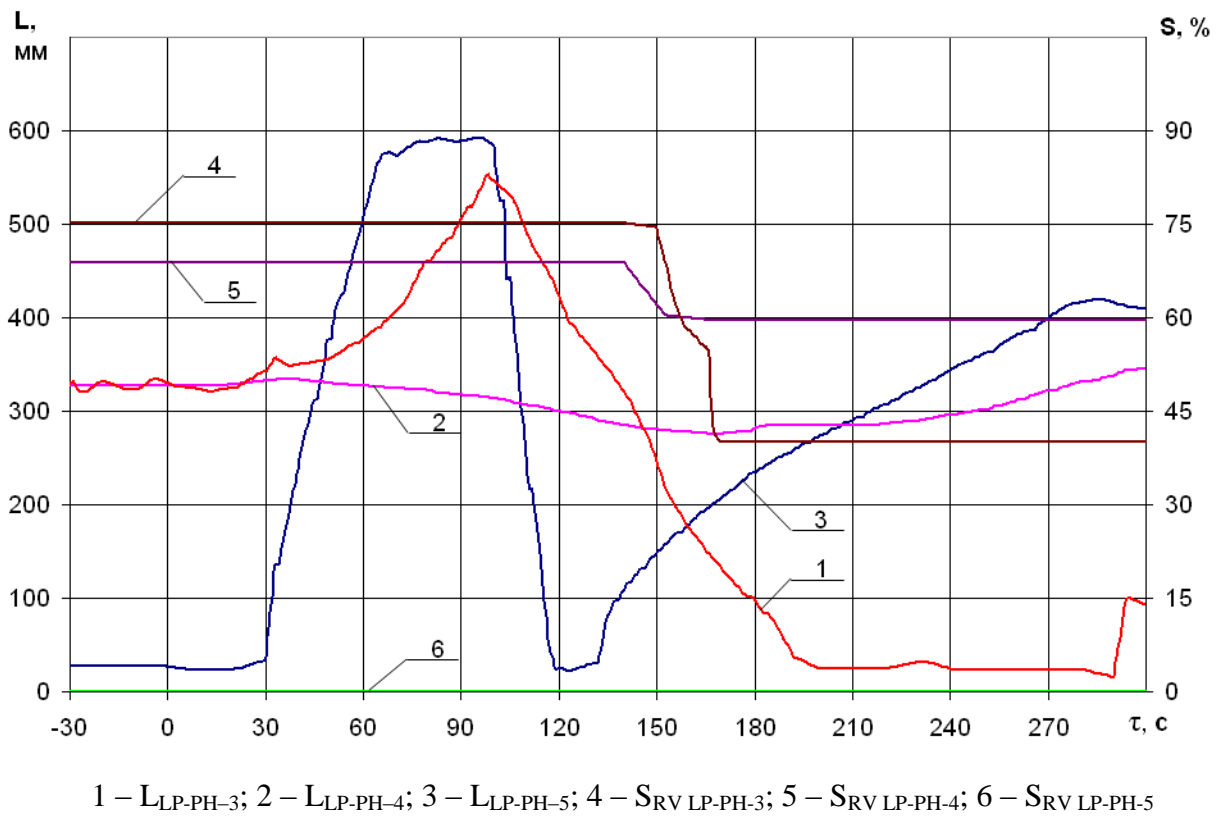


Fig. 73 – Condensate level time-histories and the positions of the level regulators of LP-PH-3-5 recorded by the UBLS

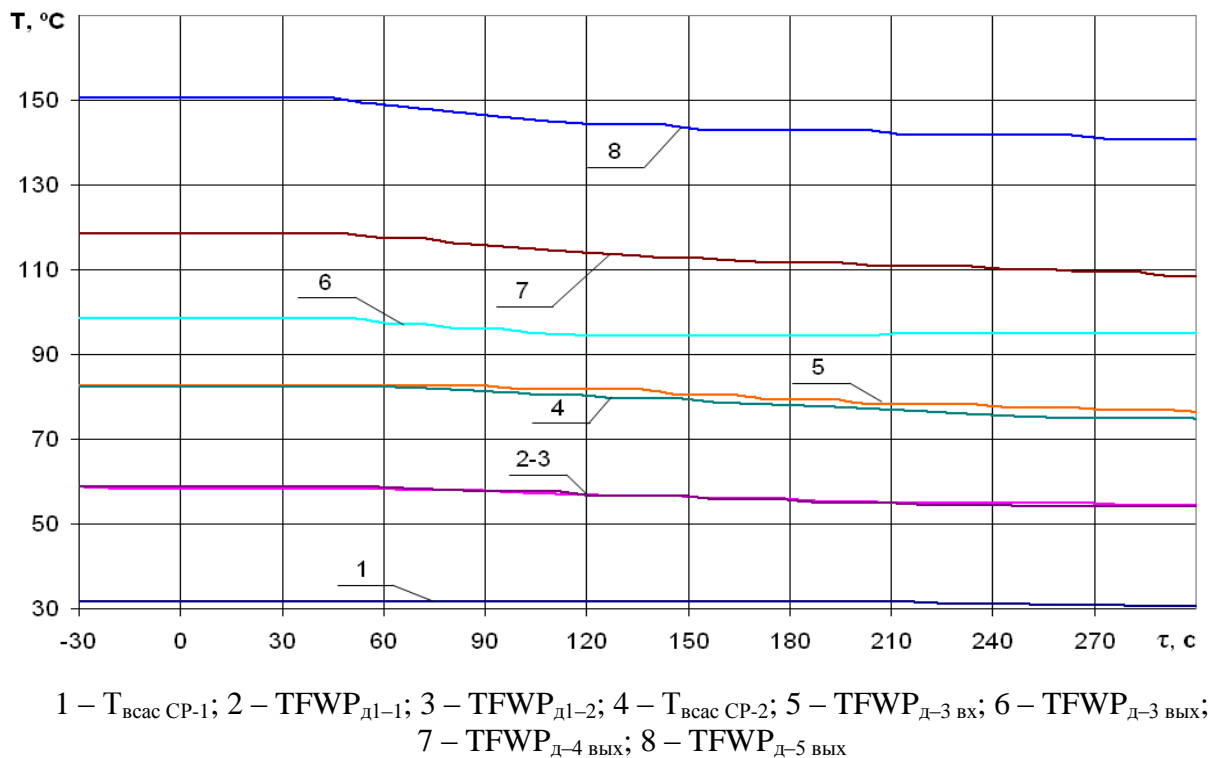


Fig. 74 – Temperature histories measured at the condensate line starting from the CP-1 till the inlet of LP-PH -#5 recorded by the UBLS

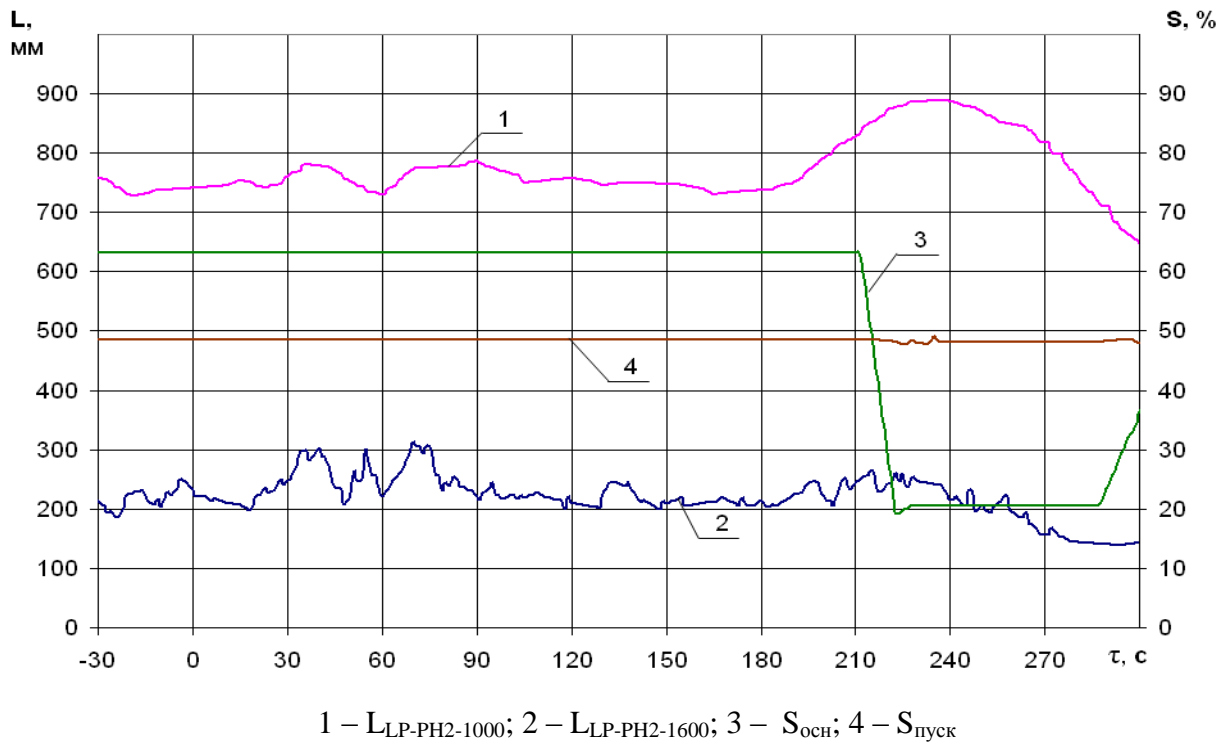


Fig. 75 – Water level histories (by level measurements based on 1000 and 1600 mm) and the position of the main and starting level control valve of the LP-PH-#2 recorded by the UBLS

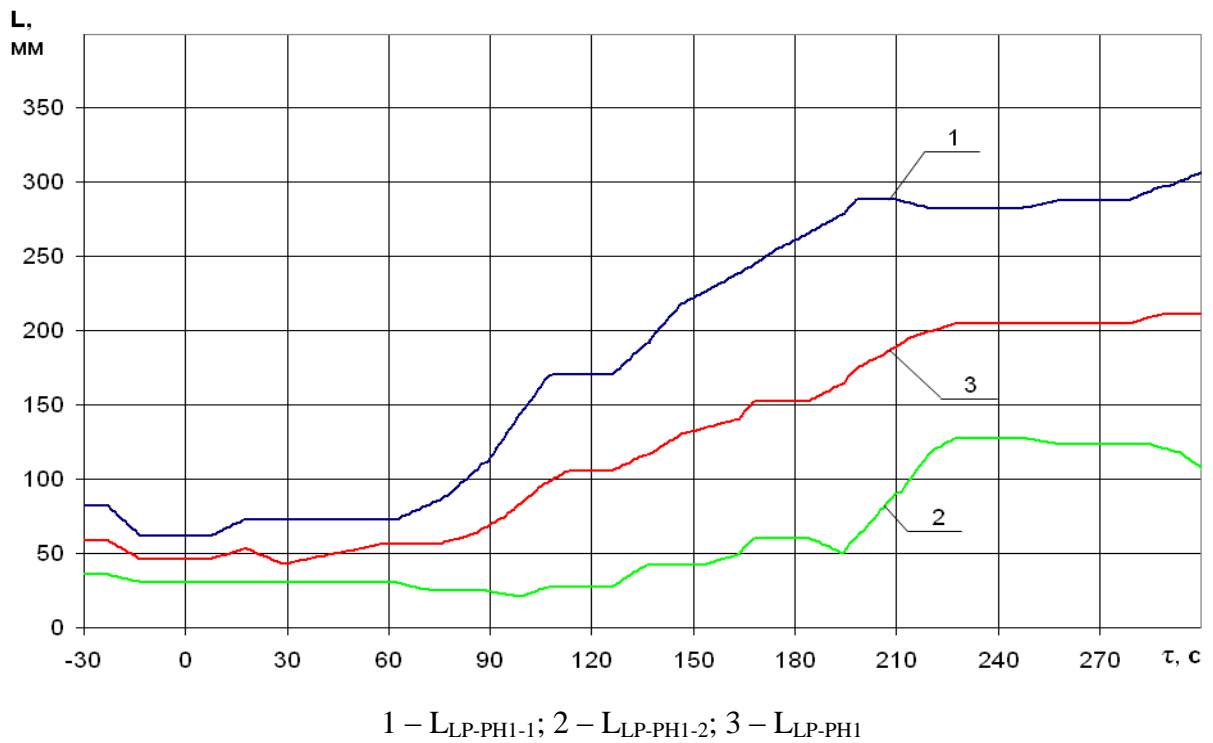


Fig. 76 – Water level histories of the LP-PH-1 recorded by the UBLS

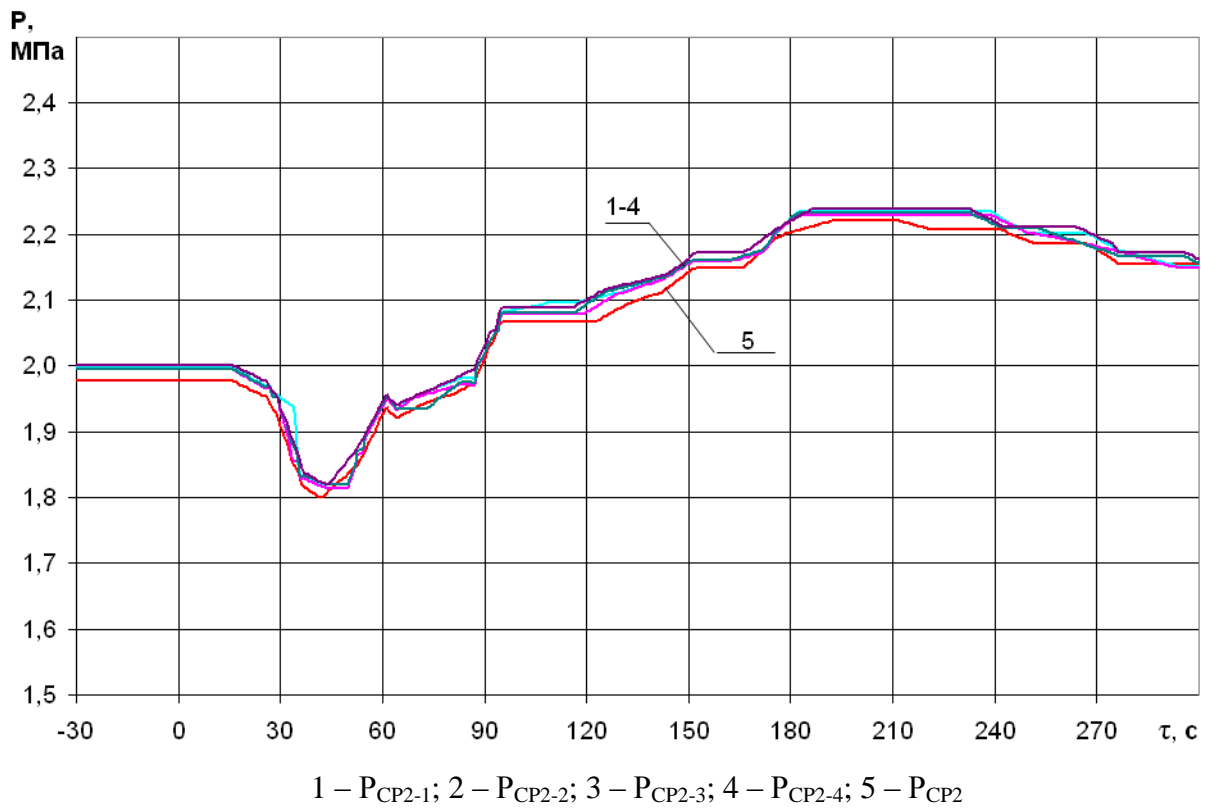


Fig. 77 – Pressure histories at the pressure side of the CP-#2 1-4 and in the collector of the CP-#2 recorded by the UBLS

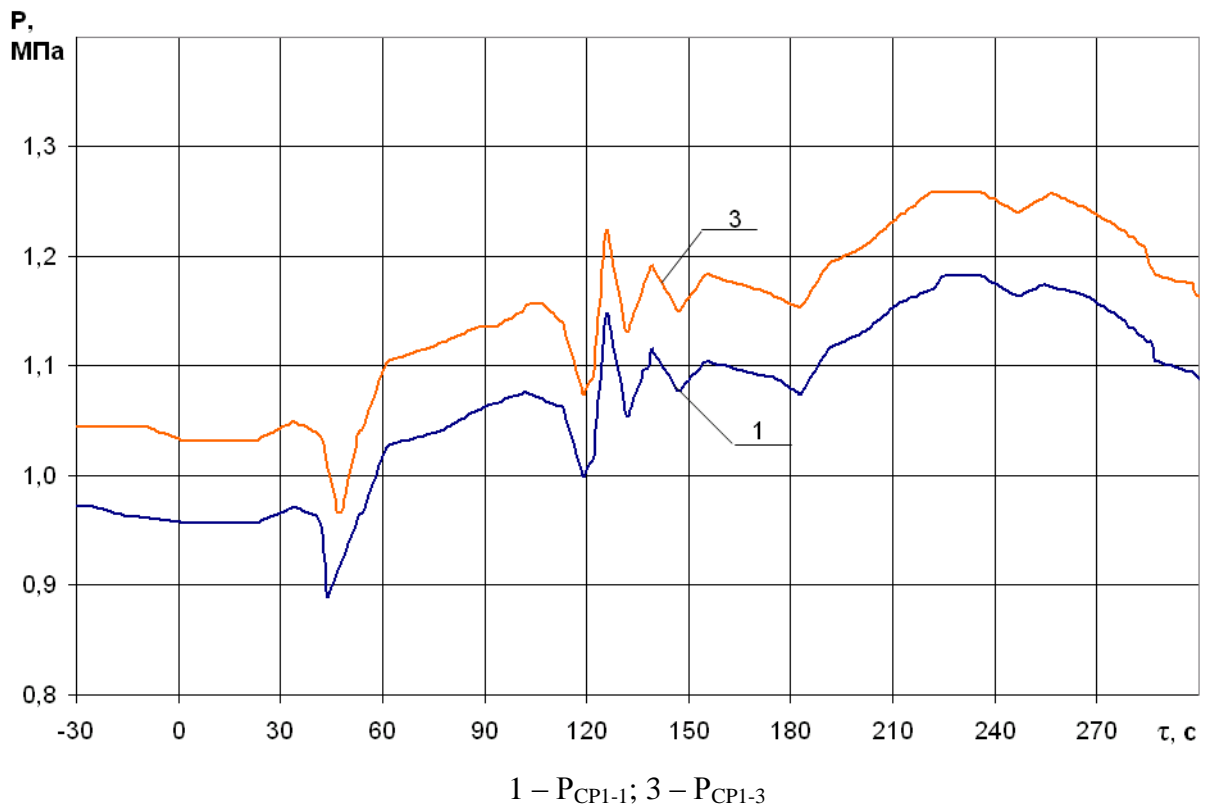


Fig. 78 – Pressure history of CP-#1 1-3 recorded by UBLS

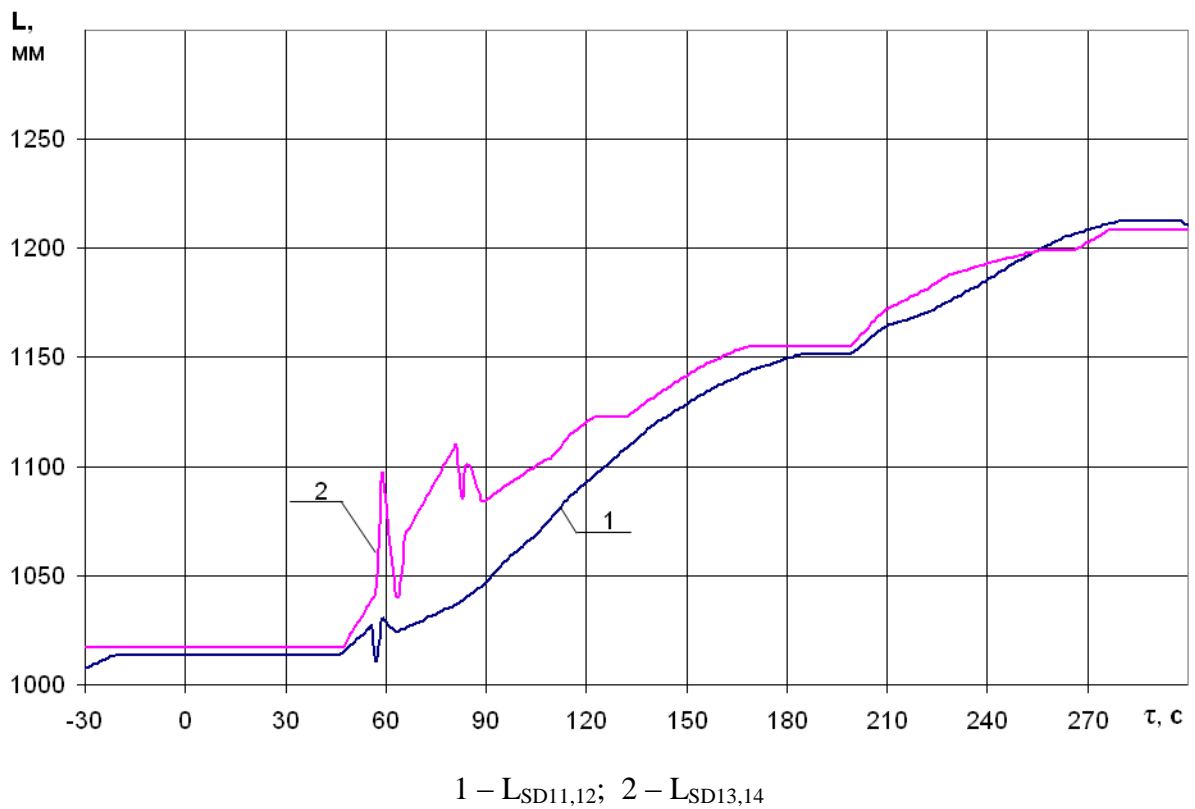


Fig. 78 – Water level time history of the turbine condensers recorded by the UBLS

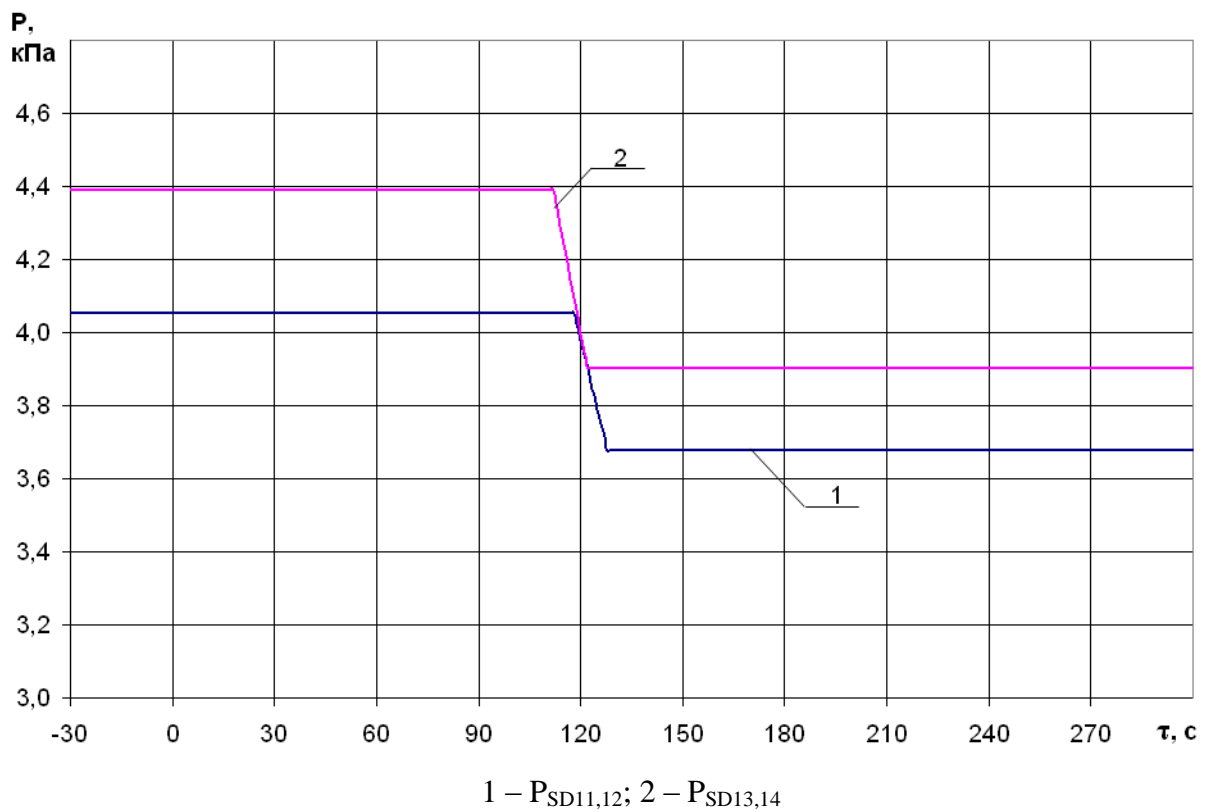


Fig. 80 –Turbine condensers water level histories recorded by the UBLS

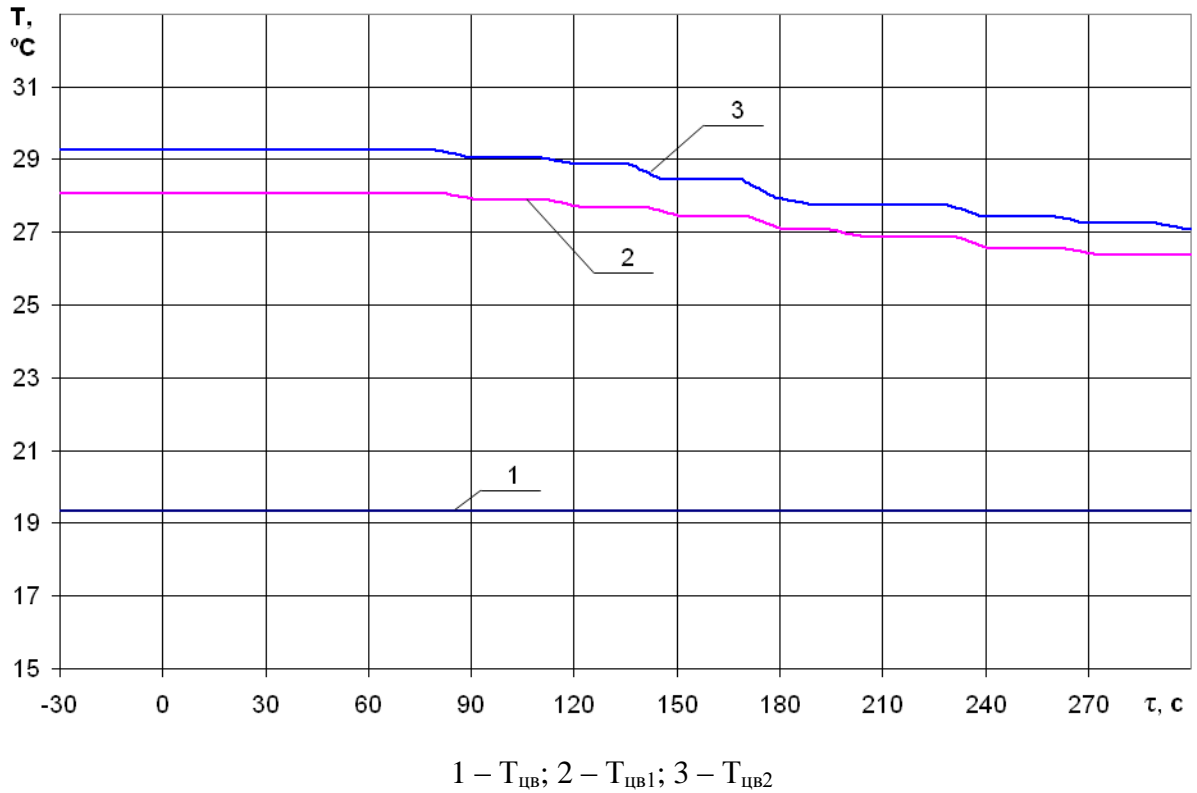


Fig. 81 – Inlet and outlet condenser (group 1 and 2) circulation water temperature histories recorded by UBLS

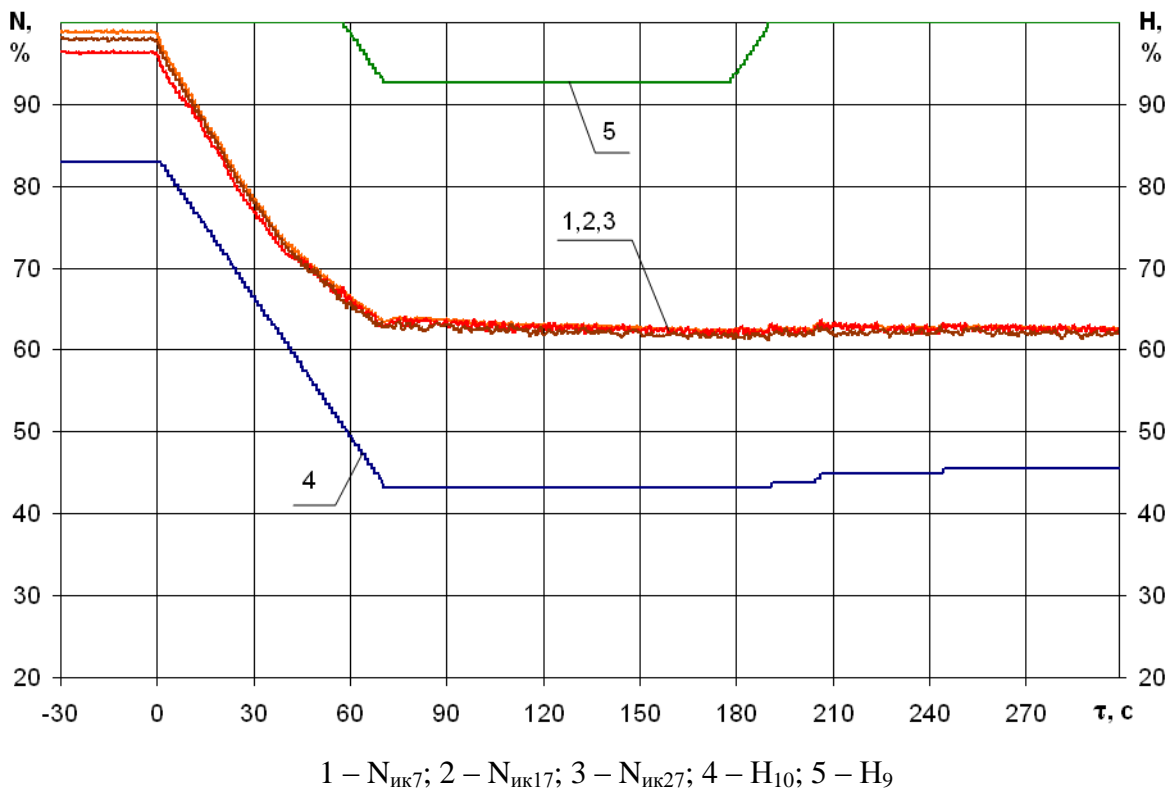


Fig. 82 – Reactor power history recorded by NFC and the position change of CPS CR #10 and #9 recorded by MMS

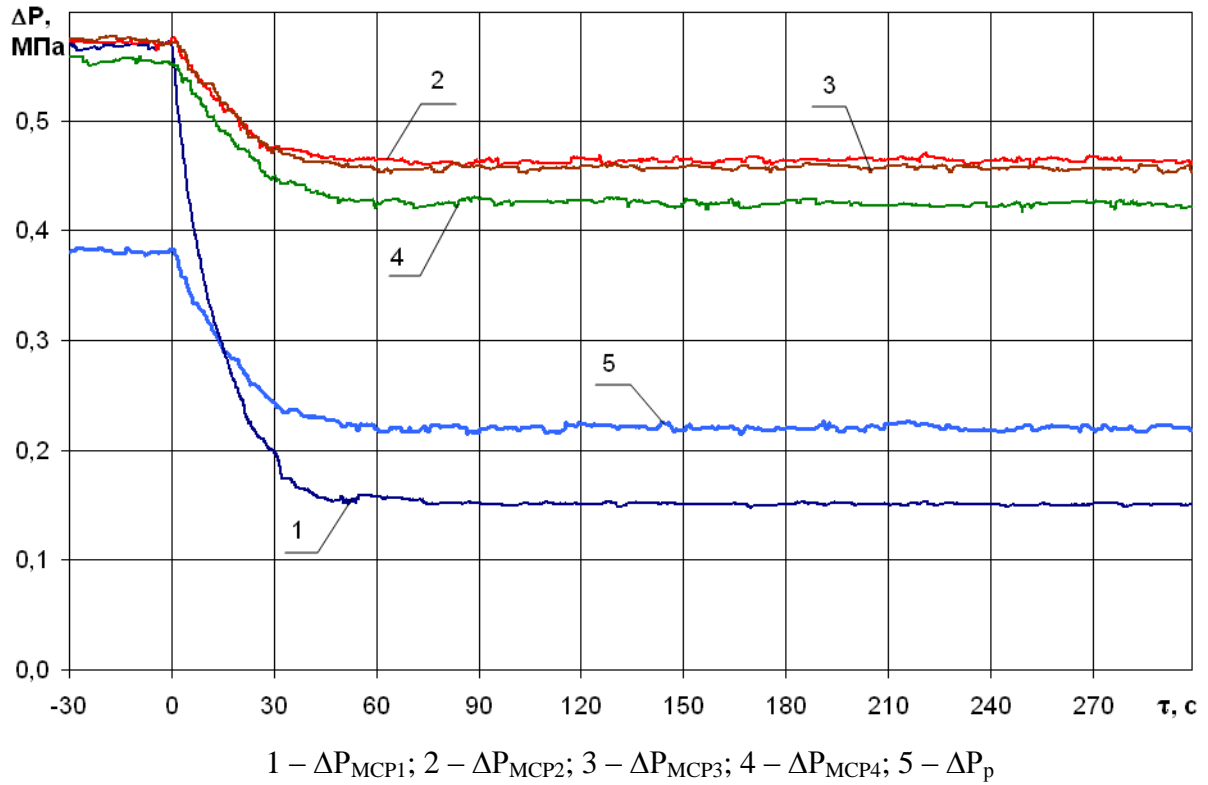


Fig. 83 – Pressure difference histories of the MCPs and the reactor recorded by MMS

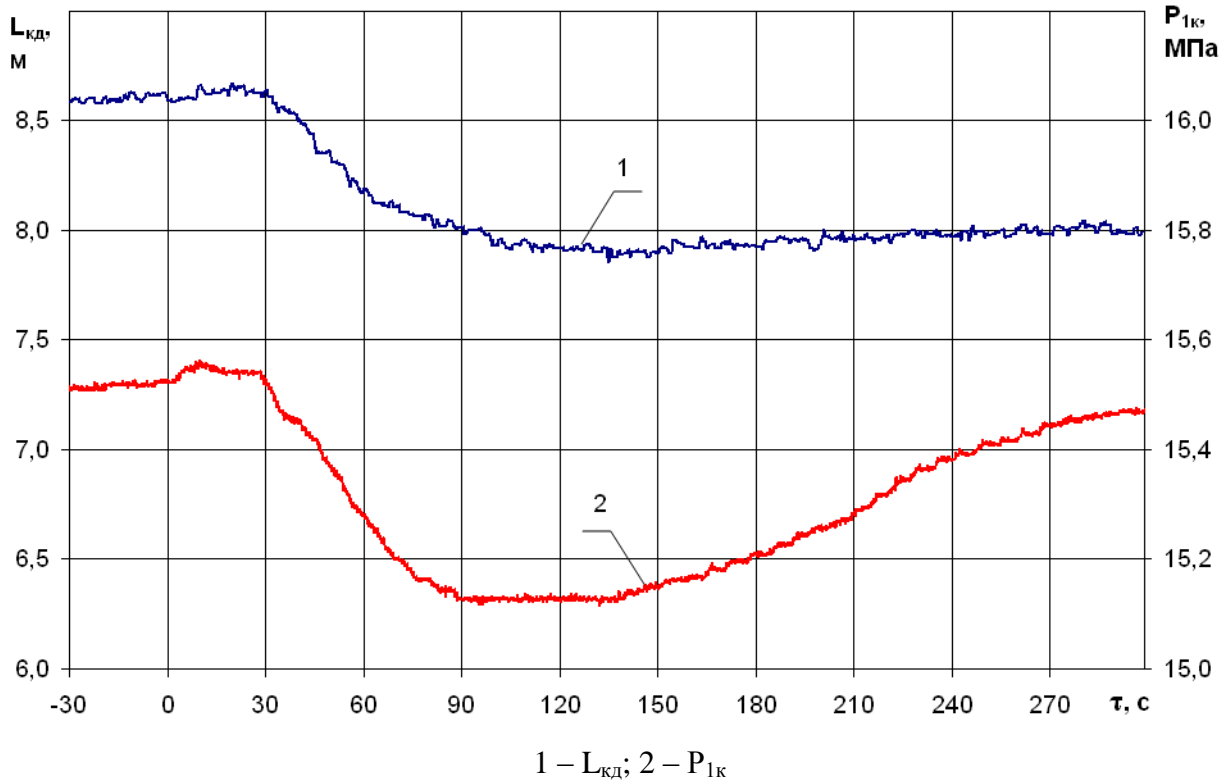


Fig. 84 – PRZ water level history and the pressure history above the core recorded by MMS

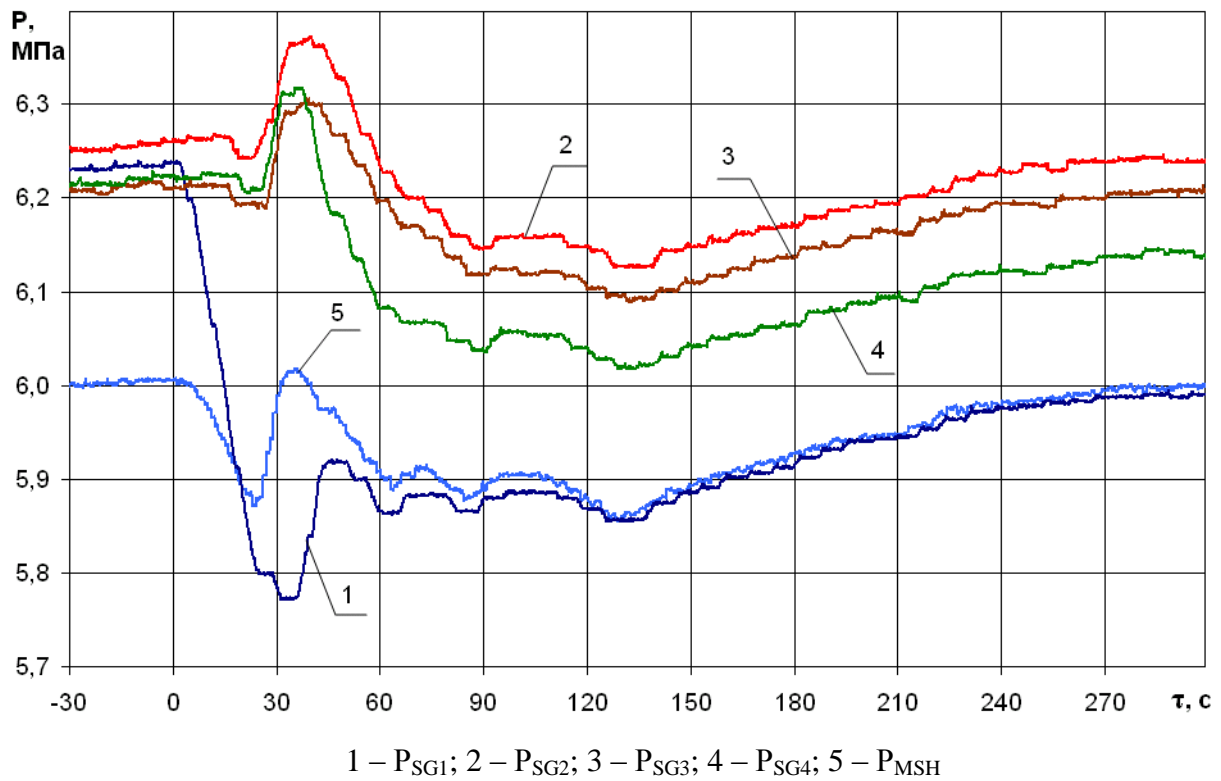


Fig. 85 – SG pressure histories and main steam collector pressure history recorded by MMS

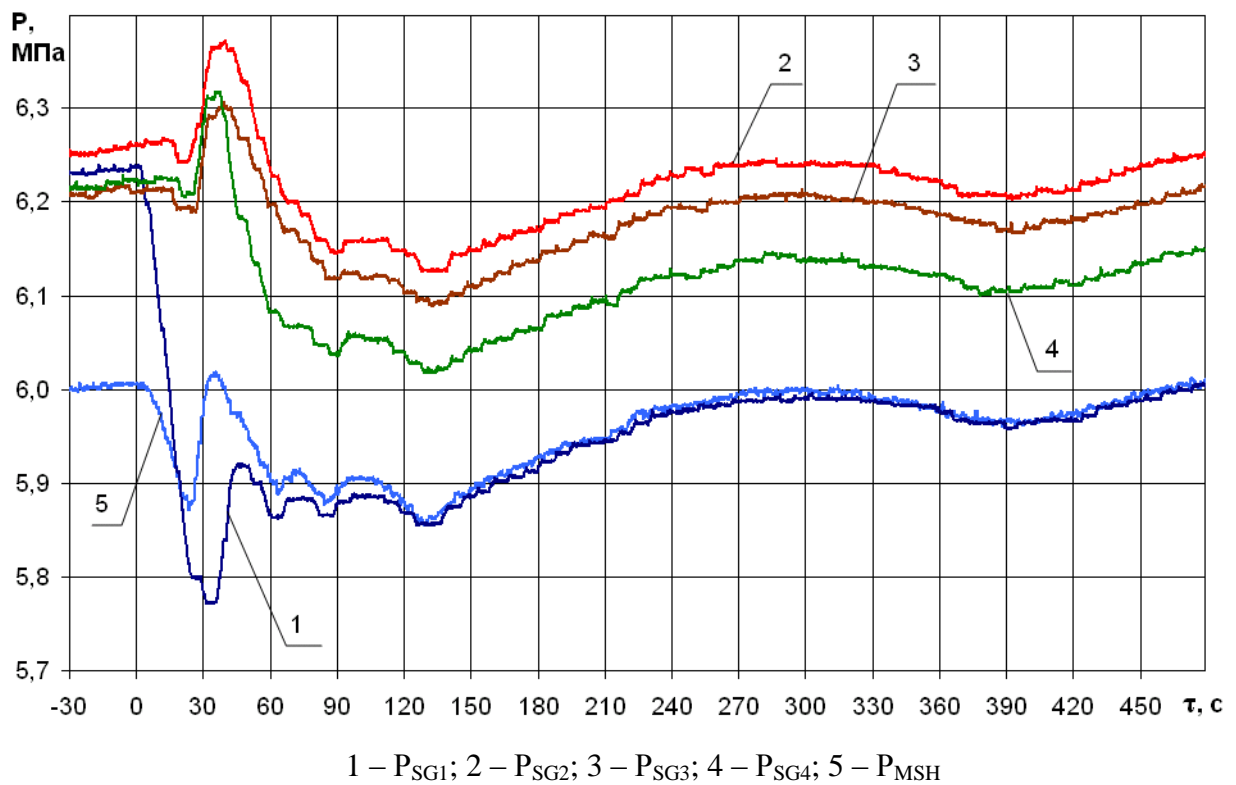


Fig. 86 – SG pressure histories and main steam collector pressure history recorded by MMS

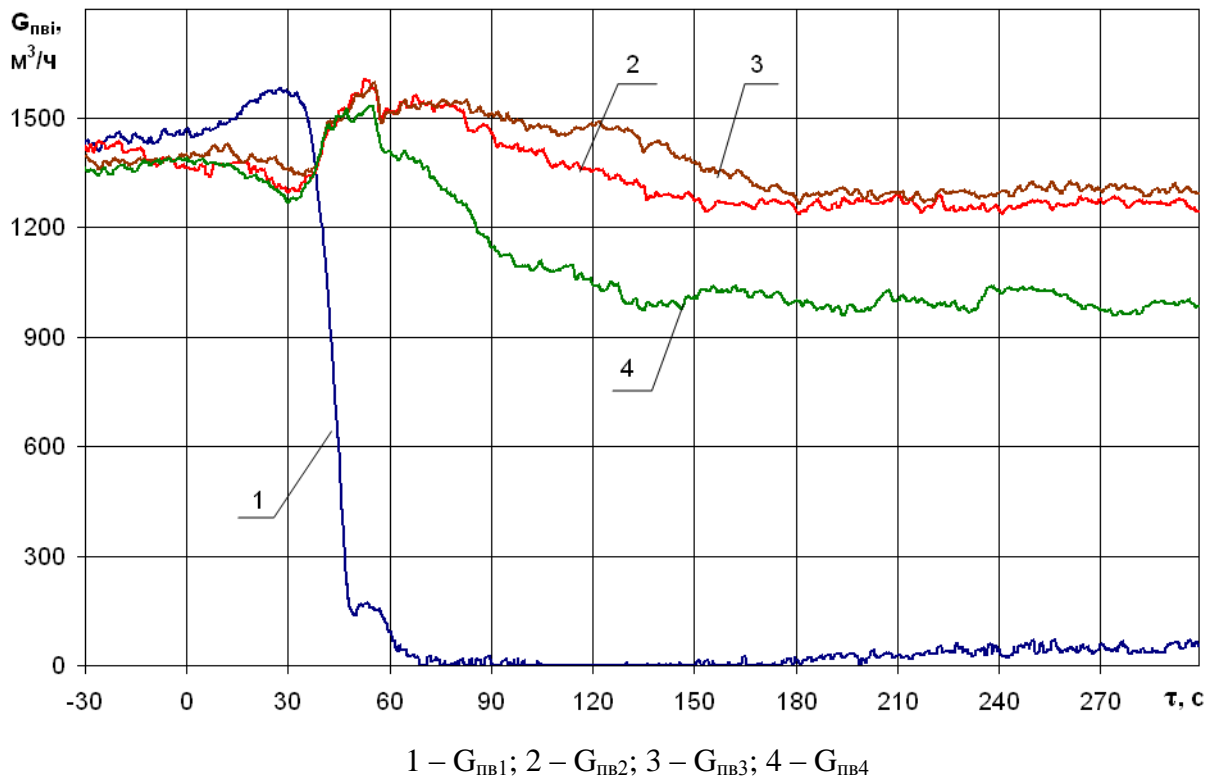


Fig. 87 – SG inlet feedwater mass flow histories recorded by the MMS

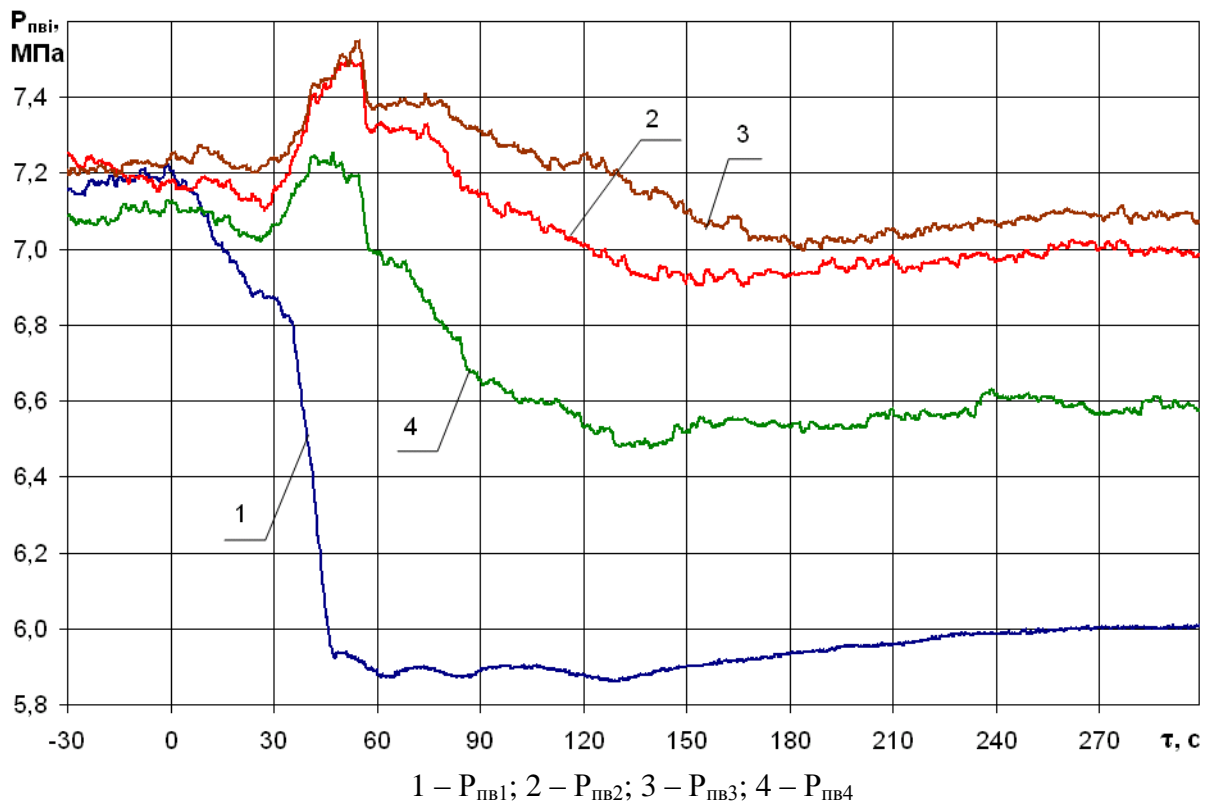


Fig. 88 – SG inlet feedwater pressure histories recorded by the MMS

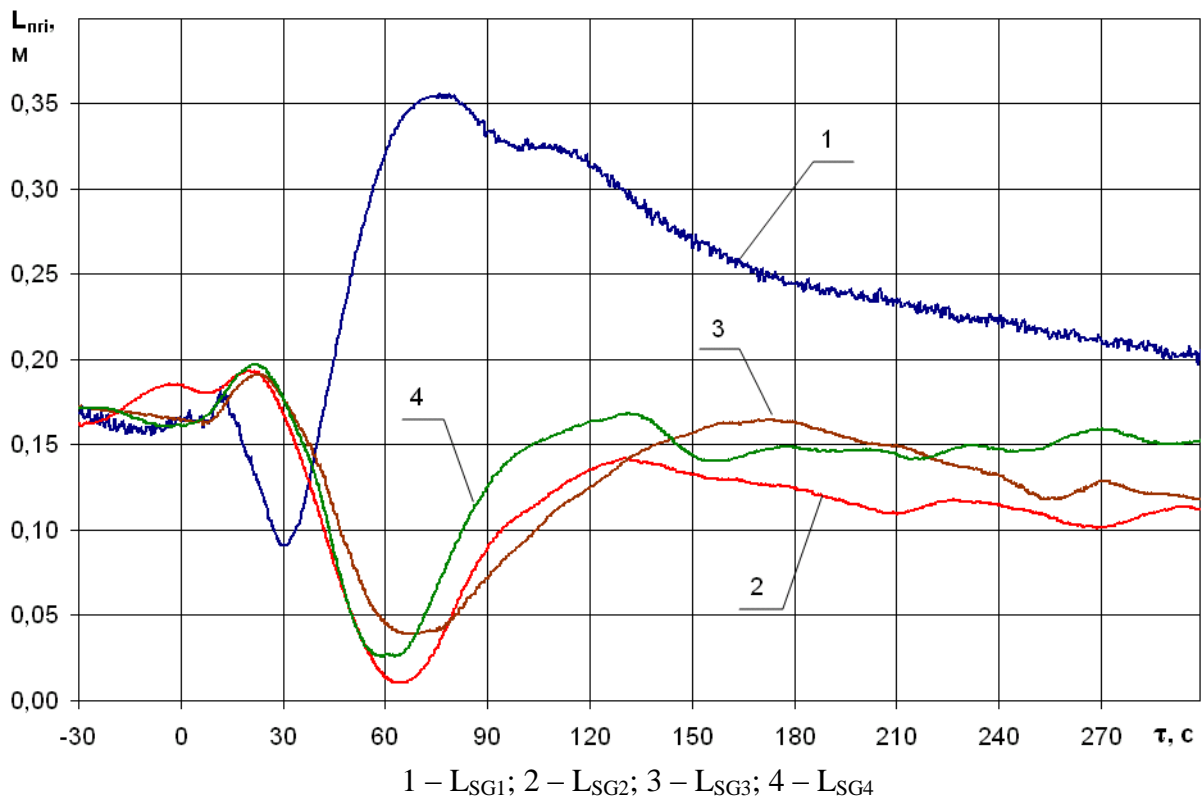


Fig. 89 – SG water level histories recorded by the MMS (measurements on “small” basis)

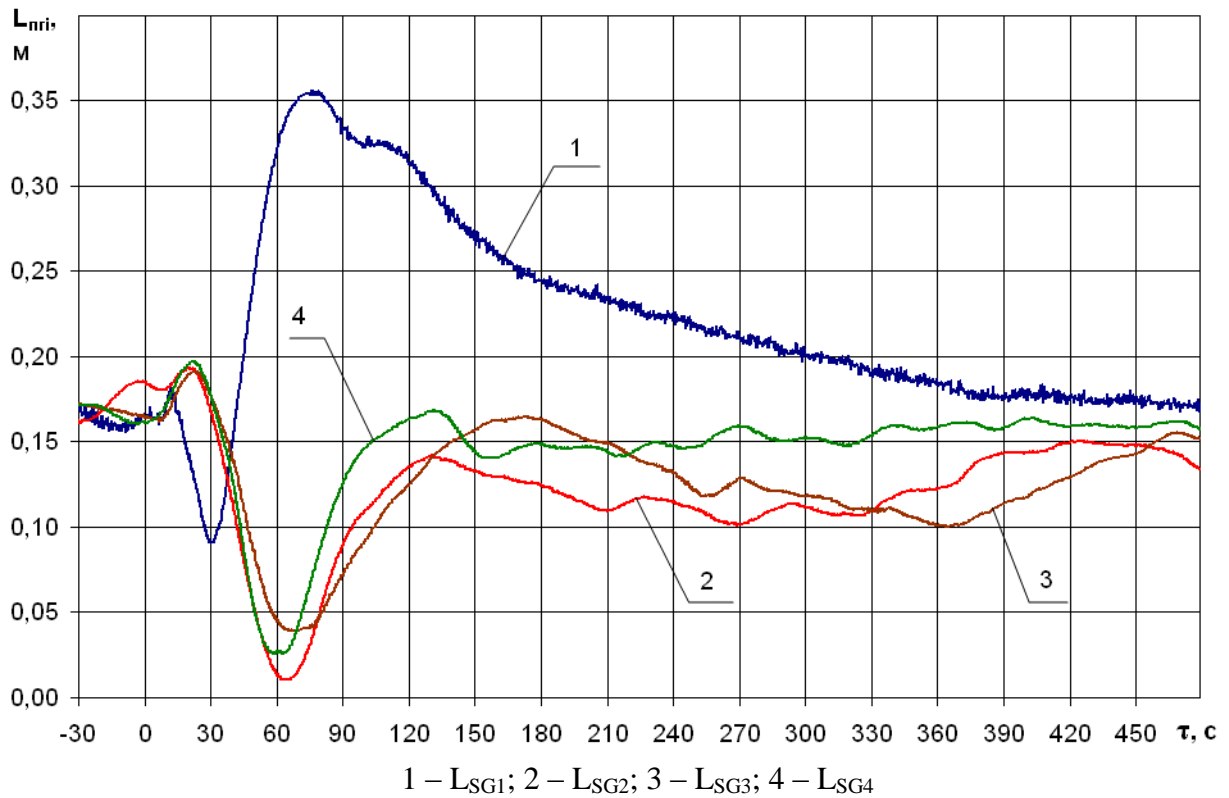


Fig. 90 – SG water level histories recorded by the MMS (measurements on “small” basis)

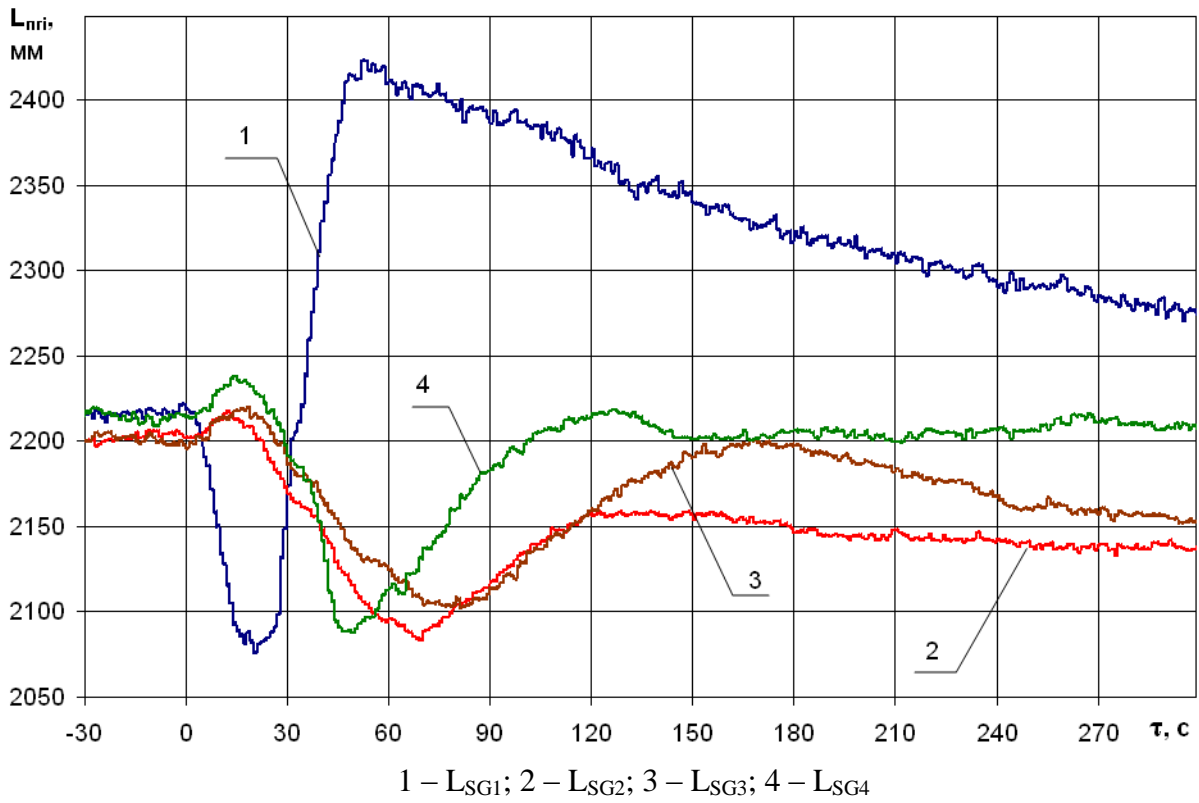


Fig. 91 – SG water level histories recorded by the MMS (measurements on “large” basis)

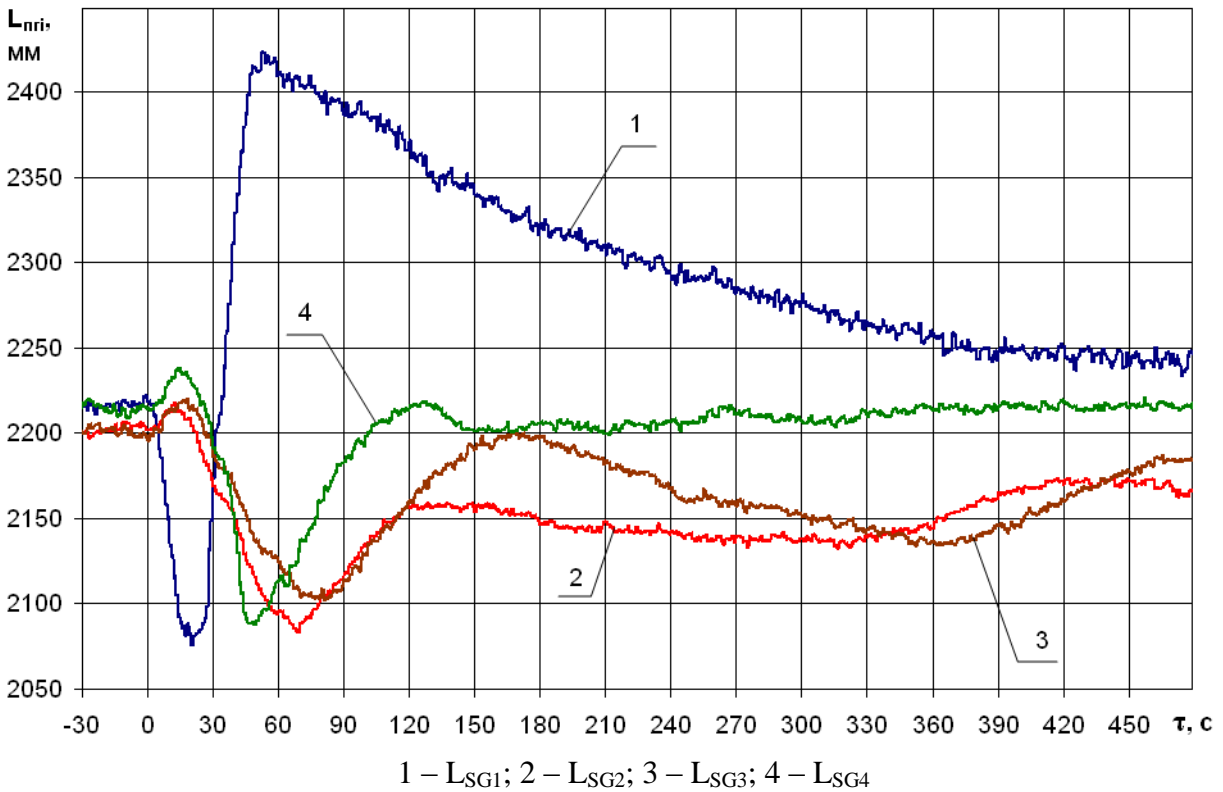


Fig. 92 – SG water level histories recorded by the MMS (measurements on “large” basis)

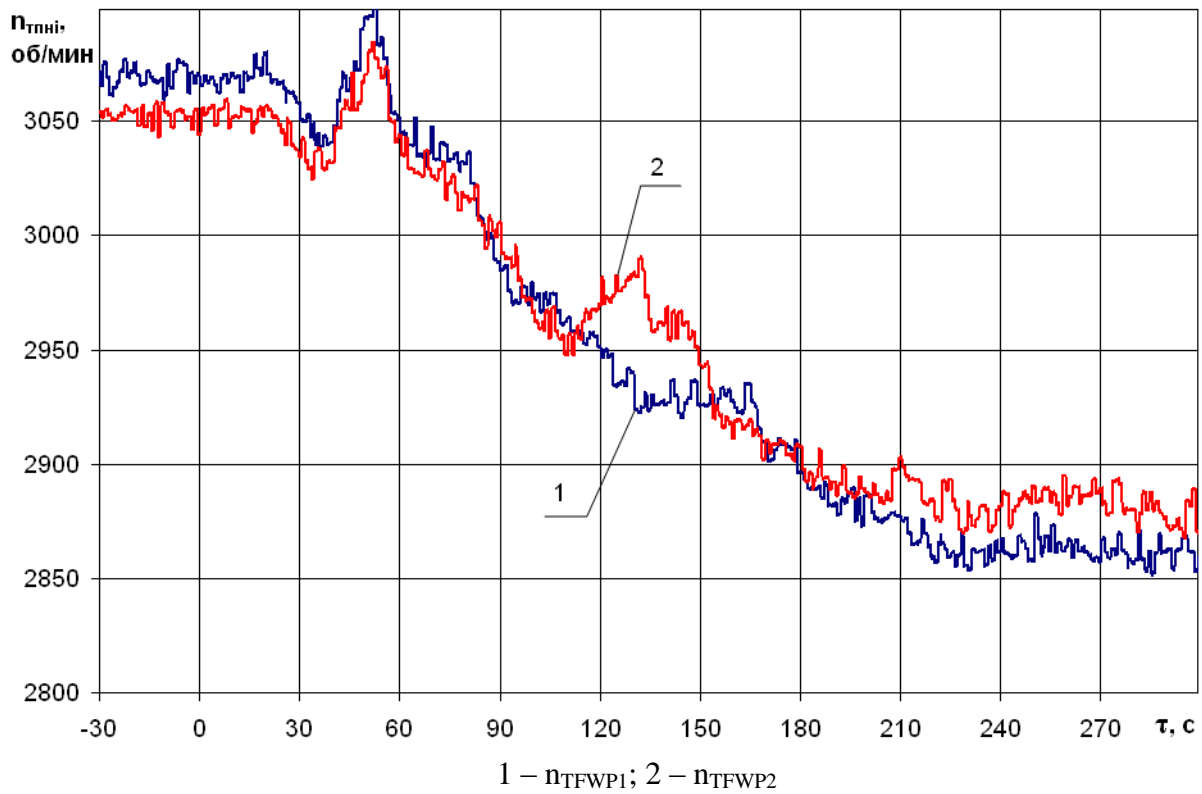


Fig. 93 – Rotation speed of TFWP recorded by MMS

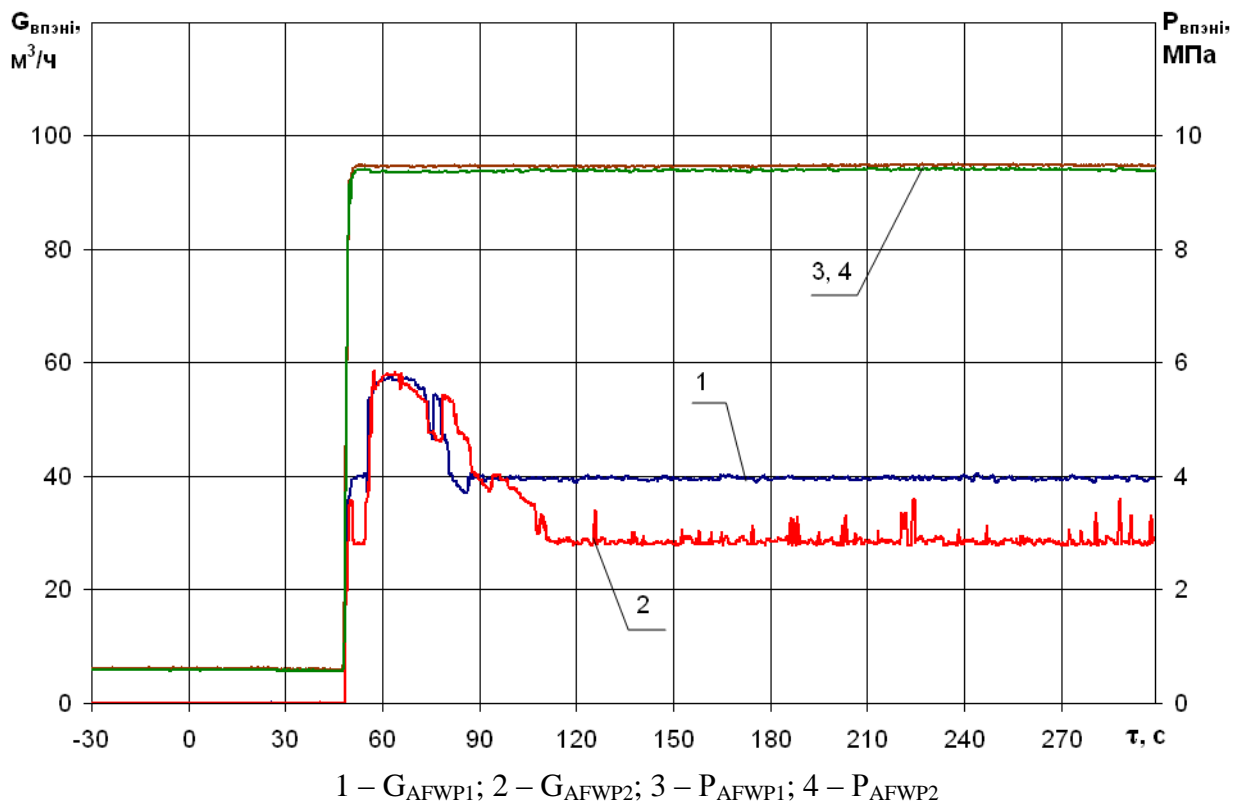


Fig. 94 – Change in feedwater flow rates and pressure at the pressure side of AFWP recorded by MMS

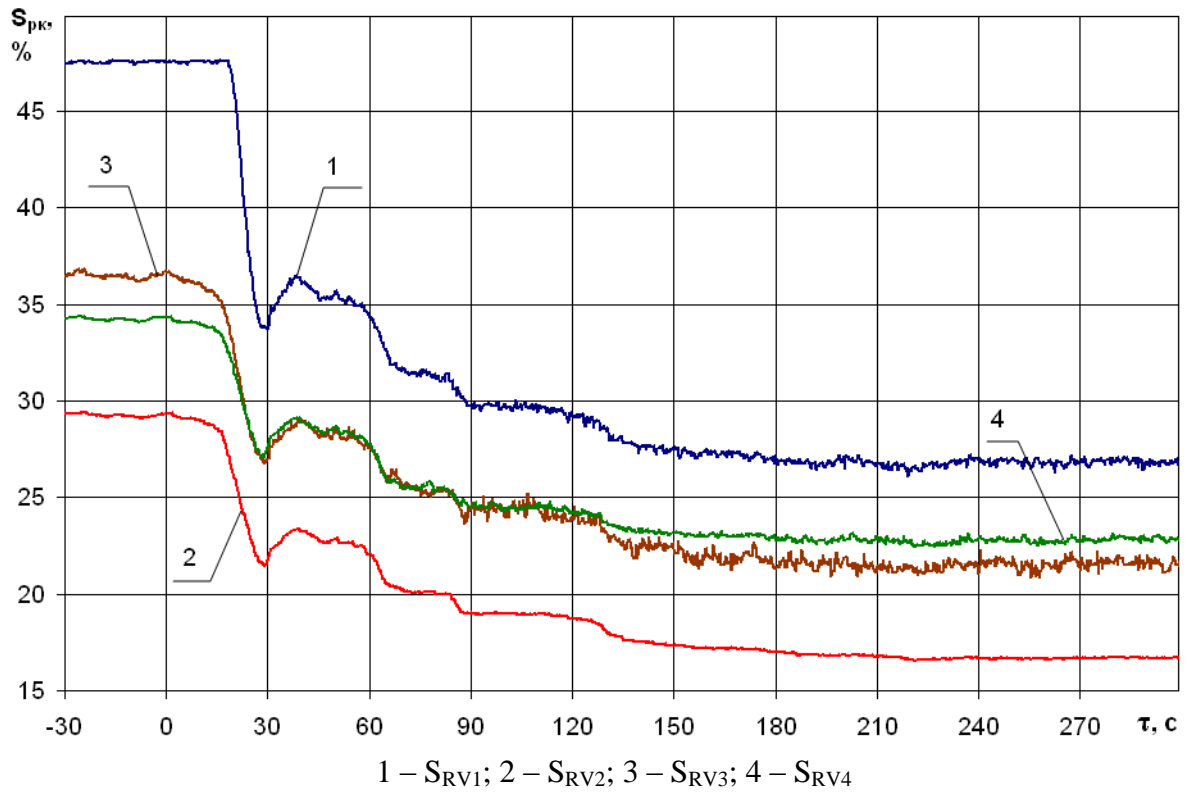


Fig. 95 – Change in the position of HP control valves of TG recorded by MMS

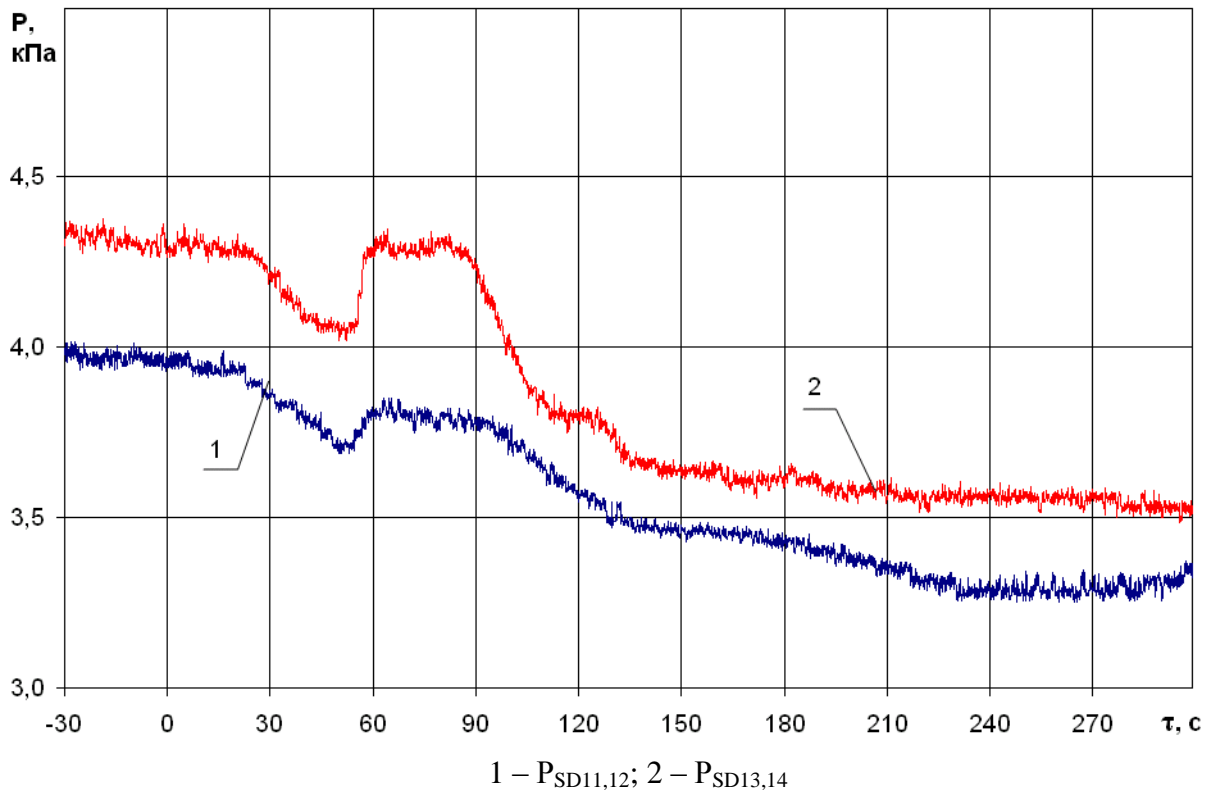


Fig. 96 – TG condenser pressure histories recorded by MMS

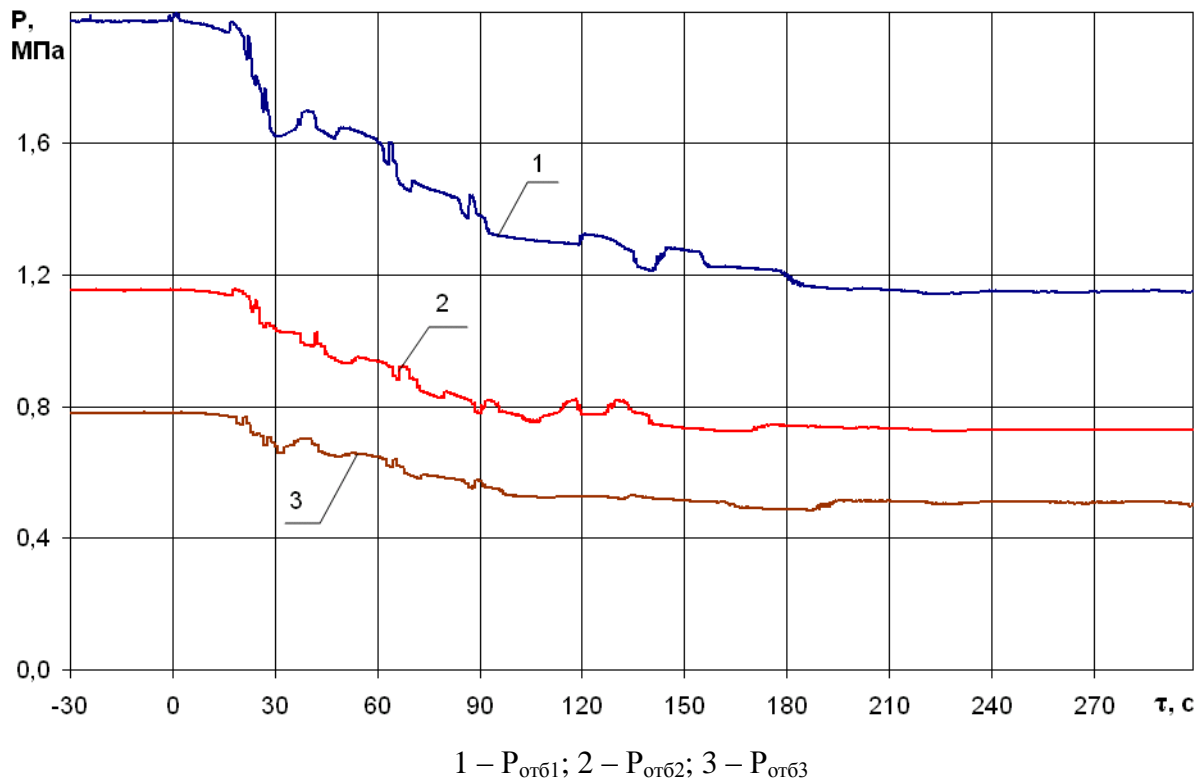


Fig. 97 – Steam pressure at the 1th, 2th and 3th intake of the turbine recorded by MMS

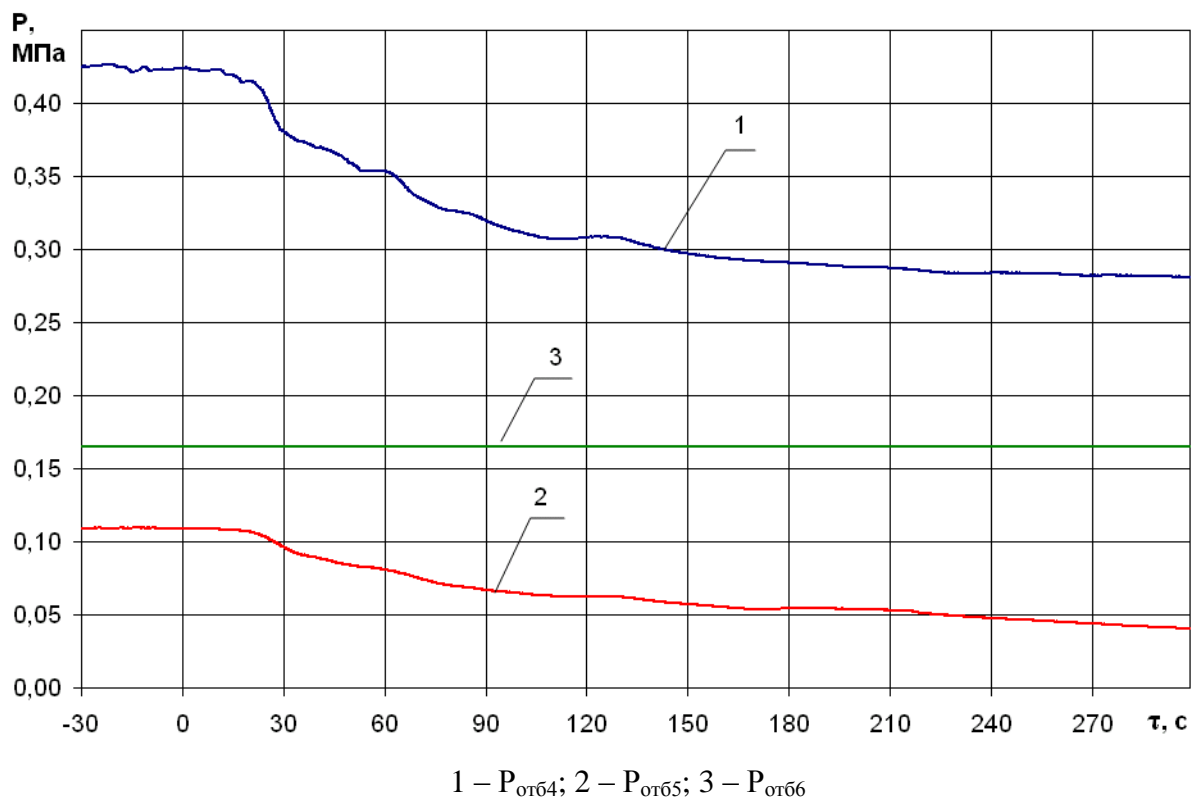


Fig. 98 – Steam pressure at the 4th, 5th and 6th intake of the turbine recorded by MMS

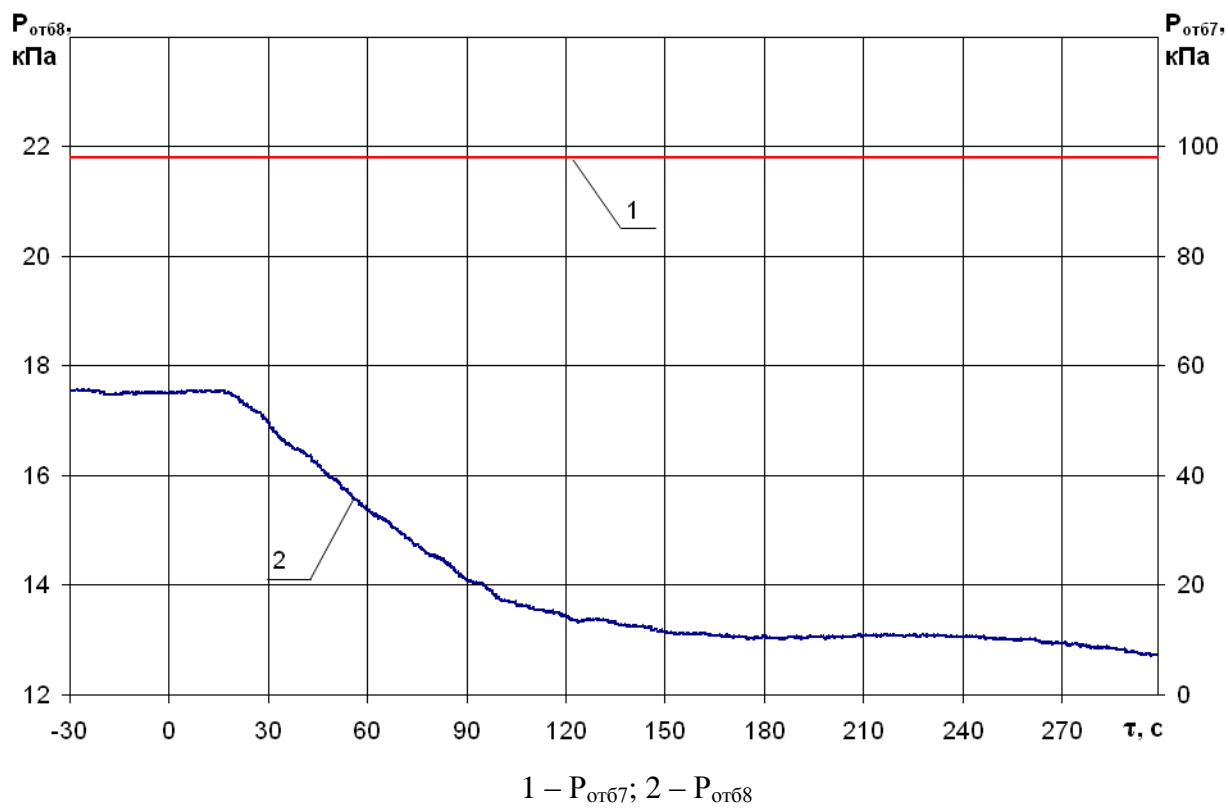


Fig. 99 – Steam pressure at the 7th and 8th intake of the turbine recorded by MMS

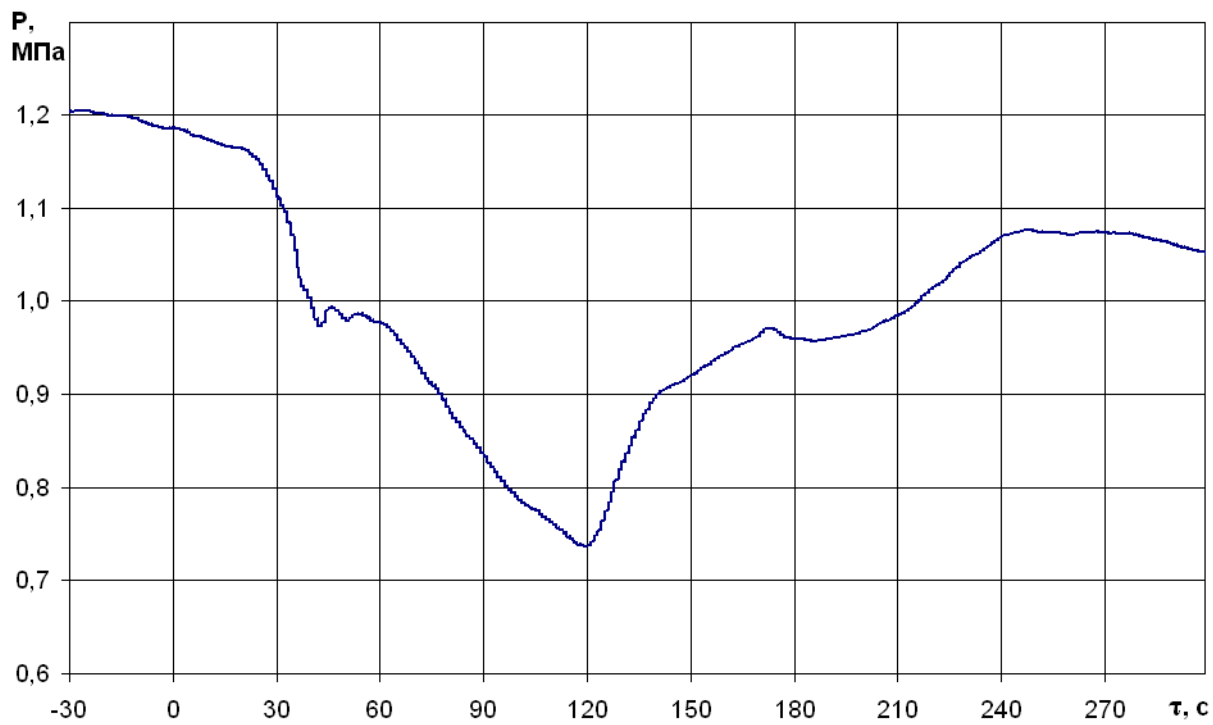


Fig. 100 – ISC steam pressure history recorded by MMS

CONCLUSIONS

1) Analyzing the results of the transient ‘Switching off of one from four operating MCP at nominal reactor power’, it can be concluded:

– the equipment and control systems (with an exception of the system TEC at operational mode ”Contr. P”), protection systems and all interlocks worked correctly according to the design;

– the parameters of PC and SC did not reach the set-points of emergency protection system activation or any acceptance criteria (FA peaking factors and core peaking factors and also the coolant heat-up in the FA) at the investigated power level;

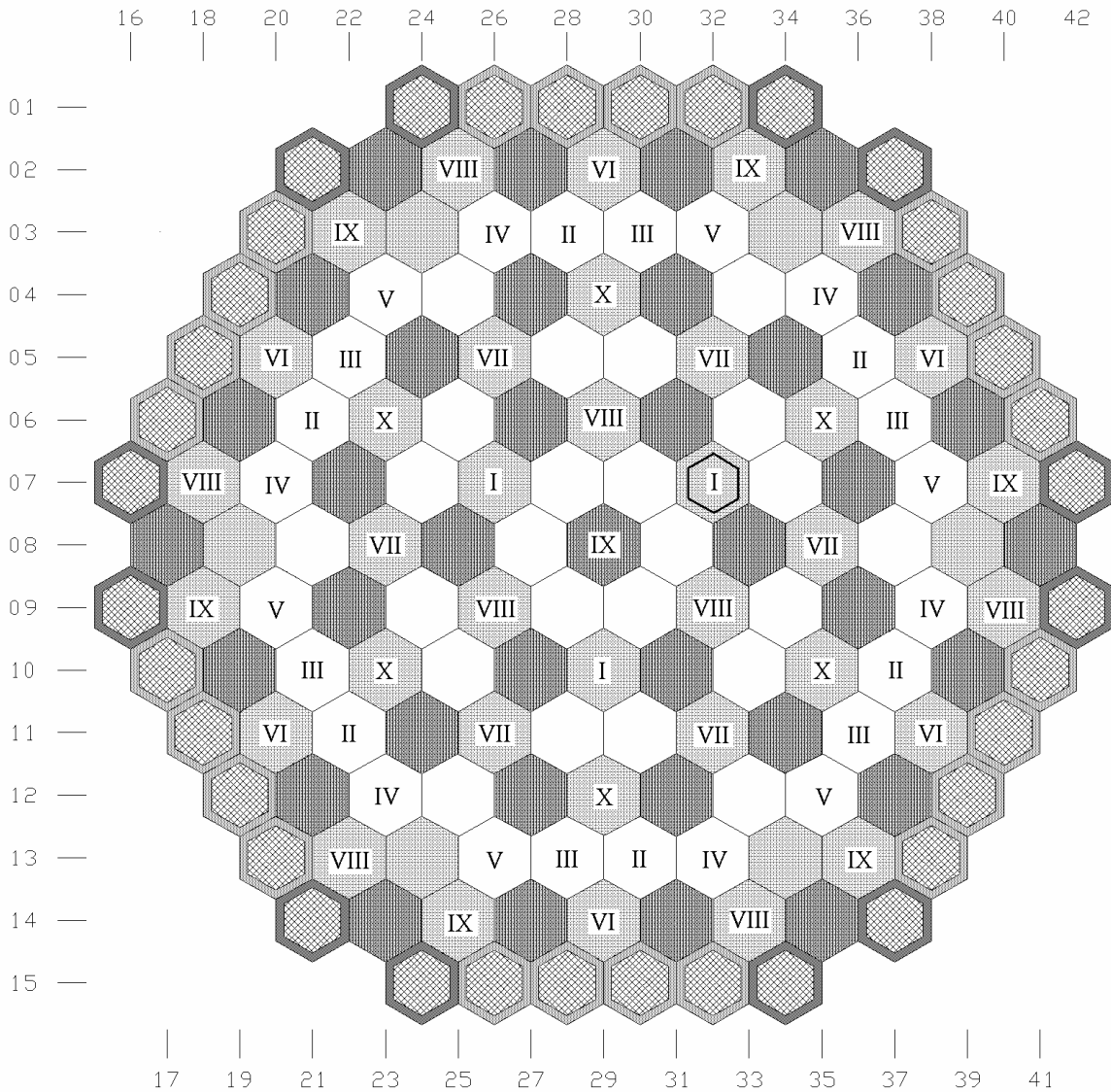
– the reactor facility passed automatically into another, lower power level corresponding to the number of operating MCP.

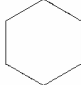
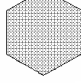
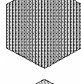
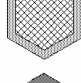
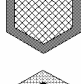
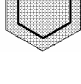
2) Unique experimental data of PC and SC parameter changes were collected needed for the analysis of the performed transient and for validation of computer code systems.

3) A relatively slow TG load-off procedure in the time interval 40 - 85 s after the switching off of MCP-1 was the reason for the relatively big, for such kind of transients, steam pressure reduction. This act in its turn, apart from the insufficient efficiency of the THE (caused by some coolant leakages, larger than the design values, through the control valves of the injection line of the PRZ), imposed an impact on the coolant temperature of the cold legs of the primary circuit loops with operating MCPs and on the PC pressure (which caused relatively big reduction of the main parameters for this reactor operation mode).

ANNEX A

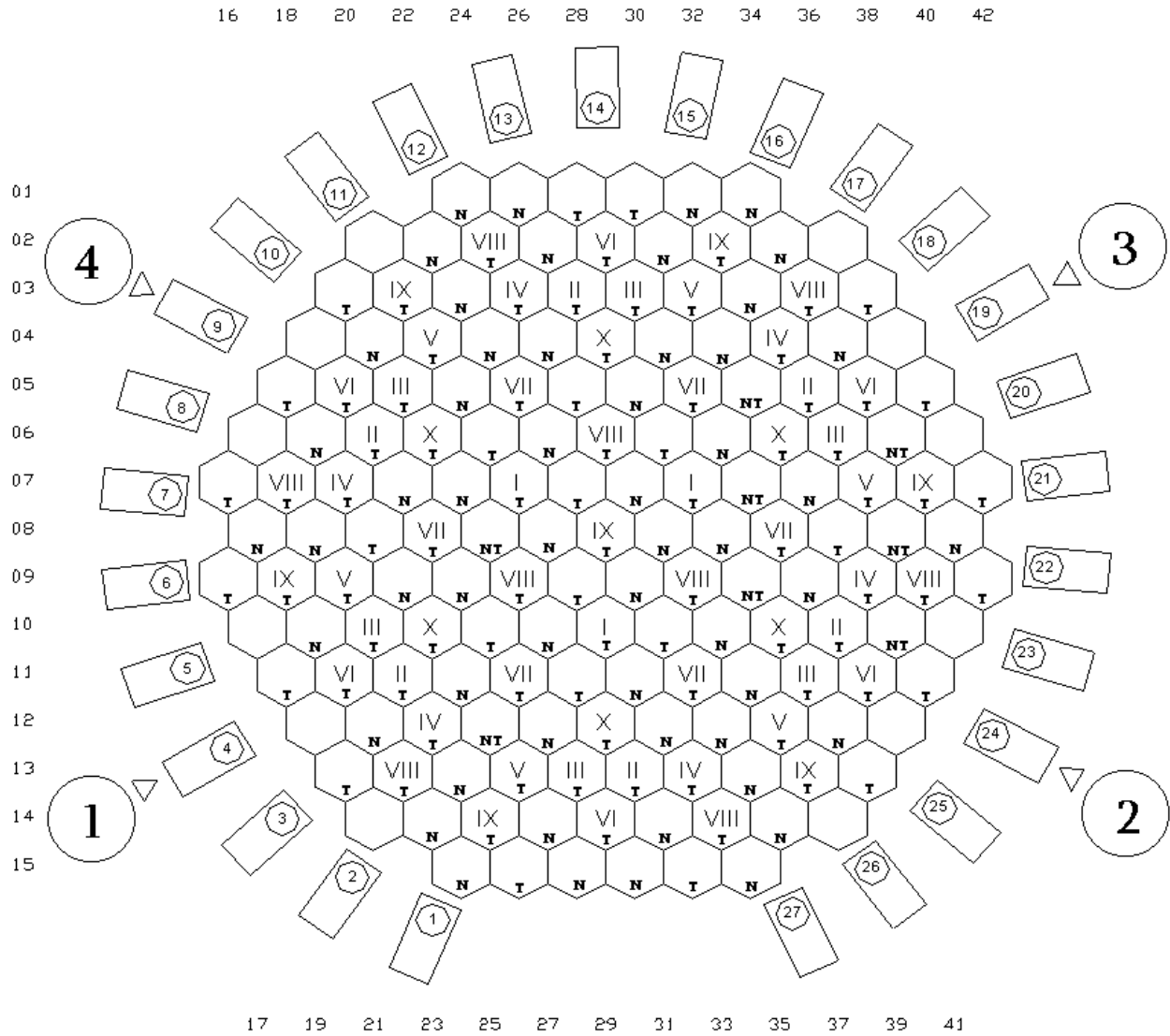
FA layout in the reactor core







- 
 - Enrichment of U-235 1.3 % - 48 FA
- 
 - Enrichment of U-235 2.2 % - 42 FA
- 
 - Average enrichment of U-235 2.98 % - 37 FA
 (303 FA with enrichment 3 %, 9 gad-FA with enrichment 2.4 %)
- 
 - Average enrichment of U-235 3.9 % - 24 „profiled“ FA
 (243 FA with enrichment 4.0 %, 60 FA with enrichment 3.6 %, 9 gad-FA with enrichment 3.3 %)
- 
 - Average enrichment of U-235 3.9 % - 12 „profiled“ FA
 (240 FA with enrichment 4.0 %, 66 FA with enrichment 3.6 %, 6 gad-FA with enrichment 3.3 %)
- 
 - Enrichment of U-235 1,6 (stainless steel)

ANNEX B

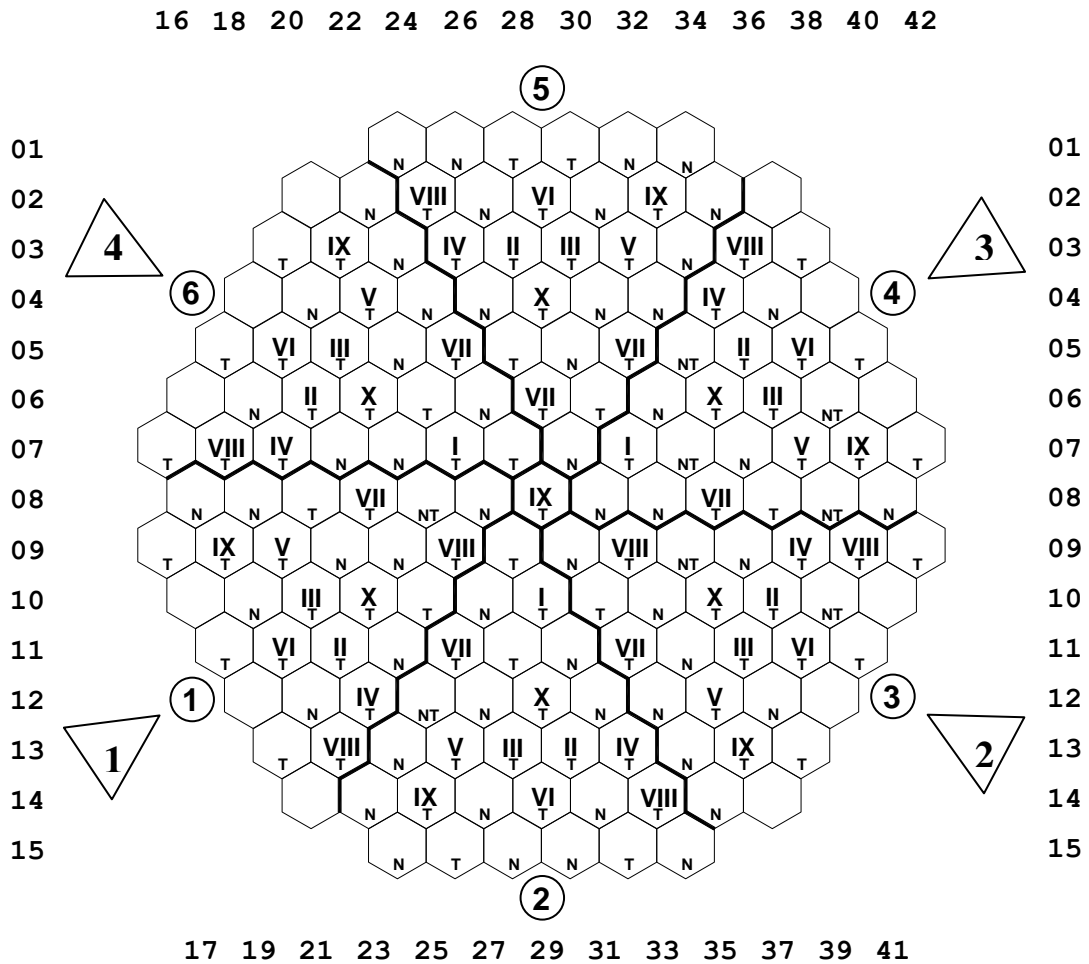
Arrangement of the ionization chamber channels; control rods of CPS and their groups' assignment; thermal control sensors at FA outlets and the arrangement of the SPND



-  - Number of the ionizing chamber channel
-  - Number of the CPS CR group
-  - Assemblies with SPND (thermal control sensors)
-  - Number of the loop

ANNEX C

Division of the reactor core in 60 °-symmetry sector, layout of FA, CPS control rods and CPS CR group allocation, layout of thermal control sensors at FA outlets and assemblies with SPND

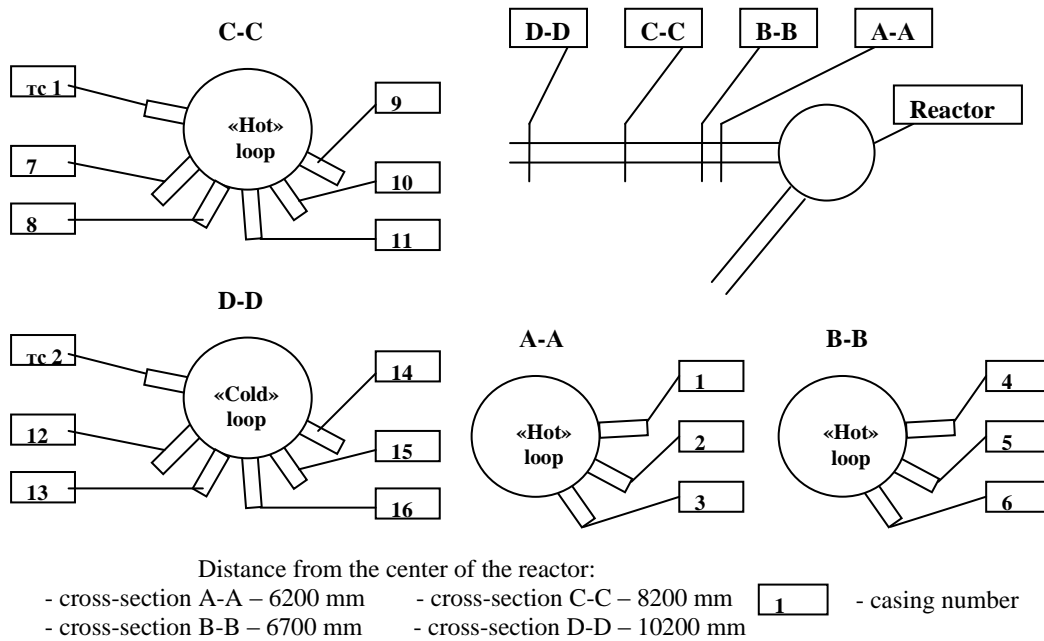


X
NT - Number of CPS CR group
 - Assembly with SPND /thermal control sensors

1 - Number of the loop 1 - Number of 60 ° symmetry sectors

ANNEX D

Location of the temperature monitoring casings in the primary circulation loops



Allocation of in-core control KKS sensors to shroud numbers of MC temperature control

KKS	Parameter	Shroud number
31YAS(11,21,31,41)CT073XQ01	Temperature of the „hot“ leg by RT	rt 1
31YAS(11,21,31,41)CT071AXQ01	Temperature of the „hot“ leg by TC1-1	4
31YAS(11,21,31,41)CT071BXQ01	Temperature of the „hot“ leg by TC1-2	5
31YAS(11,21,31,41)CT071CXQ01	Temperature of the „hot“ leg by TC1-3	6
33YAS(11,21,31,41)CT072AXQ01	Temperature of the „hot“ leg by TC2-1	1
33YAS(11,21,31,41)CT072BXQ01	Temperature of the „hot“ leg by TC2-2	2
33YAS(11,21,31,41)CT072CXQ01	Temperature of the „hot“ leg by TC2-3	3
31YAS(12,22,32,42)CT073XQ01	Temperature of the „hot“ leg by RT	rt 2
31YAS(12,22,32,42)CT071AXQ01	Temperature of the „hot“ leg by TC1-1	13
31YAS(12,22,32,42)CT071BXQ01	Temperature of the „hot“ leg by TC1-2	14
31YAS(12,22,32,42)CT071CXQ01	Temperature of the „hot“ leg by TC1-3	12
33YAS(12,22,32,42)CT072AXQ01	Temperature of the „hot“ leg by TC2-1	13
33YAS(12,22,32,42)CT072BXQ01	Temperature of the „hot“ leg by TC2-2	14
33YAS(12,22,32,42)CT072CXQ01	Temperature of the „hot“ leg by TC2-3	16

Annex E

Parameters recorded by UBLS

Parameter	Unit	Code KKS	Signals No.
Generator's active power	MW	30GTR00CU003_XQ01	1
Turbine rotor rotation speed TFWP-1	rot/min	30SER51CG911_XQ01	1
Flow rate at pressure side of feedwater pump TFWP-1	m ³ /h	30RLR41CF901_XQ01	1
Flow rate at pressure side of feedwater pump TFWP-2	m ³ /h	30RLR42CF901_XQ01	1
Pressure at pressure side of feedwater pump TFWP-2	MPa	30RLR42CP902_XQ01	1
Pressure at pressure side of feedwater pump TFWP-1	MPa	30RLR41CP902_XQ01	1
Position of RV for cooling water supply to the suction of the feedwater pump	%	30UAR30AS801_XQ02	1
Pressure in deaerator D7-1 RL21B01	MPa	30RLR21CP001_XQ01	1
Pressure in deaerator D7-2 RL22B01	MPa	30RLR22CP001_XQ01	1
Pressure of the 3 rd intake	MPa	30RDR30CP001_XQ01	1
Temperature of the 3 rd intake	°C	30RDR30CT001_XQ01	1
Level in D7-1 RL21B01 (0-4000)	mm	30RLR21CL901_XQ01	1
Level in deaerator D7-2 RL22B01 (0-4000)	mm	30RLR22CL901_XQ01	1
Position of RV of heating steam to deaerator D7-1	%	30RQR21AS808_XQ02	1
Position of RV of heating steam to deaerator D7-2	%	30RQR22AS808_XQ02	1
Rotation speed of the turbine rotor TFWP-2	rot/min	30SER52CG911_XQ01	1
Flow rate of feedwater at the inlet to SG-1	t/h	30RLR71CF901_XQ01	1
Temperature of feedwater at the inlet to SG-1	°C	30RLR71CT001_XQ01	1
Flow rate of feedwater at the inlet to SG-2	t/h	30RLR72CF901_XQ01	1
Temperature of feedwater at the inlet to SG-2	°C	30RLR72CT001_XQ01	1
Flow rate of feedwater at the inlet to SG-3	t/h	30RLR73CF901_XQ01	1
Temperature of feedwater at the inlet to SG-3	°C	30RLR73CT001_XQ01	1
Flow rate of feedwater at the inlet to SG-4	t/h	30RLR74CF901_XQ01	1
Temperature of feedwater at the inlet to SG4	°C	30RLR74CT001_XQ01	1
Feedwater level in SG-1 (0-1000)	mm	30YBR10CL901_XQ01	1
Feedwater level in SG-1 (0-4000)	mm	30YBR10CL935_XQ01	1
Feedwater level in SG-2 (0-1000)	mm	30YBR20CL901_XQ01	1
Feedwater level in SG-2 (0-4000)	mm	30YBR20CL935_XQ01	1
Feedwater level in SG-3 (0-1000)	mm	30YBR30CL901_XQ01	1
Feedwater level in SG-3 (0-4000)	mm	30YBR30CL935_XQ01	1
Feedwater level in SG-4 (0-1000)	mm	30YBR40CL901_XQ01	1
Feedwater level in SG-4 (0-4000)	mm	30YBR40CL935_XQ01	1
Feedwater pressure in SG-1	MPa	30RLR71CP001_XQ01	1
Feedwater pressure in SG-2	MPa	30RLR72CP001_XQ01	1
Feedwater pressure in SG-3	MPa	30RLR73CP001_XQ01	1
Feedwater pressure in SG-4	MPa	30RLR74CP001_XQ01	1
Steam pressure in MSH	MPa	30RCR11CP901_XQ01	1
Steam pressure upstream MSS-1 (main steam slide)	MPa	30RAR11CP002_XQ01	1
Steam pressure upstream MSS-2	MPa	30RAR12CP002_XQ01	1
Steam pressure upstream MSS-3	MPa	30RAR13CP002_XQ01	1

Cont. Annex E

Parameter	Unit	Code KKS	Signals No.
Steam pressure upstream MSS-4	MPa	30RAR14CP002_XQ01	1
Pressure of the 2 nd intake	MPa	30RDR20CP901_XQ01	1
Pressure in ISC	MPa	30RQR50CP901_XQ01	1
Pressure of the 2 nd intake в HP-PH-6	MPa	30RDR20CP001_XQ01	1
Feedwater temperature in HP-PH6-1	°C	30RLR61CT003_XQ01	1
Feedwater temperature in HP-PH 6-2 RD22W01	°C	30RLR62CT003_XQ01	1
Pressure of the 1 st intake in HP-PH-7	MPa	30RDR10CP001_XQ01	1
Temperature of the 1 st intake in HP-PH-7	°C	30RDR10CT001_XQ01	1
Temperature of the 2 nd intake in HP-PH-6	°C	30RDR20CT001_XQ01	1
Flow rate of the feedwater to HP-PH -A	m ³ /h	30RLR61CF001_XQ01	1
Feedwater pressure downstream HP-PH-A	MPa	30RLR61CP002_XQ01	1
Feedwater temperature downstream HP-PH7-1	°C	30RLR61CT001_XQ01	1
Feedwater temperature HP-PH7-1	°C	30RLR61CT002_XQ01	1
Feedwater temperature downstream HP-PH7-1	°C	30RLR61CT004_XQ01	1
Feedwater temperature downstream HP-PH7-1	°C	30RLR61CT005_XQ01	1
Feedwater temperature downstream HP-PH7-1	°C	30RLR61CT006_XQ01	1
Flow rate of feedwater to HP-PH-B	m ³ /h	30RLR62CF001_XQ01	1
Feedwater pressure downstream HP-PH -B	MPa	30RLR62CP002_XQ01	1
Feedwater temperature downstream HP-PH7-2	°C	30RLR62CT001_XQ01	1
Feedwater temperature HP-PH7-2	°C	30RLR62CT002_XQ01	1
Feedwater temperature downstream HP-PH7-2	°C	30RLR62CT004_XQ01	1
Feedwater temperature downstream HP-PH7-2	°C	30RLR62CT005_XQ01	1
Feedwater temperature downstream HP-PH7-2	°C	30RLR62CT006_XQ01	1
Position of RV-1 of HPTP	%	30RAR11CS003_XQ01	1
Position of RV-2 of HPTP	%	30RAR12CS003_XQ01	1
Position of RV-3 of HPTP	%	30RAR13CS003_XQ01	1
Position of RV-4 of HPTP	%	30RAR14CS003_XQ01	1
Steam pressure upstream LPTP-1	MPa	30RBR11CP003_XQ01	1
Position of RV of LPTP-1	%	30RBR11CS002_XQ01	1
Steam temperature downstream LPTP-1,2 (left)	°C	30RBR11CT002_XQ01	1
Steam pressure upstream LPTP-2	MPa	30RBR12CP003_XQ01	1
Position of RV of LPTP-2	%	30RBR12CS002_XQ01	1
Steam temperature downstream LPTP-1,2 (right)	°C	30RBR12CT002_XQ01	1
Steam pressure upstream LPTP-3	MPa	30RBR13CP003_XQ01	1
Position of RV of LPTP-3	%	30RBR13CS002_XQ01	1
Steam temperature downstream LPTP-3,4 (left)	°C	30RBR13CT002_XQ01	1
Steam pressure upstream LPTP4	MPa	30RBR14CP003_XQ01	1
Position of RV of LPTP-4	%	30RBR14CS002_XQ01	1
Steam temperature downstream LPTP-3,4 (right)	°C	30RBR14CT002_XQ01	1
Steam pressure at the outlet from HPTP-1	MPa	30SAR10CP002_XQ01	1
Position of RV in steam supply line to high pressure SSSH	%	30RAR20CS001_XQ01	1
Heating steam pressure at the inlet to high pressure SSSH	MPa	30RAR20CP001_XQ01	1
Flow rate of heating steam of SSSH1-4	t/h	30RAR20CF001_XQ01	1
Heating steam temperature at the inlet to high pressure SSSH	°C	30RAR20CT001_XQ01	1
Heating steam pressure at the inlet to SSSH-1	MPa	30RAR21CP001_XQ01	1
Heating steam pressure at the inlet to SSSH-1	MPa	30RAR21CP002_XQ01	1
Heating steam pressure at the inlet to SSSH-2	MPa	30RAR22CP001_XQ01	1
Heating steam pressure at the inlet to SSSH-2	MPa	30RAR22CP002_XQ01	1
Heating steam pressure at the inlet to SSSH-3	MPa	30RAR23CP001_XQ01	1

Cont. Annex E

Parameter	Unit	Code KKS	Signals No.
Heating steam pressure at the inlet to SSSH-3	MPa	30RAR23CP002_XQ01	1
Heating steam pressure at the inlet to SSSH-4	MPa	30RAR24CP001_XQ01	1
Heating steam pressure at the inlet to SSSH-4	MPa	30RAR24CP002_XQ01	1
Steam pressure at the outlet from HPTP-2	MPa	30RBR11CP001_XQ01	1
Steam pressure at the outlet from HPTP-3	MPa	30RBR12CP001_XQ01	1
Steam pressure at the outlet from HPTP-4	MPa	30RBR13CP001_XQ01	1
Steam pressure downstream SSSH-4 RB14W01	MPa	30RBR14CP001_XQ01	1
Level in CCB of SSSH RB20B01 (0-1600)	mm	30RBR20CL001_XQ01	1
Average level in CCB of SSSH RB20B01 (0-1600)	mm	30RBR20CL901_XQ01	1
Steam pressure in CCB of SSSH RB20B01	MPa	30RBR20CP001_XQ01	1
Steam pressure upstream SSSH-1	MPa	30RDR41CP002_XQ01	1
Steam pressure upstream SSSH-2	MPa	30RDR42CP002_XQ01	1
Steam pressure upstream SSSH-3	MPa	30RDR43CP002_XQ01	1
Steam pressure upstream SSSH-4	MPa	30RDR44CP002_XQ01	1
Condensate level in the condensate collector of SSSH (0-1000)	mm	30RNR70CL001_XQ01	1
Heating steam pressure in the condensate collector of SSSH	MPa	30RNR70CP001_XQ01	1
Heating steam temperature downstream the condensate collector of SSSH	°C	30RNR70CT001_XQ01	1
Steam pressure in the turbine condenser SD11,12	kPa	30SDR11CP901_XQ01	1
Circuit water temperature downstream the turbine condenser SD11	°C	30SDR11CT001_XQ01	1
Steam pressure in the turbine condenser SD13,14	kPa	30SDR13CP901_XQ01	1
Circuit water temperature downstream the turbine condenser SD13	°C	30SDR13CT001_XQ01	1
Circuit water temperature at the inlet to the turbine condenser (the 1st group)	°C	30VCR11CT002_XQ01	1
Circuit water temperature at the outlet from the turbine condenser (the 1st group)	°C	30VCR11CT003_XQ01	1
Circuit water temperature at the inlet to the turbine condenser (the 1st group)	°C	30VCR12CT002_XQ01	1
Circuit water temperature at the outlet from the turbine condenser (the 1st group)	°C	30VCR12CT003_XQ01	1
Circuit water temperature at the inlet to the turbine condenser (the 2nd group)	°C	30VCR13CT002_XQ01	1
Circuit water temperature at the outlet from the turbine condenser (the 2nd group)	°C	30VCR13CT003_XQ01	1
Circuit water temperature at the inlet to the turbine condenser (the 2nd group)	°C	30VCR14CT002_XQ01	1
Circuit water temperature at the outlet from the turbine condenser (the 2nd group)	°C	30VCR14CT003_XQ01	1
Condensate flow rate to deaerator D7-1 RL21B01	m ³ /h	30RMR80CF001A_XQ01	1
Condensate flow rate to deaerator D7-2 RL22B01	m ³ /h	30RMR80CF002A_XQ01	1
Average level of the condensate in LP-PH-2 (0-1600)	mm	30RHR70CL901_XQ01	1
Condensate level in LP-PH1-1 RH80W01 (0-1000)	mm	30RHR80CL001_XQ01	1
Condensate pressure in LP-PH1-1 RH80W01	kPa	30RHR80CP001_XQ01	1
Condensate pressure in LP-PH1-1 RH80W01	kPa	30RHR81CP001_XQ01	1
Condensate temperature in LP-PH1-1 RH80W01	°C	30RHR81CT001_XQ01	1
Condensate pressure in LP-PH1-1 RH80W01 0-100	kPa	30RHR82CP001_XQ01	1
Condensate temperature in LP-PH1-1 RH80W01	°C	30RHR82CT001_XQ01	1
Condensate pressure in LP-PH1-2 RH80W01	kPa	30RHR83CP001_XQ01	1

Cont. Annex E

Parameter	Unit	Code KKS	Signals No.
Condensate temperature in LP-PH1-2 RH80W02	°C	30RHR83CT001_XQ01	1
Condensate pressure in LP-PH1-2 RH80W01	kPa	30RHR84CP001_XQ01	1
Condensate temperature in LP-PH1-2 RH80W02	°C	30RHR84CT001_XQ01	1
Position of the main RV for the level in deaerator D-7	%	30RMR70AS802_XQ02	1
Position of the starting RV for the level in deaerator D-7	%	30RMR72AS802_XQ02	1
Average condensate level in the turbine condenser SD11 (0-1600)	mm	30SDR11CL901_XQ01	1
Average condensate level in the turbine condenser SD13 (0-1600)	mm	30SDR13CL901_XQ01	1
Position of RV for cooling water supply to the deaerator	%	30UAR20AS803_XQ02	1
Average pressure in the pressure collector CP-2	MPa	30RMR70CP901_XQ01	1
Condensate pressure in LP-PH-5 RD40W01	MPa	30RDR40CP002_XQ01	1
Condensate level in LP-PH-5 RD40W01 (0-1600)	mm	30RDR40CL001_XQ01	1
Average condensate level in LP-PH-5 (0-1600)	mm	30RDR40CL901_XQ01	1
Average condensate level in LP-PH-5 (0-630)	mm	30RDR40CL902_XQ01	1
Condensate pressure in LP-PH-5 RD40W01	MPa	30RDR40CP001_XQ01	1
Average condensate pressure in LP-PH-5 RD40W01	MPa	30RDR40CP901_XQ01	1
Condensate temperature in LP-PH-5	°C	30RDR40CT001_XQ01	1
Condensate level in LP-PH-4 RH50W01 (0-1600)	mm	30RHR50CL001_XQ01	1
Condensate level in LP-PH-4 RH50W01 (0-630)	mm	30RHR50CL002_XQ01	1
Condensate level in LP-PH-4 RH50W01 (0-1600)	mm	30RHR50CL003_XQ01	1
Condensate level in LP-PH-4 RH50W01 (0-1600)	mm	30RHR50CL004_XQ01	1
Average condensate level in LP-PH-4 (0-1600)	mm	30RHR50CL901_XQ01	1
Average condensate level in LP-PH-4 (0-630)	mm	30RHR50CL902_XQ01	1
Condensate pressure upstream LP-PH-4 RH50W01	MPa	30RHR50CP001_XQ01	1
Condensate pressure upstream LP-PH-4 RH50W01	MPa	30RHR50CP002_XQ01	1
Condensate pressure upstream the return valve of RH50S01	MPa	30RHR50CP004_XQ01	1
Condensate temperature upstream LP-PH-4 RH50W01	°C	30RHR50CT001_XQ01	1
Condensate temperature upstream the return valve of RH50S01	°C	30RHR50CT002_XQ01	1
Condensate level in LP-PH3 (0-1600)	mm	30RHR60CL901_XQ01	1
Condensate level in LP-PH3 (0-630)	mm	30RHR60CL902_XQ01	1
Position of RV for the level in LP-PH-3	%	30RNR60AS801_XQ02	1
Turbine shaft rotation speed (0-4000)	rot/min	30SBR11CS901_XQ02	1
Position of the turbine control device	%	30SER60AS006_XQ02	1
Generator electrical power	MW	30SPR10CE903_XQ01	1
Steam temperature downstream SSSH-1 RB11W01	°C	30RBR11CT001_XQ01	1
Steam temperature downstream SSSH-2 RB11W01	°C	30RBR12CT001_XQ01	1
Steam temperature downstream SSSH-3 RB11W01	°C	30RBR13CT001_XQ01	1
Steam temperature downstream SSSH-4 RB11W01	°C	30RBR14CT001_XQ01	1
Position of the heating steam RV to D7-1	%	30RQR21AS808_AA01	1
Position of the heating steam RV to D7-2	%	30RQR22AS808_AA01	1
Position of main RV in the feedwater supply to SG-1	%	30RLR71AS802_AA01	1
Position of starting RV in the feedwater supply to SG-1	%	30RLR71AS804_AA01	1
Position of main RV in the feedwater supply to SG-1	%	30RLR72AS802_AA01	1
Position of starting RV in the feedwater supply to SG-1	%	30RLR72AS804_AA01	1
Position of main RV in the feedwater supply to SG-1	%	30RLR73AS802_AA01	1
Position of starting RV in the feedwater supply to SG-1	%	30RLR73AS804_AA01	1
Position of main RV in the feedwater supply to SG-1	%	30RLR74AS802_AA01	1
Position of starting RV in the feedwater supply to SG-1	%	30RLR74AS804_AA01	1

Cont. Annex E

Parameter	Unit	Code KKS	Signals No.
Position of (fast acting relief valve to condenser) BRUK-3	%	30RCR12AS801_AA01	1
Position of (fast acting relief valve to condenser) BRUK-4	%	30RCR12AS802_AA01	1
Position of (fast acting steam discharge into the collector) FASB-HL1	%	30RQR11AS801_AA01	1
Position of (fast acting steam discharge into the collector) FASB-HL2	%	30RQR12AS801_AA01	1
Position of (fast acting relief valve to condenser) BRUK-1	%	30RCR11AS801_AA01	1
Position of (fast acting relief valve to condenser) BRUK-2	%	30RCR11AS802_AA01	1
Position of (fast acting steam discharge into the atmosphere) BRUA-4	%	31TXS80AS005_AA01	1
Sensor of the BRUA-4 position	%	31TXS80AS005_XQ02	1
Position of (fast acting steam discharge into the atmosphere) BRUA-2	%	32TXS60AS005_AA01	1
Sensor of the BRUA-2 position	%	32TXS60AS005_XQ02	1
Position of (fast acting steam discharge into the atmosphere) BRUA-3	%	32TXS70AS005_AA01	1
Sensor of the BRUA-3 position	%	32TXS70AS005_XQ02	1
Position of (fast acting steam discharge into the atmosphere) BRUA-1	%	33TXS50AS005_AA01	1
Sensor of the BRUA -1 position	%	33TXS50AS005_XQ02	1
Coolant level in PRESSURIZER	m	31YPS10FL905_XQ02	1
Flow rate of PC make-up	m ³ /h	31TKS30CF001_XQ02	1
Flow rate of PC blowdown (downstream TK80S03)	m ³ /h	31TKS80CF001_XQ02	1
Feedwater level in SG-1	m	31YBS10FL905_XQ02	1
Feedwater level in SG-2	m	31YBS20FL905_XQ02	1
Feedwater level in SG-3	m	31YBS30FL905_XQ02	1
Feedwater level in SG-4	m	31YBS40FL905_XQ02	1
Position of RV for BRUA-4	%	31TXS80AS005_XQ02	1
Position of RV for BRUA-2	%	32TXS60AS005_XQ02	1
Position of RV for BRUA-3	%	32TXS70AS005_XQ02	1
Position of RV for BRUA-3	%	32TXS70AS005R_XQ02	1
Position of RV for BRUA-1	%	33TXS50AS005_XQ02	1
Position of the device BRUA-4	%	31TXS80AS005_AA01	1
PC supply pressure	MPa	30TKR30CP901_XQ02	1
Flow rate in the pressure side header of the feedwater pump	m ³ /h	30TKR50CF901_XQ02	1
Difference of flow rates in PC volume control system	m ³ /h	30TKR00FF901_XQ01	1
Boron concentration in PC supply	g/dm ³	30TKR30CQ001_XQ02	1
RV position in blowdown TK81S02	%	30TKR81AS002_XQ02	1
RV position in blowdown TK82S02	%	30TKR82AS002_XQ02	1
RV position in supply TK31S02	%	30TKR31AS002_XQ02	1
RV position in supply TK32S02	%	30TKR32AS002_XQ02	1
Position of RV of „fine“ injection	%	30YPR13AS002_XQ02	1
Water level in PRESSURIZER	m	30YPR10FL002_XQ02	1
Water level in PRESSURIZER	m	30YPR10FL901_XQ02	1
Water level in PRZ	m	30YPR10FL903_XQ02	1
Feedwater level in SG-1	m	30YBR10CL903_XQ02	1
Main steam pressure SG-1	MPa	30YBR10CP010_XQ02	1
Feedwater level in SG-2	m	30YBR20CL903_XQ02	1
Main steam pressure SG-2	MPa	30YBR20CP010_XQ02	1
Feedwater level in SG-3	m	30YBR30CL903_XQ02	1
Main steam pressure SG-3	MPa	30YBR30CP010_XQ02	1

Parameter	Unit	Code KKS	Signals No.
Feedwater level in SG-4	m	30YBR40CL903_XQ02	1
Main steam pressure SG-4	MPa	30YBR40CP010_XQ02	1
Boron concentration in the intake from PRZ	g/dm ³	30TVR50CQ001_XQ02	1
Boron concentration in the intake from the reactor	g/dm ³	30TVR30CQ001_XQ02	1
Boron concentration in the intake from the reactor	g/dm ³	30TVR40CQ001_XQ02	1
RV position in blowdown TK81S02	%	30TKR81AS002_AA01	1
RV position in blowdown TK82S02	%	30TKR82AS002_AA01	1
RV position in supply TK31S02	%	30TKR31AS002_AA01	1
RV position in supply TK32S02	%	30TKR32AS002_AA01	1
Coolant pressure difference in MCP-1	MPa	31YAS10CP051AXQ01	1
Coolant pressure difference in MCP-2	MPa	31YAS20CP051AXQ01	1
Coolant pressure difference in MCP-3	MPa	31YAS30CP051AXQ01	1
Reactor power recorded by NFC ion. chamber 2 OR-2	%	31YCS00FX005AXQ01	1
Reactor power recorded by NFC ion. chamber 2 OR-1	%	31YCS00FX001AXQ01	1
Reactor power recorded by NFC ion. chamber 2 PD	%	31YCS00FX019AXQ01	1
Reactivity recorded by ion. chamber 2	β_{ef}	31YCS00FX200AXQ01	1
Reactor power recorded by NFC ion. chamber 12 OR-2	%	31YCS00FX005BXQ01	1
Reactor power recorded by NFC ion. chamber 12 OR-1	%	31YCS00FX001BXQ01	1
Reactor power recorded by NFC ion. chamber 12 PD	%	31YCS00FX019BXQ01	1
Reactivity recorded by ion. chamber 12	β_{ef}	31YCS00FX200BXQ01	1
Reactor power recorded by NFC ion. chamber 22 OR-2	%	31YCS00FX005CXQ01	1
Reactor power recorded by NFC ion. chamber 22 OR-1	%	31YCS00FX001CXQ01	1
Reactor power recorded by NFC ion. chamber 22 PD	%	31YCS00FX019CXQ01	1
Reactivity recorded by ion. chamber 22	β_{ef}	31YCS00FX200CXQ01	1
Reactor power recorded by NFC ion. chamber 7 OR-2	%	33YCS00FX006AXQ01	1
Reactor power recorded by NFC ion. chamber 7 OR-1	%	33YCS00FX002AXQ01	1
Reactor power recorded by NFC ion. chamber 7 PD	%	33YCS00FX020AXQ01	1
Reactivity recorded by ion. chamber 7	β_{ef}	33YCS00FX201AXQ01	1
Coolant pressure difference in MCP-1	MPa	33YAS10CP052BXQ01	1
Coolant pressure difference in MCP-2	MPa	33YAS20CP052BXQ01	1
Coolant pressure difference in MCP-3	MPa	33YAS30CP052BXQ01	1
Coolant pressure difference in MCP-4	MPa	33YAS40CP052BXQ01	1
Reactor power recorded by NFC ion. chamber 17 OR-2	%	33YCS00FX006BXQ01	1
Reactor power recorded by NFC ion. chamber 17 OR-1	%	33YCS00FX002BXQ01	1
Reactor power recorded by NFC ion. chamber 17 PD	%	33YCS00FX020BXQ01	1
Reactivity recorded by ion. chamber 17	β_{ef}	33YCS00FX201BXQ01	1
Supply frequency of MCP-1	Hz	33YDS10CH052CXQ01	1
Supply frequency of MCP-2	Hz	33YDS20CH052CXQ01	1
Supply frequency of MCP-3	Hz	33YDS30CH052CXQ01	1
Supply frequency of MCP-4	Hz	33YDS40CH052CXQ01	1
Reactor power recorded by NFC ion. chamber 27 OR-2	%	33YCS00FX006CXQ01	1
Reactor power recorded by NFC ion. chamber 27 OR-1	%	33YCS00FX002CXQ01	1
Reactor power recorded by NFC ion. chamber 27 PD	%	33YCS00FX020CXQ01	1
Reactivity recorded by ion. chamber 27	β_{ef}	33YCS00FX201CXQ01	1
Average coolant temperature in the „cold“ leg of loop 1	°C	30YAR12FT901XQ01	1
Average coolant temperature in the „cold“ leg of loop 2	°C	30YAR22FT901XQ01	1
Average coolant temperature in the „cold“ leg of loop 3	°C	30YAR32FT901XQ01	1
Average coolant temperature in the „cold“ leg of loop 4	°C	30YAR42FT901XQ01	1
Average coolant temperature at the inlet to reactor	°C	30YAR00FT901XQ01	1
Average coolant temperature in the „hot“ leg of loop 1	°C	30YAR11FT901XQ01	1

Cont. Annex E

Parameter	Unit	Code KKS	Signals No.
Average coolant temperature in the „hot“ leg of loop 2	°C	30YAR21FT901XQ01	1
Average coolant temperature in the „hot“ leg of loop 3	°C	30YAR31FT901XQ01	1
Average coolant temperature in the „hot“ leg of loop 4	°C	30YAR41FT901XQ01	1
Average coolant temperature at the outlet of reactor	°C	30YAR00FT901XQ03	1
Minimal value of DNB factor	rel. unit	30YQR08FX904XQ01	1
Summary volume flow rate through the reactor	m ³ /h	30YCR10FF903XQ01	1
Average reactor power (core)	MW	30YQR00FX901XQ01	1
Position of CPS-rods group 10	%	30YVS00FG910XQ02	1
Thermal power loop 1	MW	30YAR10FU001XQ01	1
Thermal power loop 2	MW	30YAR20FU001XQ01	1
Thermal power loop 3	MW	30YAR30FU001XQ01	1
Thermal power loop 4	MW	30YAR40FU001XQ01	1
Reactor thermal power recorded by PC parameters	MW	30YAR00FX001XQ01	1
Coolant average pressure in the reactor	MPa	30YCR10FP901XQ01	1
Coolant pressure difference in the reactor	MPa	30YCR10CP071XQ01	1
Calculated feedwater temperature in SG-1	°C	30RLR71FT001XQ01	1
Calculated feedwater temperature in SG-2	°C	30RLR72FT001XQ01	1
Calculated feedwater temperature in SG-3	°C	30RLR73FT001XQ01	1
Calculated feedwater temperature in SG-4	°C	30RLR74FT001XQ01	1
Reactor thermal power by parameters of SC to SG	MW	30RLR00FX903XQ03	1
Reactor power recorded by DCS	MW	30YQR00FX001XQ01	1
Reactor power recorded by NFC	MW	30YCR00FX001XQ01	1
Feedwater temperature upstream HP-PH7-1	°C	30RLR61CT003_XQ01	1
Feedwater temperature downstream HP-PH7-1	°C	30RLR61CT004_XQ01	1
Feedwater temperature downstream HP-PH7-1	°C	30RLR61CT005_XQ01	1
Feedwater temperature downstream HP-PH7-1	°C	30RLR61CT006_XQ01	1
Feedwater temperature upstream HP-PH7-2	°C	30RLR62CT003_XQ01	1
Feedwater temperature downstream HP-PH7-2	°C	30RLR62CT004_XQ01	1
Feedwater temperature downstream HP-PH7-2	°C	30RLR62CT005_XQ01	1
Feedwater temperature downstream HP-PH7-2	°C	30RLR62CT006_XQ01	1
Steam average pressure in MSH	MPa	30RCR11CP901_XQ01	1
Main RV position for feedwater to SG-1	%	30RLR71AS802_AA01	1
Starting RV position for feedwater to SG-1	%	30RLR71AS804_AA01	1
Feedwater flow rate in SG-1	t/h	30RLR71CF901_XQ01	1
Main RV position for feedwater to SG-2	%	30RLR72AS802_AA01	1
Starting RV position for feedwater to SG-2	%	30RLR72AS804_AA01	1
Feedwater flow rate in SG-2	t/h	30RLR72CF901_XQ01	1
Main RV position for feedwater to SG-3	%	30RLR73AS802_AA01	1
Starting RV position for feedwater to SG-3	%	30RLR73AS804_AA01	1
Feedwater flow rate in SG-3	t/h	30RLR73CF901_XQ01	1
Main RV position for feedwater to SG-4	%	30RLR74AS802_AA01	1
Starting RV position for feedwater to SG-4	%	30RLR74AS804_AA01	1
Feedwater flow rate in SG-1	t/h	30RLR74CF901_XQ01	1
Feedwater level in SG-1 (0-1000)	mm	30YBR10CL901_XQ01	1
Feedwater level in SG-1 (0-4000)	mm	30YBR10CL935_XQ01	1
Feedwater level in SG-2 (0-1000)	mm	30YBR20CL901_XQ01	1
Feedwater level in SG-2 (0-4000)	mm	30YBR20CL935_XQ01	1
Feedwater level in SG-3 (0-1000)	mm	30YBR30CL901_XQ01	1
Feedwater level in SG-3 (0-4000)	mm	30YBR30CL935_XQ01	1
Feedwater level in SG-4 (0-1000)	mm	30YBR40CL901_XQ01	1

Cont. Annex E

Parameter	Unit	Code KKS	Signals No.
Feedwater level in SG-4 (0-4000)	mm	30YBR40CL935_XQ01	1
Feedwater level in HP-PH7-1 (0-6300)	mm	30RDR11CL001_XQ01	1
Feedwater level in HP-PH7-1 (0-6300)	mm	30RDR11CL002_XQ01	1
Feedwater level in HP-PH7-1 (0-6300)	mm	30RDR11CL003_XQ01	1
Feedwater level in HP-PH7-1 (0-1000)	mm	30RDR11CL004_XQ01	1
Feedwater average level in HP-PH7-1 (0-6300)	mm	30RDR11CL901_XQ01	1
Feedwater level in HP-PH7-2 (0-6300)	mm	30RDR12CL001_XQ01	1
Feedwater level in HP-PH7-2 (0-6300)	mm	30RDR12CL002_XQ01	1
Feedwater level in HP-PH7-2 (0-6300)	mm	30RDR12CL003_XQ01	1
Feedwater level in HP-PH7-2 (0-1000)	mm	30RDR12CL004_XQ01	1
Feedwater average level in HP-PH7-2 (0-6300)	mm	30RDR12CL901_XQ01	1
Feedwater level in HP-PH 6-1 (0-6300)	mm	30RDR21CL001_XQ01	1
Feedwater level in HP-PH 6-1 (0-6300)	mm	30RDR21CL002_XQ01	1
Feedwater level in HP-PH 6-1 (0-6300)	mm	30RDR21CL003_XQ01	1
Feedwater level in HP-PH 6-1 (0-1000)	mm	30RDR21CL004_XQ01	1
Feedwater average level in HP-PH 6-1 (0-6300)	mm	30RDR21CL901_XQ01	1
Feedwater level in HP-PH 6-2 (0-6300)	mm	30RDR22CL001_XQ01	1
Feedwater level in HP-PH 6-2 (0-6300)	mm	30RDR22CL002_XQ01	1
Feedwater level in HP-PH 6-2 (0-6300)	mm	30RDR22CL003_XQ01	1
Feedwater level in HP-PH 6-2 (0-1000)	mm	30RDR22CL004_XQ01	1
Feedwater average level in HP-PH 6-2 (0-6300)	mm	30RDR22CL901_XQ01	1
Condensate level in the turbine condenser confluent chamber SD21	mm	30VCR01CL001_XQ01	1
Condensate level in the turbine condenser confluent chamber SD22	mm	30VCR02CL001_XQ01	1
Condensate level in the turbine condenser confluent chamber SD23	mm	30VCR03CL001_XQ01	1
Condensate level in the turbine condenser confluent chamber SD24	mm	30VCR04CL001_XQ01	1
Condensate pressure in LP-PH-2 RH70W01	kPa	30RHR70CP001_XQ01	1
Average condensate level in LP-PH-2 (0-1600)	mm	30RHR70CL901_XQ01	1
Average condensate level in LP-PH-2 (0-1000)	mm	30RHR70CL904_XQ01	1
Pressure in the 7th intake in LP-PH-2	kPa	30RHR71CP001_XQ01	1
Condensate temperature upstream LP-PH-2 RH70W01	°C	30RHR71CT001_XQ01	1
Pressure in the 7th intake LP-PH-2	kPa	30RHR72CP001_XQ01	1
Condensate temperature upstream LP-PH-2 RH70W01	°C	30RHR72CT001_XQ01	1
Condensate level in LP-PH1-1 RH80W01 (0-1000)	mm	30RHR80CL001_XQ01	1
Condensate level in LP-PH1-2 RH80W02 (0-4000)	mm	30RHR80CL002_XQ01	1
Condensate level in LP-PH1-2 RH80W02 (0-1000)	mm	30RHR80CL003_XQ01	1
Average condensate level in LP-PH-1 (0-1000)	mm	30RHR80CL901_XQ01	1
Condensate pressure in LP-PH1-1 RH80W01	kPa	30RHR80CP001_XQ01	1
Condensate pressure in LP-PH1-2 RH80W02	kPa	30RHR80CP002_XQ01	1
Condensate pressure in LP-PH1-1 RH80W01	kPa	30RHR80CP901_XQ01	1
Condensate pressure in LP-PH1-1 RH80W01	kPa	30RHR81CP001_XQ01	1
Condensate temperature in LP-PH1-1 RH80W01	°C	30RHR81CT001_XQ01	1
Condensate pressure in LP-PH1-1 RH80W01	kPa	30RHR82CP001_XQ01	1
Condensate temperature in LP-PH1-1 RH80W01	°C	30RHR82CT001_XQ01	1

Cont. Annex E

Parameter	Unit	Code KKS	Signals No.
Condensate pressure in LP-PH1-2 RH80W01	kPa	30RHR83CP001_XQ01	1
Condensate temperature in LP-PH1-2 RH80W02	°C	30RHR83CT001_XQ01	1
Condensate pressure in LP-PH1-2 RH80W01	kPa	30RHR84CP001_XQ01	1
Condensate temperature in LP-PH1-2 RH80W02	°C	30RHR84CT001_XQ01	1
Condensate temperature at the suction side of CP-1	°C	30RMR10CT001_XQ01	1
Condensate temperature at the suction side of CP-1	°C	30RMR10CT002_XQ01	1
Condensate temperature in LP-PH1-1 RH80W01	°C	30RMR50CT001_XQ01	1
Condensate temperature in LP-PH1-2 RH80W02	°C	30RMR50CT002_XQ01	1
Condensate temperature at the suction side of CP-2	°C	30RMR60CT001_XQ01	1
Condensate level in the turbine condenser SD11 (0-1600)	mm	30SDR11CL001_XQ01	1
Condensate level in the turbine condenser SD11 (0-1600)	mm	30SDR11CL002_XQ01	1
Average condensate level in the turbine condenser SD11 (0-1600)	mm	30SDR11CL901_XQ01	1
Condensate level in the turbine condenser SD13 (0-1600)	mm	30SDR13CL001_XQ01	1
Condensate level in the turbine condenser SD13 (0-1600)	mm	30SDR13CL002_XQ01	1
Average condensate level in the turbine condenser SD13 (0-1600)	mm	30SDR13CL901_XQ01	1
Condensate average pressure at pressure collector CP-2	MPa	30RMR70CP901_XQ01	1
Condensate at pressure collector CP-2	MPa	30RMR70CP001A_XQ01	1
Condensate at pressure collector CP-2	MPa	30RMR70CP001B_XQ01	1
Condensate pressure in LP-PH-5 RD40W01	MPa	30RDR40CP901_XQ01	1
Condensate temperature in LP-PH-5 RD40W01	°C	30RDR40CT001_XQ01	1
Condensate pressure upstream LP-PH-4 RH50W01	MPa	30RHR50CP001_XQ01	1
Condensate pressure upstream LP-PH-4 RH50W01	MPa	30RHR50CP002_XQ01	1
Condensate pressure upstream the return valve of RH50S01	MPa	30RHR50CP004_XQ01	1
Condensate temperature upstream LP-PH-4 RH50W01	°C	30RHR50CT001_XQ01	1
Condensate temperature upstream the return valve of RH50S01	°C	30RHR50CT002_XQ01	1
Condensate pressure upstream LP-PH-3 RH60W01	kPa	30RHR61CP001_XQ01	1
Condensate pressure upstream LP-PH-3 RH60W01	kPa	30RHR61CP002_XQ01	1
Condensate pressure upstream the return valve of LP-PH-3	kPa	30RHR61CP004_XQ01	1
Condensate pressure upstream LP-PH-3 RH60W01	°C	30RHR61CT001_XQ01	1
Condensate temperature upstream the return valve of LP-PH-3	°C	30RHR61CT002_XQ01	1
RV-device position for the level in HP-PH 6-1 with the discharge to deaerator D-7	%	30RNR21AS803_AA01	1
RV-device position for the level in HP-PH 6-1 with the discharge to the turbine condenser	%	30RNR21AS811_AA01	1
RV-device position for the level in HP-PH 6-2 with the discharge to deaerator D-7	%	30RNR22AS811_AA01	1
RV-device position for the level in HP-PH 6-2 with the discharge to the turbine condenser	%	30RNR22AS803_AA01	1
RV-device position for the level in HP-PH7-2	%	30RNR12AS801_AA01	1
RV-device position for the level in HP-PH7-1	%	30RNR11AS801_AA01	1
RV-device position for the level in LP-PH-5	%	30RNR41AS802_AA01	1
RV-device position for the level in LP-PH-4	%	30RNR50AS801_AA01	1
RV-device position for the level in LP-PH-3	%	30RNR60AS801_AA01	1
Position of RV of (fast acting discharge into condenser) BRUK-1	%	30RCR11AS801_XQ02	1
Position of RV of (fast acting discharge into condenser) BRUK-2	%	30RCR11AS802_XQ02	1
Position of RV of (fast acting discharge into condenser)	%	30RCR12AS801_XQ02	1

Cont. Annex E

Parameter	Unit	Code KKS	Signals No.
BRUK-3			
Position of RV of (fast acting discharge into condenser) BRUK-4	%	30RCR12AS802_XQ02	1
Average condensate level in the condensate collector SSSH (0-1000)	mm	30RNR70CL901_XQ01	1
Temperature at the pressure side of the pump for the discharge of the condensate SSSH	⁰ C	30RNR80CT001_XQ01	1
Pressure at the suction side of the pump for the discharge of the condensate RN81D01	MPa	30RNR81CP001_XQ01	1
Pressure at the pressure side of the pump for the discharge of the condensate RN81D01	MPa	30RNR81CP002_XQ01	1
Condensate flow rate to deaerator D7-1 RL21B01	m ³ /h	30RMR80CF001A_XQ01	1
Condensate flow rate to deaerator D7-2 RL22B01	m ³ /h	30RMR80CF002A_XQ01	1
Condensate pressure at pressure collector CP1-1	MPa	30RMR11CP902_XQ01	1
Condensate pressure at pressure collector CP1-2	MPa	30RMR12CP902_XQ01	1
Condensate pressure at collector CP1-3	MPa	30RMR13CP902_XQ01	1
Condensate flow rate downstream BOU (deionising device)	t/h	30RMR40CF901_XQ01	1
Condensate pressure downstream BOU	MPa	30RMR40CP001_XQ01	1
Condensate temperature downstream BOU	⁰ C	30RMR40CT001_XQ01	1
Condensate average pressure at pressure collector CP-2	MPa	30RMR70CP901_XQ01	1
Condensate at pressure collector CP2-1	MPa	30RMR61CP902_XQ01	1
Condensate at pressure collector CP2-2	MPa	30RMR62CP902_XQ01	1
Condensate at pressure collector CP2-3	MPa	30RMR63CP902_XQ01	1
Condensate at pressure collector CP2-4	MPa	30RMR64CP902_XQ01	1
Condensate at pressure collector CP2-5	MPa	30RMR65CP902_XQ01	1
Condensate temperature downstream LP-PH-5 RD40W01	⁰ C	30RMR80CT008_XQ01	1
Condensate temperature upstream LP-PH-3 RH60W01	⁰ C	30RMR80CT001_XQ01	1
Condensate temperature downstream LP-PH-3 RH60W01	⁰ C	30RMR80CT002_XQ01	1
Condensate temperature upstream LP-PH-4 RH50W01	⁰ C	30RMR80CT003_XQ01	1
Condensate temperature downstream LP-PH-4 RH50W01	⁰ C	30RMR80CT004_XQ01	1
Condensate temperature upstream LP-PH-5 RD40W01	⁰ C	30RMR80CT005_XQ01	1
Condensate temperature downstream LP-PH-5 RD40W01	⁰ C	30RMR80CT006_XQ01	1
Condensate temperature downstream LP-PH-5 RD40W01	⁰ C	30RMR80CT007_XQ01	1
Position of the mechanism for injection slide PPU-2 (steam valve)	%	30RCR32AS801_AA01	1
Position of the mechanism for injection slide PPU-1 (steam valve)	%	30RCR31AS801_AA01	1
Position of RV (for main regulator) of the level in LP-PH-2	%	30RMR40AS802_AA01	1
Position of RV (for start regulator) of the level in LP-PH-2	%	30RMR40AS806_AA01	1
Position of RV (for main regulator) of the level in deaerator D-7	%	30RMR70AS802_AA01	1
Position of RV (for start regulator) of the level in deaerator D7	%	30RMR72AS802_AA01	1
Boron concentration in the intake from PRZ	g/dm ³	30TVR50CQ001_XQ02	1
Boron concentration in the intake from PRZ	%	30TVR50CQ001_XQ04	1
Boron concentration in the intake from the reactor	g/dm ³	30TVR30CQ001_XQ02	1
Boron concentration in the intake from the reactor	%	30TVR30CQ001_XQ04	1
Boron concentration in the intake from the reactor	g/dm ³	30TVR40CQ001_XQ02	1
Boron concentration in the intake from the reactor	%	30TVR40CQ001_XQ04	1
Coolant pressure in the reactor	MPa	31YCS10CP051AXQ01	1
Coolant level in PRZ	m	31YPS10CL051AXQ01	1
Steam pressure in MSH	MPa	31RCS12CP051AXQ01	1

Cont. Annex E

Parameter	Unit	Code KKS	Signals No.
Coolant pressure in the reactor	MPa	31YCS10CP051BXQ01	1
Coolant level in PRZ	m	31YPS10CL051BXQ01	1
Steam pressure in MSH	MPa	31RCS12CP051BXQ01	1
Coolant pressure in the reactor	MPa	31YCS10CP051CXQ01	1
Coolant level in PRZ	m	31YPS10CL051CXQ01	1
Steam pressure in MSH	MPa	31RCS12CP051CXQ01	1
Coolant pressure in the reactor	MPa	33YCS10CP052AXQ01	1
Coolant level in PRZ	m	33YPS10CL052AXQ01	1
Steam pressure in MSH	MPa	33RCS12CP052AXQ01	1
Coolant pressure in the reactor	MPa	33YCS10CP052BXQ01	1
Coolant level in PRZ	m	33YPS10CL052BXQ01	1
Steam pressure in MSH	MPa	33RCS12CP052BXQ01	1
Coolant pressure in the reactor	MPa	33YCS10CP052CXQ01	1
Coolant level in PRZ	m	33YPS10CL052CXQ01	1
Steam pressure in MSH	MPa	33RCS12CP052CXQ01	1
Position of RV of (fast acting discharge into condenser) BRUK-1	%	30RCR11AS801_XQ02	1
Position of RV of (fast acting discharge into condenser) BRUK-2	%	30RCR11AS802_XQ02	1
Position of RV of (fast acting discharge into condenser) BRUK-3	%	30RCR12AS801_XQ02	1
Position of RV of (fast acting discharge into condenser) BRUK-4	%	30RCR12AS802_XQ02	1
Relative power release coeff. by FA 1-163	rel. unit	30YQR02FX(001-163)XQ01	163
Max. FA power peaking factor	rel. unit	30YQR02FX902XQ01	1
Max. core power peaking factor	rel. unit	30YQR01FX902XQ01	1
Max. FA power peaking factor	rel. unit	30YQR02FX902XQ01	1
Coordinate of the FA with max. peaking factor	-	30YQR02FG001XQ02	1
Max. value of offset in FA	%	30YQR03FX902XQ01	1
Coordinate of the FA with the max. offset value	-	30YQR03FG001XQ02	1
Min. value of offset in FA	%	30YQR03FX904XQ01	1
Coordinate of the FA with the min. offset value	-	30YQR03FG002XQ02	1
Max. value of linear power release	W/cm	30YQR06FX902XQ01	1
Coordinate of the FA with max. value of linear power release	-	30YQR06FG001XQ02	1
Position of the point with max. linear power release in the fuel rod	%	30YQR06FG002XQ01	1
Max. FA power peaking factor in the core	rel. unit	30YQR01FX902XQ01	1
Coordinate of the FA with max. power release in the core volume	-	30YQR01FG001XQ02	1
Number of the layer with max. power peaking factor	-	30YQR01FG002XQ01	1
Minimal margin to the allowable core power peaking factor	rel. unit	30YQR05FX904XQ01	1
Coordinate of FA with min. margin to the allowable core power peaking factor	-	30YQR05FG001XQ02	1
Number of the layer with min. margin to the allowable core power peaking factor	-	30YQR05FG002XQ01	1
Min. margin to the allowable value of the coolant temperature at the outlet from the FA	°C	30YQR00FT904XQ02	1
Coordinate of FA with min. margin to the allowable value of the coolant temperature at the outlet from the FA	-	30YQR00FG001XQ02	1
Max. heat-up of the coolant in the FA	°C	30YQR02FT902XQ01	1

Cont. Annex E

Parameter	Unit	Code KKS	Signals No.
Coordinate of FA with max. heat-up of the coolant in the FA	-	30YQR02FG002XQ02	1
Min. margin to the allowable heat-up of the coolant in the FA	⁰ C	30YQR03FT904XQ01	1
Coordinate of the FA with min. margin to the allowable value of the coolant heat-up in the FA	-	30YQR03FG003XQ02	1
Number of the layer with max. value of linear power release	-	30YQR07FG002XQ01	1
Minimal value of DNB	rel. unit	30YQR08FX904XQ01	1
Coordinate of the FA with min. DNB	-	30YQR08FG001XQ02	1
Temperature downstream the coolant of the blowdown TK80W02	⁰ C	30TKR80CT901_XQ02	1
Temperature downstream RTO of the blow-down TK80W01	⁰ C	30TKR40CT001_XQ02	1
Steam temperature in PRZ	⁰ C	30YPR10CT001_XQ02	1
Coolant temperature from the PC to PRZ	⁰ C	30YPR10CT902_XQ02	1
Coolant temperature from the PC to PRZ	⁰ C	30YPR10CT002A_XQ02	1
Coolant temperature from the PC to PRZ	⁰ C	30YPR10CT002B_XQ02	1
Coolant temperature in the line from PRZ to MCC	⁰ C	30YPR10CT007_XQ02	1
Coolant temperature in the line from PRZ to MCC	⁰ C	30YPR10CT008_XQ02	1
Water temperature in the pressure suppression pool	⁰ C	30YPR20CT002_XQ02	1
Interim circuit water temperature downstream the cooler of MCP-1	⁰ C	30TFR11CT001_XQ02	1
Interim circuit water temperature downstream the cooler of MCP-2	⁰ C	30TFR12CT001_XQ02	1
Interim circuit water temperature downstream the cooler of controlled leakages 3TY10W01	⁰ C	30TFR13CT001_XQ02	1
Interim circuit water temperature downstream the cooler of PC blow-down 3TK80W02	⁰ C	30TFR15CT001_XQ02	1
Interim circuit water temperature downstream the cooler of MCP-3	⁰ C	30TFR16CT001_XQ02	1
Interim circuit water temperature downstream the cooler of MCP-4	⁰ C	30TFR17CT001_XQ02	1
Water temperature upstream the interim circuit heat exchanger	⁰ C	30TFR20CT001_XQ02	1
Water temperature downstream the interim circuit heat exchanger TF21W01	⁰ C	31TFR21CT001A_XQ02	1
Water temperature downstream the interim circuit heat exchanger TF21W01	⁰ C	31TFR21CT001B_XQ02	1
Water temperature downstream the interim circuit heat exchanger TF21W01	⁰ C	31TFR21CT901_XQ02	1
Water temperature downstream the interim circuit heat exchanger TF22W01	⁰ C	31TFR22CT001A_XQ02	1
Water temperature downstream the interim circuit heat exchanger TF22W01	⁰ C	31TFR22CT001B_XQ02	1
Water temperature downstream the interim circuit heat exchanger TF22W01	⁰ C	31TFR22CT901_XQ02	1
Water temperature downstream the interim circuit heat exchanger TF21W01	⁰ C	32TFR21CT002A_XQ02	1
Water temperature downstream the interim circuit heat exchanger TF21W01	⁰ C	32TFR21CT002B_XQ02	1
Water temperature downstream the interim circuit heat exchanger TF21W01	⁰ C	32TFR21CT902_XQ02	1
Water temperature downstream the interim circuit heat exchanger TF22W01	⁰ C	32TFR22CT002A_XQ02	1
Water temperature downstream the interim circuit heat exchanger TF22W01	⁰ C	32TFR22CT002B_XQ02	1

Parameter	Unit	Code KKS	Signals No.
changer TF22W01			
Water temperature downstream the interim circuit heat exchanger TF22W01	°C	32TFR22CT902_XQ02	1
Water temperature downstream the interim circuit heat exchanger TF21W01	°C	33TFR21CT003A_XQ02	1
Water temperature downstream the interim circuit heat exchanger TF21W01	°C	33TFR21CT003B_XQ02	1
Water temperature downstream the interim circuit heat exchanger TF21W01	°C	33TFR21CT903_XQ02	1
Water temperature downstream the interim circuit heat exchanger TF22W01	°C	33TFR22CT003A_XQ02	1
Water temperature downstream the interim circuit heat exchanger TF22W01	°C	33TFR22CT003B_XQ02	1
Water temperature downstream the interim circuit heat exchanger TF22W01	°C	33TFR22CT903_XQ02	1
Calculated value of the axial offset	rel. unit	31YCS00FX300AXQ01	1
Calculated value of axial peaking factor in layer 1	rel. unit	31YCS00FX302AXQ01	1
Calculated value of axial peaking factor in layer 2	rel. unit	31YCS00FX304AXQ01	1
Calculated value of axial peaking factor in layer 3	rel. unit	31YCS00FX306AXQ01	1
Calculated value of axial peaking factor in layer 4	rel. unit	31YCS00FX308AXQ01	1
Calculated value of axial peaking factor in layer 5	rel. unit	31YCS00FX310AXQ01	1
Calculated value of axial peaking factor in layer 6	rel. unit	31YCS00FX312AXQ01	1
Calculated value of axial peaking factor in layer 7	rel. unit	31YCS00FX314AXQ01	1
Calculated value of axial peaking factor in layer 8	rel. unit	31YCS00FX316AXQ01	1
Calculated value of axial peaking factor in layer 9	rel. unit	31YCS00FX318AXQ01	1
Calculated value of axial peaking factor in layer 10	rel. unit	31YCS00FX320AXQ01	1
Local power release value	W/m	31YCS00FX400AXQ01	1
Calculated value for DNB	rel. unit	31YCS00FX402AXQ01	1
Calculated value of the axial offset	rel. unit	31YCS00FX300BXQ01	1
Calculated value of axial peaking factor in layer 1	rel. unit	31YCS00FX302BXQ01	1
Calculated value of axial peaking factor in layer 2	rel. unit	31YCS00FX304BXQ01	1
Calculated value of axial peaking factor in layer 3	rel. unit	31YCS00FX306BXQ01	1
Calculated value of axial peaking factor in layer 4	rel. unit	31YCS00FX308BXQ01	1
Calculated value of axial peaking factor in layer 5	rel. unit	31YCS00FX310BXQ01	1
Calculated value of axial peaking factor in layer 6	rel. unit	31YCS00FX312BXQ01	1
Calculated value of axial peaking factor in layer 7	rel. unit	31YCS00FX314BXQ01	1
Calculated value of axial peaking factor in layer 8	rel. unit	31YCS00FX316BXQ01	1
Calculated value of axial peaking factor in layer 9	rel. unit	31YCS00FX318BXQ01	1
Calculated value of axial peaking factor in layer 10	rel. unit	31YCS00FX320BXQ01	1
Local power release value	W/m	31YCS00FX400BXQ01	1
Calculated value for DNB	rel. unit	31YCS00FX402BXQ01	1
Calculated value of the axial offset	rel. unit	31YCS00FX300CXQ01	1
Calculated value of axial peaking factor in layer 1	rel. unit	31YCS00FX302CXQ01	1
Calculated value of axial peaking factor in layer 2	rel. unit	31YCS00FX304CXQ01	1
Calculated value of axial peaking factor in layer 3	rel. unit	31YCS00FX306CXQ01	1
Calculated value of axial peaking factor in layer 4	rel. unit	31YCS00FX308CXQ01	1
Calculated value of axial peaking factor in layer 5	rel. unit	31YCS00FX310CXQ01	1
Calculated value of axial peaking factor in layer 6	rel. unit	31YCS00FX312CXQ01	1
Calculated value of axial peaking factor in layer 7	rel. unit	31YCS00FX314CXQ01	1
Calculated value of axial peaking factor in layer 8	rel. unit	31YCS00FX316CXQ01	1
Calculated value of axial peaking factor in layer 9	rel. unit	31YCS00FX318CXQ01	1

Cont. Annex E

Parameter	Unit	Code KKS	Signals No.
Calculated value of axial peaking factor in layer 10	rel. unit	31YCS00FX320CXQ01	1
Local power release value	W/m	31YCS00FX400CXQ01	1
Calculated value for DNB	rel. unit	31YCS00FX402CXQ01	1
Calculated value of the axial offset	rel. unit	33YCS00FX301AXQ01	1
Calculated value of axial peaking factor in layer 1	rel. unit	33YCS00FX303AXQ01	1
Calculated value of axial peaking factor in layer 2	rel. unit	33YCS00FX305AXQ01	1
Calculated value of axial peaking factor in layer 3	rel. unit	33YCS00FX307AXQ01	1
Calculated value of axial peaking factor in layer 4	rel. unit	33YCS00FX309AXQ01	1
Calculated value of axial peaking factor in layer 5	rel. unit	33YCS00FX311AXQ01	1
Calculated value of axial peaking factor in layer 6	rel. unit	33YCS00FX313AXQ01	1
Calculated value of axial peaking factor in layer 7	rel. unit	33YCS00FX315AXQ01	1
Calculated value of axial peaking factor in layer 8	rel. unit	33YCS00FX317AXQ01	1
Calculated value of axial peaking factor in layer 9	rel. unit	33YCS00FX319AXQ01	1
Calculated value of axial peaking factor in layer 10	rel. unit	33YCS00FX321AXQ01	1
Local power release value	W/m	33YCS00FX401AXQ01	1
Calculated value for DNB	rel. unit	33YCS00FX403AXQ01	1
Calculated value of the axial offset	rel. unit	33YCS00FX301BXQ01	1
Calculated value of axial peaking factor in layer 1	rel. unit	33YCS00FX303BXQ01	1
Calculated value of axial peaking factor in layer 2	rel. unit	33YCS00FX305BXQ01	1
Calculated value of axial peaking factor in layer 3	rel. unit	33YCS00FX307BXQ01	1
Calculated value of axial peaking factor in layer 4	rel. unit	33YCS00FX309BXQ01	1
Calculated value of axial peaking factor in layer 5	rel. unit	33YCS00FX311BXQ01	1
Calculated value of axial peaking factor in layer 6	rel. unit	33YCS00FX313BXQ01	1
Calculated value of axial peaking factor in layer 7	rel. unit	33YCS00FX315BXQ01	1
Calculated value of axial peaking factor in layer 8	rel. unit	33YCS00FX317BXQ01	1
Calculated value of axial peaking factor in layer 9	rel. unit	33YCS00FX319BXQ01	1
Calculated value of axial peaking factor in layer 10	rel. unit	33YCS00FX321BXQ01	1
Local power release value	W/m	33YCS00FX401BXQ01	1
Calculated value for DNB	rel. unit	33YCS00FX403BXQ01	1
Calculated value of the axial offset	rel. unit	33YCS00FX301CXQ01	1
Calculated value of axial peaking factor in layer 1	rel. unit	33YCS00FX303CXQ01	1
Calculated value of axial peaking factor in layer 2	rel. unit	33YCS00FX305CXQ01	1
Calculated value of axial peaking factor in layer 3	rel. unit	33YCS00FX307CXQ01	1
Calculated value of axial peaking factor in layer 4	rel. unit	33YCS00FX309CXQ01	1
Calculated value of axial peaking factor in layer 5	rel. unit	33YCS00FX311CXQ01	1
Calculated value of axial peaking factor in layer 6	rel. unit	33YCS00FX313CXQ01	1
Calculated value of axial peaking factor in layer 7	rel. unit	33YCS00FX315CXQ01	1
Calculated value of axial peaking factor in layer 8	rel. unit	33YCS00FX317CXQ01	1
Calculated value of axial peaking factor in layer 9	rel. unit	33YCS00FX319CXQ01	1
Calculated value of axial peaking factor in layer 10	rel. unit	33YCS00FX321CXQ01	1
Local power release value	W/m	33YCS00FX401CXQ01	1
Calculated value for DNB	rel. unit	33YCS00FX403CXQ01	1

ANNEX F

Parameters recorded by the in-core control

Parameter	Unit	Code KKS	Signals No.
Coolant average pressure above the core	MPa	30YCR10FP901XQ01	1
Coolant pressure difference in reactor	MPa	30YCR10CP071XQ01	1
Coolant average pressure difference in MCP-1	MPa	YA10P18	1
Coolant average pressure difference in MCP-2	MPa	YA20P18	1
Coolant average pressure difference in MCP-3	MPa	YA30P18	1
Coolant average pressure difference in MCP-4	MPa	YA40P18	1
Mass flow rate of the coolant in loop 1	t/h	30YAR10FF001XQ01	1
Mass flow rate of the coolant in loop 2	t/h	30YAR20FF001XQ01	1
Mass flow rate of the coolant in loop 3	t/h	30YAR30FF001XQ01	1
Mass flow rate of the coolant in loop 4	t/h	30YAR40FF001XQ01	1
Total mass flow rate of the coolant through the reactor	t/h	30YCR10FF903XQ02	1
Coolant volume flow rate in loop 1	m ³ /h	YA10F_O	1
Coolant volume flow rate in loop 2	m ³ /h	YA20F_O	1
Coolant volume flow rate in loop 3	m ³ /h	YA30F_O	1
Coolant volume flow rate in loop 4	m ³ /h	YA40F_O	1
Total volume flow rate of the coolant through the reactor	m ³ /h	30YCR10FF903XQ01	1
Average coolant heat-up in loop 1	°C	30YAR10FT001XQ01	1
Average coolant heat-up in loop 2	°C	30YAR20FT001XQ01	1
Average coolant heat-up in loop 3	°C	30YAR30FT001XQ01	1
Average coolant heat-up in loop 4	°C	30YAR40FT001XQ01	1
Average heat-up of coolant in the loops	°C	30YCR10FT901XQ01	1
Thermal power loop 1	MW	30YAR10FU001XQ01	1
Thermal power loop 3	MW	30YAR20FU001XQ01	1
Thermal power loop 2	MW	30YAR30FU001XQ01	1
Thermal power loop 4	MW	30YAR40FU001XQ01	1
Reactor thermal power through parameters of the primary circuit	MW	30YAR00FX001XQ01	1
Feedwater mass flow rate upstream HP-PH -A, (not corrected)	t/h	30RLR61CF071XQ01	1
Feedwater mass flow rate upstream HP-PH -B, (not corrected)	t/h	30RLR62CF071XQ01	1
Feedwater mass flow rate in SG-1, (not corrected)	t/h	30RLR71CF071XQ01	1
Feedwater mass flow rate in SG-2, (not corrected)	t/h	30RLR72CF071XQ01	1

Cont. Annex F

Parameter	Unit	Code KKS	Signals No.
Feedwater mass flow rate in SG-3, (not corrected)	t/h	30RLR73CF071XQ01	1
Feedwater mass flow rate in SG-4, (not corrected)	t/h	30RLR74CF071XQ01	1
Total feedwater mass flow rate in SG	t/h	30RLR00FF903XQ01	1
Steam pressure in SG-1	MPa	30YBR10CP071XQ01	1
Steam pressure in SG-2	MPa	30YBR20CP071XQ01	1
Steam pressure in SG-3	MPa	30YBR30CP071XQ01	1
Steam pressure in SG-4	MPa	30YBR40CP071XQ01	1
Feedwater pressure at the inlet to SG-1	MPa	30RLR71CP071XQ01	1
Feedwater pressure at the inlet to SG-2	MPa	30RLR72CP071XQ01	1
Feedwater pressure at the inlet to SG-3	MPa	30RLR73CP071XQ01	1
Feedwater pressure at the inlet to SG-4	MPa	30RLR74CP071XQ01	1
Feedwater saturation temperature in SG-1	°C	30RLR10FT001XQ01	1
Feedwater saturation temperature in SG-2	°C	30RLR20FT001XQ01	1
Feedwater saturation temperature in SG-3	°C	30RLR30FT001XQ01	1
Feedwater saturation temperature in SG-4	°C	30RLR40FT001XQ01	1
Outlet feedwater temperature HP-PH -A	°C	30RLR61FT001XQ01	1
Outlet feedwater temperature HP-PH -B	°C	30RLR62FT001XQ01	1
Feedwater temperature at the inlet to SG-1	°C	30RLR71FT001XQ01	1
Feedwater temperature at the inlet to SG-2	°C	30RLR72FT001XQ01	1
Feedwater temperature at the inlet to SG-3	°C	30RLR73FT001XQ01	1
Feedwater temperature at the inlet to SG-4	°C	30RLR74FT001XQ01	1
Thermal power SG-1	MW	30RLR10FU001XQ01	1
Thermal power SG-2	MW	30RLR20FU001XQ01	1
Thermal power SG-3	MW	30RLR30FU001XQ01	1
Thermal power SG-4	MW	30RLR40FU001XQ01	1
Feedwater pressure downstream HP-PH -7	MPa	30RLR60FP001XQ01	1
Feedwater temperature upstream HP-PH -A	°C	30RLR61FT003XQ01	1
Feedwater temperature upstream HP-PH -B	°C	30RLR62FT003XQ01	1
Thermal power HP-PH -A	MW	30RLR61FX001XQ01	1
Thermal power HP-PH -B	MW	30RLR62FX001XQ01	1
Thermal power of the reactor by parameters of SC in the line HP-PH	MW	30RLR00FX903XQ01	1
Reactor power	MW	30YQR00FX001XQ01	1
Reactor power recorded by NFC	MW	30YCR00FX001XQ01	1
Reactor power recorded by NFC ion. chamber 2 OR-1	%	31YCS00FX005AXQ2	1
Reactor power recorded by NFC ion. chamber 12 OR-1	%	31YCS00FX005BXQ2	1
Reactor power recorded by NFC ion. chamber 22 OR-1	%	31YCS00FX005CXQ2	1
Reactor power recorded by NFC ion. chamber 7 OR-1	%	33YCS00FX006AXQ2	1
Reactor power recorded by NFC ion. chamber 17 OR-1	%	33YCS00FX006BXQ2	1
Reactor power recorded by NFC ion. chamber 27 OR-1	%	33YCS00FX006CXQ2	1
Reactor average power (core)	MW	30YQR00FX901XQ01	1
TG electric power	%	30SPR00FE001XQ01	1
Offset recorded by DCS (OFED)	%	30YQR00FU005XQ01	1
Offset on the basis of the restored power release field (offset)	%	30YQR00FU901XQ01	1
Reactor effective operation time	eff. days	30YQR00FU002XQ01	1
Boron concentration in the reactor	g/dm ³	30TVR30FQ001XQ01	1
Coolant pressure difference in MCP-1	MPa	31YAS10CP071AXQ1	1
Coolant pressure difference in MCP-1	MPa	31YAS10CP071BXQ1	1
Coolant pressure difference in MCP-1	MPa	31YAS10CP071CXQ1	1

Cont. Annex F

Parameter	Unit	Code KKS	Signals No.
Coolant pressure difference in MCP-1	MPa	33YAS10CP072AXQ1	1
Coolant pressure difference in MCP-1	MPa	33YAS10CP072BXQ1	1
Coolant pressure difference in MCP-1	MPa	33YAS10CP072CXQ1	1
Coolant pressure difference in MCP-2	MPa	33YAS20CP072AXQ1	1
Coolant pressure difference in MCP-2	MPa	33YAS20CP072BXQ1	1
Coolant pressure difference in MCP-2	MPa	33YAS20CP072CXQ1	1
Coolant pressure difference in MCP-3	MPa	33YAS30CP072AXQ1	1
Coolant pressure difference in MCP-3	MPa	33YAS30CP072BXQ1	1
Coolant pressure difference in MCP-3	MPa	33YAS30CP072CXQ1	1
Coolant pressure difference in MCP-4	MPa	33YAS40CP072AXQ1	1
Coolant pressure difference in MCP-4	MPa	33YAS40CP072BXQ1	1
Coolant pressure difference in MCP-4	MPa	33YAS40CP072CXQ1	1
Coolant pressure difference in MCP-2	MPa	31YAS20CP071AXQ1	1
Coolant pressure difference in MCP-2	MPa	31YAS20CP071BXQ1	1
Coolant pressure difference in MCP-2	MPa	31YAS20CP071CXQ1	1
Coolant pressure difference in MCP-3	MPa	31YAS30CP071AXQ1	1
Coolant pressure difference in MCP-3	MPa	31YAS30CP071BXQ1	1
Coolant pressure difference in MCP-3	MPa	31YAS30CP071CXQ1	1
Coolant pressure difference in MCP-4	MPa	31YAS40CP071AXQ1	1
Coolant pressure difference in MCP-4	MPa	31YAS40CP071BXQ1	1
Coolant pressure difference in MCP-4	MPa	31YAS40CP071CXQ1	1
Feedwater flow rate in SG-4	t/h	30RLR74CF01BXQ01	1
Feedwater flow rate in SG-4	t/h	30RLR74CF01AXQ01	1
Feedwater flow rate in SG-2	t/h	30RLR72CF01AXQ01	1
Feedwater flow rate in SG-2	t/h	30RLR72CF01BXQ01	1
Feedwater flow rate to HP-PH -B RD12,22W01	m3/h	30RLR62CF001XQ01	1
Feedwater flow rate at the pressure side of the feedwater pump	m3/h	30TKR21CF02AXQ04	1
Feedwater flow rate at the pressure collector of the feedwater pumps	m3/h	30TKR40CF901XQ02	1
Feedwater flow rate to HP-PH -A RD11,21W01	m3/h	30RLR61CF001XQ01	1
Feedwater flow rate in SG-3	t/h	30RLR73CF01AXQ01	1
Feedwater flow rate in SG-3	t/h	30RLR73CF01BXQ01	1
Feedwater flow rate in SG-1	t/h	30RLR71CF01AXQ01	1
Coolant volume flow rate in loop 4	m3/h	GPTO_TEST4	1
Coolant volume flow rate in loop 3	m3/h	GPTO_TEST3	1
Coolant volume flow rate in loop 2	m3/h	GPTO_TEST2	1
Coolant volume flow rate in loop 1	m3/h	GPTO_TEST1	1
Feedwater flow rate in SG-1	t/h	30RLR71CF01BXQ01	1
Flow rate in the pipe of pumps with controlled leakages	m3/h	30TER00CF001XQ02	1
Flow rate in the pipe upstream the blowdown of the primary circuit	m3/h	30TER00CF002XQ02	1
Coolant volume flow rate in loop 1	m3/h	YA10F_O	1
Coolant volume flow rate in loop 2	m3/h	YA20F_O	1
Coolant volume flow rate in loop 3	m3/h	YA30F_O	1
Coolant volume flow rate in loop 4	m3/h	YA40F_O	1
Coolant average pressure difference in MCP-1	MPa	YA10P18	1
Coolant average pressure difference in MCP-2	MPa	YA20P18	1
Coolant average pressure difference in MCP-3	MPa	YA30P18	1
Coolant average pressure difference in MCP-4	MPa	YA40P18	1
Coolant temperature in the „cold“ leg of loop 1 recorded by	°C	31YAS12CT071AXQ1	1

Parameter	Unit	Code KKS	Signals No.
RT-1			
Coolant temperature in the „cold“ leg of loop 1 recorded by RT-2	°C	31YAS12CT071BXQ1	1
Coolant temperature in the „cold“ leg of loop 1 recorded by RT-3	°C	31YAS12CT071CXQ1	1
Coolant temperature in the „cold“ leg of loop 1 recorded by RT-4	°C	33YAS12CT072AXQ1	1
Coolant temperature in the „cold“ leg of loop 1 recorded by RT-4	°C	33YAS12CT072BXQ1	1
Coolant temperature in the „cold“ leg of loop 1 recorded by RT-6	°C	33YAS12CT072CXQ1	1
Coolant temperature in the „cold“ leg of loop 1 by RT	°C	31YAS12CT073XQ01	1
Coolant temperature in the „cold“ leg of loop 2 recorded by RT-1	°C	31YAS22CT071AXQ1	1
Coolant temperature in the „cold“ leg of loop 2 recorded by RT-2	°C	31YAS22CT071BXQ1	1
Coolant temperature in the „cold“ leg of loop 2 recorded by RT-3	°C	31YAS22CT071CXQ1	1
Coolant temperature in the „cold“ leg of loop 2 recorded by RT-4	°C	33YAS22CT072AXQ1	1
Coolant temperature in the „cold“ leg of loop 2 recorded by RT-4	°C	33YAS22CT072BXQ1	1
Coolant temperature in the „cold“ leg of loop 2 recorded by RT-6	°C	33YAS22CT072CXQ1	1
Coolant temperature in the „cold“ leg of loop 2 by RT	°C	31YAS22CT073XQ01	1
Coolant temperature in the „cold“ leg of loop 3 recorded by RT-1	°C	31YAS32CT071AXQ1	1
Coolant temperature in the „cold“ leg of loop 3 recorded by RT-2	°C	31YAS32CT071BXQ1	1
Coolant temperature in the „cold“ leg of loop 3 recorded by RT-3	°C	31YAS32CT071CXQ1	1
Coolant temperature in the „cold“ leg of loop 3 recorded by RT-4	°C	33YAS32CT072AXQ1	1
Coolant temperature in the „cold“ leg of loop 3 recorded by RT-4	°C	33YAS32CT072BXQ1	1
Coolant temperature in the „cold“ leg of loop 3 recorded by RT-6	°C	33YAS32CT072CXQ1	1
Coolant temperature in the „cold“ leg of loop 3 by RT	°C	31YAS32CT073XQ01	1
Coolant temperature in the „cold“ leg of loop 4 recorded by RT-1	°C	31YAS42CT071AXQ1	1
Coolant temperature in the „cold“ leg of loop 4 recorded by RT-2	°C	31YAS42CT071BXQ1	1
Coolant temperature in the „cold“ leg of loop 4 recorded by RT-3	°C	31YAS42CT071CXQ1	1
Coolant temperature in the „cold“ leg of loop 4 recorded by RT-4	°C	33YAS42CT072AXQ1	1
Coolant temperature in the „cold“ leg of loop 4 recorded by RT-4	°C	33YAS42CT072BXQ1	1
Coolant temperature in the „cold“ leg of loop 4 recorded by RT-6	°C	33YAS42CT072CXQ1	1
Coolant temperature in the „cold“ leg of loop 4 by RT	°C	31YAS42CT073XQ01	1

Cont. Annex F

Parameter	Unit	Code KKS	Signals No.
Average coolant temperature in the „cold“ leg of loop 1	°C	30YAR12FT901XQ01	1
Average coolant temperature in the „cold“ leg of loop 2	°C	30YAR22FT901XQ01	1
Average coolant temperature in the „cold“ leg of loop 3	°C	30YAR32FT901XQ01	1
Average coolant temperature in the „cold“ leg of loop 4	°C	30YAR42FT901XQ01	1
Coolant average pressure above the core	MPa	30YCR10FP901XQ01	1
Min. margin on the basis of the coolant heat-up in the FA till the allowed value	°C	30YQR03FT904XQ01	1
Coordinate of FA with maximal offset value	-	30YQR03FG001XQ01	1
Coolant temperature in PRZ	°C	30YPR10CT02AXQ02	1
Coolant temperature in PRZ	°C	30YPR10CT02BXQ02	1
Steam temperature in PRZ	°C	30YPR10CT001XQ02	1
Coolant temperature in the surge line (upwards)	°C	30YPR10CT007XQ02	1
Coolant temperature in the surge line (downwards)	°C	30YPR10CT008XQ02	1
Level in PRZ	m	30YPR10CL901XQ02	1
Maximal value of the relative power release by fuel assemblies in the core	rel. unit	30YQR02FX902XQ01	1
Coordinate of the FA with maximal value of the relative power release coeff. by FA in the core	-	30YQR02FG001XQ01	1
Supply frequency of MCP-1	Hz	33YDS10CH72AXQ01	1
Supply frequency of MCP-2	Hz	33YDS20CH72AXQ01	1
Supply frequency of MCP-3	Hz	33YDS30CH72AXQ01	1
Supply frequency of MCP-4	Hz	33YDS40CH72AXQ01	1
Power of MCP-4	MW	33YDS40CN72AXQ01	1
Power of MCP-3	MW	33YDS30CN72AXQ01	1
Power of MCP-2	MW	33YDS20CN72AXQ01	1
Power of MCP-1	MW	33YDS10CN72AXQ01	1
Temperature downstream the heat exchanger TK80W01	°C	30TKR40CT001XQ02	1
Flow rate at pressure side of HP-PH	m ³ /h	30TKR40CF901XQ02	1
Feedwater level in SG-1 (0-1000)	m	30YBR10CL903XQ02	1
Feedwater level in SG-2 (0-1000)	m	30YBR20CL903XQ02	1
Feedwater level in SG-3 (0-1000)	m	30YBR30CL903XQ02	1
Feedwater level in SG-4 (0-1000)	m	30YBR40CL903XQ02	1
Feedwater temperature at the inlet to SG-4	°C	30RLR74CT001XQ01	1
Feedwater temperature at the inlet to SG-3	°C	30RLR73CT001XQ01	1
Feedwater temperature at the inlet to SG-2	°C	30RLR72CT001XQ01	1
Feedwater temperature at the inlet to SG-1	°C	30RLR71CT001XQ01	1
Feedwater temperature downstream HP-PH7-2	°C	30RLR62CT006XQ01	1
Feedwater temperature downstream HP-PH7-2	°C	30RLR62CT005XQ01	1
Feedwater temperature downstream HP-PH7-2	°C	30RLR62CT004XQ01	1
Feedwater temperature upstream HP-PH7-2	°C	30RLR62CT003XQ01	1
Feedwater temperature downstream HP-PH7-1	°C	30RLR61CT006XQ01	1
Feedwater temperature downstream HP-PH7-1	°C	30RLR61CT005XQ01	1
Feedwater temperature downstream HP-PH7-1	°C	30RLR61CT004XQ01	1
Feedwater temperature upstream HP-PH7-1	°C	30RLR61CT003XQ01	1
Feedwater pressure at the inlet to SG-1	MPa	30RLR71CP071XQ01	1
Feedwater pressure at the inlet to SG-1	MPa	30RLR71CP001XQ01	1
Feedwater pressure at the inlet to SG-2	MPa	30RLR72CP071XQ01	1
Feedwater pressure at the inlet to SG-2	MPa	30RLR72CP001XQ01	1
Feedwater pressure at the inlet to SG-3	MPa	30RLR73CP071XQ01	1
Feedwater pressure at the inlet to SG-3	MPa	30RLR73CP001XQ01	1

Parameter	Unit	Code KKS	Signals No.
Feedwater pressure at the inlet to SG-4	MPa	30RLR74CP071XQ01	1
Feedwater pressure at the inlet to SG-4	MPa	30RLR74CP001XQ01	1
Feedwater pressure downstream HP-PH7-1	MPa	30RLR61CP001XQ01	1
Feedwater pressure downstream HP-PH7-2	MPa	30RLR62CP001XQ01	1
Feedwater pressure upstream HP-PH 6-2	MPa	30RLR61CP002XQ01	1
Feedwater pressure upstream HP-PH 6-2	MPa	30RLR62CP002XQ01	1
TG electrical power	MW	30SPR10CE903XQ01	1
Boron concentration in PC supply	g/dm ³	30TKR30CQ001XQ02	1
Boron concentration in PRZ	g/dm ³	30TVR50CQ001XQ02	1
Reactor thermal power by SC parameters	MW	30RLR00FX903XQ03	1
Reactor power recorded in channels of ion. chamber 2 in OR-2 NFC	%	31YCS00FX001AXQ2	1
Reactor power recorded in channels of ion. chamber 12 in OR-2 NFC	%	31YCS00FX001BXQ2	1
Reactor power recorded in channels of ion. chamber 22 in OR-2 NFC	%	31YCS00FX001CXQ2	1
Steam pressure at MSH	MPa	30RCR11CP901XQ01	1
Feedwater level in SG-1 (0-4000)	mm	30YBR10CL935XQ01	1
Feedwater level in SG-2 (0-4000)	mm	30YBR20CL935XQ01	1
Feedwater level in SG-3 (0-4000)	mm	30YBR30CL935XQ01	1
Feedwater level in SG-4 (0-4000)	mm	30YBR40CL935XQ01	1
Reactor power recorded in channels of ion. chamber 7 in OR-2 NFC	%	33YCS00FX002AXQ2	1
Reactor power recorded in channels of ion. chamber 17 in OR-2 NFC	%	33YCS00FX002BXQ2	1
Reactor power recorded in channels of ion. chamber 27 in OR-2 NFC	%	33YCS00FX002CXQ2	1
Coolant temperature in the „cold“ leg of loop 1 recorded by RT-3	°C	31YAS12CT071CXQ1	1
Coolant temperature in the „cold“ leg of loop 1 recorded by RT-2	°C	31YAS12CT071BXQ1	1
Coolant temperature in the „cold“ leg of loop 1 recorded by RT-1	°C	31YAS12CT071AXQ1	1
Coolant temperature in the „cold“ leg of loop 1 recorded by RT-6	°C	33YAS12CT072CXQ1	1
Coolant temperature in the „cold“ leg of loop 1 recorded by RT-5	°C	33YAS12CT072BXQ1	1
Coolant temperature in the „cold“ leg of loop 1 recorded by RT-4	°C	33YAS12CT072AXQ1	1
Coolant temperature in the „cold“ leg of loop 1 by RT	°C	31YAS12CT073XQ01	1
Coolant temperature in the „cold“ leg of loop 2 recorded by RT-3	°C	31YAS22CT071CXQ1	1
Coolant temperature in the „cold“ leg of loop 2 recorded by RT-2	°C	31YAS22CT071BXQ1	1
Coolant temperature in the „cold“ leg of loop 2 recorded by RT-1	°C	31YAS22CT071AXQ1	1
Coolant temperature in the „cold“ leg of loop 2 recorded by RT-6	°C	33YAS22CT072CXQ1	1
Coolant temperature in the „cold“ leg of loop 2 recorded by RT-5	°C	33YAS22CT072BXQ1	1
Coolant temperature in the „cold“ leg of loop 2 recorded by RT-4	°C	33YAS22CT072AXQ1	1

Cont. Annex F

Parameter	Unit	Code KKS	Signals No.
RT-4			
Coolant temperature in the „cold“ leg of loop 2 by TC	°C	31YAS22CT073XQ01	1
Coolant temperature in the „cold“ leg of loop 3 recorded by RT-3	°C	31YAS32CT071CXQ1	1
Coolant temperature in the „cold“ leg of loop 3 recorded by RT-2	°C	31YAS32CT071BXQ1	1
Coolant temperature in the „cold“ leg of loop 3 recorded by RT-1	°C	31YAS32CT071AXQ1	1
Coolant temperature in the „cold“ leg of loop 3 recorded by RT-6	°C	33YAS32CT072CXQ1	1
Coolant temperature in the „cold“ leg of loop 3 recorded by RT-5	°C	33YAS32CT072BXQ1	1
Coolant temperature in the „cold“ leg of loop 3 recorded by RT-4	°C	33YAS32CT072AXQ1	1
Coolant temperature in the „cold“ leg of loop 3 by RT	°C	31YAS32CT073XQ01	1
Coolant temperature in the „cold“ leg of loop 4 recorded by RT-3	°C	31YAS42CT071CXQ1	1
Coolant temperature in the „cold“ leg of loop 4 recorded by RT-2	°C	31YAS42CT071BXQ1	1
Coolant temperature in the „cold“ leg of loop 4 recorded by RT-1	°C	31YAS42CT071AXQ1	1
Coolant temperature in the „cold“ leg of loop 4 recorded by RT-6	°C	33YAS42CT072CXQ1	1
Coolant temperature in the „cold“ leg of loop 4 recorded by RT-5	°C	33YAS42CT072BXQ1	1
Coolant temperature in the „cold“ leg of loop 4 recorded by RT-4	°C	33YAS42CT072AXQ1	1
Coolant temperature in the „cold“ leg of loop 4 by RT	°C	31YAS42CT073XQ01	1
Average coolant temperature in the „cold“ leg of loop 4	°C	30YAR42FT901XQ01	1
Average coolant temperature in the „cold“ leg of loop 3	°C	30YAR32FT901XQ01	1
Average coolant temperature in the „cold“ leg of loop 2	°C	30YAR22FT901XQ01	1
Average coolant temperature in the „cold“ leg of loop 1	°C	30YAR12FT901XQ01	1
Average coolant temperature at the inlet to reactor	°C	30YAR00FT901XQ01	1
Coolant temperature in the „hot“ leg of loop 1 recorded by RT-3	°C	31YAS11CT071CXQ1	1
Coolant temperature in the „hot“ leg of loop 1 recorded by RT-2	°C	31YAS11CT071BXQ1	1
Coolant temperature in the „hot“ leg of loop 1 recorded by RT-1	°C	31YAS11CT071AXQ1	1
Coolant temperature in the „hot“ leg of loop 1 recorded by RT-6	°C	33YAS11CT072CXQ1	1
Coolant temperature in the „hot“ leg of loop 1 recorded by RT-5	°C	33YAS11CT072BXQ1	1
Coolant temperature in the „hot“ leg of loop 1 recorded by RT-4	°C	33YAS11CT072AXQ1	1
Coolant temperature in the „hot“ leg of loop 1 by RT	°C	31YAS11CT073XQ01	1
Coolant temperature in the „hot“ leg of loop 2 recorded by RT-3	°C	31YAS21CT071CXQ1	1
Coolant temperature in the „hot“ leg of loop 2 recorded by RT-2	°C	31YAS21CT071BXQ1	1
Coolant temperature in the „hot“ leg of loop 2 recorded by	°C	31YAS21CT071AXQ1	1

Cont. Annex F

Parameter	Unit	Code KKS	Signals No.
RT-1			
Coolant temperature in the „hot“ leg of loop 2 recorded by RT-6	°C	33YAS21CT072CXQ1	1
Coolant temperature in the „hot“ leg of loop 2 recorded by RT-5	°C	33YAS21CT072BXQ1	1
Coolant temperature in the „hot“ leg of loop 2 recorded by RT-4	°C	33YAS21CT072AXQ1	1
Coolant temperature in the „hot“ leg of loop 2 by RT	°C	31YAS21CT073XQ01	1
Coolant temperature in the „hot“ leg of loop 3 recorded by RT-3	°C	31YAS31CT071CXQ1	1
Coolant temperature in the „hot“ leg of loop 3 recorded by RT-2	°C	31YAS31CT071BXQ1	1
Coolant temperature in the „hot“ leg of loop 3 recorded by RT-1	°C	31YAS31CT071AXQ1	1
Coolant temperature in the „hot“ leg of loop 3 recorded by RT-6	°C	33YAS31CT072CXQ1	1
Coolant temperature in the „hot“ leg of loop 3 recorded by RT-5	°C	33YAS31CT072BXQ1	1
Coolant temperature in the „hot“ leg of loop 3 recorded by RT-4	°C	33YAS31CT072AXQ1	1
Coolant temperature in the „hot“ leg of loop 3 by RT	°C	31YAS31CT073XQ01	1
Coolant temperature in the „hot“ leg of loop 4 recorded by RT-3	°C	31YAS41CT071CXQ1	1
Coolant temperature in the „hot“ leg of loop 4 recorded by RT-2	°C	31YAS41CT071BXQ1	1
Coolant temperature in the „hot“ leg of loop 4 recorded by RT-1	°C	31YAS41CT071AXQ1	1
Coolant temperature in the „hot“ leg of loop 4 recorded by RT-6	°C	33YAS41CT072CXQ1	1
Coolant temperature in the „hot“ leg of loop 4 recorded by RT-5	°C	33YAS41CT072BXQ1	1
Coolant temperature in the „hot“ leg of loop 4 recorded by RT-4	°C	33YAS41CT072AXQ1	1
Coolant temperature in the „hot“ leg of loop 4 by RT	°C	31YAS41CT073XQ01	1
Average coolant temperature in the „hot“ leg of loop 1	°C	30YAR11FT901XQ01	1
Average coolant temperature in the „hot“ leg of loop 2	°C	30YAR21FT901XQ01	1
Average coolant temperature in the „hot“ leg of loop 3	°C	30YAR31FT901XQ01	1
Average coolant temperature in the „hot“ leg of loop 4	°C	30YAR41FT901XQ01	1
Average coolant temperature at the outlet of reactor	°C	30YAR00FT901XQ03	1
Position of CPS-rods 08-23 Group 7	cm	30YVS00FG001XQ01	1
Position of CPS-rods 09-18 Group 9	cm	30YVS00FG002XQ01	1
Position of CPS-rods 09-20 Group 5	cm	30YVS00FG003XQ01	1
Position of CPS-rods 10-21 Group 3	cm	30YVS00FG004XQ01	1
Position of CPS-rods 11-20 Group 6	cm	30YVS00FG005XQ01	1
Position of CPS-rods 13-22 Group 8	cm	30YVS00FG006XQ01	1
Position of CPS-rods 12-23 Group 4	cm	30YVS00FG007XQ01	1
Position of CPS-rods 11-22 Group 2	cm	30YVS00FG008XQ01	1
Position of CPS-rods 10-23 Group 10	cm	30YVS00FG009XQ01	1
Position of CPS-rods 09-26 Group 8	cm	30YVS00FG010XQ01	1
Position of CPS-rods 11-26 Group 7	cm	30YVS00FG011XQ01	1
Position of CPS-rods 10-29 Group 1	cm	30YVS00FG012XQ01	1

Cont. Annex F

Parameter	Unit	Code KKS	Signals No.
Position of CPS-rods 14-25 Group 9	cm	30YVS00FG013XQ01	1
Position of CPS-rods 13-26 Group 5	cm	30YVS00FG014XQ01	1
Position of CPS-rods 13-28 Group 3	cm	30YVS00FG015XQ01	1
Position of CPS-rods 14-29 Group 6	cm	30YVS00FG016XQ01	1
Position of CPS-rods 13-30 Group 2	cm	30YVS00FG017XQ01	1
Position of CPS-rods 13-32 Group 4	cm	30YVS00FG018XQ01	1
Position of CPS-rods 14-33 Group 8	cm	30YVS00FG019XQ01	1
Position of CPS-rods 12-29 Group 10	cm	30YVS00FG020XQ01	1
Position of CPS-rods 08-29 Group 9	cm	30YVS00FG021XQ01	1
Position of CPS-rods 11-32 Group 7	cm	30YVS00FG022XQ01	1
Position of CPS-rods 10-35 Group 10	cm	30YVS00FG023XQ01	1
Position of CPS-rods 13-36 Group 9	cm	30YVS00FG024XQ01	1
Position of CPS-rods 12-35 Group 5	cm	30YVS00FG025XQ01	1
Position of CPS-rods 11-36 Group 3	cm	30YVS00FG026XQ01	1
Position of CPS-rods 11-38 Group 6	cm	30YVS00FG027XQ01	1
Position of CPS-rods 10-37 Group 2	cm	30YVS00FG028XQ01	1
Position of CPS-rods 09-40 Group 8	cm	30YVS00FG029XQ01	1
Position of CPS-rods 09-38 Group 4	cm	30YVS00FG030XQ01	1
Position of CPS-rods 09-32 Group 8	cm	30YVS00FG031XQ01	1
Position of CPS-rods 08-35 Group 7	cm	30YVS00FG032XQ01	1
Position of CPS-rods 07-38 Group 5	cm	30YVS00FG033XQ01	1
Position of CPS-rods 07-40 Group 9	cm	30YVS00FG034XQ01	1
Position of CPS-rods 06-37 Group 3	cm	30YVS00FG035XQ01	1
Position of CPS-rods 05-38 Group 6	cm	30YVS00FG036XQ01	1
Position of CPS-rods 05-36 Group 2	cm	30YVS00FG037XQ01	1
Position of CPS-rods 04-35 Group 4	cm	30YVS00FG038XQ01	1
Position of CPS-rods 03-36 Group 8	cm	30YVS00FG039XQ01	1
Position of CPS-rods 06-35 Group 10	cm	30YVS00FG040XQ01	1
Position of CPS-rods 07-32 Group 1	cm	30YVS00FG041XQ01	1
Position of CPS-rods 05-32 Group 7	cm	30YVS00FG042XQ01	1
Position of CPS-rods 06-29 Group 8	cm	30YVS00FG043XQ01	1
Position of CPS-rods 04-29 Group 10	cm	30YVS00FG044XQ01	1
Position of CPS-rods 02-33 Group 9	cm	30YVS00FG045XQ01	1
Position of CPS-rods 03-32 Group 5	cm	30YVS00FG046XQ01	1
Position of CPS-rods 03-30 Group 3	cm	30YVS00FG047XQ01	1
Position of CPS-rods 02-29 Group 6	cm	30YVS00FG048XQ01	1
Position of CPS-rods 03-28 Group 2	cm	30YVS00FG049XQ01	1
Position of CPS-rods 03-26 Group 4	cm	30YVS00FG050XQ01	1
Position of CPS-rods 02-25 Group 8	cm	30YVS00FG051XQ01	1
Position of CPS-rods 07-26 Group 1	cm	30YVS00FG052XQ01	1
Position of CPS-rods 05-26 Group 7	cm	30YVS00FG053XQ01	1
Position of CPS-rods 06-23 Group 10	cm	30YVS00FG054XQ01	1
Position of CPS-rods 05-22 Group 3	cm	30YVS00FG055XQ01	1
Position of CPS-rods 04-23 Group 5	cm	30YVS00FG056XQ01	1
Position of CPS-rods 03-22 Group 9	cm	30YVS00FG057XQ01	1
Position of CPS-rods 05-20 Group 6	cm	30YVS00FG058XQ01	1
Position of CPS-rods 06-21 Group 2	cm	30YVS00FG059XQ01	1
Position of CPS-rods 07-20 Group 4	cm	30YVS00FG060XQ01	1
Position of CPS-rods 07-18 Group 8	cm	30YVS00FG061XQ01	1
Coolant temperature under the reactor lid	°C	30YQR00CT028XQ02	1

Cont. Annex F

Parameter	Unit	Code KKS	Signals No.
Coolant temperature under the reactor lid	⁰ C	30YQR00CT077XQ02	1
Coolant temperature under the reactor lid	⁰ C	30YQR00CT098XQ02	1
Coolant temperature at the outlet from FA01-28	⁰ C	30YQR00CT001XQ02	1
Coolant temperature at the outlet from FA02-25	⁰ C	30YQR00CT002XQ02	1
Coolant temperature at the outlet from FA03-32	⁰ C	30YQR00CT003XQ02	1
Coolant temperature at the outlet from FA03-26	⁰ C	30YQR00CT004XQ02	1
Coolant temperature at the outlet from FA03-28	⁰ C	30YQR00CT005XQ02	1
Coolant temperature at the outlet from FA04-29	⁰ C	30YQR00CT006XQ02	1
Coolant temperature at the outlet from FA06-29	⁰ C	30YQR00CT007XQ02	1
Coolant temperature at the outlet from FA03-20	⁰ C	30YQR00CT008XQ02	1
Coolant temperature at the outlet from FA04-23	⁰ C	30YQR00CT009XQ02	1
Coolant temperature at the outlet from FA05-22	⁰ C	30YQR00CT010XQ02	1
Coolant temperature at the outlet from FA05-26	⁰ C	30YQR00CT011XQ02	1
Coolant temperature at the outlet from FA05-28	⁰ C	30YQR00CT012XQ02	1
Coolant temperature at the outlet from FA06-23	⁰ C	30YQR00CT013XQ02	1
Coolant temperature at the outlet from FA06-25	⁰ C	30YQR00CT014XQ02	1
Coolant temperature at the outlet from FA05-18	⁰ C	30YQR00CT015XQ02	1
Coolant temperature at the outlet from FA05-20	⁰ C	30YQR00CT016XQ02	1
Coolant temperature at the outlet from FA06-21	⁰ C	30YQR00CT017XQ02	1
Coolant temperature at the outlet from FA07-20	⁰ C	30YQR00CT018XQ02	1
Coolant temperature at the outlet from FA07-26	⁰ C	30YQR00CT019XQ02	1
Coolant temperature at the outlet from FA07-28	⁰ C	30YQR00CT020XQ02	1
Coolant temperature at the outlet from FA08-25	⁰ C	30YQR00CT021XQ02	1
Coolant temperature at the outlet from FA07-16	⁰ C	30YQR00CT022XQ02	1
Coolant temperature at the outlet from FA07-18	⁰ C	30YQR00CT023XQ02	1
Coolant temperature at the outlet from FA08-21	⁰ C	30YQR00CT024XQ02	1
Coolant temperature at the outlet from FA08-29	⁰ C	30YQR00CT025XQ02	1
Coolant temperature at the outlet from FA09-16	⁰ C	30YQR00CT026XQ02	1
Coolant temperature at the outlet from FA09-18	⁰ C	30YQR00CT027XQ02	1
Coolant temperature at the outlet from FA08-23	⁰ C	30YQR00CT029XQ02	1
Coolant temperature at the outlet from FA09-20	⁰ C	30YQR00CT030XQ02	1
Coolant temperature at the outlet from FA09-28	⁰ C	30YQR00CT031XQ02	1
Coolant temperature at the outlet from FA10-21	⁰ C	30YQR00CT032XQ02	1
Coolant temperature at the outlet from FA10-25	⁰ C	30YQR00CT033XQ02	1
Coolant temperature at the outlet from FA11-18	⁰ C	30YQR00CT034XQ02	1
Coolant temperature at the outlet from FA11-20	⁰ C	30YQR00CT035XQ02	1
Coolant temperature at the outlet from FA09-26	⁰ C	30YQR00CT036XQ02	1
Coolant temperature at the outlet from FA10-23	⁰ C	30YQR00CT037XQ02	1
Coolant temperature at the outlet from FA11-22	⁰ C	30YQR00CT038XQ02	1
Coolant temperature at the outlet from FA11-26	⁰ C	30YQR00CT039XQ02	1
Coolant temperature at the outlet from FA11-28	⁰ C	30YQR00CT040XQ02	1
Coolant temperature at the outlet from FA12-23	⁰ C	30YQR00CT041XQ02	1
Coolant temperature at the outlet from FA13-20	⁰ C	30YQR00CT042XQ02	1
Coolant temperature at the outlet from FA12-25	⁰ C	30YQR00CT043XQ02	1
Coolant temperature at the outlet from FA13-22	⁰ C	30YQR00CT044XQ02	1
Coolant temperature at the outlet from FA13-26	⁰ C	30YQR00CT045XQ02	1
Coolant temperature at the outlet from FA13-28	⁰ C	30YQR00CT046XQ02	1
Coolant temperature at the outlet from FA14-25	⁰ C	30YQR00CT047XQ02	1
Coolant temperature at the outlet from FA14-29	⁰ C	30YQR00CT048XQ02	1
Coolant temperature at the outlet from FA15-26	⁰ C	30YQR00CT049XQ02	1

Cont. Annex F

Parameter	Unit	Code KKS	Signals No.
Coolant temperature at the outlet from FA10-29	⁰ C	30YQR00CT050XQ02	1
Coolant temperature at the outlet from FA12-29	⁰ C	30YQR00CT051XQ02	1
Coolant temperature at the outlet from FA13-30	⁰ C	30YQR00CT052XQ02	1
Coolant temperature at the outlet from FA13-32	⁰ C	30YQR00CT053XQ02	1
Coolant temperature at the outlet from FA13-36	⁰ C	30YQR00CT054XQ02	1
Coolant temperature at the outlet from FA14-33	⁰ C	30YQR00CT055XQ02	1
Coolant temperature at the outlet from FA15-32	⁰ C	30YQR00CT056XQ02	1
Coolant temperature at the outlet from FA09-32	⁰ C	30YQR00CT057XQ02	1
Coolant temperature at the outlet from FA10-31	⁰ C	30YQR00CT058XQ02	1
Coolant temperature at the outlet from FA10-35	⁰ C	30YQR00CT059XQ02	1
Coolant temperature at the outlet from FA11-32	⁰ C	30YQR00CT060XQ02	1
Coolant temperature at the outlet from FA11-36	⁰ C	30YQR00CT061XQ02	1
Coolant temperature at the outlet from FA12-35	⁰ C	30YQR00CT062XQ02	1
Coolant temperature at the outlet from FA13-38	⁰ C	30YQR00CT063XQ02	1
Coolant temperature at the outlet from FA08-35	⁰ C	30YQR00CT064XQ02	1
Coolant temperature at the outlet from FA09-34	⁰ C	30YQR00CT065XQ02	1
Coolant temperature at the outlet from FA09-38	⁰ C	30YQR00CT066XQ02	1
Coolant temperature at the outlet from FA10-37	⁰ C	30YQR00CT067XQ02	1
Coolant temperature at the outlet from FA10-39	⁰ C	30YQR00CT068XQ02	1
Coolant temperature at the outlet from FA11-38	⁰ C	30YQR00CT069XQ02	1
Coolant temperature at the outlet from FA11-40	⁰ C	30YQR00CT070XQ02	1
Coolant temperature at the outlet from FA07-40	⁰ C	30YQR00CT071XQ02	1
Coolant temperature at the outlet from FA07-42	⁰ C	30YQR00CT072XQ02	1
Coolant temperature at the outlet from FA08-37	⁰ C	30YQR00CT073XQ02	1
Coolant temperature at the outlet from FA08-39	⁰ C	30YQR00CT074XQ02	1
Coolant temperature at the outlet from FA09-40	⁰ C	30YQR00CT075XQ02	1
Coolant temperature at the outlet from FA09-42	⁰ C	30YQR00CT076XQ02	1
Coolant temperature at the outlet from FA05-38	⁰ C	30YQR00CT078XQ02	1
Coolant temperature at the outlet from FA05-40	⁰ C	30YQR00CT079XQ02	1
Coolant temperature at the outlet from FA06-39	⁰ C	30YQR00CT080XQ02	1
Coolant temperature at the outlet from FA06-38	⁰ C	30YQR00CT081XQ02	1
Coolant temperature at the outlet from FA07-32	⁰ C	30YQR00CT082XQ02	1
Coolant temperature at the outlet from FA07-34	⁰ C	30YQR00CT083XQ02	1
Coolant temperature at the outlet from FA07-38	⁰ C	30YQR00CT084XQ02	1
Coolant temperature at the outlet from FA03-38	⁰ C	30YQR00CT085XQ02	1
Coolant temperature at the outlet from FA04-35	⁰ C	30YQR00CT086XQ02	1
Coolant temperature at the outlet from FA05-32	⁰ C	30YQR00CT087XQ02	1
Coolant temperature at the outlet from FA05-34	⁰ C	30YQR00CT088XQ02	1
Coolant temperature at the outlet from FA05-36	⁰ C	30YQR00CT089XQ02	1
Coolant temperature at the outlet from FA06-31	⁰ C	30YQR00CT090XQ02	1
Coolant temperature at the outlet from FA06-35	⁰ C	30YQR00CT091XQ02	1
Coolant temperature at the outlet from FA01-30	⁰ C	30YQR00CT092XQ02	1
Coolant temperature at the outlet from FA02-29	⁰ C	30YQR00CT093XQ02	1
Coolant temperature at the outlet from FA02-33	⁰ C	30YQR00CT094XQ02	1
Coolant temperature at the outlet from FA03-30	⁰ C	30YQR00CT095XQ02	1
Coolant temperature at the outlet from FA03-32	⁰ C	30YQR00CT096XQ02	1
Coolant temperature at the outlet from FA03-36	⁰ C	30YQR00CT097XQ02	1
Coordinate of FA with maximal value of core power peaking factor	-	30YQR01FG001XQ01	1
Max. coeff. of core power peaking factor	rel. unit	30YQR01FX902XQ01	1

Cont. Annex F

Parameter	Unit	Code KKS	Signals No.
Coordinate of FA with maximal value of relative power re-lease coeff. related to FA in the core	-	30YQR02FG001XQ01	1
Number of the layer with min. margin for core power peaking factor	-	30YQR05FG002XQ01	1
Min. margin of core power peaking factor	rel. unit	30YQR05FX904XQ01	1
Number of the layer with max. value of core power peaking factor	-	30YQR01FG002XQ01	1
Max. value of power peaking factor based on FA in the core	rel. unit	30YQR02FX902XQ01	1
Coordinate of the FA with the min. margin to DNB	-	30YQR08FG001XQ01	1
Coolant heat-up in FA01-28	⁰ C	30YQR02FT001XQ01	1
Coolant heat-up in FA02-25	⁰ C	30YQR02FT002XQ01	1
Coolant heat-up in FA03-32	⁰ C	30YQR02FT003XQ01	1
Coolant heat-up in FA03-26	⁰ C	30YQR02FT004XQ01	1
Coolant heat-up in FA03-28	⁰ C	30YQR02FT005XQ01	1
Coolant heat-up in FA04-29	⁰ C	30YQR02FT006XQ01	1
Coolant heat-up in FA06-29	⁰ C	30YQR02FT007XQ01	1
Coolant heat-up in FA03-20	⁰ C	30YQR02FT008XQ01	1
Coolant heat-up in FA04-23	⁰ C	30YQR02FT009XQ01	1
Coolant heat-up in FA05-22	⁰ C	30YQR02FT010XQ01	1
Coolant heat-up in FA05-26	⁰ C	30YQR02FT011XQ01	1
Coolant heat-up in FA05-28	⁰ C	30YQR02FT012XQ01	1
Coolant heat-up in FA06-23	⁰ C	30YQR02FT013XQ01	1
Coolant heat-up in FA06-25	⁰ C	30YQR02FT014XQ01	1
Coolant heat-up in FA05-18	⁰ C	30YQR02FT015XQ01	1
Coolant heat-up in FA05-20	⁰ C	30YQR02FT016XQ01	1
Coolant heat-up in FA06-21	⁰ C	30YQR02FT017XQ01	1
Coolant heat-up in FA07-20	⁰ C	30YQR02FT018XQ01	1
Coolant heat-up in FA07-26	⁰ C	30YQR02FT019XQ01	1
Coolant heat-up in FA07-28	⁰ C	30YQR02FT020XQ01	1
Coolant heat-up in FA08-25	⁰ C	30YQR02FT021XQ01	1
Coolant heat-up in FA07-16	⁰ C	30YQR02FT022XQ01	1
Coolant heat-up in FA07-18	⁰ C	30YQR02FT023XQ01	1
Coolant heat-up in FA08-21	⁰ C	30YQR02FT024XQ01	1
Coolant heat-up in FA08-29	⁰ C	30YQR02FT025XQ01	1
Coolant heat-up in FA09-16	⁰ C	30YQR02FT026XQ01	1
Coolant heat-up in FA09-18	⁰ C	30YQR02FT027XQ01	1
Coolant heat-up in FA08-23	⁰ C	30YQR02FT029XQ01	1
Coolant heat-up in FA09-20	⁰ C	30YQR02FT030XQ01	1
Coolant heat-up in FA09-28	⁰ C	30YQR02FT031XQ01	1
Coolant heat-up in FA10-21	⁰ C	30YQR02FT032XQ01	1
Coolant heat-up in FA10-25	⁰ C	30YQR02FT033XQ01	1
Coolant heat-up in FA11-18	⁰ C	30YQR02FT034XQ01	1
Coolant heat-up in FA11-20	⁰ C	30YQR02FT035XQ01	1
Coolant heat-up in FA09-26	⁰ C	30YQR02FT036XQ01	1
Coolant heat-up in FA10-23	⁰ C	30YQR02FT037XQ01	1
Coolant heat-up in FA11-22	⁰ C	30YQR02FT038XQ01	1
Coolant heat-up in FA11-26	⁰ C	30YQR02FT039XQ01	1
Coolant heat-up in FA11-28	⁰ C	30YQR02FT040XQ01	1
Coolant heat-up in FA12-23	⁰ C	30YQR02FT041XQ01	1
Coolant heat-up in FA13-20	⁰ C	30YQR02FT042XQ01	1

Cont. Annex F

Parameter	Unit	Code KKS	Signals No.
Coolant heat-up in FA12-25	⁰ C	30YQR02FT043XQ01	1
Coolant heat-up in FA13-22	⁰ C	30YQR02FT044XQ01	1
Coolant heat-up in FA13-26	⁰ C	30YQR02FT045XQ01	1
Coolant heat-up in FA13-28	⁰ C	30YQR02FT046XQ01	1
Coolant heat-up in FA14-25	⁰ C	30YQR02FT047XQ01	1
Coolant heat-up in FA14-29	⁰ C	30YQR02FT048XQ01	1
Coolant heat-up in FA15-26	⁰ C	30YQR02FT049XQ01	1
Coolant heat-up in FA10-29	⁰ C	30YQR02FT050XQ01	1
Coolant heat-up in FA12-29	⁰ C	30YQR02FT051XQ01	1
Coolant heat-up in FA13-30	⁰ C	30YQR02FT052XQ01	1
Coolant heat-up in FA13-32	⁰ C	30YQR02FT053XQ01	1
Coolant heat-up in FA13-36	⁰ C	30YQR02FT054XQ01	1
Coolant heat-up in FA14-33	⁰ C	30YQR02FT055XQ01	1
Coolant heat-up in FA15-32	⁰ C	30YQR02FT056XQ01	1
Coolant heat-up in FA09-32	⁰ C	30YQR02FT057XQ01	1
Coolant heat-up in FA10-31	⁰ C	30YQR02FT058XQ01	1
Coolant heat-up in FA10-35	⁰ C	30YQR02FT059XQ01	1
Coolant heat-up in FA11-32	⁰ C	30YQR02FT060XQ01	1
Coolant heat-up in FA11-36	⁰ C	30YQR02FT061XQ01	1
Coolant heat-up in FA12-35	⁰ C	30YQR02FT062XQ01	1
Coolant heat-up in FA13-38	⁰ C	30YQR02FT063XQ01	1
Coolant heat-up in FA08-35	⁰ C	30YQR02FT064XQ01	1
Coolant heat-up in FA09-34	⁰ C	30YQR02FT065XQ01	1
Coolant heat-up in FA09-38	⁰ C	30YQR02FT066XQ01	1
Coolant heat-up in FA10-37	⁰ C	30YQR02FT067XQ01	1
Coolant heat-up in FA10-39	⁰ C	30YQR02FT068XQ01	1
Coolant heat-up in FA11-38	⁰ C	30YQR02FT069XQ01	1
Coolant heat-up in FA11-40	⁰ C	30YQR02FT070XQ01	1
Coolant heat-up in FA07-40	⁰ C	30YQR02FT071XQ01	1
Coolant heat-up in FA07-42	⁰ C	30YQR02FT072XQ01	1
Coolant heat-up in FA08-37	⁰ C	30YQR02FT073XQ01	1
Coolant heat-up in FA08-39	⁰ C	30YQR02FT074XQ01	1
Coolant heat-up in FA09-40	⁰ C	30YQR02FT075XQ01	1
Coolant heat-up in FA09-42	⁰ C	30YQR02FT076XQ01	1
Coolant heat-up in FA05-38	⁰ C	30YQR02FT078XQ01	1
Coolant heat-up in FA05-40	⁰ C	30YQR02FT079XQ01	1
Coolant heat-up in FA06-39	⁰ C	30YQR02FT080XQ01	1
Coolant heat-up in FA06-38	⁰ C	30YQR02FT081XQ01	1
Coolant heat-up in FA07-32	⁰ C	30YQR02FT082XQ01	1
Coolant heat-up in FA07-34	⁰ C	30YQR02FT083XQ01	1
Coolant heat-up in FA07-38	⁰ C	30YQR02FT084XQ01	1
Coolant heat-up in FA03-38	⁰ C	30YQR02FT085XQ01	1
Coolant heat-up in FA04-35	⁰ C	30YQR02FT086XQ01	1
Coolant heat-up in FA05-32	⁰ C	30YQR02FT087XQ01	1
Coolant heat-up in FA05-34	⁰ C	30YQR02FT088XQ01	1
Coolant heat-up in FA05-36	⁰ C	30YQR02FT089XQ01	1
Coolant heat-up in FA06-31	⁰ C	30YQR02FT090XQ01	1
Coolant heat-up in FA06-35	⁰ C	30YQR02FT091XQ01	1
Coolant heat-up in FA01-30	⁰ C	30YQR02FT092XQ01	1
Coolant heat-up in FA02-29	⁰ C	30YQR02FT093XQ01	1

Cont. Annex F

Parameter	Unit	Code KKS	Signals No.
Coolant heat-up in FA02-33	°C	30YQR02FT094XQ01	1
Coolant heat-up in FA03-30	°C	30YQR02FT095XQ01	1
Coolant heat-up in FA03-32	°C	30YQR02FT096XQ01	1
Coolant heat-up in FA03-36	°C	30YQR02FT097XQ01	1
Coolant max. heating in FA	°C	30YQR02FT902XQ01	1
Calculated coolant heat-up in FA 1-163	°C	30YQR04FT(001-163)XQ01	163
Corrected current recorded by DCS 1-7 for neutron flux control 1-23	mkA	31YQS(01-23)CX(001-007)XQ01	161
Corrected current recorded by DCS 1-7 for neutron flux control 24-46	mkA	31YQS(24-46)CX(001-007)XQ01	161
Corrected current recorded by DCS 1-7 for neutron flux control 47-64	mkA	31YQS(47-64)CX(001-007)XQ01	126
Minimal margin to DNB	rel. unit	30YQR08FX904XQ01	1
Coeff. of margin till the heat exchange crisis in FA 1-80	rel. unit	30YQR08FX(001-080)XQ01	80
Coeff. of margin till the heat exchange crisis in FA 1-80	rel. unit	30YQR08FX(081-163)XQ01	83
Linear thermal flow in FA 1-80 in layer 1	W/cm	30YQR06FX(001-080)XQ01	80
Linear thermal flow in FA 81-163 in layer 1	W/cm	30YQR06FX(081-163)XQ01	83
Linear thermal flow in FA 1-80 in layer 2	W/cm	30YQR06FX(001-080)XQ02	80
Linear thermal flow in FA 81-163 in layer 2	W/cm	30YQR06FX(081-163)XQ02	83
Linear thermal flow in FA 1-80 in layer 3	W/cm	30YQR06FX(001-080)XQ03	80
Linear thermal flow in FA 81-163 in layer 3	W/cm	30YQR06FX(081-163)XQ03	83
Linear thermal flow in FA 1-80 in layer 4	W/cm	30YQR06FX(001-080)XQ04	80
Linear thermal flow in FA 81-163 in layer 4	W/cm	30YQR06FX(081-163)XQ04	83
Linear thermal flow in FA 1-80 in layer 5	W/cm	30YQR06FX(001-080)XQ05	80
Linear thermal flow in FA 81-163 in layer 5	W/cm	30YQR06FX(081-163)XQ05	83
Linear thermal flow in FA 1-80 in layer 6	W/cm	30YQR06FX(001-080)XQ06	80
Linear thermal flow in FA 81-163 in layer 6	W/cm	30YQR06FX(081-163)XQ06	83
Linear thermal flow in FA 1-80 in layer 7	W/cm	30YQR06FX(001-080)XQ07	80
Linear thermal flow in FA 81-163 in layer 7	W/cm	30YQR06FX(081-163)XQ07	83
Power peaking factor of FA 1-80 in layer 1	rel. unit	30YQR04FX(001-080)XQ01	80
Power peaking factor of FA 81-163 in layer 1	rel. unit	30YQR04FX(081-163)XQ01	83
Power peaking factor of FA 1-80 in layer 2	rel. unit	30YQR04FX(001-080)XQ02	80
Power peaking factor of FA 81-163 in layer 2	rel. unit	30YQR04FX(081-163)XQ02	83
Power peaking factor of FA 1-80 in layer 3	rel. unit	30YQR04FX(001-	80

Cont. Annex F

Parameter	Unit	Code KKS	Signals No.
		080)XQ03	
Power peaking factor of FA 81-163 in layer 3	rel. unit	30YQR04FX(081-163)XQ03	83
Power peaking factor of FA 1-80 in layer 4	rel. unit	30YQR04FX(001-080)XQ04	80
Power peaking factor of FA 81-163 in layer 4	rel. unit	30YQR04FX(081-163)XQ04	83
Power peaking factor of FA 1-80 in layer 5	rel. unit	30YQR04FX(001-080)XQ05	80
Power peaking factor of FA 81-163 in layer 5	rel. unit	30YQR04FX(081-163)XQ05	83
Power peaking factor of FA 1-80 in layer 6	rel. unit	30YQR04FX(001-080)XQ06	80
Power peaking factor of FA 81-163 in layer 6	rel. unit	30YQR04FX(081-163)XQ06	83
Power peaking factor of FA 1-80 in layer 7	rel. unit	30YQR04FX(001-080)XQ07	80
Power peaking factor of FA 81-163 in layer 7	rel. unit	30YQR04FX(081-163)XQ07	83
Relative power release coeff. by FA 1-163	rel. unit	30YQR02FX(001-163)XQ01	163

Annex G
Parameters recorded by MMS

Parameter	Code KKS	Signals No.
Coolant pressure in the reactor	30YCR10CP901	1
Coolant pressure difference in the core	30YCR(1-4)0CP002	4
Pressure difference in MCP 1-4	30YAR(1-4)0CP901	4
Main steam pressure in steam line SG 1-4	30YBR(1-4)0CP010	4
Coolant level in PRZ	33YPS10CL007A	1
Pressure in condenser SD11,12,13,14	30SDR(11,13)CP901E	2
Main steam pressure in collector upstream BRU-K	30RCR11CP901E	1
Steam pressure in intake I	30RDR10CP001E	1
Steam pressure in intake II	30RDR20CP001E	1
Steam pressure in intake III	30RDR30CP001E	1
Steam pressure in intake IV	30RDR40CP901E	1
Steam pressure in intake V	30RHR50CP004E	1
Steam pressure in intake VI	30RHR61CP004E	1
Steam pressure in intake VII	30RHR70CP901E	1
Steam pressure in intake VIII	30RHR80CP901E	1
Steam pressure in deaerator RL(21,22)B01	30RLR(21,22)CP001E	2
Steam pressure in in-service collector	30RQR50CP901E	1
Pressure of the steam to HP-PH 6-1,2	30RDR(21,22)CP001E	2
Pressure of the steam to HP-PH7-1,2	30RDR(11,12)CP001E	2
Feedwater pressure in SG 1-4	30RLR(71-74)CP001E	4
Feedwater pressure at pressure side of AFWP-1,2	30RLR(51,52)CP004E	2
Feedwater pressure at pressure side of TFWP-1,2	30RLR(41,42)CP902E	2
HP regulating valves position 1-4	30RAR(11-14)CS003E	4
Feedwater flow rate downstream TFWP-1,2	30RLR(41,42)CF901E	2
Feedwater flow rate upstream HP-PH -A,B	30RLR(61,62)CF001E	2
Feedwater flow rate to SG 1-4	30RLR(71-74)CF901E	4
Feedwater flow rate downstream AFWP-1,2	30RLR(51,52)CF001E	2
Turbine rotor rotation speed TF	30SBR11CS905E	1
Turbine rotor rotation speed TFWP-1,2	30SER(51,52)CG911E	2
Feedwater temperature κ SG 1-4	30RLR(71-74)CT001E	4
Level in deaerator RL(21,22)B01	30RLR(21,22)CL901E	2
Level in HP-PH 6-1,2	30RDR(21,22)CL901E	2
Level in HP-PH7-1,2	30RDR(11,12)CL901E	2
Feedwater level in SG 1-4 (“big” basis)	30YBR(1-4)0CL901E	4
Feedwater level in SG 1-4 (“small” basis)	30YBR(1-4)0CL902E	4
Position of CPS-rods	-	61
Current ion. chamber KNK-4 3,14,25	-	3

Power recorded by ion. chamber 2,12,22,7,17,27, operation sub-range of NFC (linear range)	-	6
---	---	---